FUNDAMENTAL STUDY ON GEOMETRICAL CONFIGURATION AND RELIABILITY OF FRAMED STRUCTURES USED FOR BRIDGES

By

Hitoshi FURUTA

Department of Civil Engineering
Kyoto University
Kyoto, Japan
July, 1980

FUNDAMENTAL STUDY ON GEOMETRICAL CONFIGURATION AND RELIABILITY OF FRAMED STRUCTURES USED FOR BRIDGES

By

Hitoshi FURUTA

Department of Civil Engineering
Kyoto University
Kyoto, Japan
July, 1980

Summary

This dissertation is devoted to the investigation of geometrical configurations and the reliability of framed structural systems used in bridges.

In the first part of this paper, some fundamental characteristics of the geometrical configurations of framed structures are studied on the basis of optimum design concepts, placing particular attention on the influence of topological and geometrical characteristics on the weight-minimized systems. In order to disclose their effects on structural configuration in the design process, the concepts of " topology " and " geometry " are specifically introduced by means of the " node system " and the " member system ". By use of the above-mentioned concepts, the weight-minimization formula is presented and a practical design procedure useful for obtaining the effective configuration is found through some numerical experimentation.

For a more practical point of view, an approximate design method is also employed, with the aid of the optimality criterion method, to reduce the computation load which is inevitable because of the complex set of mutual correlations between factors involved in the design process.

The latter part deals with the safety analysis and design methods based on the reliability concepts. As the measure of safety, two different parameters, failure probability and safety index, are adopted for evaluating the influence of uncertainties on structural design. While failure probability is used to discuss the structural characteristics under the environment with variational loads and resistances, a safety index is employed to make the reliability-based design practical. Here, particular attention is placed on the evaluation of the reliability of indeterminate structural systems, the influence of statistical uncertainty on the structural safety, and the application of the reliability theory to the load factor design.

Acknowledgements

The author would like to express his deepest gratitude to Professor Emeritus Ichiro Konishi and Professor Naruhito Shiraishi of Kyoto University for their constant encouragement during the course of his studies, and for the many hours of consultation and advice that were invaluable toward the compilation of the manuscript.

To Professor Masaru Matsumoto, the author wishes to express his sincere thanks for his valuable suggestions in compiling the dissertation. He is also indebted to lecturer Takeo Taniguchi of Okayama University who has been a continuing source of inspiration.

He is thankful to Messr's Shigeki Kitazono, Shingo Irie and Kenji Ikejima for their stimulating discussions concerning the first part of this thesis. And to Messr's Kunihiro Tarumi, Masanori Nakano and Katsuhiko Goto, he is grateful for their constructive criticisms about the latter part.

This is a good opportunity for the author to extend his appreciation to his parents for their understanding and support throughout his course of studies. His wife Tami is given his special acknowledgement for typing the thesis.

CONTENTS

	Summary	(i)
	Acknowledgements	(ii)
Chapter 1	Introduction	1
1.1	Structural Design	1
1.2	Bridge Design	3
1.3	Objectives and Layout of This Dissertation	6
	References	9
Chapter 2	Geometrical Configurations of Trussed Structural Systems Used for Bridges	10
2.1	Geometrical Configurations of Trussed Structures	10
2.2	Configurational Characteristics of Trussed Bridges	11
2.3	Recognition of Truss Configuration	14
2.4	Mechanical Design Factors	15
2.5	Some Optimization Schemes and Their Relationship to the Decision of Geometrical Configurations	16
2.6	The Relationship between Topology and Geometry	21
2.7	The Influence of Mechanical Properties on Geometrical Configurations	27
2.8	Conclusions	40
	References	43
Chapter 3	The Practical Design Method of Bridge Structures Regarding Configurational Variation	47
3.1	Design Procedure	47
3.2	Partitioning of Design Variables	49
3.3	Approximate Design Method Based on Optimality Criterion	52
3.4	Sub-Optimization of Members	54
3.5	Applications of Approximate Method to Truss Design	61
3.6	Applications of Approximate Method to Arch Design	65
3.7	Design Examples	67
3.8	Conclusions	86
	References	89
Chapter 4	Safety Analysis and Minimum-Weight Design of Framed Structures Using Failure Probability	91

4.1 Safety of Structure 91
4.2 Failure Probability of Framed Structure 92
4.3 Reliability of Indeterminate Structural Systems 94
4.4 Reliability Analysis Including Statistical Uncertainty 110
4.5 Minimum-Weight Design of Rigid Frames with Failure Probability Constraint 124
4.6 Minimum-Weight Design of Trussed Systems with Failure Probability Constraint 137
4.7 Conclusions 145
References 147
Chapter 5 Safety Index and Its Application to Reliability Analysis 152
5.1 Reliability Analysis Based on Second-Moment First-Order Approximation 152
5.2 The Influence of Statistical Uncertainty on Safety Index 153
5.3 Safety Index and Correction Factor 159
5.4 Reliability Analysis of Structural Systems with Multiple Failure Modes 166
5.5 Evaluation of the Effects of Each Failure Mode on System Reliability 170
5.6 Numerical Examples (Documentation) 173
5.7 Conclusions 183
References 185
Appendix 187
Chapter 6 Structural Design Based on Second-Moment Theory 189
6.1 Second-Moment Design Format 189
6.2 Usual Reliability-Based Design Methods 190
6.3 Failure Point 193
6.4 Iterative Design Method Using Failure Point 197
6.5 Determination of Partial Load Factors 203
6.6 Numerical Examples 209
6.7 Conclusions 229
References 230
Chapter 7 Concluding Remarks 232

Chapter 1 Introduction

1.1 Structural Design

" Where economic law reigns supreme and mathematical exactness is jointed to daring and imagination : that is beauty! "

- Le Corbusier -

Before the Industrial Revolution, the word " design " had been scarcely used except in the field of the fine and applied arts. Today, it can be seen in the various fields other than the artistic fields. One of these designs is structural design which may be defined here :

" Structural design is to decide the definite form, interiors and details of a structure which offers maximum benefit from a limited investiment through its expected service period. "

A process of structural design can be illustrated in Fig. 1.1, using the concept of mapping.[1] Here, the design process consists of four abstract spaces ; data space D, type space T, proportional space M and norm space N. Data space contains the uncontrollable primitive constraints due to design requirements. Type space stands for various types of structures, and each point of proportional space represents a resulting design. Therefore, in the narrow sense of selecting member sizes and proportion, design can be interpreted as an establishment of correspondence between data space and proportional space, in which both scalar mapping function and norm space present a criterion to evaluate the efficiency of design.

Numerous investigations have been made on improvements of structural design with emphasis on various stages involved in the design process. By use of the afore-mentioned concept, they can be classified into the following categories[2] ;

1) On determination of a rational mapping function without reference to norm space
2) On examination of structural characteristics from a designing point of views, by calling attention to data and type spaces

3) On influence of norm space on structural design

4) On optimization of design process, itself, including the examination of norm space

Most of studies belong to category 1, which aim to determine the rational combination of design parameters according to the current design codes. Category 2 contains the studies relevant to the decision of geometrical configuration and the examination of structural behavior of new typed structures. The objective of the studies in category 3 is to elucidate the influence of factors whose treatment is not established in the current design codes. Those investigations are generally based upon the new design concepts such as limit state design, probabilistic design. As a whole, design process is discussed in category 4, in which the risk assessment and the code-optimization are involved.

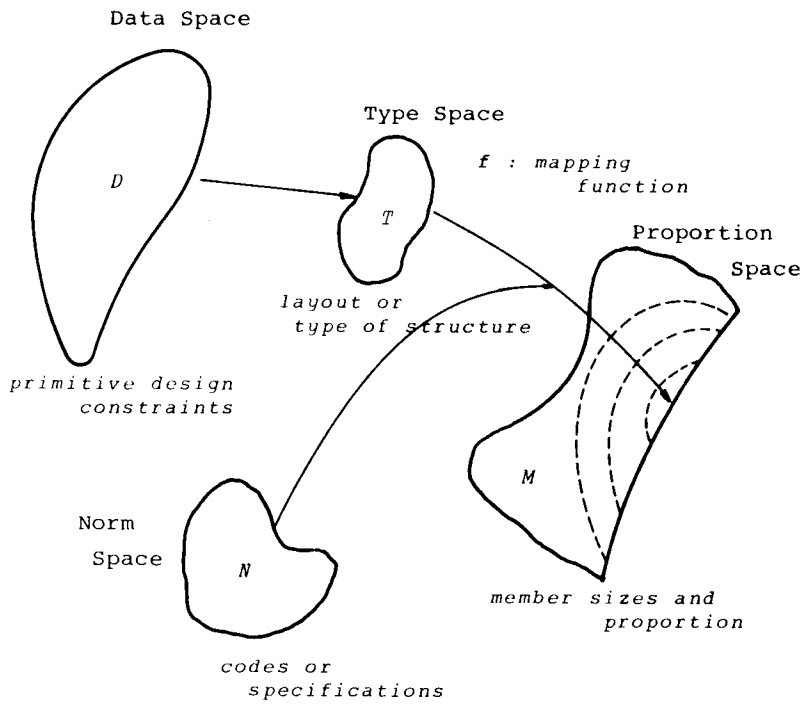

Fig. 1.1 Design Process as a Mapping

1.2 Bridge Design

" Of all the human artifacts, none can beat the great bridge : for power, for grace, for the reflection of period and the taste of progress, for the illumination of a setting or the honouring of old vitality "

- James Morris - [3]

Procedure of Bridge Design

Bridge design forms a hierarchy as well as other structural designs. According to A. Templeman[4], it is classified as four stages;

1) Topology of the structure
2) Geometry of the structure
3) Overall sizes of structure members
4) Detailed design of elements

For trussed bridges, " topology " means the number of nodes or members and their connectivity, and " geometry " means the locations of nodes and the lenghts of members. In stage 3, the cross sectional areas and the proportion of members are determined. Stage 4 means the detailed design such as the selection of plate thickness, depth of cross section, etc. Through the decisions concerned with the above four stages, a design is completed. It is, however, quite difficult to obtain a design which produces the maximum benefit, because each stage involved in the design process is not independent but inter-related.

Generally, bridge design process is quite different from the analysis. Design process consists of comparison and decision to reach many feasible solutions, while a unique solution can generally be obtained in structural analysis.

Application of Mathematical Programming to Structural Design

If the objective of structural design is to obtain a structure which produces the maximum benefit, the concept of optimization should be introduced into the design process. Then, the interpretation of design should be transferred from the analysis-oriented method to the design-oriented one. Increasing the neccesity of rationality in structural de-

sign, structural optimization has been developed in recent years. In accordance with the development of the digital computer, remarkable advances have been shown in this field since 1960 when the modern form of structural optimization was born by L. A. Schmit[5]. There are, however, many difficulties to overcome for the full potential of optimization to be realized. In designs of civil engineering structures, the difficulties involved in the structural optimization seem to appear quite explicitly, because many requirements are imposed on these designs ;

1) Usefulness---convenience, comfort, and maintenance
2) Safety---sufficient strength, durability and stability for the applied forces and weather conditions during the life of structure
3) Economy---choice of type of structure and materials
4) Harmony with the environment

Some of these requirements are intractable in the optimization procedure because of the difficulty in expressing them numerically. In addition, a great deal of the design variables induce difficulties, such as a poor convergency and an excessive computation load. In order to reduce the computation load, some special treatments, for instance, approximation or decomposition, should be introduced into the design procedure, by calling attention to the characteristics of the underlying problems that are large, multivariable, nonlinear, constrained problems.

Geometrical Configurations of Bridges

To many people the bridge is one of man's most beautiful and useful works, and symbolic of man's achievements. The aesthetic factor has played a quite important role in the design of bridge. As noted from the elegant shapes of ancient stone arches and those of modern suspended bridges, a number of investigations[6)-9)] have been performed to disclose the relationships between structural configurations and mechanical properties. The process of pursuing the mechanical rationality in structural design problems is greatly concerned with the determining configurations of a structural system, which is vested with so many kinds of possibilities of selections, based on the high reliability of materials and the recent development of construction method. It should be mentioned here

that the economical consideration takes one of the most important roles in the decision process for structural design.

The first step for obtaining the effective configuration is to clarify the factors which constitute the configuration. Next, the recognition of configuration should be performed by means of those factors specified previously. After these processes, an interest is focused on fundamental characteristics of geometrical configurations, placing attention on inherent mechanical aspects of bridges. An effective procedure to determine the configuration will be achieved through the numerical experiments. When the establishment of design process is made, it is desirable to derive an approximate method in which the geometrical variation can be taken into accout, to save the memory capacity and computation time necessary for the optimization.

Reliability of Bridges

It is well known that bridge structures as well as other civil engineering structures must withstand the severe environments. Because of this, it is necessary to evaluate the influence of environmental uncertainties on structural safety. Generally, the uncertainties involved in the design process are due to the dispersions of the loads and resistances, and errors occurring in analysis and construction, etc., whether it is possible or not to perform the probabilistic evaluation under artificial controls. As a rule, those uncertainties have been taken into consideration by the introduction of safety factor. Needless to say, the accumulated experiments or observation data obtained in the past are reflected in the determination of safety factor, but the probabilistic or statistical treatment is preferable from the standpoint of rational design.

Numerical investigations have been made on the application of probabilistic concepts to structural problems since the intensive work by A. Freudenthal in 1947. An excellent review of the development in this field so far is given by the 1972 Task Committee on Structural Safety of ASCE[10]. Up to the present the probabilistic interpretation of structural safety has gained acceptance on the belief that this approach can be implemented without difficulty within the framework of conventional structural analysis and design.

Recent research is roughly divided into five subjects ;

1) Application to practical design ; rationalization of current design codes, minimization of total expected cost, etc.
2) Extension of reliability analysis ; probabilistic evaluation of structural instability, estimation of structural safety of complex or large systems.
3) Fundamental consideration on the theoretical framework of reliability theory ; establishment of new safety measure, management of various uncertainties.
4) Application to time-dependent problems ; safety analysis and design against seismic or wind load, application of random process theory.
5) Application to prediction problems ; risk assessment, statistical decision making.

1.3 Objectives and Layout of This Dissertation

This dissertation deals with two separate subjects ; geometrical configuration of framed structure and safety analysis and design based on the reliability concepts.

Some fundamental characteristics of geometrical configuration of framed structures are investigated on the basis of the optimum design concepts, placing particular attention on the influence of topological and geometrical characteristics on the weight alleviated systems. In order to disclose their effects on structural configuration, the concepts of " topology " and " geometry " are specifically introduced by means of the " node system " and the " member system ". By use of the abovementioned concept, the weight-minimization formulation is constructed, and also an approximation is introduced into the design process so as to reduce the computation load associated with complex optimization problems. From the standpoint of structural design, this subject is referred to the one with respect to the type space described in section 1.1.

Next, the influence of uncertainties unavoidably involved in various stages of the design process on structural safety and design is

studied on the basis of both the classical theory and the second-moment theory. The classical theory is used to discuss the safety of structural system with the variated strength under the random load. Using the fiducial statistics or Bayesian decision theory, the effect of sampling on structural safety is examined with interests on the number of data and the sampling method. And the weight-minimization design with failure probability constraints is formulated for the indeterminate structural systems with many possible failure modes.

Based on the second-moment theory, a practical design method is proposed and applied to the load factor design. Comparing with several reliability-based design methods, the efficiency and applicability of the proposed method is discussed through some numerical examples.

Chapter 2 contributes to clarify the configurational characteristics of trussed systems. A distinctive feature of the configuration of trussed bridge is illustrated compared with other trussed structures. Geometrical configuration of trussed system is graphically interpreted by introducing the concepts of " topology " and " geometry ". Furthermore, two abstract systems, the " node system " and the " member system ", are considered to disclose the influence of topological and geometrical characteristics on weight-minimization. Examination of mutual relationship between geometrical configuration and mechanical properties of members provides a rough but useful guide for the design procedure.

In Chapter 3, from a practical point of views an approximate design method is studied to reduce the computation load associated with large optimization problems with many variables and a large number of nonlinear constraints. A least-weight structure is sought with the aid of a two-step approach, in which the design variables, cross sectional areas of members and nodal coordinates, are treated in two separate but dependent design spaces. Cross sectional areas can be expressed as functions of the nodal coordinates, using the sub-optimization of members and the optimality criterion. A truss example whose dimension and configuration are the same as the Amakusa 1-Go Bridge is employed to demonstrate the efficiency and applicability of the method. This design method is also applicable to arched structures, and the characteristics of trussed and arched structures are discussed with interests on their geometrical con-

figurations through numerical examples.

Chapter 4 deals with the safety analysis and the minimum-weight design of framed structures based upon the calssical reliability theory in which structural safety is evaluated by means of failure probability. For indeterminate structural systems with many possible failure modes, a simple method presenting a good upper bound of failure probability is derived by using the correlations between every two failure modes. By use of the fiducial statistics and Bayesian decision theory the influence of sampling or measurement is discussed. Also, the minimum-weight design with reliability constraints is outlined and an approximate method is proposed for a large system, which decomposes the possible failure modes into basic and non-basic modes.

Safety index is adopted as a measure of safety in Chapter 5. The influence of statistical uncertainty is discussed by considering the safety index as a random variable. To evaluate the safety of structural systems with different kinds of failure modes, the reliability analysis based on the second-moment theory is extended by calling attention to the definition of safety index presented by A. Hasofer and N. Lind.

Chapter 6 presents a reliability-based design method without dependence on mathematical assumption or approximation. The design formulation is constructed by paying attention to the " failure point " which indicates the most unsafety situation. In order to make the reliability-based design practical, the method proposed here is applied for the load factor design. Performing the calibration to the current code, resistance and load factors are determined. Then, it becomes possible to examine the safety of present bridges through numerical experiments.

Main conclusions obtained through these chapters are comprehensively reviewed in Chapter 7 accompanied with some proposals for structural design and the prospects for the future studies to be continued.

References for Chapter 1

1) Lind, N. C., " The Design of Structural Norms ", J. of Structural Mechanics, Vol.3, (3), 1973, pp357-370
2) Furuta, H., " Theory of Optimum Design ", manuscript for Chapter 5 of " Design Method in Civil Engineering " by Y.Osaka, M.Hoshiya and N.Takaoka, to appear from Gihodo Co. (in Japanese)
3) Shirley-Smith, H., " The World's Great Bridges ", Harper and Row Publishers, 1964
4) Templeman, A. B., " Optimization Concepts and Techniques in Structural Design ", IABSE 10th Congress, Inductory Report, Tokyo 1975, pp41-60
5) Schmit, L. A., " Structural Design by Systematic Synthesis ", ASCE 2nd Conference on Electronic Computation, 1960
6) Michell, A., " The Limit of Economy of Material in Frame-Structures ", Philosophical Magazine, London, Series 6, Vol.8, No.47, Nov., 1904
7) Prager, W., " A Note on Discretized Michell Structures ", J. of Computer Methods in Applied Mechanics and Engineering, 3, 1974, pp349-355
8) Ghista, D., " Optimum Frameworks under Single Load System ", Proc. ASCE, ST5, Oct., 1966, pp261-286
9) Prager, W., " Geometric Discussion on the Optimal Design of a Simple Truss ", J. of Structural Mechanics, 4(1), 1976, pp57-63
10) The Task Committee on Structural Safety of the Administractive Committee on Analysis and Design of the Structural Division, " Structural Safety - A Literature Review ", Proc. ASCE, ST4, Apr., 1972, pp845-884

Chapter 2 Geometrical Configurations of Trussed Structural Systems Used for Bridges

2.1 Geometrical Configurations of Trussed Structures

There are some kinds of trussed structures ; transmission tower, space truss used for roof and dome, trussed bridge, etc., which possess mutually different geometrical configurations to comply with their purpose of use. (" geometrical configuration " will be frequently abbreviated as " configuration " hereafter) In truss design, the designer can freely determine the interior layout of the structure, while the exterior is frequently constrained. Although many factors affect the determination of truss configuration, economy must be one of important factors. In fact, a number of design examples has made it clear that it is possible to obtain more economic designs by introducing the variety of configuration into the design process.

Up to the present many efforts have been made to disclose the configurational characteristics of truss. The first important contribution to the decision of structural configuration was made by J. Maxwell[1]. Later, A. Michell[2] recognized the importance of Maxwell's theorem, applied it to determine the least-weight structure. H. Cox[3], W. Hemp[4], D. Ghista[5] and et al[6)-13)] developed the classical theorem by Maxwell and Michell and gave examples of optimum configurations for certain load cases. However, their works are essentially based on the analytical method, and are not suitable for practical design because of the lack of generality.

In recent years the search for rational configuration has been carried out with the aid of mathematical programmings. Using the Linear Programming (LP), W. Dorn and et al[14] determined the optimum layout of members, eliminating the unnecessary members from the " ground structure " which is formed by connecting the truss members between every possible nodes. Also, A. Palmer and D. Sheppard[15] derived the effective layout by use of the Dynamic Programming (DP). In addition, many papers[16)-22)] have been presented for this field.

Despite of many contributions as listed above, there remain some difficulties in the treatment of configuration in the design process. Evidently, it is impossible to simultaneously take thought of all design factors pertaining to the configuration, and even if possible, the implementation of design work will be prohibitive and time-consuming. Then, it is inevitable to disclose the intrinsic properties of present structures and further the effect of design factors on structural configuration. It is obvious that the loading condition is the most important factor among all design factors, and that the paths between the loading points and the supporting points are closely related with the configuration.

Generally, trussed structure is defined as a pin-jointed framework whose members do not resist bending but carry only axial forces. For this specific structural character, truss configuration is constructed as a superposition of triangles which are the basic patterns to hold the stability of structure. For example, a typical one is Warren truss which consists of the " isomorphic " triangles, and in which the " degree " of nodes is less than four.

Unlike the decision of the configuration of continuous media, the numbers of nodes and members, the lengths of members, the locations of nodes and the connectivity are important to specify the configuration of truss. By means of these quantities the efficiency of configuration is discussed in this paper.

2.2 Configurational Characteristics of Trussed Bridges

Trussed bridge is considered as a system which resists the bending action as a whole. On account of the functional requirements, its configuration is horizontally long and also the vertical load due to the gravity force is excellent among the applied loads. Generally, usual trussed bridges consist of chord members and hanger members. Truss type (e.g. Pratt truss, Warren truss, etc.) is mainly recognized by the layout of hanger members. Here, in order to clarify the character-

istics of trussed bridges, the concepts of " exterior " and " interior " are introduced.[23] The exterior means the chord members and a part of the hanger members, which distinguish the space occupied by truss itself from the other space. The interior means the remains of members.

By use of the above-mentioned concepts, the configurational characteristics of trussed bridges are investigated through some simple design examples. Consider example 1 shown in Fig. 2.1. Under the supporting and loading conditions given in this figure, the configuration shown in Fig. 2.1(b) can be considered optimal, because the force is directly transmitted from the applied point to the supporting points. In this case, the interior members are unnecessary since the buckling failure does not occur at the exterior members. The same load is reversely applied in example 2, where the load induces the compressive force in members. Unless the buckling occurs, the system shown in Fig. 2.2(b) is optimum. But, if the buckling effect can not be ignored, the resulting system will change, for instance, to the one shown in Fig. 2.2(c). Example 3 represents a model for trussed bridge. In the former two cases, the configurations of the exterior can be similarly determined without difficulty, though those of the interior are different. The determination of the exterior can be carried out by considering the transmission paths from the loading point to the supporting points. However, in example 3 it is difficult to find the effective transmitting paths. The direct connection of the loading and supporting points yields the system shown in Fig. 2.3(b), whose members give no contribution. If the load is allowed to move along the acting line, various configurations can be considered for the exterior with correspondence to individual applied points. Furthermore, the member force may change from compressive to tensile or vice versa as the location of node changes. Since the buckling effect should be taken into consideration for the design of compressive members, the layout of the interior becomes important to reduce the weight or cost.

As mentioned before, the loading condition is one of the most important factors to determine the configuration. Here, the configurational characteristics are argued with interests on the relations between

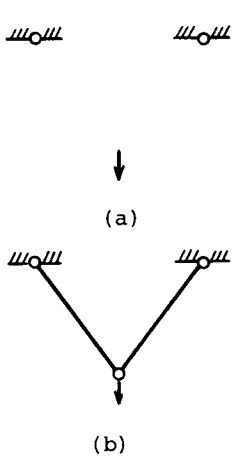

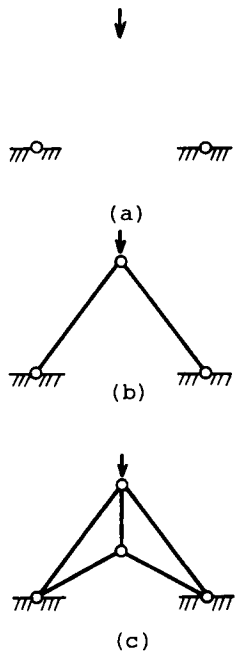

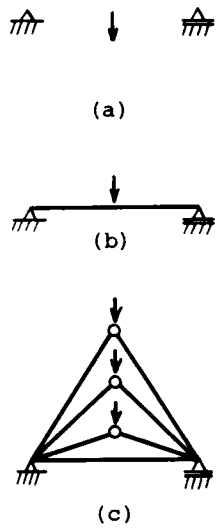

Fig. 2.1 Example 1 Fig. 2.2 Example 2 Fig. 2.3 Example 3

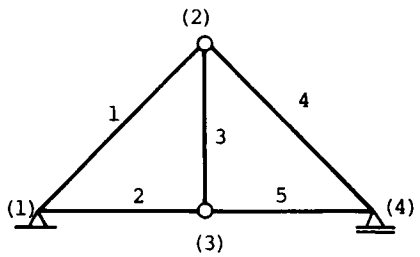

Fig. 2.4 Triangular Truss

the loading condition and the arrangement of members. Consider a triangular truss shown in Fig. 2.4, in which the vertical load is applied at the center of span and the buckling effect is not taken into account. In this example, node (2) must be translated upwards to coincide the directions of some members with that of the load. The necessary cross sectional areas of member 1 and member 4 are reduced by the translation of node (2), but the lengths of those members become larger. The optimum position will be determined as a point where the increase and decrease on weight due to the above phenomena are balanced. As observed in these examples, the difficulty involved in the decision of truss configuration lies in the fact that truss is a discrete system whose elements are chosen relatively free.

2.3 Recognition of Truss Configuration[24)]

The problem treated here can be specified as " to determine an optimal configuration which satisfies the functional requirement and is safe against an external load ". Then, it is of importance how to recognize and specify the configuration.

With the aid of the graph theory[25)-29)], the configuration of the truss system can be expressed by a linear graph consisting of only nodes and lines, which is here expressed by the term " topology ". And the mechanical characteristics of the structural system considered here can be determined by specifying geometrical dimensions of members used, which are termed as " geometry ". Thus, the factors to define the configuration consist of the " node system " and the " member system ", namely

Node System
- factors with respect to topology
  - ----- number of nodes
- factors with respect to geometry
  - ----- locations of nodes

Member System
- factors with respect to topology
  - ----- number and layout of members
- factors with respect to geometry
  - ----- lengths and sectional areas of members

The optimum problem here is, therefore, composed of the following four steps ;[30)]

(1) How many nodes shall the truss have ?

(2) Where shall the nodes be located ?

(3) How shall the nodes be connected by members ?

(4) What cross sectional areas shall they be assigned ?

These questions are, as well known, so mutually correlated that the questions should be solved simultaneously to reach the optimum solution.

2.4 Mechanical Design Factors

As observed in the previous examples, the buckling effect is considered influential on the determination of the configuration of truss. Representative factors as to mechanical properties are enumerated as follows ;[31)]

Limit allowable stress Under allowable stress constraints, the validity of configuration can be evaluated to some extent by tracing the path from loading point to datum point. However, the search of the optimal configuration for a trussed bridge tends to be involved on account of complicated paths due to the bending action.

Limit strength for buckling For the buckling strength, length of member becomes significant since the buckling strength usually decreases in accordance with the square of member length. Note that this factor greatly affects configuration.

Rigidity The deflection constraint is often specified in design of bridges. Generally, trussed bridges are relatively rigid compared with other types of bridge structures. However, if the deflection constraint is violated, most factors pertaining to the configuration should be modified, since the limitation of deflection may also affect the determination of configuration.

Supporting condition The path from loading point to datum point depends on supporting conditions and the decision is closely related with this path.

Loading condition This loading condition is considered as the most

important factor. Note that moving load remarkably affects the structural configuration since induced stresses vary from positive to negative according to the location of the load and vice versa.

Other properties The effects of secondary stress, kind of material, construction method, etc.

2.5 Some Optimization Schemes and Their Relationship to the Design of Geometrical Configurations

The configurations of actual structures are determined based on aesthetic, economic and functional factors. Evidently, functional factors should be first taken into account in the designing process. Thus, it is postulated here that necessary conditions for the functional requirement are given at the first stage of such design process as the optimal principle which is discussed on the basis of the weight-minimization concept.

Here, configurational optimization is performed by use of the mathematical programmings, different from Michell's work. Since none of usual optimization methods can simultaneously treat all design factors, some appropriate methods should be adopted for the representative design cases. The optimization methods employed here are shown as follows :

1) Linear Programming (LP)[32)-34)]

Linear programming is used to investigate the effect of topology regarding the member system when the number and the locations of the nodes are given. According to the method proposed in Ref. 14, the optimal configuration is obtained by deleting the unnecessary members from the ground structure. In the case, the problem is referred to as

$$\textit{To find} \qquad A_i \quad (i = 1, \cdots, m)$$

$$\textit{such that} \qquad f = \sum_{i=1}^{m} \rho_i A_i L_i \rightarrow \textit{Minimize} \tag{2.1}$$

$$\textit{subject to} \qquad -\sigma_{ac} \underline{A} < \underline{P}_m < \sigma_{at} \underline{A} \tag{2.2}$$

where $\underline{P}_m = \underline{C}^{-1} \underline{P}$, and Eqs (2.1) and (2.2) can be rewritten by introducing the redundant force $\underline{r}$.[35)36)]

$$\begin{bmatrix} \hat{\underline{P}}_m \\ \hline \underline{r} \end{bmatrix} = \begin{bmatrix} \hat{\underline{C}}_0^{-1} & \tilde{\underline{C}}_0^{-1} \\ \hline \underline{O} & \underline{I} \end{bmatrix} \begin{bmatrix} \tilde{\underline{P}} \\ \hline \underline{r} \end{bmatrix} \tag{2.3}$$

$$-\sigma_{ac}\,\hat{\underline{A}} \leq \hat{\underline{C}}_0^{-1}\,\underline{P} + \tilde{\underline{C}}_0^{-1}\,\underline{r} \leq \sigma_{at}\,\hat{\underline{A}} \tag{2.4}$$

$$-\sigma_{ac}\,\tilde{\underline{A}} \leq \underline{r} \leq \sigma_{at}\,\tilde{\underline{A}} \tag{2.5}$$

where σ_{at} , σ_{ac} : allowable tensile and compressive stresses

$\underline{P}_m$: member force vector

$\underline{A}$: vector of sectional areas

$\underline{P}$: external load vector

$\underline{C}$: incidence matrix

$\underline{O}$: zero matrix

$\underline{I}$: unit matrix

Notations $\hat{}$ and $\sim$ denote the determinate basic system and redundant member, respectively and subscript 0 designates the sub-matrix. Also, the underlined symbol means a vector or a matrix.

Necessary and unnecessary members are recognized by corresponding to " basic variables " and " non-basic variables " in linear programming.

2) Linear Programming with Monte Carlo Method

Linear programming method is combined with the Monte Carlo method to include the effect of node positions. In this case, it is necessary to make use of nonlinear programming, because node positions are variables and the preceding method is not applicable. The method can provide a reasonable solution without any nonlinear programming.

The permissible space is divided into some sub-spaces, where a node is generated by using the Monte Carlo method. By repeting this procedure and comparing the results obtained at each step, one can reach the final solution. This treatment excludes complicated procedures caused by taking the node positions as variables.

3) Sequential Linear Programming (SLP)[37)-39)]

In order to obtain more accurate node positions and to investigate the effect of geometry, the sequential programming is utilized. Then, the design variables consist of sectional areas A_i and nodal coordinates X_j. Using the Taylor expansion, it follows that

$$\textit{To find ;}\ \Delta A_i\ ,\ \Delta X_j \qquad \begin{cases} i = 1,\cdots\cdots,m & m : \textit{number of members} \\ j = 1,\cdots\cdots,n & n : \textit{number of moving direction of nodes} \end{cases}$$

such that

$$\Delta f = \sum_{i=1}^{m} \rho_i L_i \Delta A_i + \sum_{j=1}^{n} \sum_{i=1}^{m} \rho_i A_i (\partial L_i/\partial X_j)\Delta X_j \ \rightarrow\ \textit{Minimize} \tag{2.6}$$

subject to

$$\sum_{\ell=1}^{m} (\partial\sigma_i/\partial A_\ell)\Delta A_\ell + \sum_{j=1}^{n} (\partial\sigma_i/\partial X_j)\Delta X_j \leq \sigma_{at} - \sigma_i^{(k)} \tag{2.7}$$

$$-\sum_{\ell=1}^{m} (\partial\sigma_i/\partial A_\ell + \partial\sigma_{aci}/\partial A_\ell)\Delta A_\ell - \sum_{j=1}^{n} (\partial\sigma_i/\partial X_j + \partial\sigma_{aci}/\partial X_j)\Delta X_j$$

$$\leq \sigma_{aci}^{(k)} - \sigma_i^{(k)} \tag{2.8}$$

or

$$-\sum_{\ell=1}^{m} (\partial\sigma_i/\partial A_\ell)\Delta A_\ell - \sum_{j=1}^{n} (\partial\sigma_i/\partial X_j)\Delta X_j \leq \sigma_{at} + \sigma_i^{(k)} \tag{2.9}$$

where σ_i is the stress of the i-th member and superscript k denotes the k-th iteration step.

4) Modified Sequential Linear Programming

Although SLP has wide applicability, some difficulties appear frequently in the actual calculation, such as enormous implementation time and poor convergency. An attempt is, therefore, made to improve SLP by classifying the constraints into active and passive ones. An outline of this method is described for two designs.

a) Application to the design with buckling constraint

Initially, the nodal coordinates are determined by using only buckling constraints. Cross sectional areas are modified at the next step by adding the stress constraints. The separation of buckling constraints reduces the memory capacity to 2/3 of that required in the usual treatment. The flow chart is shown in Fig. 2.5.

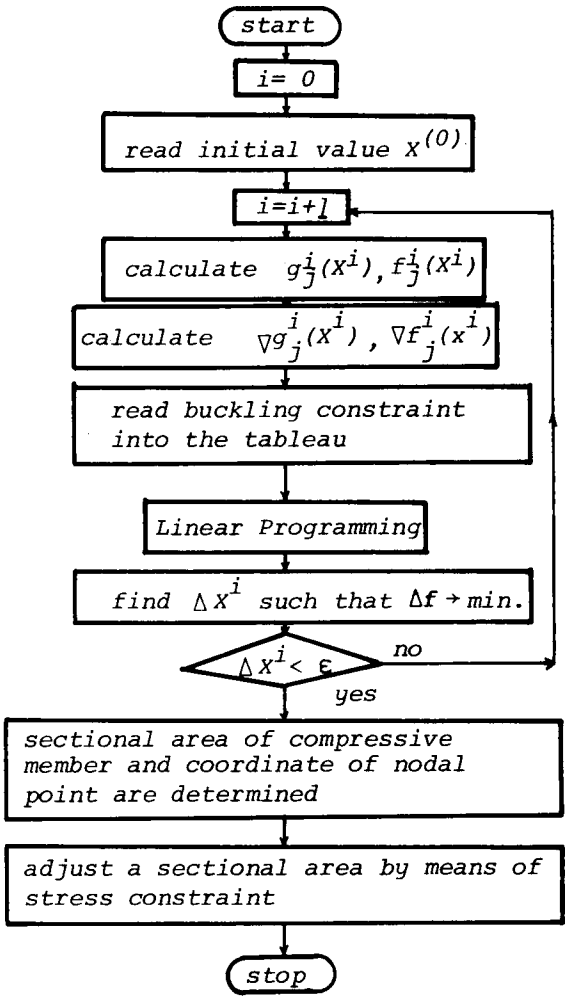

Fig. 2.5 Macro Flow Chart of Modified Sequential Linear Programming Method

b) Application to the design subjected to multiple loading conditions

For n-cases of multiple loading conditions, the number of constraints become n times larger than the case for single loading condition. Generally, the influence line method is used to analyze trussed bridges subjected to the moving load. However, the influence line changes as the nodal coordinates change, and hence the moving load is equivalently replaced by multiple load, which may invoke the increase of constraints as aforementioned. For such problems, two ways of selecting the active constraints are utilized : one is by taking three constraints, which correspond to the absolutely maximum stresses (tensile, compressive and buckling) among n loading cases, for a member, while the other is to use a single constraint by finding the most dangerous situation. They are called " Method 1 " and " Method 2 ".

5) Mixed Integer Programming[40)-42)]

In certain design cases, some design variables need to be treated as integer or discrete variables on account of their intrinsic characteristics. One of those design problems is the selection of materials in which the variables representing the grade of materials are considered discrete. By use of a special integer variable whose value is 1 or 0, the problem can be reduced to a mixed integer programming problem.[43)] It is noted that in this case cost should be chosen as the objective function instead of the weight, because the use of the high grade material makes a remarkable contribution to the weight-alleviation unless economy is taken into consideration.

To find ; ΔA_i , ΔX_j , $\delta_{\ell i}$ $\quad \ell = 1,\cdots,p$ $\quad p$: *number of kinds of materials*

such that

$$\sum_{\ell=1}^{m} A_i L_i (\partial C_i(\sigma_a)/\partial \sigma_{ai}) \sum_{\ell=1}^{p} \tilde{\sigma}_{a\ell}\delta_{\ell i} + \sum_{i=1}^{m} C_i(\sigma_a) L_i \Delta A_i + \sum_{j=1}^{n}\sum_{i=1}^{m} C_i(\sigma_a) A_i (\partial L_i/\partial X_j)\Delta X_j \rightarrow \textit{Minimize} \tag{2.10}$$

subject to

$$-\sum_{\ell=1}^{p} \tilde{\sigma}_{a\ell}\delta_{\ell i} + (\partial\sigma_i/\partial A_i)\Delta A_i + \sum_{j=1}^{n} (\partial\sigma_i/\partial X_j)\Delta X_j \leq -\sigma_i \qquad (2.11)$$

$$-\sum_{\ell=1}^{p} \tilde{\sigma}_{a\ell}\delta_{\ell i} - (\partial\sigma_i/\partial A_i)\Delta A_i - \sum_{j=1}^{n} (\partial\sigma_i/\partial X_j)\Delta X_j \leq \sigma_i \qquad (2.12)$$

where $\tilde{\sigma}_{a\ell}$ is the allowable stress of the ℓ-th kind of material and $C_i(\cdot)$ denotes the cost function.

2.6 The Relationship between Topology and Geometry

Fundamental characteristics of geometrical configurations of trussed bridges are discussed by placing particular attention on their topological properties. According to the afore-mentioned classification (the node system and the member system), the effects of topology and geometry on the weight minimized system are examined through some numerical examples. Attention is particularly paid to the correlation between topology and geometry, which has been scarcely argued.

1) Topology of the Member System and Geometry of the Node System

At first, presented are some considerations on the changes of topology and geometry in the optimization procedure. Consider the model of a trussed bridge, which is simply supported. It consists of four panels and the span length is *40 m*. The convergency and the topology obtained at each design step are illustrated in Fig. 2.6. In this case, an optimal topology is obtained by deleting the unnecessary members from the ground structure. Then, the linear programming is used for the optimization, because the number and positions of nodes are fixed. Some distinct changes on the topology can be seen in the optimization, in which the solution at each step is systematically compared from one to another. Whether a member is necessary or not is judged by corresponding it to the basic or non-basic variable. Unnecessary members are eliminated through the pivot operation. Fig. 2.7 shows the effect of the truss height on weight-minimization, where the parameter α is

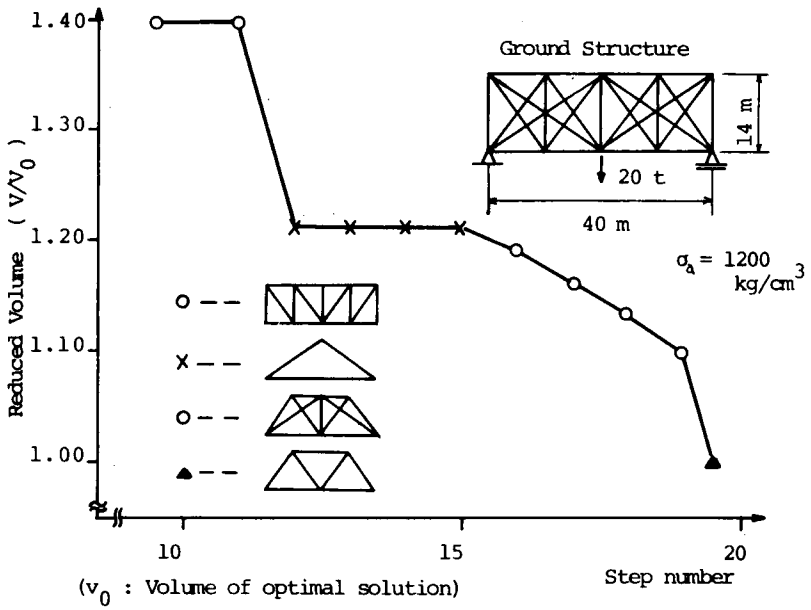

Fig. 2.6 Change of Topology of the Member System

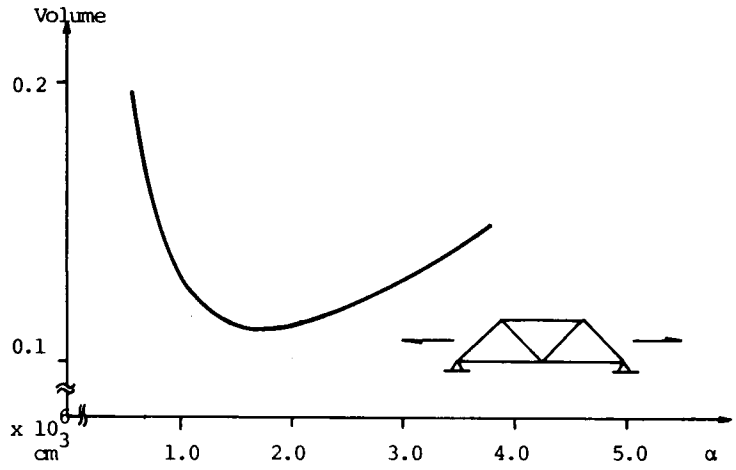

Fig. 2.7 Relation between Truss Height and Volume

the rate of the panel length and the truss height. The least volume (the volume is often used as the objective function) is obtained at $\alpha = 1.85$.

In the next example, the nodes of the upper chord are variable, while the nodes of the lower chord are fixed. Similarly to the previous example, the ground structure is formed on the basis of the nodal pattern generated by the Monte Carlo method. By use of the linear programming combined with the Monte Carlo method, the correlation between the topology of member and the geometry of node can be examined without difficulty.

The representative configurations obtained for the generated nodal pattern are presented in Fig. 2.8. It is observed from this figure that types *a*, *b* and *d* cover most of the configurations obtained here. Although a truss belonging to type *a* has the least members, its weight is heavier than that of type *b* or type *d*. A truss of type *b* shows the least weight within a range where the *y*-coordinates of node *3* is less than *15 m*. Through the successive use of the above procedure, the optimal configuration is obtained, as shown in Fig. 2.9.

Next, let's consider the change of geometry in the optimization. With the aid of SLP, the optimal node positions are sought without varying the topology of member. The change of geometry is seen in Fig. 2.10, where the initial configuration (Pratt truss) gradually transfers to the final configuration (Warren truss). It is to be noted that node *2* tends to approach to node *1* and then the induced force of the *4*th member is almost zero. This fact means that the treatment of variational geometry enables to make a rough estimation of the optimal topology of member. Thus, one can prove that node positions are so important that topology of the member system may change according to the change of node positions. Namely, node positions are so dominant to specify topology of the member system.

2) Topology of the Member System and Topology of the Node System

The number of generated nodes is increased from 5 (4-panel model) to 7 (6-panel model) or 9 (8-panel model) to investigate the relation between the layout of members and the number of nodes. The configurations obtained for the latter two cases are shown in Fig. 2.11

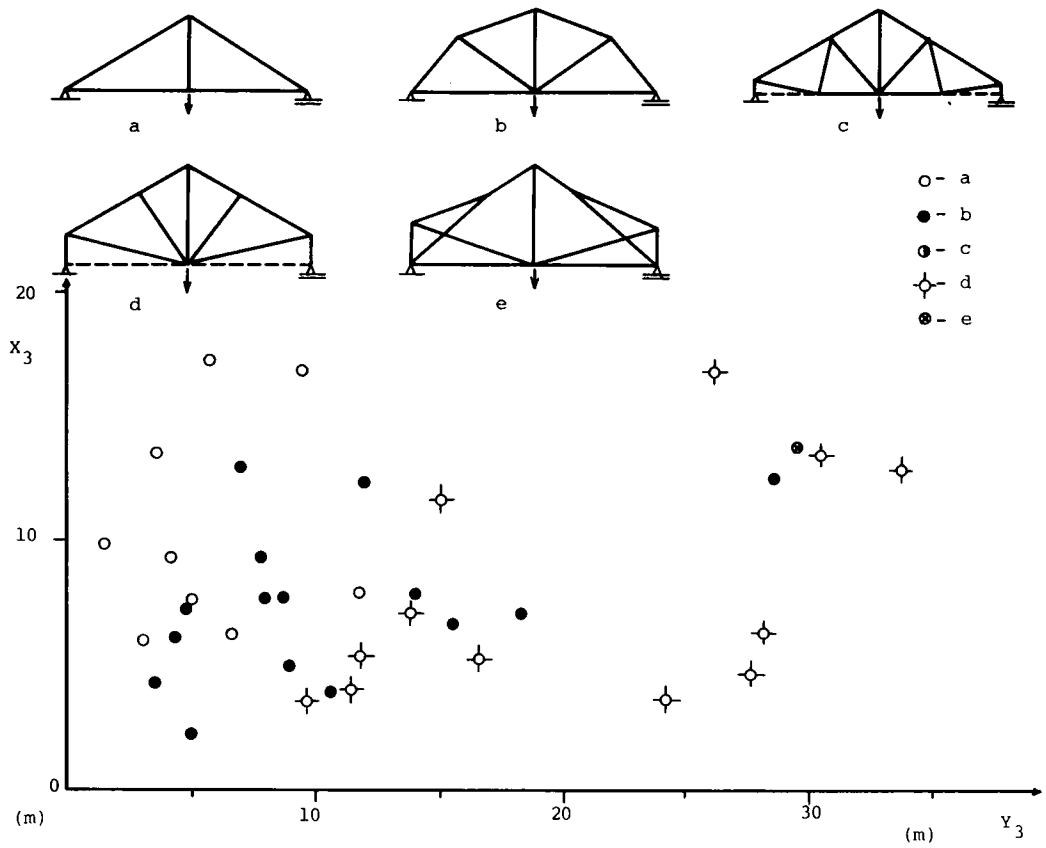

Fig. 2.8 Representative Configurations Obtained by LP with Monte Carlo Method

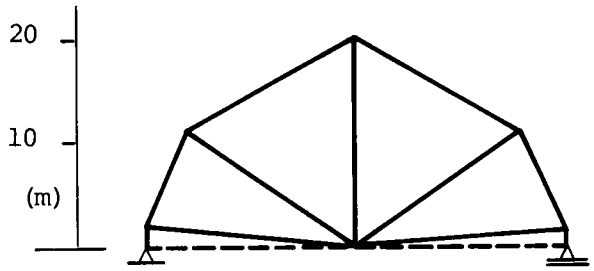

Fig. 2.9 Optimal Configuration

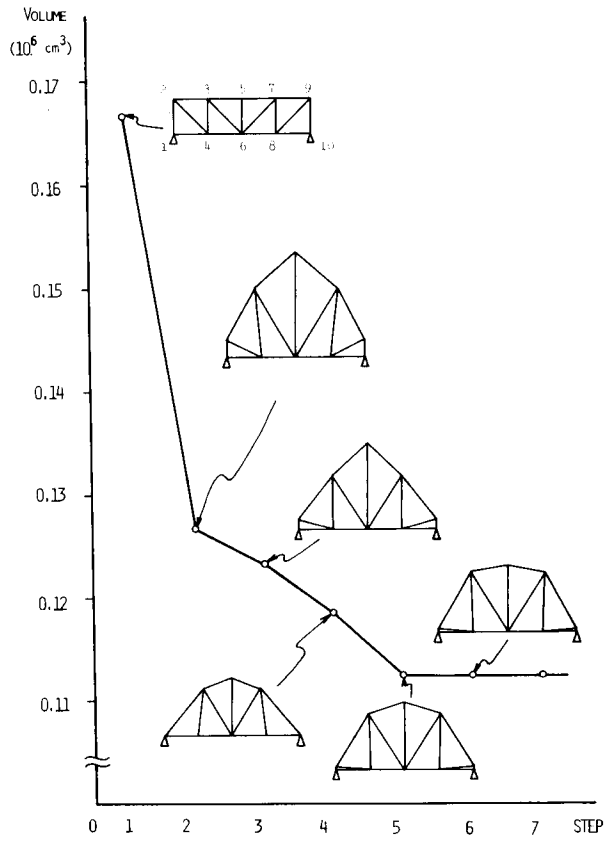

Fig. 2.10 Truss Configuration according to Each Design Step

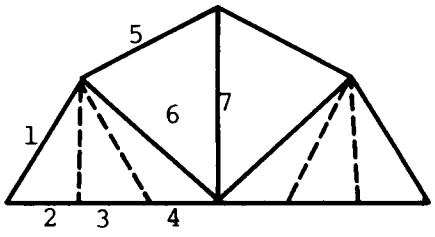

Fig. 2.11 Configuration Obtained for 6-panel Model by LP with Monte Carlo Method

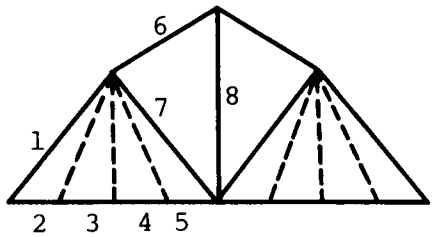

Fig. 2.12 Configuration Obtained for 8-panel Model by LP with Monte Carlo Method

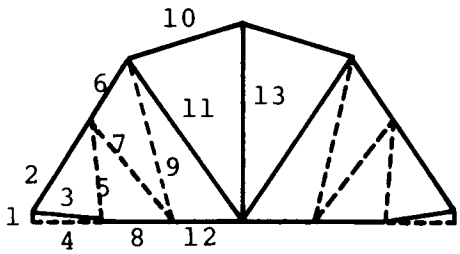

Fig. 2.13 Optimal Configuration of 6-panel Model Obtained by SLP

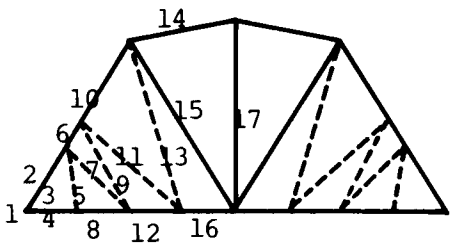

Fig. 2.14 Optimal Configuration of 8-panel Model Obtained by SLP

and Fig. 2.12. Note that there exsist non-basic (unnecessary) nodes other than non-basic members and that similar configurations were obtained for three cases in spite of the number of nodes. If the members whose sectional areas are close to zero are ignored, topology of members for each case is the same.

To further discussion on the effect of node numbers, 6-, 8-, 10- and 12-panel models are designed by use of SLP. Among them, the configurations obtained for 6- and 8-panel models are shown in Fig. 2.13 and Fig. 2.14. These results lead to the conclusion that for this loading condition the optimal topology of members is the one obtained for 2-panel model shown in Fig. 2.15.

Through these design examples, it can be said that an optimum number of nodes exsists for each topology of members. In other words, it is effective to assign the number of nodes before determining the topology of members, and that the use of an appropriate number of nodes possibly reduces a certain amount of the weight of the structure.

2.7 The Influence of Mechanical Properties on Geometrical Configurations

Through some numerical examples, the effects of mechanical properties on truss configuration are discussed in detail.

1) Influence of Buckling Effect

The buckling effect is introduced by using an approximate formula which was proposed by G. Vanderplaats and F. Moses[44] for the pipe sections. (see Fig. 2.16)

$$P_{cr} = \frac{14.13\ \pi EA}{8\ L^2} \qquad (D/t = 15.0) \qquad (2.13)$$

where P_{cr} : limit strength for buckling, E : Young's modulus, A : cross sectional area, L : member length, D : diameter, t : thickness

Let's consider a 4-panel truss model similar to the previous example. The calcualted configuration shows low height and similar mem-

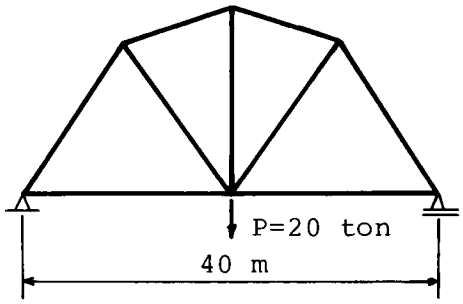

Fig. 2.15 Optimal Configuration of 2-panel Model

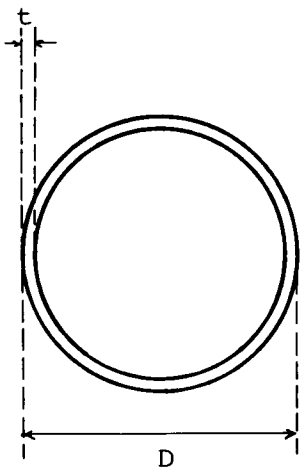

Fig. 2.16 Pipe Section

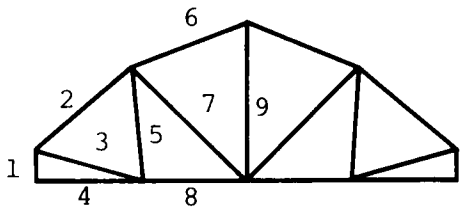

Fig. 2.17 Optimal Configuration Obtained by Considering Buckling Effect

ber lengths. (see Fig. 2.17) Considering the effect of buckling, all members are meaningful and useful for reducing the weight, while some members are useless for the case without buckling constraint. These results can be easily inferred from Eq.(2.13), for it implies that the necessary cross sectional areas increase proportionally to the square of member length. Naturally, the volume obtained for the case with buckling constraint is more than two times of the weight obtained for the case without buckling constraint. Also, the modified sequential linear programming method can reduce the computation time to the half of that needed for usual methods.

More design examples are employed to clarify the influence of buckling effect on the number of nodes. The results are summarized in Fig. 2.18, where the design conditions are as follows :

case *a* : designs of Pratt truss whose configuration is fixed, where the buckling effect is not included.

case *b* : designs of Pratt truss with buckling constraint.

case *c* : designs of truss with variable configurations (only allowable stress limit)

case *d* : designs with buckling constraint, whose configuration is that given by case *c*.

case *e* : designs with variable configurations, where the buckling effect is directly introduced into the optimization.

From this figure, the following items can be obtained : in case *a*, the optimum number of panels is *2* or *4*. There is no difference in volume between them. However, considering the buckling effect, the optimum number becomes *4*. (see the curve of case *b*) The curve of case *c* ascertains the conclusion that there is an optimal configuration under the design condition in which only the allowable stress limit is imposed. In this curve, the value of the volume is unchanged regardless of the number of panels. The curve of case *d* indicates that the greater the number of panels, the lighter the truss. While the configurations given by case *c* have almost the same configuration with respect to the exterior members, they have different numbers of interior members. As the number of the interior members increases, the lengths of the exterior members become shorter. This is useful for a design which is considering the

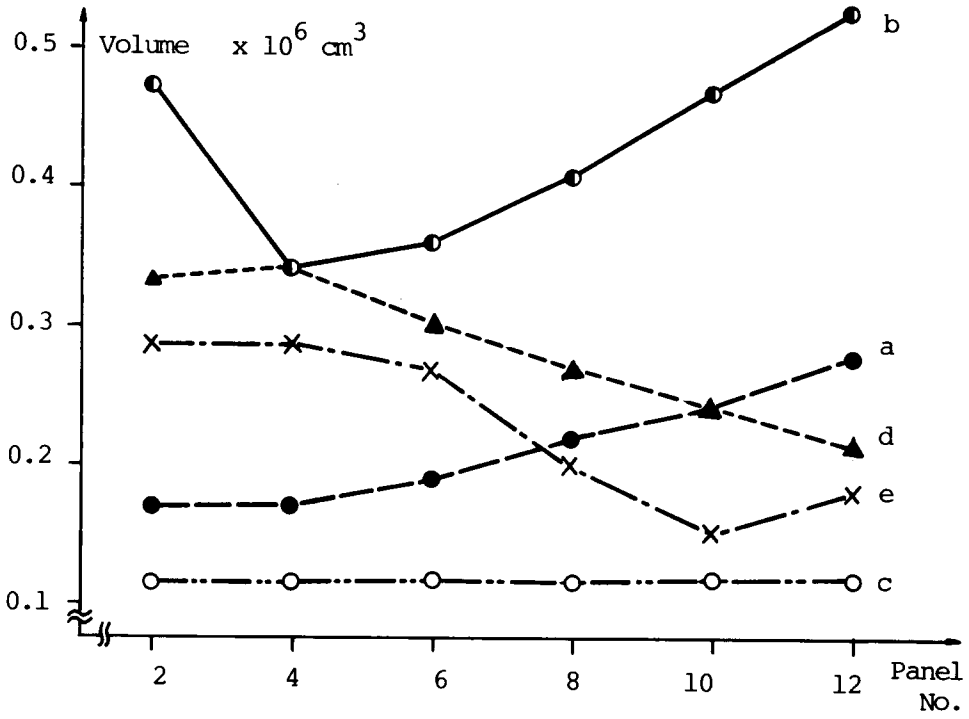

Fig. 2.18 Relations between Panel Number and Volume

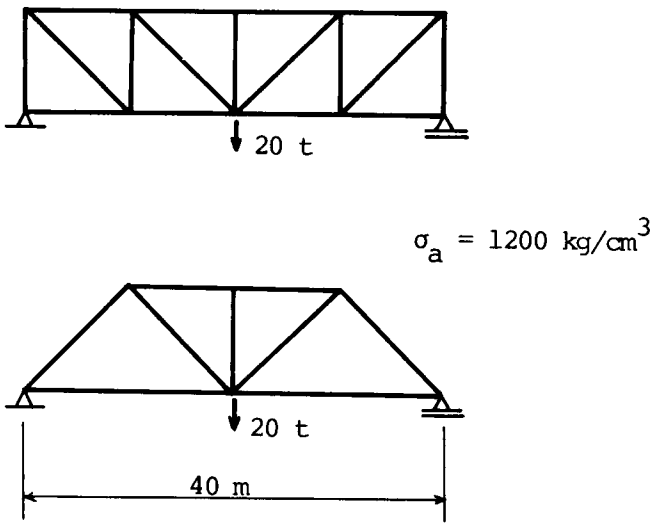

Fig. 2.19 Pratt Truss and Warren Truss

buckling effect.

Case *e* shows the least volume, and then, the optimum number is obtained as *10*. It may be considered that the increase caused by the addition of interior members and the decrease caused by the shortening of exterior members are balanced at this number. Also, these results lead to the conclusion that the optimum number of panel will change, if the variation of configuration is taken into account in the design process.

2) Influence of Rigidity

As mentioned before, the deflection constraint is often important in the design of bridge structure. It can be also considered that the limitation of deflection affects the determination of truss configuration. Here, only the correlation between deflection and weight is discussed for determinate trussed systems, because a detail discussion on the effect of a deflection constraint will be presented in chapter 3.

Consider two truss models, Pratt truss and Warren truss, whose configurations are fixed and presented in Fig. 2.19. The volumes and the deflections of the center of span calculated for these trusses are $0.1667 \times 10^6\ cm^3$, $5.714\ cm$ and $0.1333 \times 10^6\ cm^3$, $4.571\ cm$, respectively. These results show that determinate trusses have a tendency that the deflection is smaller as the weight is lighter. One can prove this fact by considering the characteristics of the weight-minimized determinate truss systems. Generally, the deflection δ is calculated by using the following formula.[45)]

$$\delta = \sum_{i=1}^{m} \frac{F_i \bar{F}_i}{E A_i} L_i \qquad (2.14)$$

where F_i and $\bar{F}_i$ denote the axial force of the i-th member induced by the external load P and the virtual unit load applied at the center of the span respectively.

Since each member reaches the " fully stressed " condition in the optimum solution, the following relations are obtained.[46)47)]

$$F_i = \sigma_a A_i \qquad (2.15)$$

$$\bar{F}_i = \sigma_a A_i / P \qquad (2.16)$$

where σ_a is the allowable stress, and its value is assumed to be equal for all members.

Substituting Eq.(2.15) and Eq.(2.16) to Eq.(2.14), the deflection is found as

$$\delta = \frac{\sigma_a^2}{E} \sum_{i=1}^{m} A_i L_i \qquad (2.17)$$

From Eq.(2.17), it can be obtained that the deflection is proportional to the volume or weight.

Further examples[48] show that this fact seems to be held for the design cases sujected to other loading conditions or buckling constraints. For instance, on account of buckling constraint, the weights and the deflections of the same models change to $0.342 \times 10^6\ cm^3$, $3.805\ cm$ and $0.288 \times 10^6\ cm^3$, $2.298\ cm$, respectively.

3) Influence of Supporting Condition[49]

Three supporting systems of simple support (Model 1), continuous support (Model 2) and cantilever support (Model 3) are employed in order to disclose the influence of supporting systems. Fig. 2.20 indicates considerable difference in configurations and it is interesting to note that the formation of upper chords is quite similar to the bending moment diagrams regarding beam models. Table 2.1 indicates that Model 1 is the heaviest and Model 3 the lightest, whether the positions of nodes are fixed or variable. It seems that each supporting condition reaches the limit of weight-minimization. This means that a feasible supporting system should be chosen at the first step of designing.

4) Influence of Loading Condition

Here, the method proposed in section 2.5 is applied to the multiple loading case. Consider the model shown in Fig. 2.21. The moving load is replaced by the six loads, P_1 - P_6, whose positions are illustrated in the same figure. Numerical results are summarized in Fig. 2.22 and Table 2.2. Fig. 2.22 shows the changes of configuration and total volume through optimization, and that the final configuration differs considerably from that obtained for the single loading case. It can be said that the loading condition is one of the most important factors, and hence

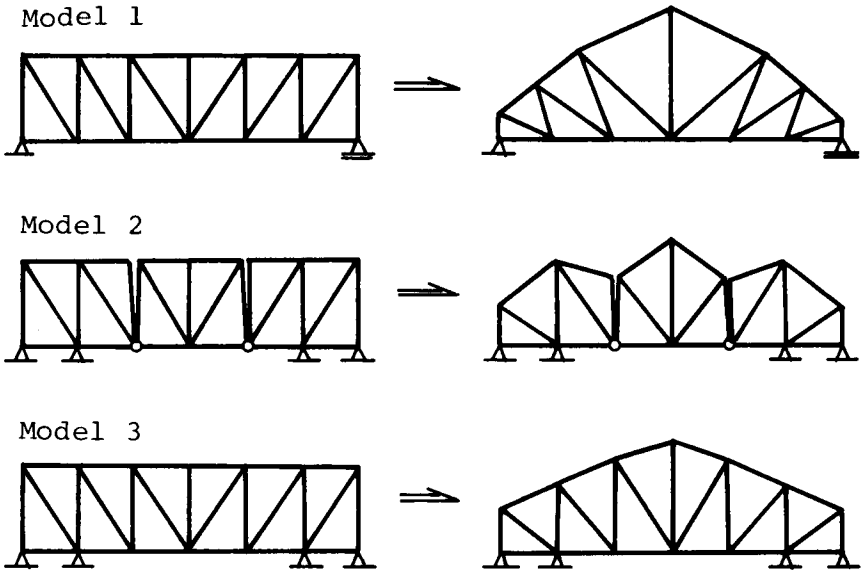

Fig. 2.20 Optimal Configurations Obtained for Some Kinds of Supports

Table 2.1 Numerical Results for Some Kinds of Supports

	Total Volume (fixed geometry)	Total Volume (variable geometry)
Model 1	0.3580	0.2657
Model 2	0.3236	0.2629
Model 3	0.2681	0.2260

$\times 10^6$ cm^3

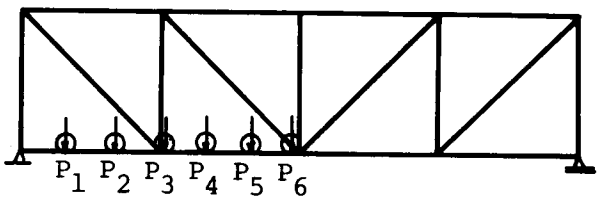

Fig. 2.21 4-Panel Model and Loading Condition

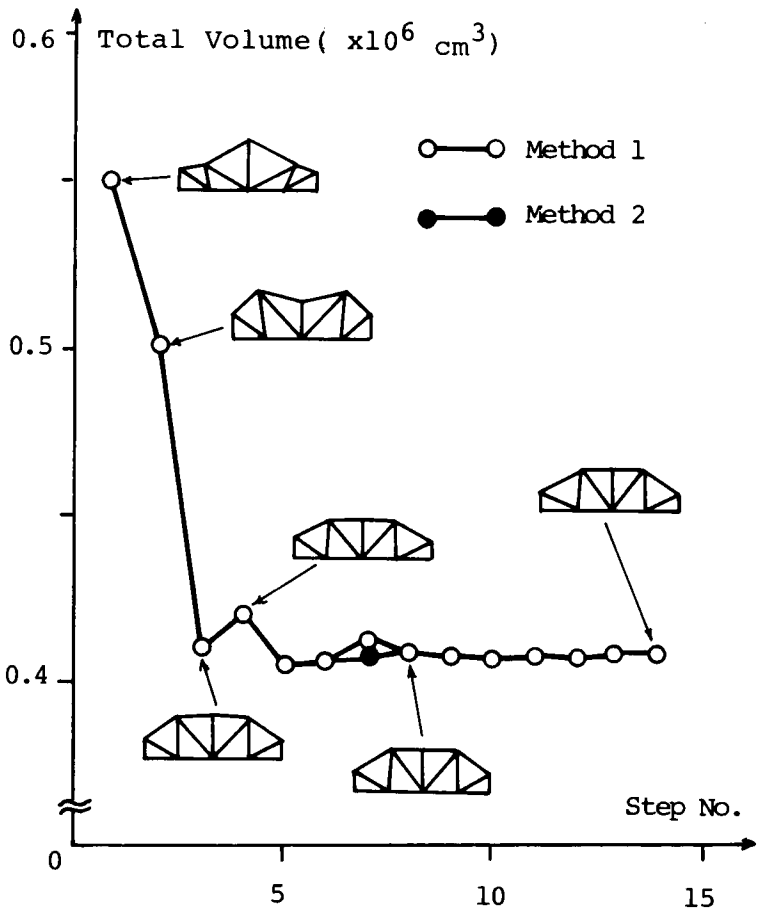

Fig. 2.22 Change of Configuration and Total Volume through Optimization

Table 2.2 Numerical Results for Multiple Loading Condition

Method 1

Member	A cm^3	L cm	R_t max	R_t min	P_{cr}	σ kg/cm^2
1	19.2	535.1	*	-15000	-15000	-781
2	46.4	1262.7	*	-15725	-15726	-339
3	13.0	1134.2	15585	*	-1528	1199
4	5.0	1000.0	0	0	-291	0
5	23.7	1153.8	12700	-4922	-4922	-208
6	34.7	896.7	*	-17490	-17490	-504
7	33.8	1457.6	12820	-6272	-6272	0186
8	10.5	1000.0	12600	*	01286	1200
9	5.0	1143.5	*	-222	-224	-45

Calculation Time 15 sec.

Method 2

Member	A cm^3	L cm	R_t max	Rt min	P_{cr}	σ kg/cm^2
1	19.2	535.1	*	-15000	-15000	-781
2	46.6	1267.1	*	-15745	-15745	-338
3	13.0	1133.7	15600	*	-1533	1200
4	5.0	1000.0	0	0	0291	0
5	23.7	1154.7	12700	-4922	-4922	-208
6	34.6	892.5	*	-17483	-17483	-505
7	33.7	1455.4	12800	-6259	-6259	-186
8	10.5	1000.0	12585	*	-1282	1199
9	5.0	1144.0	*	-222	-223	-45

Calculation Time 11 sec.

that an accurate modeling of load condition is inevitable to determine the configurations of trussed bridges. Compared with the computation time, the proposed method is able to solve the problem in half the time. Therefore, Method 2 is preferable.

5) Influence of Secondary Stress

For trussed bridges, the secondary stress is mainly due to the bending moment which occurs in each member. Generally, the effect of bending moment is not taken into account in the analysis of trussed structures, because of simplicity and small difference between the strict and approximate treatments. However, this effect is no longer ignored for the design of trusses whose members have high rigidity, large eccentricity and long length.

It is quite difficult to investigate the effect of secondary stress on configuration, because the secondary stress can be evaluated only when all design parameters are completely determined. Here, the effect of secondary stress is examined by use of a design example shown in Fig. 2.17. Numerical results are presented in Table 2.3, which shows that the secondary stress tends to increase in the upper chord and the vertical members subjected to the compressive force, and that the ratio of secondary stress and original stress is from 10 to 20 per cent. Considering the effect of secondary stress, the configuration should be determined to diminish the axial forces for the compressive members.

6) Influence of the Grade of Material[50)51)]

Three kinds of material, M1, M2 and M3 (which correspond to *SS41*, *SM50* and *SM58* steels) are employed to disclose the effect of the grade of material. The optimal configurations are obtained for three design cases. In case 1, M1 is used for all members. In case 2 and case 3, M1 is also used for the hanger members, while M2 and M3 are used for the chord members, respectively. As shown in Fig. 2.23, truss height tends to become smaller as the higher grade material is employed for the chord members.

Next, the search for the optimal configuration is carried out on the basis of the cost-optimization formulation in which the costs of M2 and M3 are *1.05* and *1.20* times that of M1 and those materials are treated as design variables. Numerical results for the 4-panel model

Table 2.3 Secondary Stresses of 4-Panel Model

Member	Member Stress (σ)	Secondary Stress (σ')	Stress Ratio σ'/σ (%)
1	-1200.0	$\sigma'_{12} = 32.23$ $\sigma'_{21} = 15.23$	2.69 1.27
2	-302.4	$\sigma'_{23} = -15.41$ $\sigma'_{32} = -5.65$	5.09 1.87
3	1200.1	$\sigma'_{24} = -7.33$ $\sigma'_{42} = -9.43$	0.01 0.79
4	0.0	$\sigma'_{41} = -69.35$ $\sigma'_{14} = -44.82$	
5	-151.6	$\sigma'_{34} = 28.99$ $\sigma'_{43} = 19.16$	19.19 12.69
6	-339.6	$\sigma'_{35} = -2.29$ $\sigma'_{53} = -31.28$	0.67 9.21
7	-1200.1	$\sigma'_{36} = 6.91$ $\sigma'_{63} = -1.45$	0.58 0.12
8	1200.0	$\sigma'_{46} = -29.00$ $\sigma'_{64} = -35.86$	2.42 2.99
9	243.3	$\sigma'_{56} = 0.00$ $\sigma'_{65} = 0.00$	0.00 0.00

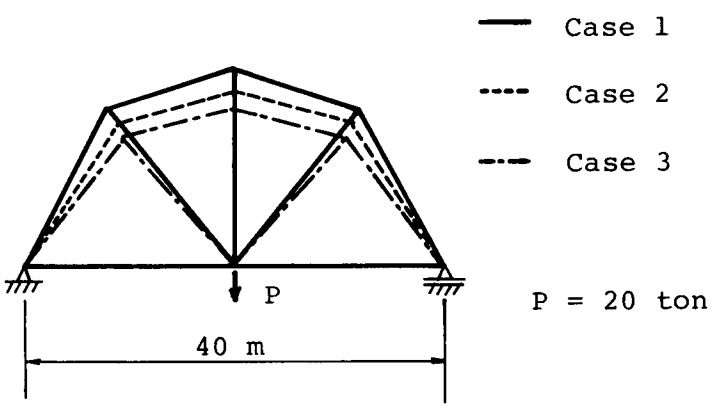

Fig. 2.23 Influence of Member Strength on Optimal Configuration

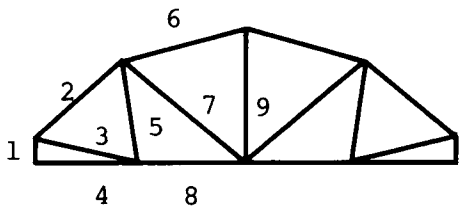

Fig. 2.24 Optimal Configuration of 4-Panel Truss with Some Grades of Materials

Table 2.4 Numerical Results of 4-Panel Model

	kind of steel	Area cm^2	Member force kg	Member length cm
1	SS41	18.00	-10000	250
2	SS41	46.47	-11777	1134
3	SM50	4.79	9103	1031
4	SS41	7.57	0	1000
5	SS41	23.19	-2232	1079
6	SS41	54.20	-15900	1188
7	SM50	4.80	9123	1524
8	SM50	4.47	8500	1000
9	SM50	4.22	8027	1300

Total Volume = 0.3365×10^6 cm^3

Total Cost = 0.3385×10^6

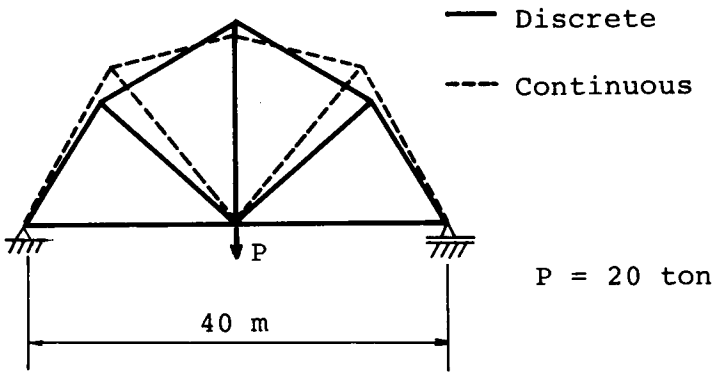

Fig. 2.25 Optimal Configuration of Truss with Discrete Components

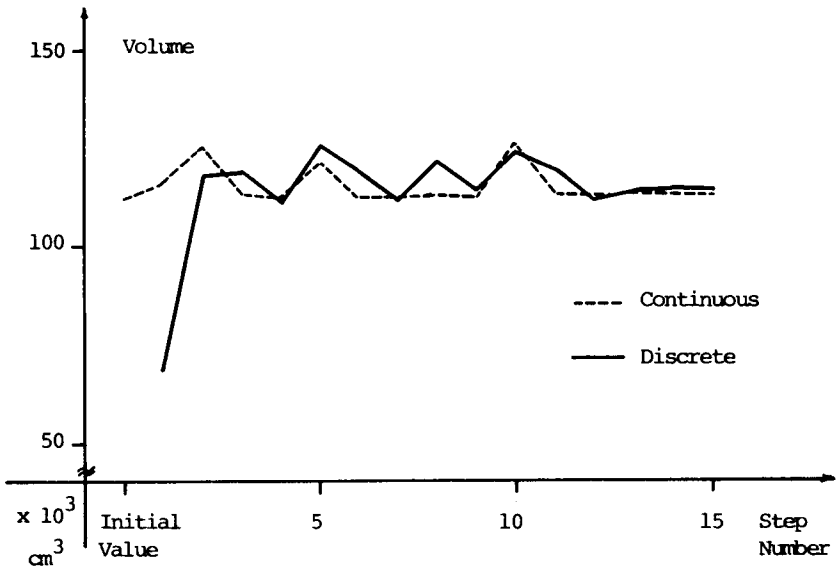

Fig. 2.26 Convergence of Truss Design with Discrete Components

are given in Fig. 2.24 and Table 2.4. It can be seen that truss height is smaller than that of the truss with the same material. Note that M1 material is chosen for the compressive members and M2 material for the tensile members. In Table 2.4, positive and negative values in member forces show tension and compression, respectively.

7) Influence of Discrete Sizing[52)-55)]

For civil engineering structures, it is often desirable to select member size as discrete values from a table of acceptable values. Here, the design problem with discrete variables is dealt with by use of a mixed integer programming. Let's consider the 2-panel truss model in which the cross sectional areas are given as discrete values, e.g., five cross sectional areas (A_1, A_2, A_3, A_4, A_5) = (5, 10, 15, 20, 25 cm^2). The resulting configuration is presented in Fig. 2.25, compared with the configuration obtained for the case with continuous variables. As expected, one can find a considerable difference in configuration, but the difference in volume is merely 2 per cent. This means that when cross sectional areas are given as discrete values, it is possible to obtain an effective design by introducing a variation of configurations into the design process.

The calculation is carried out by use of Doig and Land's algorithm[56)] based on the branch bound method. Fig. 2.26 shows the convergency in the optimization. It is seen that this problem has an uneven convergence, which is caused by the replacements of discrete variables. As known from the poor convergency, the problem requires more computation time, about 7 times that of the usual treatments. From a practical point of views, the design problem with discrete variables requires a special treatment to reduce the computation time and memory capacity.

2.8 Conclusions

In this chapter, the influence of geometrical factors and mechanical properties on configuration are investigated by placing attention on topological and geometrical characteristics of trussed bridges. Through numerical results, one may conclude as follows :

1) Graphical representation is useful to recognize the geometrical configurations of trussed structures. Based on the concepts of the topology and geometry, the characteristics of truss configuration can be elucidated by means of the classification of the member system and the node system.

2) It is confirmed that a considerable weight reduction can often be achieved by introducing the variation of configurations into the designing process. For trussed bridges, " geometry " is more important than " topology " to determine structural configurations. Namely, the topology of the member system is specified to a great extent by the node positions. There is an optimal configuration when only stress constraints are taken into consideration. Then, the number of nodes does not play an important role.

3) Buckling effect is of primary importance in the decision of configuration. Using the approximate method proposed in this chapter, it is possible to reach the optimum solution or a reasonable solution in a comparatively simplified manner. Note that the method is also applicable for the moving load case.

4) Needless to say, the loading condition is the most important factor to determine structural configurations, and the loading condition should be modeled to correspond well to the real state. From the points of practical computation, it is accepted to replace the moving load by the decomposed multiple loads.

5) Also, supporting condition affects the decision of truss configuration. A feasible supporting condition should be chosen at the first step of design, because each supporting condition used in the present designs has the limit of weight-minimization, regardless of whether the configuration is fixed or variable.

6) Seemingly, deflection constraint is not so important in the decision of geometrical configurations of statically determinate trussed systems, because those trusses have more rigidity as they are lighter.

7) The use of some grades of materials contributes to reduce the cost and weight when some constraints are imposed on configuration. However, it is inconvenient to implement the selection of materials

by means of the mixed integer programmings, because of the enormous computation time and memory capacity.

8) Consequently, the following procedure is considered effective to decide the configuration of a trussed bridge.

   i) Determine the supporting condition.

   ii) Assume the number of nodes and topology of the member system.

   iii) Perform the optimization by taking the nodal coordinates and the cross sectional areas of members as design variables.

References for Chapter 2

1) Maxwell, J., " On the Calculation of the Equilibrium and Stiffness of Frames ", The Scientific Papers of James Clerk Maxwell, Cambridge Univ. Press, Cambridge, England, 1890
2) Michell, A. G. M., " The Limit of Economy of Material in Frame-Structures ", Philosophical Magazine, London, England, Series 6, Vol.8, No.47, November, 1904
3) Cox, H. L., " The Design of Structures of Least Weight ", Pergamon Press, 1965
4) Hemp, W. S., " Optimum Structures ", Oxford Engineering Series, Clarendon Press, Oxford, England, 1973
5) Ghista, D. N., " Optimum Frameworks under Single Load System ", Proc. ASCE, ST5, October, 1966, pp261-286
6) Reinschmidt, F. and Russel, D., " Application of Linear Programming in Structural Layout and Optimization ", Int. J. of Computers and Structures, Vol.4, 1974, pp855-869
7) Alspaugh, W. and Kunoo, K., " Optimum Configurational and Dimensional Design of Truss Structures ", Int. J. of Computers and Structures, Vol.4, 1974, pp755-770
8) Lapay, S. and Goble, G., " Optimum Design of Trusses for Ultimate Loads ", Proc. ASCE, ST1, Jan., 1971, pp157-172
9) Spillers, W. and Friedland, L., " On Adaptive Structural Design ", Proc. ASCE, ST10, Oct., 1972, pp2155-2163
10) Poter-Goff, R., " Decision Theory and the Shapes of Structures ", J. of the Royal Aeronautical Society, Vol.70, Mar., 1966, pp448-452
11) McCornell, R., " Limit Weight Frameworks for Load Across Span ", Proc. ASCE, EM5, Oct., 1974, pp885-901
12) Pedersen, P., " On the Optimal Layout of Multi-Purpose Trusses ", Int. J. of Computers and Structures, Vol.2, 1972, pp695-712
13) Lipson, S. and Agrawal, K., " Weight Optimization of Plane Trusses ", Proc. ASCE, ST5, May, 1974, pp865-879
14) Dorn, W., Gomory, R. and Greenberg, H., " Automatic Design of Optimal Structures ", J. de Mechanique, Vol.3, Mars, 1964, pp25-52

15) Palmer, A. and Sheppard, D., " Optimizing the Shape of Pin Jointed Structures ", Proc. ICE, Vol.47, London, England, Nov., 1970, pp363-376

16) Patnaik, S. and Srivastava, N., " On Automated Optimum Design of Trusses ", J. of Computer Methods in Applied Mechanics and Engineering, 9, 1976, pp245-265

17) Majid, K. I., " Optimum Design of Structures ", Butterworth and Co. (publishers) Ltd., 1974

18) Majid, K. I. and Elliot, D., " Topological Design of Pin Jointed Structures by Non-Linear Programming ", Proc. ICE, 55, March, 1973, pp129-149

19) Pedersen P., " Optimal Joint Positions for Space Trusses ", Proc. ASCE, ST12, Dec., 1973, pp2459-2476

20) Corcoran, P., " Configurational Optimization of Structures ", Int. J. of Mech. Sci. Vol.12, 1970, pp459-462

21) Ho, J., " Optimal Design of Multi-Stage Structures : A Nested Decomposition Approach ", Int. J. of Computers and Structures, Vol.5, 1975, pp249-255

22) Schmidt, L. C., " Minimum Weight Layout of Elastic, Statically Determinate, Triangulated Frames under Alternative Load Systems ", J. of Mech. Phy. Solid, Vol.10, 1962, pp139-149

23) Kitazono, S., " A Study on Geometrical Configuration of Trussed Structures ", Master of Engineering Thesis, Kyoto Univ., 1977 (in Japanese)

24) Hooshin, H., " Algebraic Representation and Processing of Structural Configuration ", Int. J. of Computers and Structures, Vol.5, 1975, pp119-130

25) Fenves, S. J. and Branin, F. H., " Network-Topological Formulation of Structural Analysis ", Proc. ASCE, ST4, 1963, pp483-514

26) Spillers, W. R., " Application of Topology in Structural Analysis ", Proc. ASCE, ST4, 1963, pp301-314

27) DiMaggio, F. L. and Spillers, W. R., " Network Analysis of Structures ", Proc. ASCE, ST1, 1966, pp199-222

28) Spillers, W. R., " Network Analogy for Linear Structures ", Proc. ASCE, EM4, 1963, pp21-29

29) Konishi, I., Shiraishi, N., Taniguchi, T. and Furuta, H., " An Application of Network-Topological Concepts to the Design of Framed Structures ", The Memoirs of the Faculty of Engineering, Kyoto Univ., Vol.36, Part 4, 1974, pp348-368

30) Friedland, L., " Geometric Structural Behavior ", the Dissertation submitted for the Degree of Doctor of Engineering Science, Columbia University, 1971

31) Shiraishi, N. and Furuta, H., " A Few Considerations on Topological and Geometrical Systems of Trussed Bridges ", Theoretical and Applied Mechanics, Vol.28, 1980, pp129-137

32) Dorn, W. S. and Greenberg, H. J., " Linear Programming and Plastic Limit Analysis of Structures ", Quarterly of Applied Mathematics, Vol.15, 1957, pp155

33) Gass, S. I., " Linear Programming Method and Applications ", MacGraw Hill Co. Ltd., 1964

34) Konishi, I., Shiraishi, N., Taniguchi, T. and Furuta, H., " Structural Analysis and Design of Rigid Frames Based on Plastic Theorem ", The Memoirs of the Faculty of Engineering, Kyoto Univ., Vol.37, Part 4, Oct., 1975, pp219-236

35) Livesley, R. K., " Matrix Method of Structural Analysis ", Pergamon Press, 1964

36) Livesley, R. K., " The Selection of Redundant Forces in Structures, with an Application to the Collapse Analysis of Frameworks ", Proc. of the Royal Society (London), Series A, Vol.301, 1967, pp493-505

37) Moses, F., " Optimum Structural Design Using Linear Programming ", Proc. ASCE, ST6, Dec., 1964, pp89-104

38) Brown, D. M. and Ang, H-S., " Structural Optimization by Nonlinear Programming ", Proc. ASCE, ST6, Dec., 1966, pp319-338

39) Okubo, S., " Optimization of Truss ", Proc. JSCE, No.177, May, 1970, pp9-19 (in Japanese)

40) Naruoka, M. and et al, " Optimum Design of Framed Structure ", JSSC, Vol.7, No.64, Apr., 1971, pp46 (in Japanese)

41) Sagara, N., " Introduction to Mathematical Programming ", Morikita Co. Ltd., 1976 (in Japanese)

42) McMillan, C., " Mathematical Programming - An Introduction to the

Design and Application of Optimal Decision Machines ", John Wiley and Sons, Inc., 1970

43) Shiraishi, N. and Furuta, H., " On Optimal Configuration of Trussed Bridges Considering the Mechanical Properties of Members ", The 27th Annual Meeting of Applied Mechanics, Tokyo, Nov., 1977, D-54 (in Japanese)

44) Vanderplaats, G. and Moses, F., " Automated Design of Trusses for Optimum Geometry ", Proc. ASCE, ST3, Mar., 1972, pp671-690

45) Konishi, I. and et al, " Structural Mechanics I ", Maruzen Co. Ltd., 1974 (2nd Edition) (in Japanese)

46) Gallagher, R. and Zienkiewicz, O. (Editors), " Optimum Design : Theory and Application ", John Wiley and Sons, Inc., 1973

47) Ghista, D. N., " Fully-Stressed Design for Alternative Loads ", Proc. ASCE, ST5, Oct., 1966, pp237-260

48) Irie, S., " Fundamental Study on Geometrical Configuration of Trussed Bridges and Its Introduction to Structural Design ", Master of Engineering Thesis, Kyoto Univ., 1978 (in Japanese)

49) Shiraishi, N. and Furuta, H., " On Geometrical Configuration of Truss Systems Used for Bridges ", The 25th Symposium on Structural Engineering, Tokyo, Feb., 1979, pp39-46 (in Japanese)

50) Schmit, L. A., " Synthesis of Material and Configuration Selection ", Proc. ASCE, ST5, June, 1962, pp79-101

51) Sridhar-Rao, J. K. and et al, " An Algorithm for Optimal Material Choice for Multifunctional Criteria ", Int. J. of Computers and Structures, Vol.3, 1973, pp715-724

52) Reinschmidt, K., " Discrete Structural Optimization ", Proc. ASCE, ST1, Jan., 1971, pp133-155

53) Toakley, A. R., " Optimum Design Using Available Sections ", Proc. ASCE, ST5, May, 1968, pp1219-1241

54) Cella, A. and Logcher, R., " Automated Optimum Design from Discrete Components ", Proc. ASCE, ST1, Jan., 1971, pp175-189

55) Lipson, S. L. and Gwin, L. B., " Discrete Sizing of Trusses for Optimal Geometry ", Proc. ASCE, ST5, May, 1977, pp1031-1045

Chapter 3 The Practical Design Method of Bridge Structures Regarding Configurational Variation

3.1 Design Procedure

In usual bridge designs, the selection of structural type is firstly made according to the prescribed span length. Generally, the effective span lengths are given for some types of bridges as follows[1] :

Plate Girder Bridge, Hybrid Girder Bridge	$< 40\ m$
Continuous Girder Bridge	$40 \sim 200\ m$
Trussed Bridge	$50 \sim 300\ m$
Cable-Stayed Bridge	$100 \sim 350\ m$
Arched Bridge	$80 \sim 500\ m$
Suspension Bridge	$100 \sim 1500\ m$

Trussed bridges treated here are suitable for the medium span from $100\ m$ to $300\ m$, for which cable-stayed bridges and arched bridges are also available.

According to the design hierarchy described in Chapter 1, the decision of structural type is closely related to the decision of topology. We obtained in the previous chapter that geometry is more important than topology to determine the geometrical configuration of trussed bridge. However, this result may be due to the limitation of structural type. If there is no limitation on structural type, topology will become more important. Accepted to use a simple expression, the configurational relations between trussed, arched and cable-stayed bridges can be considered as shown in Fig. 3.1. Conceptually, bridge structures can be expressed as a model shown at the top of the figure on account of its definition that bridge is a structure which connects the two separate points. Then, some kinds of discretization are introduced to reduce the weight or cost. It may be said that present typical bridge structures have been developed by pursuiting the effective discretization with a mechanical rationality. Also, it is observed in the figure that sup-

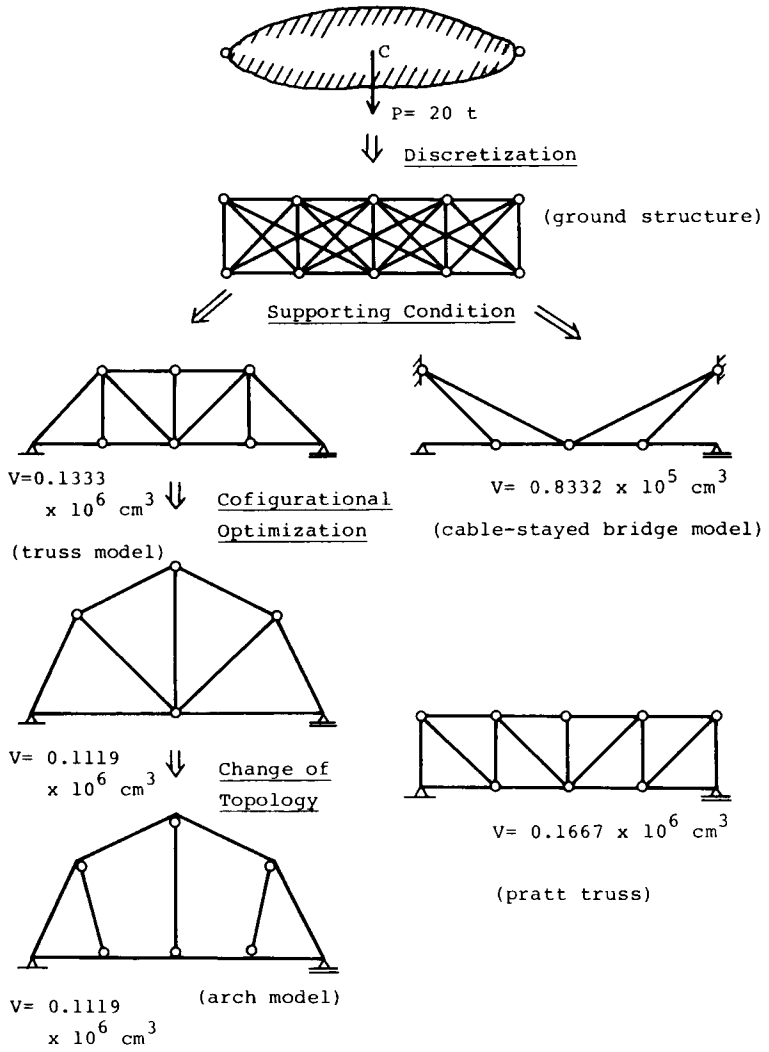

Fig. 3.1 Relations between Trussed, Arched and Cable-Stayed Bridges

porting condition is quite important in the decision of configuration, and that the truss and arch models, which have the same supports, show no distinctive difference.

In this chapter, configurational optimization of trussed and arched bridges are treated on the assumption that the supporting condition and topology of the member system are given as fixed. Then, the design problem to be considered reduces to a decision problem of optimal geometry.

To determine the effective geometry, two kinds of parameters, cross sectional areas and nodal coordinates, need to be taken into account in the optimization procedure. The treatment of nodal coordinates apparently results in the increase of the number of design variables, which often induces some difficulties in the application of mathematical programming. Large scale optimization problems gererally have a poor convergency to require excessive computation time or memory capacity. For such problems, U. Kirsch[2] proposed a decomposition approach and showed its efficiency by some design examples.

Here, a search for least-weight geometry is carried out by a two-step treatment based on Kirsch's approach. The cross sectional areas and the nodal coordinates are treated in two separate but dependent design spaces. Based on the optimality criterion and the sub-optimization of members, the cross sectional areas can be expressed as functions of the nodal coordinates. Also, this treatment can include the effects of buckling constraints or deflection constraints and the grade of materials. While attention is particularly placed on the design of trussed bridges, a brief comparison of trussed and arched bridges is done with emphasis on their geometrical configurations, and also the relation between span length and weight is investigated.

3.2 Partitioning of Design Variables[2]

Formally, it is easy to include a change of geometry into a design formulation. This can be done by introducing the nodal coordinates into the set of design variables. Then, the design variables consist of cross

sectional areas and nodal coordinates, which have different characteristics and different orders of magnitude. In a practical use of mathematical programming, the increase of design variables induced by the addition of nodal coordinates and the mixing of variables having different dimensions will cause such difficulties as a poor convergency and an excessive computation load. Using the modified sequential linear programming method, a considerable reduction of computation time and memory capacity is achieved. Although this method is applicable to any kind of non-linear optimization problem, more improvements on computation and convergence are necessary to treat the configurational optimization problems which have a large number of design variables and constraints.

G. Vanderplaats and F. Moses[3] attempted to treat this problem in two separate but dependent design spaces, one for the cross sectional areas of members and one for the nodal coordinates. They obtained good results for a considerably large transmission tower example. In this chapter, a similar treatment is employed to remove the difficulties in conjunction with computation. Cross sectional areas are considered to be completely dependent on nodal coordinates. It is not so difficult to find the optimum set of cross sectional areas if the configuration is fixed. Furthermore, for a special case, it is possible to find an effective relation or an optimality criterion. Here, the search for effective configuration is carried out, using the optimality criterion and mathematical programming. Although this method has no guarantee that a global optimum solution can be obtained, it is advantageous from an engineering point of view.

At first, a two-level formulation is shown based on Kirsch's approach in order to explain how to deal with the design variables in the optimization procedure.

General optimum design problems can be mathematically written as follows :

Find W

such that the objective function

$$Z = f(W) \rightarrow \textit{Minimize} \tag{3.1}$$

subject to

$$I\ (\ W\ )\ =\ 0 \tag{3.2}$$

$$g\ (\ W\ )\ \leq\ 0 \tag{3.3}$$

$$W^L \leq W \leq W^U \tag{3.4}$$

in which W^L and W^U are the lower and upper bounds for design variables W, and Eqs (3.2) and (3.3) are the equality and inequality conditions, respectively. In truss problems, Eq.(3.2) represents the relation between the variables. For instance, they are derived from the symmetry condition and the fabrication requirements. Eq.(3.3) represents the design requirements with respect to safety or performance.

Here, the design variables W consist of cross sectional areas, A, and nodal coordinates, X.

$$W\ =\ \begin{bmatrix} A \\ X \end{bmatrix} \tag{3.5}$$

Then, the problem expressed by Eqs (3.1) - (3.4) is treated as a two-level problem.

At the first level, the nodal coordinates represented by X are considered to be fixed and not to be variables. The initial values are given with a range where all the imposed constraints are satisfied.

$$X = X_0 \tag{3.6}$$

X_0 is the initial value selected for nodal coordinates. Using X_0, we find A such that

$$I\ (\ A\ ,\ X_0\ )\ =\ 0 \tag{3.7}$$

$$g\ (\ A\ ,\ X_0\ )\ \leq\ 0 \tag{3.8}$$

$$A^L \leq A \leq A^U \tag{3.9}$$

$$\textit{Minimize}\quad Z = f\ (\ A\ ,\ X_0\ ) \tag{3.10}$$

The next step is to solve the second level problem.

$$X^L \leq X \leq X^U \tag{3.11}$$

$$\textit{Minimize} \quad Z = f\ (\ A_0\ ,\ X\ ) \tag{3.12}$$

where A_0 represents the cross sectional areas calculated in the previous step (as the first level) and, in turn, X is treated as a variable. The alternate steps are repeated until a sufficient design is achieved. The method mentioned above is called the modal coordination method. Although this method has also no security that the optimum solution can be obtained, it is advantageous from a point of practical computation, since the iteration can always be terminated with a feasible solution. It should be, of course, noted that some treatments are necessary for programming in order to improve the convergency.

3.3 Approximate Design Method Based on Optimality Criterion[4)]

Here, in order to make the calculation easier, further simplifications are introduced into the decision process of cross sectional areas. Namely, it is assumed that the cross sectional areas completely depends on the nodal coordinates and can be expressed as functions of them by using the optimality criterion derived from the inherent characteristics of framed structures.

It is said that in the majority of minimum-weight designs of test problems, a fully stressed design is an optimal one, or that the resulting design has a weight close to that of the true solution.[5)] By using this condition (fully stressed) as an optimality criterion, the cross sectional areas A can be expressed as a function of the nodal coordinates X.

$$A = A^*\ (\ X\ ) \tag{3.13}$$

In general, the design problem including a geometrical variation is formulated as follows.

Find A_i , X_j $\quad \begin{cases} i = 1, \cdots\cdots, m \\ j = 1, \cdots\cdots, n \end{cases}$

such that

$$Z = \rho \sum_{i=1}^{m} A_i \, L_i(X_j) \rightarrow \textit{Minimize} \qquad (3.14)$$

subject to

$$- \sigma_{aci} \leq \sigma_i \leq \sigma_{ai} \qquad (3.15)$$

where σ_i and σ_{aci} denote the induced stress and the allowable compressive stress of the i-th member, respectively.

Using Eq.(3.13), the above design problem is reduced to an unconstrained optimization problem.

Find X_j

such that

$$Z = \rho \sum_{i=1}^{m} A_i^*(X_j) \, L_i(X_j) \rightarrow \textit{Minimize} \qquad (3.16)$$

Then, it is obvious that the search for unconstrained problems is much easier than that for constrained ones. In the case, the improving direction can be easily obtained by using the derivatives of Eq.(3.16).

$$\frac{\partial Z}{\partial X_j} = \rho \sum_{i=1}^{m} \left\{ \frac{\partial A^*(X_j)}{\partial X_j} \, L_i(X_j) + A^*(X_j) \, \frac{\partial L_i(X_j)}{\partial X_j} \right\} \qquad (3.17)$$

It is noted that the design variables treated in Eq.(3.16) are reduced to only the nodal coordinates and the reduction of design variables remarkably contributes to mitigate the computation time and memory capacity.

Treatment of Multiple Loading Condition[6)-10)]

Fully stressed condition is also applied for the multiple loading condition. Namely, the cross sectional area A is determined by the ab-

solutely maximum value of the member forces F^n, which are induced by n-cases external load P^n.

$$F^n = \underline{K}^{-1} P^n \tag{3.18}$$

$$\tilde{F}^n = \max_n \{F^n\} \tag{3.19}$$

where $\underline{K}$ is the stiffness matrix.
For truss problems, the cross sectional area is calculted as

$$A = \tilde{F}^n / \sigma_a \tag{3.20}$$

Treatment of Indeterminate Systems[11]

In indeterminate structures, the member forces are determined not only by the external load and the structural configuration, but also by the cross sectional areas of individual members. In other words, the induced force of each member affects the decision of the cross sectional areas of other members. Since it is impossible to express the member force by only the nodal coordinates, an approximate treatment is neccessary for dealing with indeterminate systems. Here, an iterative procedure[7] is utilized so as to calculate the cross sectional areas. (see Fig. 3.2)

At first, assume the initial values for cross sectional areas, remaining the configuration fixed. By use of the structural analysis, calculate the member forces, from which new cross sectional areas are determined. Terminate the iterative procedure when the cross sectional areas converge to certain values. Otherwise, repeat the above steps.

3.4 Sub-Optimization of Members[4]

In a case where the stress limitation is solely employed as constraints and the allowable stress is constant, the optimal set of cross sectional areas can be determined by using the member force F.

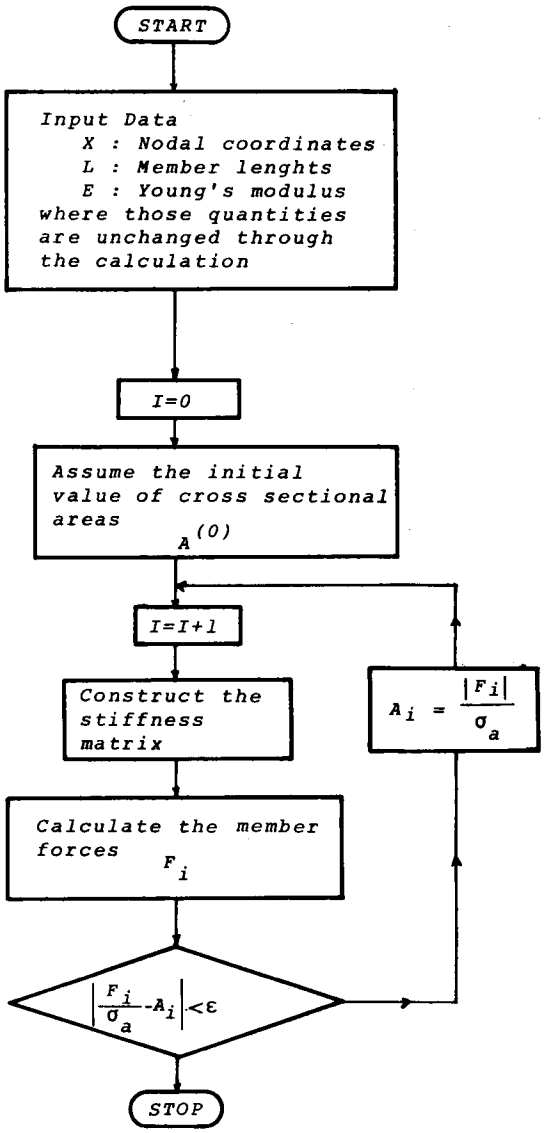

Fig. 3.2 Flow Chart for Determination of Cross Sectional Area

$$A_i = \sigma_a^{-1} F_i(X) \tag{3.21}$$

Then, the design formulation (Eq.(3.16)) is found as

Find X_j

such that

$$Z = \frac{\rho}{\sigma_a} \sum_{i=1}^{m} F_i(X_j)\ L_i(X_j) \rightarrow \textit{Minimize} \tag{3.22}$$

In a case with buckling constraints, the allowable stress σ_a is a function of X.

$$A = \sigma_a^{-1}(X)\ F(X) \tag{3.23}$$

In checking the safety against a buckling failure, the slenderness ratio is very important factor. It is said that the allowable strength for each compressive member should be determined according to its slenderness ratio. Then, the cross sectional areas can no longer be expressed as explicit functions of the nodal coordinates. However, using an approximate formula such as Eq.(2.13), the cross sectional area of the i-th member, A_i, can be obtained for pipe section

$$A_i = K_i \sqrt{F_i(X)}\ \ L_i(X) \tag{3.24}$$

in which K_i is a constant and $K_i\{\ F_i(X)\ \}^{-1/2} L_i(X)$ corresponds to $\sigma_a^{-1}(X)$ in Eq.(3.23). Using Eq.(3.24), the objective function Z is expressed as

$$Z = \rho \left\{ \sum_{i=1}^{m'} \sigma_{ai}^{-1} F_i(X)\ L_i(X) + \sum_{i=m'+1}^{m} K_i \sqrt{F_i(X)}\ \ L_i(X) \right\} \tag{3.25}$$

where m' is the number of tensile members.

For generality, buckling effects are treated herein by means of a preoperational technique called " sub-optimization ".[12] This technique has been developed to obtain a simple formula which relates the cross

sectional areas to the nodal coordinates, for general sections such as rectangular or square box sections. There are some studies[13)14)] with application to a truss design in which the configuration is fixed. When the length and the induced force of a member are given, the optimal cross sectional areas can be calculated with the aid of the optimality criterion " fully stressed ".

The moment inertia I and the cross sectional area A of the pipe section with the thickness t are calculated as

$$I = \frac{\pi D^4}{64} - \frac{\pi (D-2t)^4}{64} \tag{3.26}$$

$$A = \frac{\pi D^2}{4} - \frac{\pi (D-2t)^2}{4} \tag{3.27}$$

where D is the diameter of the pipe section.
Then, the slenderness ratio R is

$$R = \frac{r}{L} = \frac{4\,L\,t}{\sqrt{2}\,\sqrt{(A/t)^2 + t^4}} \tag{3.28}$$

in which L and r denote the length of member and the radius of gyration, respectively.

According to the formula which the Japan Road Association recommends, the allowable compressive strength σ_{ac} is found as

$$\sigma_{ac} = j_1\{ k_1 - j_2 k_4 (\frac{L}{r} - k_2)\} + (1-j_1) \frac{1.2 \times 10^7}{k_5 + (L/r)^2} \quad (kg/cm^2) \tag{3.29}$$

where

$$\left.\begin{aligned} k_2 > L/r \quad &; \quad j_1 = 1 \,,\; j_2 = 0 \\ k_2 \leq L/r \leq k_3 \quad &; \quad j_1 = 1 \,,\; j_2 = 1 \\ k_3 \leq L/r \quad &; \quad j_1 = 0 \,,\; j_2 = 1 \end{aligned}\right\} \tag{3.30}$$

The parameters k_1 - k_5 are constants dependent on the kinds of steel.

(see Table 3.1) Using Eq.(3.28), Eq.(3.30) is rewritten as

$$\left.\begin{array}{ll} R < k_2 \ ; & \pi\sqrt{8(L/k_2)^2 - 1} \leq A \\ k_2 \leq R < k_3 \ ; & \pi\sqrt{8(L/k_3)^2 - 1} < A < \pi\sqrt{8(L/k_2)^2 - 1} \\ k_3 \leq R \ ; & A \leq \pi\sqrt{8(L/k_3)^2 - 1} \end{array}\right\} \quad (3.31)$$

Observing the results of sub-optimization for *SS41* steel , the following formula can be obrained for a given length.

$$\left.\begin{array}{ll} A(x) = a\sqrt{F(X)} + b & 93 \leq R \\ A(X) = F(X)/1568 + c & 20 \leq R < 93 \\ A(X) = F(X)/1400 & R < 20 \end{array}\right\} \quad (3.32)$$

(cm^2)

where a, b and c are constants to be obtained by the curve in Fig. 3.3. (see Table 3.2)
Using Eq.(3.32), the cross sectional areas can be immediately calculated when the member force is given.

For box sections, the following relations were presented by S. Okubo[13].

$$\left.\begin{array}{ll} A_i(X) = \dfrac{1}{\alpha_i}\left(F_i(X) - \gamma_i \right)^{n_i} + \beta_i & F_i(X) \leq F_{0i} \\ A_i(X) = \dfrac{1}{\delta_i}\left(F_i(X) - \varepsilon_i \right) & F_{0i} < F_i(X) \end{array}\right\} \quad (3.33)$$

where α_i, β_i, γ_i, δ_i and n_i are constants to be determined from the *A-F* curve and F_{0i} indicates the branching point of the *A-F* curve.

On the other hand, the automatic selection of materials can be made by use of the sub-optimization technique without any integer programming. Namely, one can choose the effective material by comparing the *A-F* curves obtained for individual materials. The resulting *A-F* curve obtained for *SS41* and *SM50* steels is shown in Fig. 3.4 as a representative case. It can be seen in this figure taht when the member force is more than *78 ton*, *SM50* steel is superior to *SS41* steel for the compressive member with *4*

Table 3.1 Values of k_1 - k_5

	SS41,SM41 SMA41	SS50	SM50	SM53 SM50Y	SM58 SMA50
k_1	1400	1700	1900	2100	2600
k_2	20	17	15	14	14
k_3	93	86	80	76	67
k_4	8.4	11.3	13	15	21
k_5	6700	5700	5000	4500	3600

Table 3.2 Sub-Optimization for SS41 Steel

A / L	$A = a\sqrt{F} + b$ (93<R)		F	$A=\frac{F}{1568}+c$	F	$A=\frac{F}{1400}$
	a	b	(R=93)		(R=20)	(R<20)
100	0.110	-0.104	6778.46	4.7	62048.0	
200	0.149	1.010	14660.80	9.5	124320.0	
300	0.181	1.932	22406.72	14.2	186550.0	
400	0.208	2.786	29933.12	19.0	248766.0	
500	0.232	3.606	37428.16	23.8	310968.0	
600	0.254	4.407	45064.32	28.5	373170.0	
700	0.274	5.197	52543.68	33.3	435386.0	
800	0.293	5.980	60164.16	38.0	497588.0	
900	0.311	6.757	67627.84	42.8	559790.0	
1000	0.328	7.531	75107.20	47.6	621964.0	
1100	0.344	8.302	82712.00	52.3	684194.0	
1200	0.363	8.804	90175.68	57.1	746396.0	
1300	0.382	9.197	97796.16	61.8	808598.0	
1400	0.403	9.525	105259.04	66.6	870800.0	
1500	0.423	9.801	112707.84	71.4	933002.0	
1600	0.445	10.035	120328.32	76.1	995190.0	
1700	0.466	10.236	127792.00	80.9	1057392.0	
1800	0.488	10.407	135396.80	85.6	1119594.0	
1900	0.510	10.556	142860.48	90.4	1181796.0	
2000	0.532	10.686	150324.16	95.2	1243889.0	

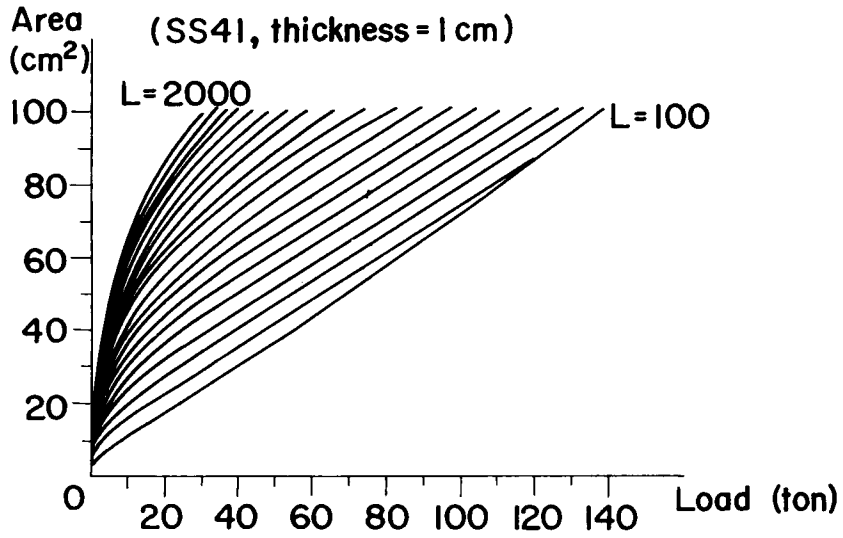

Fig. 3.3 Sub-Optimization for SS41 Steel

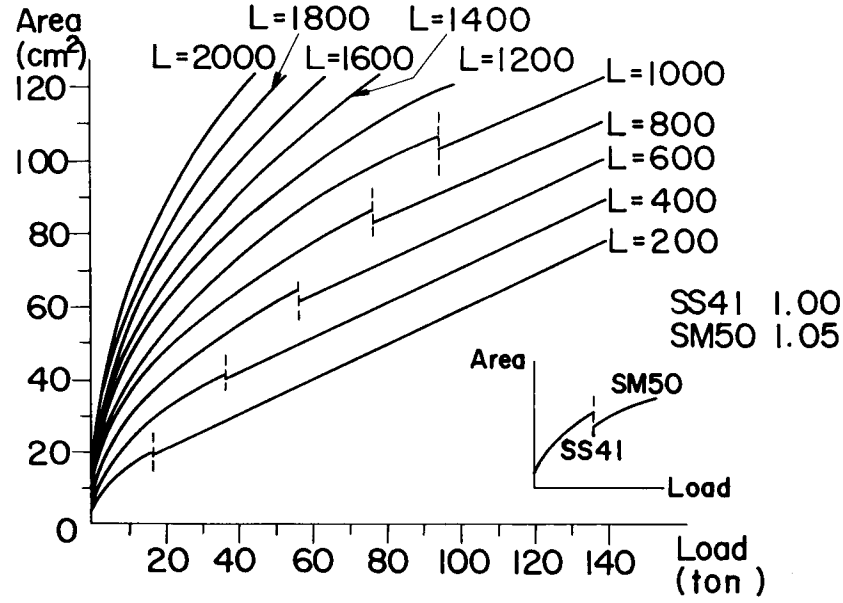

Fig. 3.4 Sub-Optimization of Axial Members

meters length. Note that this figure is made by comparing the material costs, whose rate is assumed to be *1 (SS41) : 1.05 (SM50)*.

3.5 Applications of Approximate Method to Truss Design

Here, the truss design including a geometrical variation is performed on the basis of the design procedure obtained in the previous chapter. Corresponding to the design hierarchy presented by A. B. Templeman[15], the design procedure is summarized as follows :

Hierarchy 1 Topology --- Assume the number of nodes and the layout of members under the prescribed supporting condition.

Hierarchy 2 Geometry --- The change of geometry is taken into account by introducing the nodal coordinates into the set of design variables.

Hierarchy 3 Overall Design --- The proportion of members is determined by dealing with the cross sectional areas as variables.

Hierarchy 4 Detail Design --- The details are determined by the sub-optimization of members.

Then, the optimal positions of nodes are calculated according to the following steps.

Step 1 Assume the initial geometry, (i.e. nodal coordinates $X^{(0)}$)

Step 2 Perform the structural analysis of the truss with the geometry determined in the previous step.

Step 3 Obtain the optimum set of cross sectional areas by using the values of member forces and member lengths calculated in Step 2.

Step 4 Search for the most effective direction S in the design space which consists of nodal coordinates, and calculate the distance α with the aid of a one-dimensional optimization scheme.

Step 5 Then, the improved geometry can be defined as

$$X^{(I)} = X^{(I-1)} - \alpha \cdot S$$

Step 6 If the value of $X^{(I)}$ converges, the procedure is terminated. Otherwise, return to Step 2 and repeat Steps 3 - 5.

The above process is expressed as a macro flow chart. (see Fig. 3.5)

In order to treat some kinds of material, the material cost should be employed as the objective function. Then, the problem is expressed as

$$\textit{Minimize} \qquad P = \sum_{i=1}^{m} \min_{k} \{ C_k A_k(F_i) \}_i L_i \qquad (3.34)$$

where P and C_k represent the total cost and the coefficient of the k-th material, respectively.

The term of $\min_{k} \{ C_k \cdot A_k(F_i) \}$ means the minimum of the product of cross sectional area and unit cost. Replacing this term by a_i, Eq.(3.34) is written as

Find X_j

such that

$$P = \sum_{i=1}^{m} a_i (F_i(X_j) , L_i(X_j)) L_i(X_j) \rightarrow \textit{Minimize} \qquad (3.35)$$

The derivatives necessary for calculating the improving direction are derived as

$$\frac{\partial P}{\partial X_j} = \frac{\partial a_i}{\partial X_j} L_i + a_i \frac{\partial L_i}{\partial X_j} = \frac{\partial a_i}{\partial F_i} \frac{\partial F_i}{\partial X_j} L_i + \frac{\partial a_i}{\partial L_i} \frac{\partial L_i}{\partial X_j} L_i + a_i \frac{\partial L_i}{\partial X_j} \qquad (3.36)$$

Thus, a truss design can be carried out without difficulty, using the relations between the member forces and the cross sectional areas. (i.e. Eq.(3.23) for a case without buckling constraints, Eq.(3.24) for a case with buckling constraints, Eqs (3.32) and (3.33) for general cases)

Next, the introduction of deflection constraint is attempted on the basis of the optimality criterion presented by A. Gellatly and L. Berke[16]. Using the generalized-virtual-load method, the deflection is give as

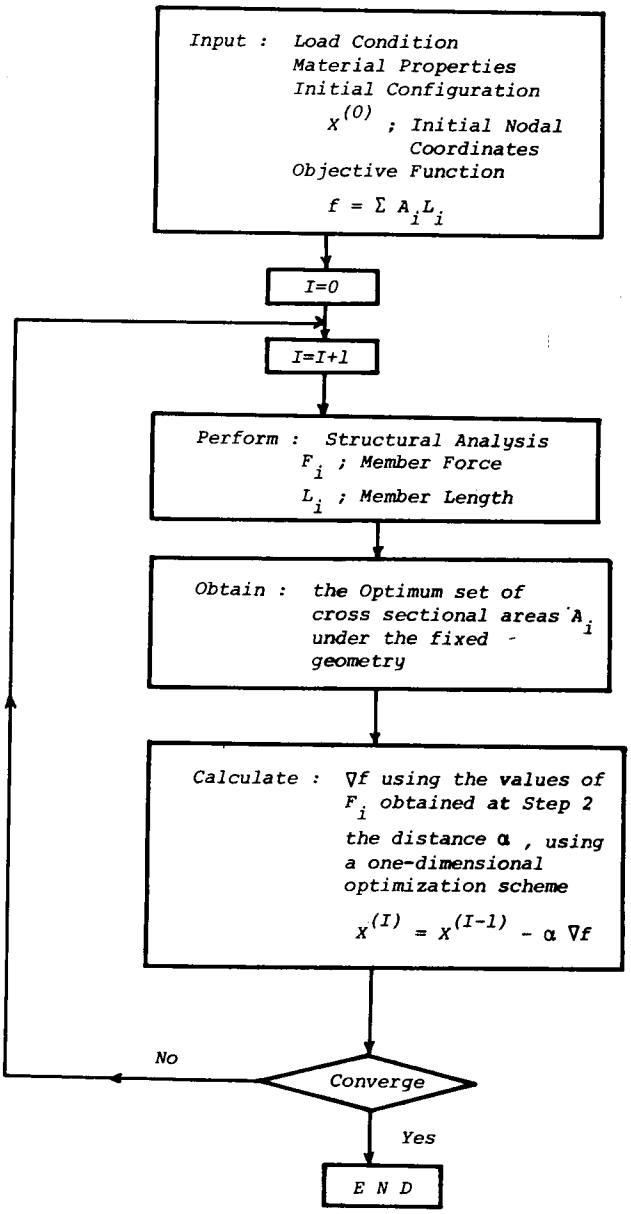

Fig. 3.5 Macro Flow Chart of Approximate Design Method

$$\delta = \sum_{i=1}^{m} \frac{F_i F_i^Q L_i}{A_i E} \tag{3.37}$$

in which F_i^Q is the force due to the virtual load Q.
The optimum structure for which the deflection has the specified value δ^* can be determined by finding the stationary value of the objective function subjected to the equality condition.

$$\delta = \delta^* \tag{3.38}$$

Using Eqs (3.37) and (3.38), the weight-minimization problem can be expressed in the following form by means of Lagrange's multiplier method.

$$\Phi = \sum_{i=1}^{m} \rho_i A_i L_i + \lambda \left(\sum_{i=1}^{m} \frac{F_i F_i^Q L_i}{A_i E} - \delta^* \right) \tag{3.39}$$

where Φ and λ are Lagrangean and Lagrange's multiplier, respectively.
For a minimum

$$\frac{\partial \Phi}{\partial A_j} = 0 = L_j \rho_j - \lambda \frac{F_j F_j^Q L_j}{A_j^2 E} + \lambda \sum_{k=1}^{m} \left(\frac{\partial F_k}{\partial A_j} F_k^Q + \frac{\partial F_k}{\partial A_j} F_k^Q \right) \frac{L_k}{A_k E} \tag{3.40}$$

$$\frac{\partial \Phi}{\partial \lambda} = \delta - \delta^* \tag{3.41}$$

Since the terms in the summation are identically zero, Eq.(3.40) becomes

$$0 = L_j \rho_j - \frac{F_j F_j^Q L_j}{A_j^2 E} \lambda \tag{3.42}$$

From Eq.(3.42), the cross sectional area is found as

$$A_j = \sqrt{\lambda} \sqrt{(F_j F_j^Q)/(E \rho_j)} \tag{3.43}$$

Finally, the cross sectional area can be expressed as a function of the

member forces F_j and F_j^Q, combining Eq.(3.41) and Eq.(3.43).

For convenience to a practical computation, the cross sectional area is expressed as a form in which structural members are divided into two groups ; active and passive members. A. Gellatly and L. Berke specify that the active members are those whose cross sectional area may be varied to achieve an optimized deflection-limited design, whereas the passive members remain unchanged. With this division, the cross sectional area can be written as

$$A_i = A_i^*(X_j) = \frac{1}{\delta^* - \delta_0} \sum_{k=1}^{\tilde{m}} L_k(X_j) \sqrt{F_k(X_j)F_k^Q(X_j)/E_k} \sqrt{F_i(X_j)F_i^Q(X_j)/E_i} \tag{3.44}$$

where $\tilde{m}$ is the number of active members and δ_0 is the contribution of passive members to the deflection.
Furthermore, Eq.(3.44) can be rewritten as a recursive form suitable for the design of indeterminate systems.

$$A_i^{(I+1)} = A_i^{(I)} \sqrt{\left(\frac{\sigma_i \sigma_i^Q}{E_i \rho_i}\right)^{(I)}} \frac{1}{\delta^* - \delta_0} \sum_{k=1}^{\tilde{m}} (A_k L_k \rho)^{(I)} \sqrt{\frac{\sigma_k \sigma_k^Q}{E_k \rho}} \tag{3.45}$$

where $\sigma_i = F_i/A_i$ and $\sigma_i^Q = F_i^Q/A_i$.
Substituting Eq.(3.44) to Eq.(3.35), the deflection constraint can be taken into account in the design of truss.

3.6 Applications of Approximate Method to Arch Design

Truss resists the external load by axial forces, whereas arch resists not only axial forces but also bending moments. This structural property of arches gives a further freedom to select the structural configuration[17]. Trussed structures have a limitation in the determination of configuration due to the stability condition. For instance, their configurations are composed of triangles. On the other hand, for arched

structures, other fundamental patterns such as square or trapezoid are allowed to choose for constituting the configuration without loss of overall stability. This means that arched structures have more freedom in the topology, and the increase of freedom may enable to achieve more weight reduction.

As well as truss designs, the design of arched bridges is formulated by use of the optimality criterion, " fully stressed ".

$$W \text{ (weight)} = \rho \sum_{i=1}^{m} A_i L_i \rightarrow \text{Minimize} \qquad (3.46)$$

In this case, it is quite difficult to find an explicit relation between the member force and the cross sectional area.

For arch members except for hanger members, the fully stressed condition is expressed by neglecting the effect of shearing force as follows.

$$\sigma_i = \frac{|N_i|}{A_i} + \frac{|M_i|}{Z_i} = \sigma_a \qquad (3.47)$$

in which N_i, M_i and Z_i signify the induced axial force, the induced bending moment and the section modulus, respectively.

It is assumed that the section modulus can be approximately expressed as a function of the cross sectional area[18].

$$Z_i = \beta A_i^{3/2} \qquad (3.48)$$

where β is a constant which depends on the shape of cross section. Then, the fiber stress σ_i is written as

$$\sigma_i = \frac{|N_i|}{A_i} + \frac{|M_i|}{\beta A_i^{3/2}} \qquad (3.49)$$

Using Eqs (3.47) and (3.49), the following relation can be obtained.

$$\sigma_a^2 A_i^3 - 2 \sigma_a |N_i| A_i^2 + |N_i| A_i - |M_i|^2 / \beta^2 = 0 \qquad (3.50)$$

Solving Eq.(3.50) analytically, the relation between the member force and the cross sectional area can be obtained. However, it is convenient to solve it numerically in the optimization procedure, where the derivatives of the objective function are given as[19)]

$$\frac{\partial W}{\partial X_j} = \rho \sum_{i=1}^{m} \{(\partial A_i/\partial X_j)\, L_i + A_i\, (\partial L_i/\partial X_j)\} \qquad (3.51)$$

in which

$$\frac{\partial A_i}{\partial X_j} = \frac{(2\sigma_a A_i^2 - 2|N_i|A_i)(\partial|N_i|/\partial X_j) + 2(|M_i|/\beta^2)(\partial|M_i|/\partial X_j)}{(3\sigma_a A_i - |N_i|)(\sigma_a A_i - |N_i|)} \qquad (3.52)$$

3.7 Design Examples

1) Nein-Bar Truss Model

This example is employed to investigate the relation between nodal coordinates and volume. The optimal geometry is shown in Fig. 3.6, with the loading condition and the selected design variables being $X_1 - X_3$. This truss is simply supported and its span length is *40 m*. Since this truss is statically determinate and subject to a single loading condition, the resulting design is fully stressed. In this case the member forces, $F_1 - F_9$, can be expressed by nodal coordinates.

$$\begin{aligned}
F_1 &= -10 \,/\, \sin\alpha \\
F_2 &= \frac{1}{\sin\gamma}\left\{\frac{\sin\beta\,(-10/\tan\alpha + 10/\tan\gamma)}{\sin\beta\,/\tan\gamma + \cos\beta} - 10\right\} \\
F_3 &= -\frac{-10/\tan\alpha + 10/\tan\gamma}{\sin\beta/\tan\gamma + \cos\beta} \\
F_4 &= 10/\tan\alpha \\
F_5 &= -2\left\{\frac{\sin\beta(-10/\tan\alpha + 10/\tan\gamma)}{\sin\beta/\tan\gamma + \cos\beta} - 10\right\} \\
F_6 &= F_2\,,\ F_7 = F_3\,,\ F_8 = F_4\,,\ F_9 = F_1
\end{aligned} \qquad (3.53)$$

where the nagative values indicate the compressive forces. Unless the buckling effect is taken into consideration, the necessary cross sectional areas are found to be

$$A_i = F_i / \sigma_a \qquad (3.54)$$

Using Eqs (3.53) and (3.54), the total volume, V, can be obtained as follows.

$$V = \frac{1}{12000}\left(\frac{20(X_1^2+X_2^2)+400X_1}{X_2} + \frac{400(X_3-X_2)}{(20-X_1)} + \frac{400\{(X_3-X_2)^2+(20-X_1)^2\}}{(20-X_1)X_3} \right.$$
$$\left. +20\{X_2^2+(20-X_1)^2\}\frac{|20X_2-X_1X_3|}{X_2X_3(20-X_1)} \right) \quad (m^3) \qquad (3.55)$$

where

$$L_1 = \sqrt{X_1^2+X_2^2} \quad , \quad L_2 = \sqrt{(X_3-X_2)^2+(20-X_1)^2} \quad , \quad L_3 = \sqrt{X_2^2+(20-X_1)^2}$$

$$L_4 = 20 \quad , \quad L_5 = X_3$$

$$\sin\alpha = X_2 / L_1 \ , \quad \cos\alpha = X_1 / L_1 \ , \quad \tan\alpha = X_2 / X_1$$

$$\sin\beta = X_2 / L_3 \ , \quad \cos\beta = (20-X_1) / L_3 \ , \quad \tan\beta = X_2 / (20-X_1)$$

$$\sin\gamma = (X_3-X_2) / L_2 \ , \quad \cos\gamma = (20-X_1) / L_2 \ , \quad \tan\gamma = (X_3-X_2)/(20-X_1)$$

$$\sigma_a = 1200 \ kg/cm^2$$

When the values of X_1 - X_3 are given, the cross sectional areas and the total volume can be calculated from Eq.(3.53) to Eq.(3.55). It is also possible to draw the contour surface of the objective function (i.e. volume). For two cases where the values of volume are specified as 0.115×10^6 cm^3 and 0.120×10^6 cm^3, the contour surfaces are shown in Fig. 3.7. Fig. 3.8 and Fig. 3.9 show the projections on the X_1-X_3 plane and the X_2-X_3 plane, respectively. Fig. 3.7 indicates that in this

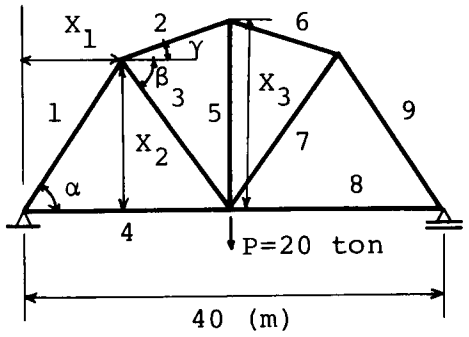

Fig. 3.6 Optimal Configuration of Nein-Bar Truss Model

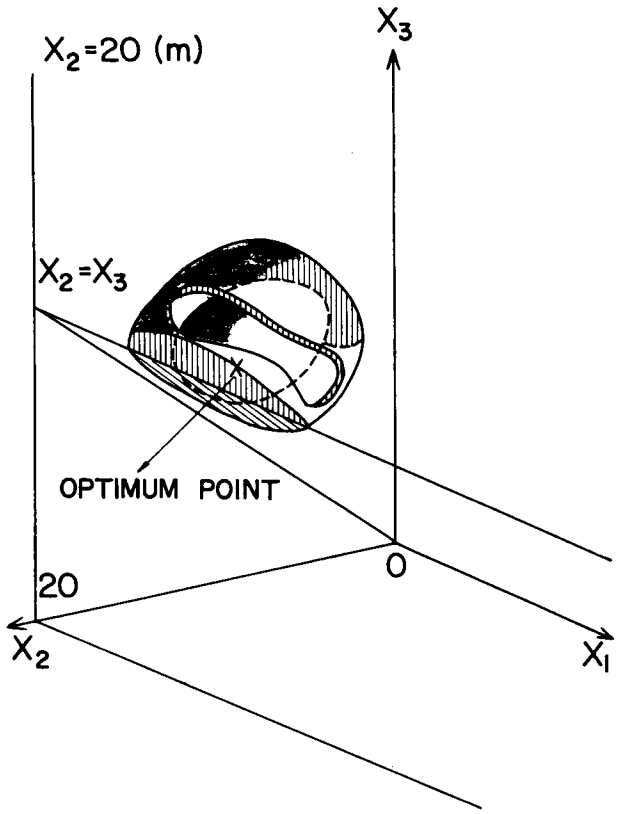

Fig. 3.7 Design Space of Nein-Bar Truss Example

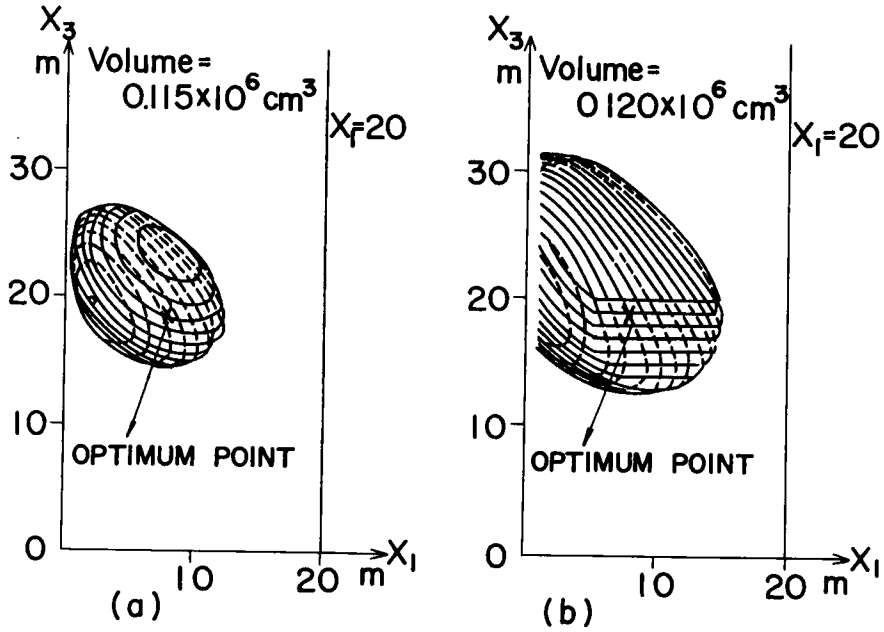

Fig. 3.8 Projection on X_1-X_3 Plane

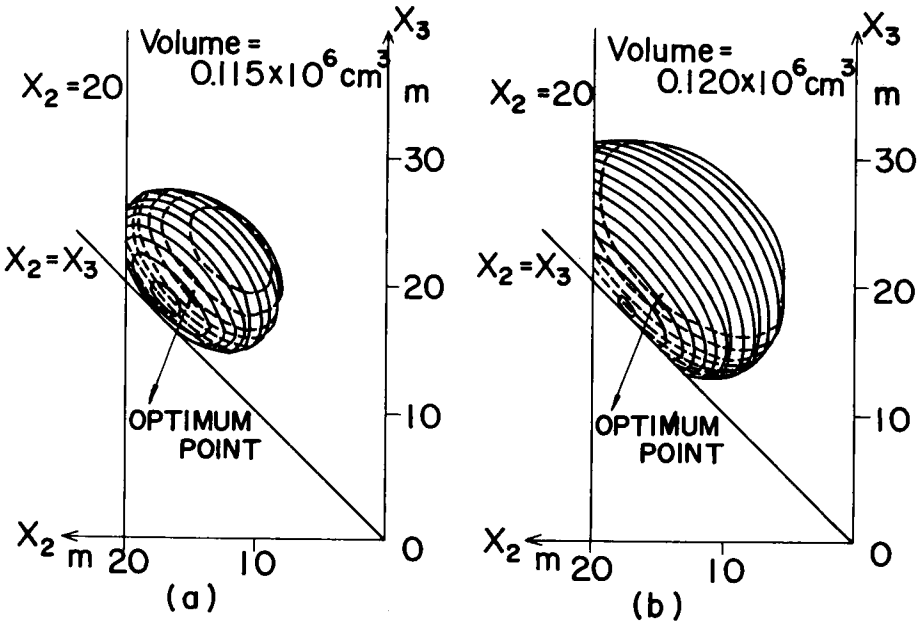

Fig. 3.9 Projection on X_2-X_3 Plane

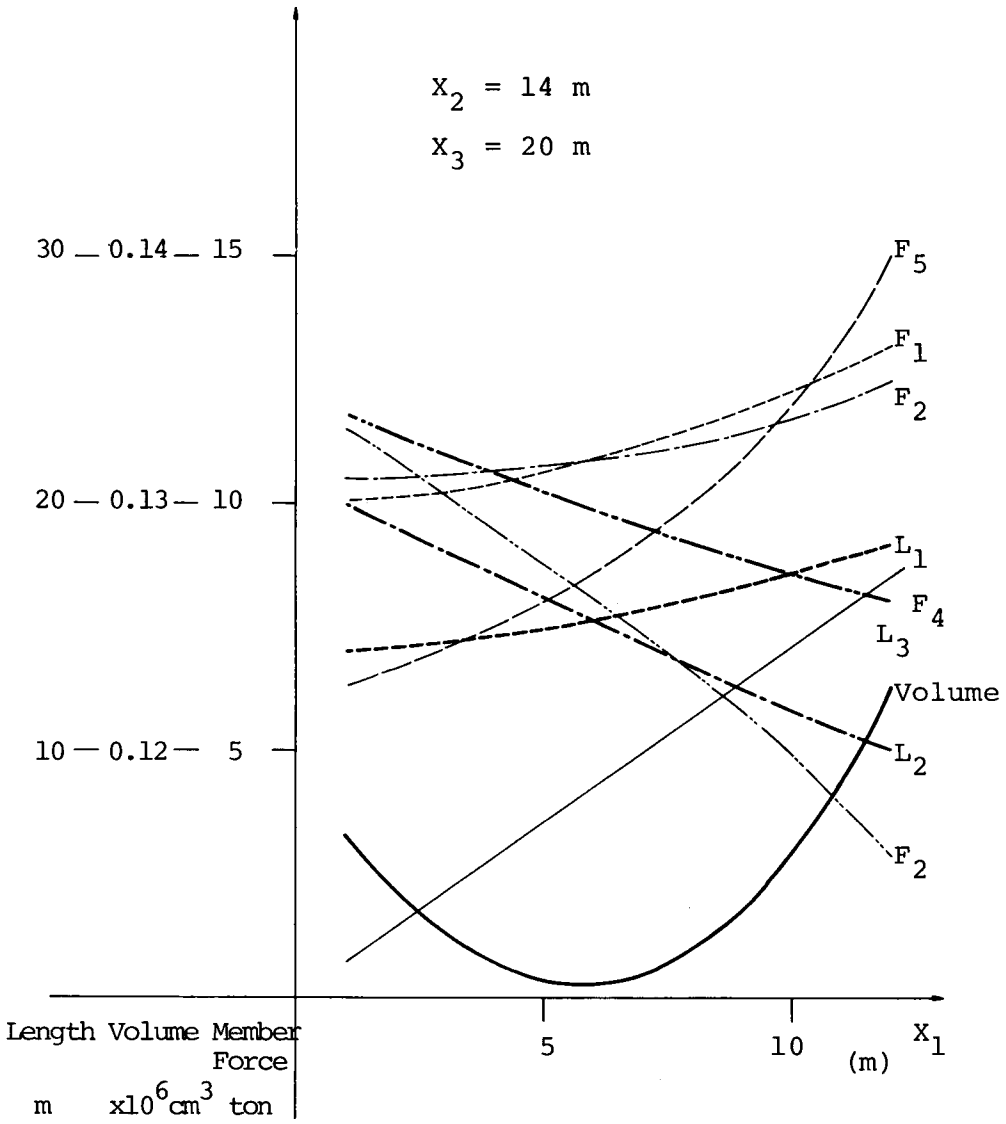

Fig. 3.10 Relation between Total Volume and X_1

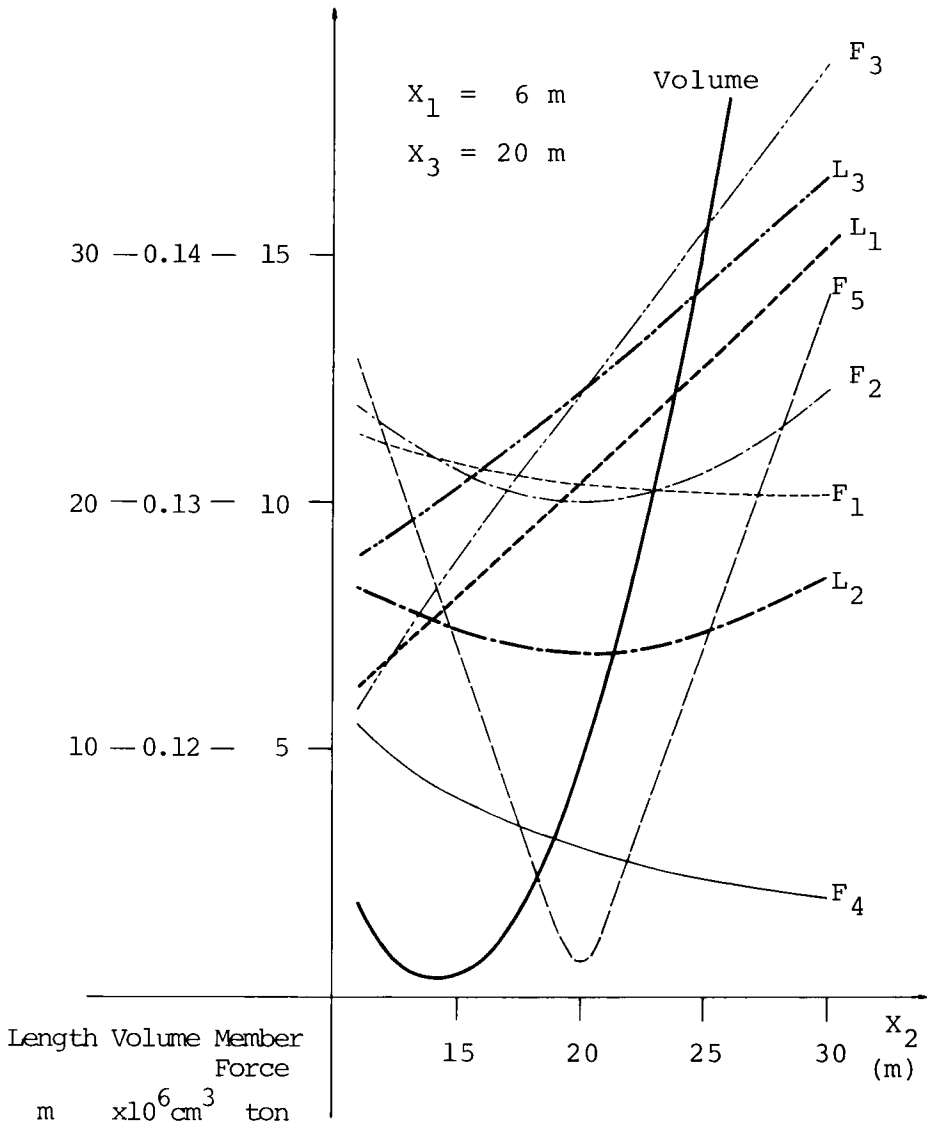

Fig. 3.11 Relation between Total Volume and X_2

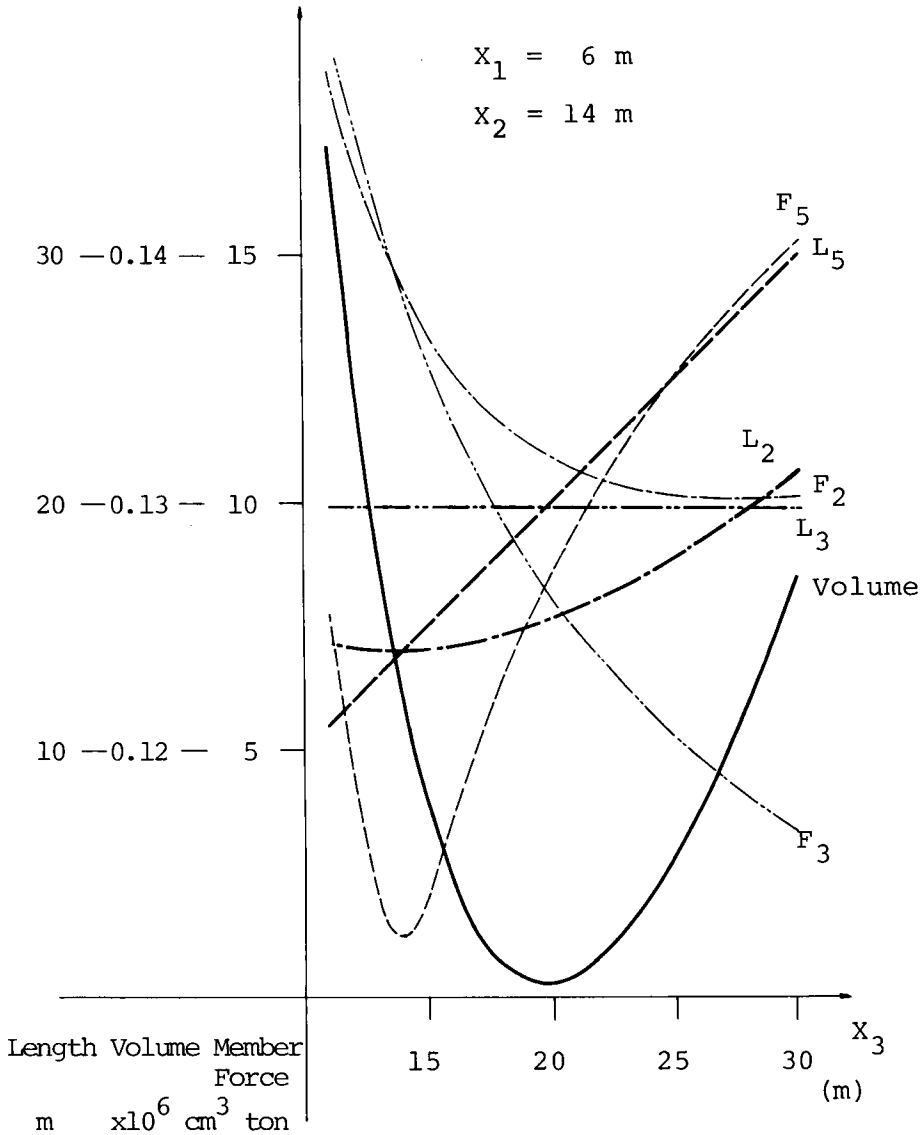

Fig. 3.12 Relation between Total Volume and X_3

model the contour surfaces have round shapes like an egg, though two ends are cut off by two planes. This is due to the side constraints imposed on the design variables X_1 and X_2.

Fig. 3.10 shows the relation between the total volume and X_1 when other variables are fixed as $X_2 = 14\ m$ and $X_3 = 20\ m$. And the relations between the total volume and X_2 or X_3 are shown in Fig. 3.11 and Fig. 3.12, respectively. From these figures, it is obtained that the optimum set of nodal coordinates is roughly estimated as $(X_1,X_2,X_3) = (6,14,20)\ (m)$ and the optimum point is located at a point near the center of the contour surfaces. The above observation leads to the conclusion that the problem treated here provides assurance that the approximate method employed in this chapter will give good results.

2) Influence of Span Length

Using the approximate method, three kinds of trussed bridges, Warren truss with vertical members (Model 1), Warren truss (Model 2) and Pratt truss (Model 3), are designed to investigate the change of the material cost for unit length due to the change of span length. The loading condition and the configuration of employed truss models are illustrated in Fig. 3.13. As shown in Fig. 3.14, the numerical results indicate that the increase of span length gives rise to the increase of the unit material cost on account of the increase of the dead load. A rapid increase can be seen where the span length is more than *140 m*. Model 1 shows the superiority in cost-minimization over all the span lengths, because of the effect of the buckling constraint. Although there is little difference between Model 2 and Model 3, Model 3 becomes superior when the span length exceeds *140 m*.

In all designs, *SS41* steel is chosen for the compressive members, whereas *SM50* steel for the tensile members. The rate of truss height and span length exsists from *1/11.5* to *1/7.5*. These values seem to be somewhat small, comparing the values *1/10 - 1/6* obtained for parallel-chord trussed bridges whose span lengths are less than *100 m*. This difference may be due to the effects of panel numbers, kinds of materials and loading condition employed herein. However, the optimal rate of truss height and span length is unchanged within a range of *0 - 100 m*,

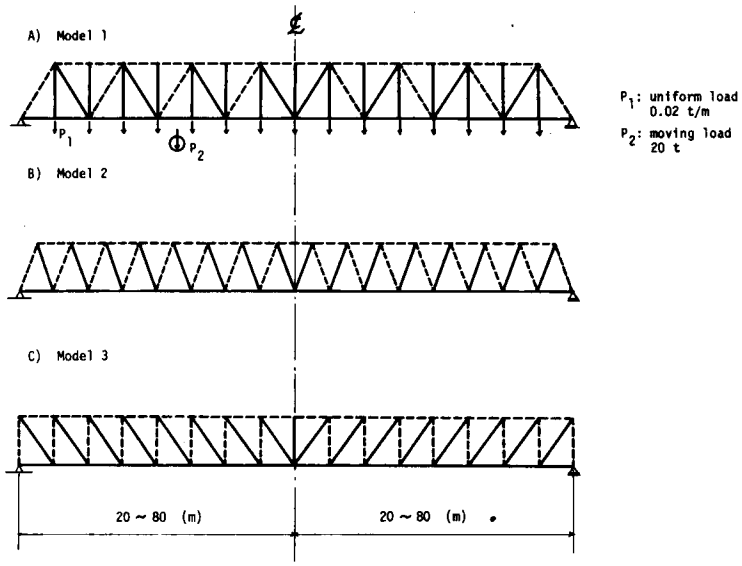

Fig. 3.13 Some Truss Models and Loading Condition

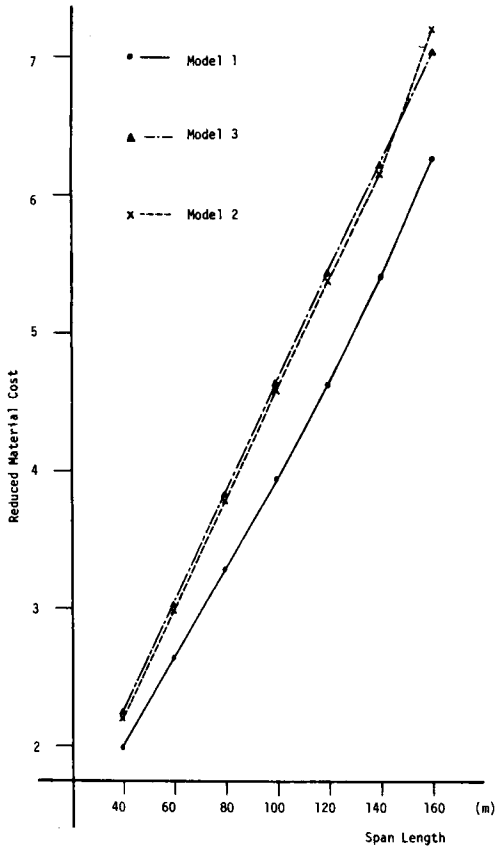

Fig. 3.14 Material Cost vs Span Length

for all trusses. One design case requires *70* seconds in computation for FACOM M-190 computer.

3) Design of Continuous Trussed Bridge (AMAKUSA 1-GO Bridge Model)

The proposed approximate method is applied for the large truss model which has *80* nodes and *157* members. The supporting condition and the loading condition are given in Fig. 3.15. This model has such limitations on configuration that the upper chord members are allocated as horizontally straight, and also the lower chord members give the clearance for the place near the center of the bridge. Considering the symmetrical and supporting conditions, *99* design variables should be taken into account in the optimization. However, the proposed method can reduce the number of design variables from *99* to *20*, eliminating the cross sectional areas from the set of design variables. In Fig. 3.16, the configuration obtained at the 4th step is shown. It is seen that the configuration tends to transfer from Pratt type to Warren type, according to the change of node positions with respect to the lower chords. Since this result is obtained under optimization and is not a final solution, the configuration shows an uneven curve for the formation of lower chord members.

At the 4th step, the material cost diminishes by 2 per cent from the initial step. It is also possible to reduce the material cost more than 8 per cent by decreasing the truss height. Finally, the configuration shown in Fig. 3.17 enables to achieve more than 16 per cent reduction. In this example, the optimization is performed by use of the conjugate gradient method. The computation time for a step is about 5 minutes, which are mainly consumed in the iterative procedure used for the structural analysis.

4) Effect of Deflection Constraint[20)]

The efficiency of the optimality criterion algorithm is first examined by a truss example shown in Fig. 3.18, whose geometry is fixed. The optimality criterion algorithm reaches the optimum solution with only one iteration, whereas SLP requires 29 iterations, starting from the same initial values. The convergency of both methods is presented in

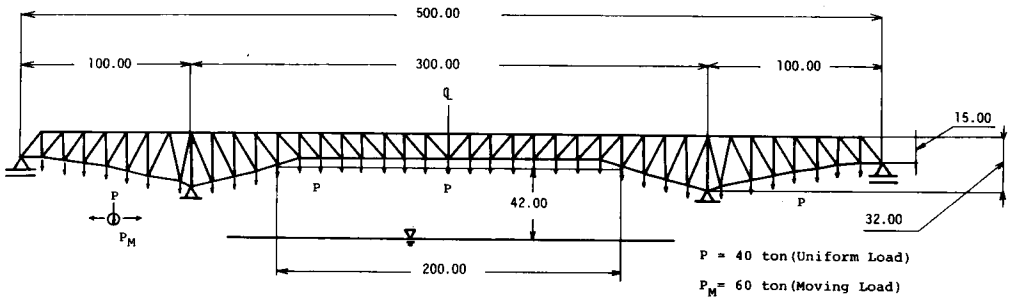

Fig. 3.15 Amakusa 1-Go Bridge Model

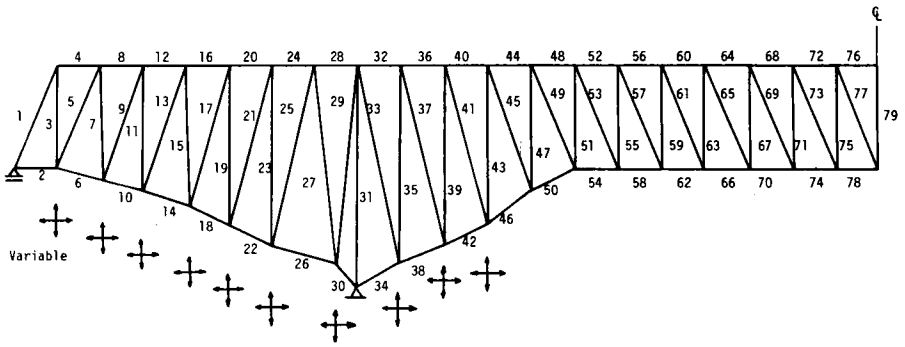

Fig. 3.16 Configuration Obtained at the 4th Step

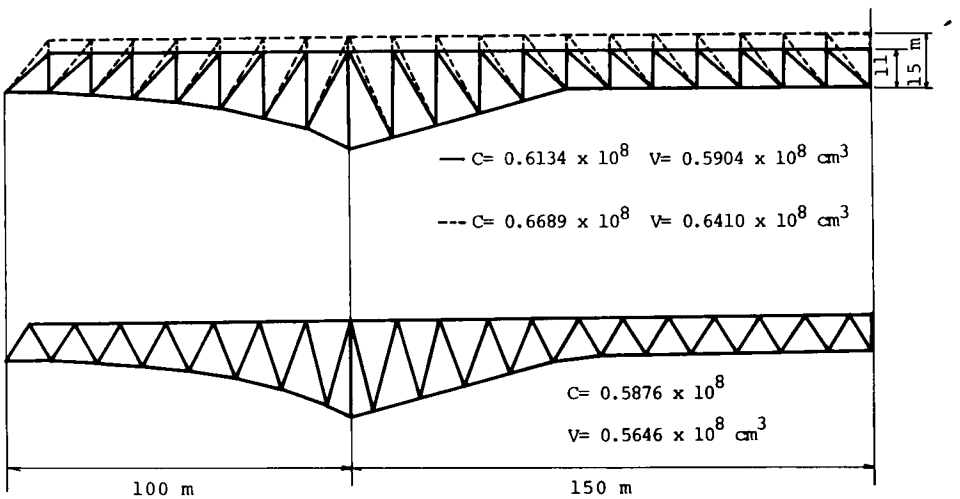

Fig. 3.17 Final Configuration of Amakusa 1-Go Bridge Model

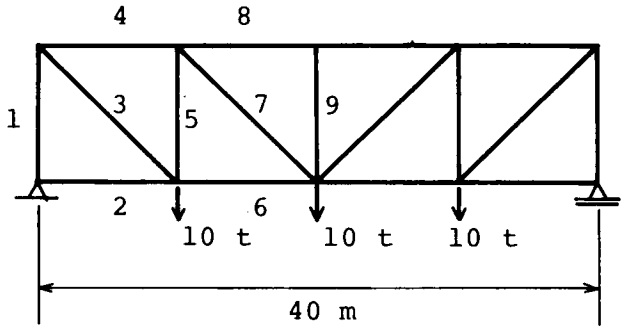

Fig. 3.18 4-Panel Pratt Truss Model

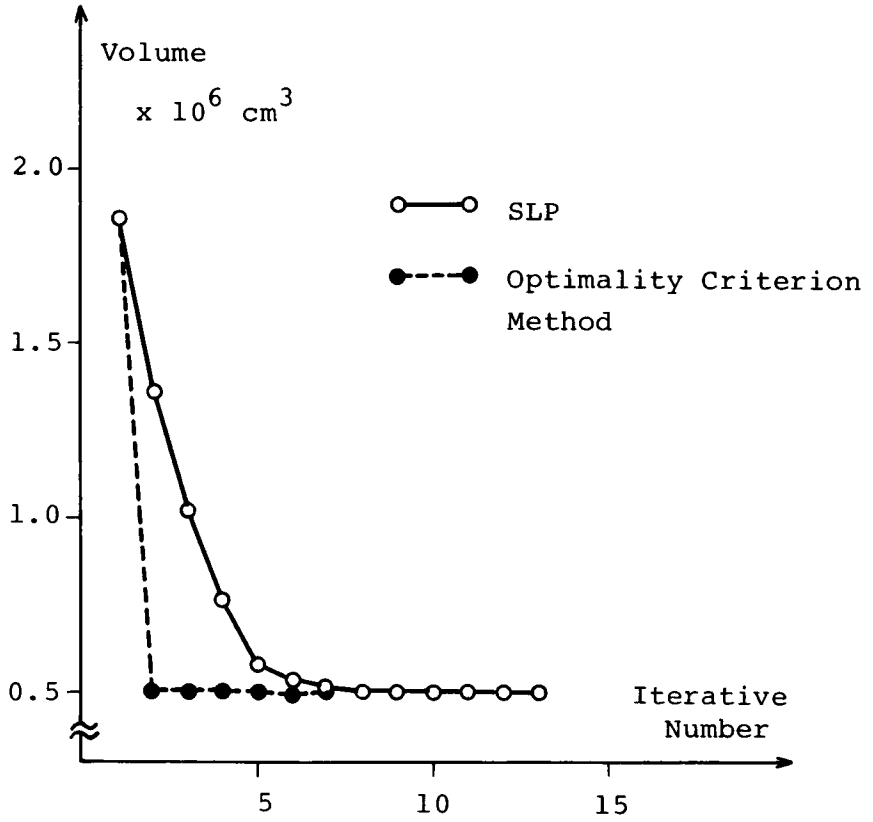

Fig. 3.19 Comparison of Optimality Criterion Method and SLP

Fig. 3.19. While the convergency of the optimality criterion method is not affected by the initial values, SLP depends on the initial values and the selection of the moving limits. It can be said that for relatively simple trusses, the optimality criterion algorithm gives an accurate solution with less computation time, independent of the initial values.

Fig. 3.20 presents the relations between the deflection constraint and the total weight, which are obtained for the truss example shown in Fig. 3.21. It is seen in this figure that the total weight is in inverse proportional to the deflection limit. This can be inferred by the fact that δ_0 in Eq.(3.44) is identically zero when the truss is statically determinate and the external load is applied at the center of span.

Next, the optimality criterion algorithm is used together with the variable metric method to search for the optimal configuration. The change of configuration through optimization is given in Fig. 3.22, where the initial configuration is a 4-panel Pratt truss. The resulting configuration is quite similar to that obtained without deflection constraints. It seems that the deflection constraint hardly affects the determination of the configuration of statically determinate trusses.

5) Comparison of Truss and Arch

Some simple arch models are designed by use of the proposed method. Fig. 3.23 shows the optimal configuration of an arch model with the same topology of members as that of the truss model shown in Fig. 3.6. Comparing Fig. 3.23 with Fig. 3.6, it is obtained that arch and truss show no distinct difference in configuration, if the topology of members is the same.

Next, consider an arch model shown in Fig. 3.24, whose topology of members is not accepted for truss models on account of the stability condition. In this case, the obtained configuration becomes quite different in spite of the same loading condition. This means that topology of members is of primary importance in the determination of the configuration of arched structures, though it is not so important in truss problems. For a 4-panel arch model subjected to the uniform load, the optimal configuration is obtained, as shown in Fig. 3.25. Then, the total weight

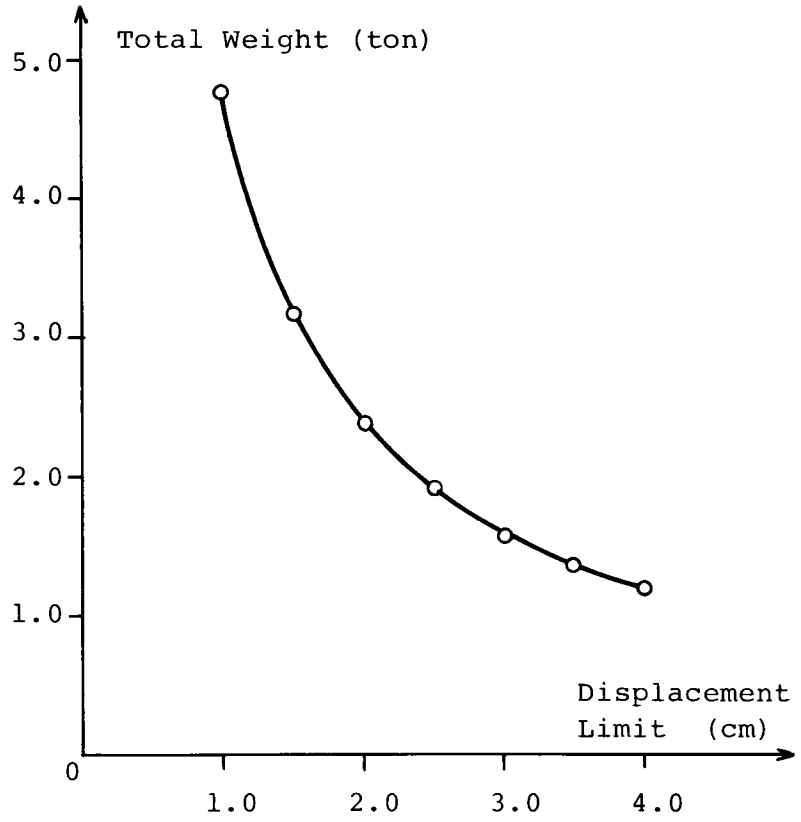

Fig. 3.20 Relation between Total Weight and Deflection Limit

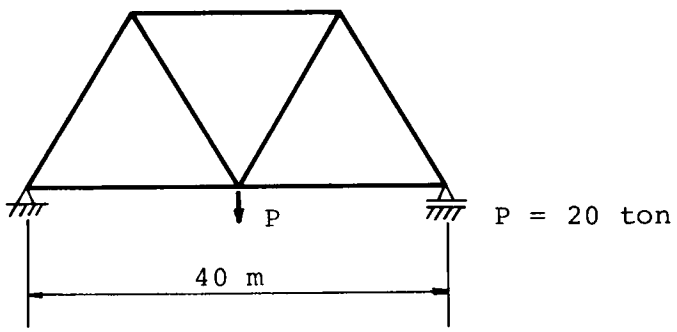

Fig. 3.21 Warren Truss Model

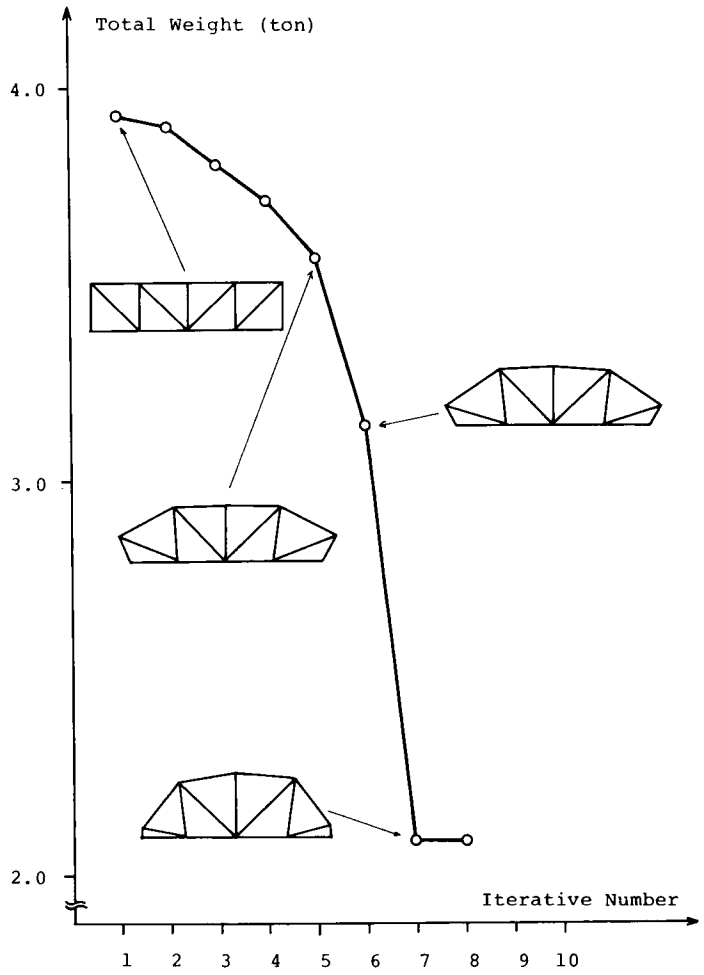

Fig. 3.22 Change of Configuration through Optimization

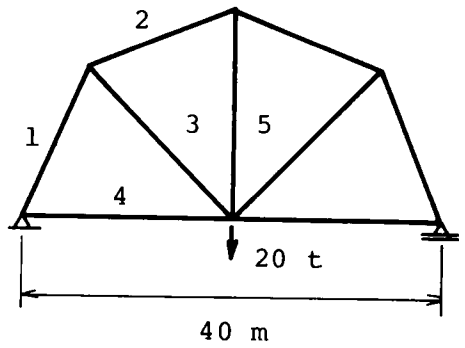

Fig. 3.23 Optimal Geometry of Arch Model with Same Topology as that of Truss Model

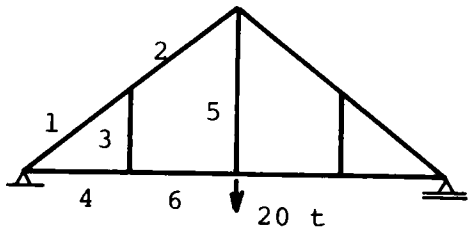

Fig. 3.24 Optimal Geometry of Arch Model with Different Topology

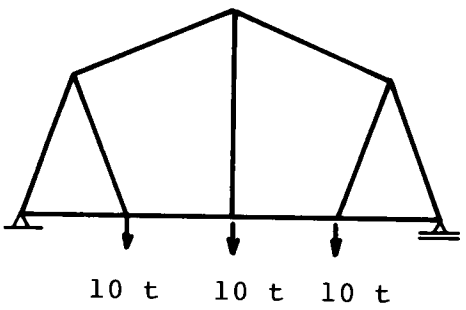

Fig. 3.25 Optimal Geometry for Uniform Load

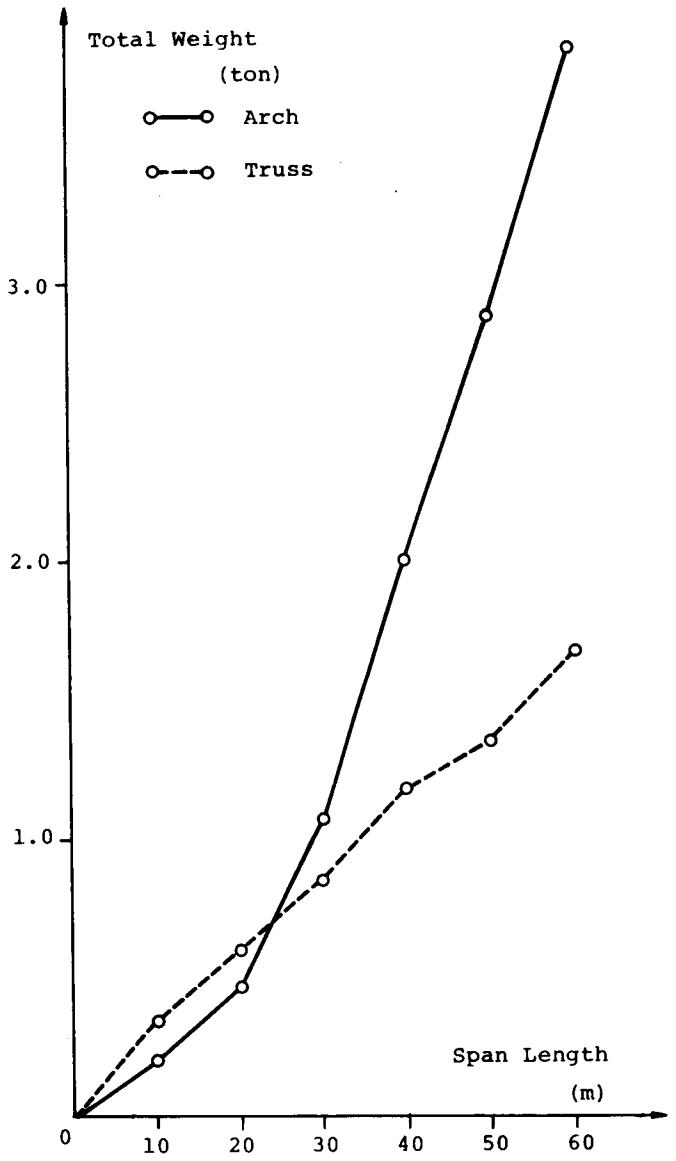

Fig. 3.26 Comparison of Truss and Arch

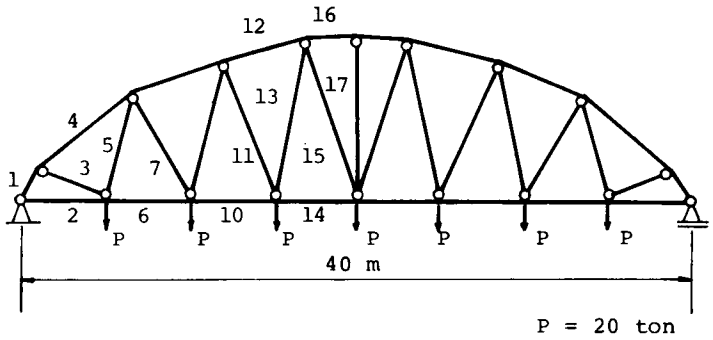

Fig. 3.27 Optimal Configuration of Model 1

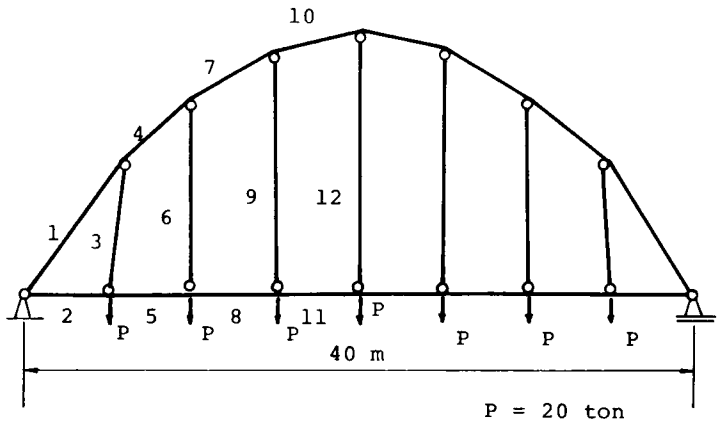

Fig. 3.28 Optimal Configuration of Model 2

Table 3.3 Numerical Results of Model 1

	Length (cm)	Area (cm^2)	Total Stress	Normal Stress	Bending Stress
1	225.1	4.88	-1181.5	-814.3	-367.2
2	500.0	1.77	1185.5	669.4	516.2
3	438.8	1.41	1214.5	1214.5	0.0
4	687.5	8.51	-580.1	-513.6	-66.5
5	643.3	0.20	1179.2	1179.2	0.0
6	500.0	2.90	1198.1	1159.3	39.0
7	720.4	0.94	1151.4	1151.4	0.0
8	616.0	7.08	-605.7	-592.7	-13.0
9	882.3	0.05	1092.6	1092.6	0.0
10	500.0	3.25	1203.5	1194.5	9.0
11	900.0	0.43	1200.0	1200.0	0.0
12	540.7	6.20	-688.2	-672.3	-15.9
13	1015.4	0.44	1198.2	1198.2	0.0
14	500.0	3.29	1202.4	1191.5	10.9
15	1019.5	0.24	1205.3	1205.3	0.0
16	252.8	3.38	-1204.9	-1182.8	-22.1
17	1000.7	0.37	1194.0	1194.0	0.0

Table 3.4 Numerical Results of Model 2

	Length (cm)	Area (cm^2)	Total Stress	Normal Stress	Bending Stress
1	330.1	7.31	-1185.2	-572.9	-612.3
2	500.0	3.20	1161.1	708.4	452.7
3	430.1	1.31	1195.4	1195.4	0.0
4	653.3	10.06	-779.6	-423.5	-356.1
5	500.0	4.05	1171.9	852.6	319.3
6	712.4	0.96	1125.7	1125.7	0.0
7	584.3	8.04	-770.4	-516.8	-253.6
8	500.0	4.29	1164.1	906.8	257.3
9	907.5	0.83	1265.1	1265.1	0.0
10	754.6	10.03	-577.9	-420.3	-157.6
11	500.0	4.39	1178.8	952.4	226.4
12	958.5	0.88	1116.9	1116.9	0.0

and the maximum deflection are *1193 kg* and *4.2 cm*, respectively. In this case, the arch model is lighter than the truss model, because the weight of the truss model becomes *1815 kg* under the same design condition.

Fig. 3.26 presents the comparison of truss and arch structures with various span lengths, where both truss and arch models have the same panel number and the same deflection limit. It can be seen that as the increase of span length the weight of arch model increases with a certain rate, while that of truss model increases rapidly. It is, however, noted that truss is superior for the case where the deflection constraint is not significant.

In order to disclose the effect of topology on the configuration of arched bridges, two different kinds of arch examples (Model 1 and Model 2) are employed. The numerical results obtained by the proposed method are summarized in Table 3.3, Table 3.4, Fig. 3.27 and Fig. 3.28. The upper chord members of both examples have the parabolic shapes similar to the bending diagram of simple beam models. From Table 3.3 and Table 3.4, it is seen that Model 1 has the bending stress less than the normal stress, though Model 2 has the larger bending stress. This implies that topology of Model 1 is effective for a trussed bridge and that of Model 2 for an arched bridge. Therefore, topological factors may play an important role in decisions concerning the selection of structural types.

3.8 Conclusions

While the importance of geometrical configuration has been sufficiently recognized in the design of bridge structures, its direct introduction has had such difficulties as poor convergency and excessive computation time. In this chapter, an approximate method based on the optimality criterion is proposed to remove the above problems concerning practical computations. Through some numerical examples, the following conclusions were reached.

1) It is confirmed that the geometrical configuration of trussed bridges can be efficiently treated with the use of the proposed method, and considerable weight or cost reduction can often be achieved. Effec-

tive use of the optimality criterion makes it possible to decrease the number of design variables, which results in a remarkable saving of computational effort.

2) The most remarkable feature of the approximate method is the fast convergence due to the simplification of unconstrained optimization problems. Although this method has no guarantee to reach the global optimum, it has an advantage from an engineering point of view. The calculation can be terminated at any design step in which a feasible solution is obtained. The design example of Amakusa 1-go bridge shows that this approximate method seems to be extremely promising in practical applications.

3) As seen in the work by H. Sugimoto and et al[21], trussed bridges without high redundancy tend to be fully stressed in the weight-minimization systems. For the reason, the optimality criterion " fully stressed " employed here is considered reasonable for the design of trussed bridges with geometrical variations.

4) Combining the sub-optimization technique with the mathematical programming, buckling effects can be taken into consideration, and also discrete variables with respect to the selection of materials can be treated without integer programming.

5) In order to search for the optimum node positions, the variable metric method seems to be superior in convergency to the conjugate gradient method. By using the band matrix method or the decomposition method in the structural analysis, one can reduce the computation time and memory capacity.

6) The optimality criterion algorithm proposed by A. Gellatly and L. Berke is very efficient for the design of trussed structures with deflection constraint. For statically determinate trusses, accurate solutions can be obtained by only one iteration, in spite of the choice of initial values. Also, for indeterminate trusses, satisfactory solutions can be obtained without difficulty.

7) Using this algorithm, it is possible to investigate the effect of deflection constraints on the decision of truss configuration. Most examples show that the deflection limitation does not change the node positions but the values of cross sectional areas.

8) It is to be noted that the proposed method is applicable for the design of arched bridges. Numerical results obtained for arch examples imply that topology of members is significant for the weight-minimization of arched bridges, whereas it is not for trussed bridges. Generally, trussed systems are lighter than arched systems for the case without deflection limitation. This tendency is due to the difference in the definition of fully stressed condition. Namely, in truss systems the induced stresses reach the allowable limit at all parts of the member, but in arched system merely at the ends of the member.

References for Chapter 3

1) Tachibana, Y., " Bridge Engineering ", Kyoritsu Publishing, 1977, pp7 (in Japanese)

2) Kirsch, U., " Multilevel Approach to Optimum Structural Design ", Proc. ASCE, ST4, Apr., 1975, pp957-974

3) Vanderplaats, G. N. and Moses, F., " Automated Design of Trusses for Optimum Geometry ", Proc. ASCE, ST3, Mar., 1972, pp671-690

4) Shiraishi, N. and Furuta, H., " On Geometry of Truss ", The Memoirs of the Faculty of Engineering, Kyoto Univ., Vol.XLI, Part 4, Oct., 1979, pp498-517

5) Kunar, P. R. and Chan, A. S. L., " A Method for the Configurational Optimisation of Structures ", J. of Computer Methods in Applied Mechanics and Engineering, Vol.7, 1976, pp331-350

6) Spillers, W. R. and Al-Banna, S., " Optimization Using Iterative Design Techniques ", Int. J. of Computers and Structures, Vol.3, 1973, pp1263-1271

7) Reinschmidt, K. F., Cornell, C. A. and Brotchie, J. F., " Iterative Design and Structural Optimization ", Proc. ASCE, ST6, Dec., 1966, pp281-318

8) Spillers, W. R. and Funaro, J., " Iterative Design with Deflection Constraints ", Int. J. of Solid and Structures, Vol.11, 1975, pp793-802

9) Spillers, W. R. and Al-Banna, S., " Convergence in Iterative Design ", Quarterly of Applied Mathematics, July, 1975, pp160-164

10) Spillers, W. R. and Lev, O., " Design for Two Loading Conditions ", Int. J. of Solid and Structures, Vol.7, 1971, pp1261-1267

11) Johnson, D. and Brotton, D. M., " Optimum Elastic Design of Redundant Trusses ", Proc. ASCE, ST12, Dec., 1969, pp2589-2610

12) Kavlie, D. and Moe, J., " Automated Design of Frame Structures ", Proc. ASCE, ST1, Jan., 1971, pp33-62

13) Okubo, S., " Optimization of Truss ", Proc. JSCE, No.177, May, 1970, pp9-19 (in Japanese)

14) Sugimoto, H., " Practical Optimization of Truss ", Proc. JSCE, No.208, Dec., 1972, pp23-31 (in Japanese)

15) Templeman, A. B., " Optimization Concepts and Techniques in Structural Design ", IABSE 10th Congress, Inductory Report, Tokyo, 1975, pp41-60

16) Gellatly, A. and Berke, L., " Optimality-Criterion-Based Algorithms, Chapter 4 of Optimum Structural Design : Theory and Application (by R. Gallagher and O. Zienkiewicz) ", John Wiley and Sons, Inc., 1973

17) Shiraishi, N. and Furuta, H., " Some Considerations on Geometrical Configurations of Bridge Structures ", The 27th Annual Meeting of Applied Mechanics, Tokyo, Nov., 1977 (in Japanese)

18) Naruoka, M. and others, " Optimum Design of Framed Structures ", JSSC, Vol.7, No.63 - Vol.8, No.74, 1971 - 1972 (in Japanese)

19) Shiraishi, N., Furuta, H. and Ikejima, K., " Configurational Optimization of Framed Structural Systems ", to appear in Theoretical and Applied Mechanics, Vol.29

20) Gellatly, R. A., Helenbrook, R. G. and Kocher, L. H., " Multiple Constraints in Structural Optimization ", Int. J. for Numerical Methods in Engineering, Vol.13, 1978, pp297-309

21) Sugimoto, H., Doi, H. and Nakamura, S., " On the Optimum Design of Long Truss Bridges by Partitioning into Substructures ", Proc. JSCE, No.261, 1977, pp1-6 (in Japanese)

Chapter 4 Safety Analysis and Minimum-Weight Design of Framed Structures Using Failure Probability

4.1 Safety of Structure[1)]

The ultimate objective of a structural engineer is to design structures which are both economically feasible and functionally reliable. In the previous chapters, attention is placed on economic design, where structures are designed on the basis of the deterministic design philosophy. The deterministic approach has been developed based on the past valuable experiences and empirical or theoretical investigations on structural safety. However, it is currently realized that there is some risk which is unavoidable, in view of numerous uncertainties underlying the design and construction of a structure. Absolute safety, therefore, is ordinarily not tenable nor practically realizable[2)].

To recognize and measure the risk, it is desirable to introduce the probabilistic approach into the design process. The foundation of the probability-based design was first given by A. M. Freudenthal in 1947[3)], and its theoretical aspects have been clarified by many researchers[4)-11)]. These refinements and clarifications of the theory are called the classical reliability theory, and thereafter A. Ang and others[12)-16)] have extended the classical theory to account for the subjective uncertainties involved in the prediction of relevant probability distributions.

In this chapter, structural safety is examined by using the failure probability as a measure of safety. To calculate the failure probability, it is necessary to specify a probability distribution function for each uncertain factor. However, the specification of distribution function is in practical quite difficult, due to the lack of sufficient data relevant to applied loads and structural resistances. Also, even if appropriate functions are found, the calculation of failure probability often requires a numerical integration which is prohibitive and time-consuming. It can be said that the

difficulties in calculation and the selection of distribution function are obstacles to a practical use of the reliability theory.

Regardless of the abovementioned problems, this approach has such significant features that it is suitable to investigate the influence of each uncertainty on structural design and the structural behavior under the unpredicting environment.

4.2 Failure Probability of Framed Structure

Assuming the independence between the applied load and the structural resistance, the failure probability of a structure with a single load can be computed as follows :[17)]

$$p_f = P_r(R < S) = \int_0^\infty (1 - F_S(r))\, f_R(r)\, dr$$

$$= \int_0^\infty F_R(S)\, f_S(S)\, dS \qquad (4.1)$$

in which $f_R(r)$ and $f_S(s)$ are the derivatives of distribution functions $F_R(r)$ and $F_S(s)$, respectively, and S and R denote the load effect and the material strength in terms of carrying capacity of load, respectively.

For mathematical convenience, both the applied load and the structural resistance are often assumed to be normally distributed or lognormally distributed. In the former case, the failure probability p_f can be expressed as

$$p_f = \Phi(-\beta_1) \qquad (4.2)$$

in which

$$\beta_1 = (\mu_R - \mu_S) / \sqrt{ \sigma_R^2 + \sigma_S^2 } \qquad (4.3)$$

$$\Phi(t) = \int_{-\infty}^{t} \frac{1}{\sqrt{2\pi}} \exp(-t^2/2)\, dt \qquad (4.4)$$

μ_R : mean value of member resistance

μ_S : mean value of load effect

σ_R^2 : variance of member resistance

σ_S^2 : variance of load effect

For the latter case, p_f is approximately found as

$$p_f \simeq \Phi(-\beta_2) \tag{4.5}$$

in which

$$\beta_2 = ln \ (\mu_R / \mu_S) \ / \ \sqrt{\delta_R^2 + \delta_S^2} \tag{4.6}$$

δ_R : coefficient of variation with respect to resistance

δ_S : coefficient of variation with respect to load effect

For general cases, the failure probability is calculated as

$$p_f = 1 - P_r(\underline{X} \in D) = 1 - \int_D f_{\underline{X}}(\underline{X}) \, d \underline{X} \tag{4.7}$$

where $\underline{X}$ is a n-dimensional vector which collects all the random quantities, and D is the safe region.

By use of the polar coordinates, Eq.(4.7) can be rewritten as[18]

$$p_f = 1 - \int_{\substack{0 \le \alpha_i \le 2\pi \\ cos\underline{\alpha}^{-t} cos\underline{\alpha}^{-} \le 1}} d\underline{\alpha}^{-} \int_0^{\beta_f(\underline{\alpha}^{-})} f_{\underline{\alpha}^{-},\beta} \ (\underline{\alpha}^{-},\beta) \ d\beta \tag{4.8}$$

where β is the distance of $\underline{X}$ from the origin and α_i is the angle between the generic axis, and vector $\underline{\alpha}$ is defined as

$$\underline{\alpha} = \begin{pmatrix} \alpha_1 \\ \alpha_2 \\ \cdot \\ \cdot \\ \alpha_n \end{pmatrix} \qquad 0 \le \alpha_i \le 2\pi \quad (i=1,\cdots,n)$$

$$cos\underline{\alpha}^{t} cos\underline{\alpha} = 1$$

and $cos \ \underline{\alpha}$: director cosines

$\underline{\alpha}^{-}$: the reduced vector which is obtained from $\underline{\alpha}$ by deleting the last component

$$\underline{\alpha}^{-} = \begin{pmatrix} \alpha_1 \\ \cdot \\ \cdot \\ \alpha_{n-1} \end{pmatrix}$$

$\beta_f(\underline{\alpha}^{-})$: safe boundary described in polar coordinates

$$\beta_f(\underline{\alpha}^{-}) = max \ \{ \ \beta \ | \ \beta \ cos \ \underline{\alpha} \in D \ \}$$

$f_{\underline{\alpha}^{-},\beta}(\underline{\alpha}^{-},\beta)$: joint distribution function described in polar coordinates

4.3 Reliability of Indeterminate Structural Systems

A safety analysis of indeterminate systems has difficult features, which are due to the fact that those systems have generally many various possible failure modes. As a rule, the approximations have been done on the assumption of statistical independence and complete dependence among failure modes. However, the resulting solution may be widely different as the number of failure modes increases. Also, usual structures have considerable dependence on their own failure mechanisms.

Indeterminate trusses can be considered to fail by the initial yielding. There are, however, many routes to reach the system collapse in indeterminate trusses, which while it is considerably difficult to trace all of them, some investigations were presented.[19)20)] While the actual collapse criterion is applied without difficulty, several mechanisms must be taken into consideration.[21)-24)]

The limit analysis concept is employed here to discuss the safety of indeterminate structures, placing attention on rigid frames. Then, only the failure due to the formation of plastic hinge is treated, so the failure through the loss of stability is not accounted for. Since the collapse mechanisms are inter-dependent, this effect is inevitable in the exact evaluation of system reliability. Here, the correlation between each failure mode is taken into account by calling attention to the events that two modes occur simultaneously.

Using the coefficient of correlation between each modal margin and an appropriate mathematical approximation, one can obtain a simple method presenting a good upper bound of system failure probability. From the view of safety design, only the value of the upper bound is necessary, but the lower bound is important to check the availability of the approximation. There is a brief discussion with regard to the lower bound. Furthermore, an improvement is attempted based on the fact that the simultaneous occurrence of three modes is considerably affected and limited by the occurrence of two of three modes. A simple mathematical model is developed to evaluate the effect of those events on the average.

Reduction of Upper Bound Formula[25)-30)]

Supposing that a structural system has n failure modes, the probability of a system failure, p_f, can be written in the terms of the modal failure events F_i as follows :

$$p_f = P_r(F_1 \cup F_2 \cup \cdots\cdots\cdots \cup F_n) \tag{4.9}$$

where the symbol " U " signifies the union of the events.
The event F_i occurs when the modal resistance R_i is less than the modal load effect S_i.

$$F_i = (R_i - S_i < 0) \tag{4.10}$$

Taking the collapse mechanisms as a typical failure mode, the failure event F_i is written by introducing the reserve strength Z_i in the following :

$$F_i = (Z_i < 0) \tag{4.11}$$

where
$$Z_i = \sum_{k=1}^{n} A_{ik} M_k - \sum_{j=1}^{m} B_{ij} S_j \tag{4.12}$$

M_k : structural resistance of a structural member at the k-th point in the structure

A_{ik} : resistance coefficient determined by the position and condition of the k-th point related to the i-th failure

S_j : effect of the j-th load on the structure

B_{ij} : load coefficient determined by the position and magnitude of the j-th load on the structure related to the i-th failure mode.

The beam failure mode of a single-bent frame shown in Fig. 4.1 is

$$Z_1 = M_B + 2M_B + M_B - 4P_1L/2 \tag{4.13}$$

If the form of Eq.(4.12) is used,

$$Z_1 = \sum_{k=1}^{7} A_{1k} M_k - \sum_{j=1}^{2} B_{1j} S_j \tag{4.14}$$

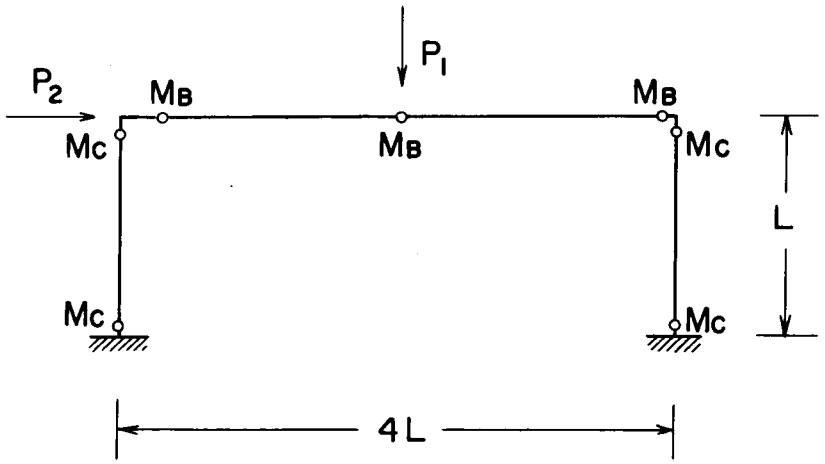

FAILURE MODES

$$Z_1 = M_B + 2M_B + M_B - 4P_1L/2$$
$$Z_2 = M_C + 2M_B + M_C - 4P_1L/2$$
$$Z_3 = M_B + 2M_B + M_C - 4P_1L/2$$
$$Z_4 = M_C + M_C + M_C + M_C - P_2L$$
$$Z_5 = M_C + M_B + M_B + M_C - P_2L$$
$$Z_6 = M_C + M_C + M_B + M_C - P_2L$$
$$Z_7 = M_C + 2M_B + 2M_C + M_C - P_2L - 4P_1L/2$$
$$Z_8 = M_C + 2M_B + 2M_B + M_C - P_2L - 4P_1L/2$$

Fig. 4.1 Single Bent Frame

where

$$M_1 = M_2 = M_6 = M_7 = M_C$$

$$M_3 = M_4 = M_5 = M_B$$

$$A_{11} = A_{12} = A_{16} = A_{17} = 0$$

$$A_{13} = A_{15} = 1 \ , \ A_{14} = 2 \qquad (4.15)$$

$$B_{11} = 0 \ , \ B_{12} = 2L$$

$$S_1 = P_2 \ , \ S_2 = P_1$$

Then, the failure probability of the i-th mode, p_{fi}, is given as

$$p_{fi} = P_r(Z_i < 0) \qquad (4.16)$$

By paying attention to the n-th event, Eq.(4.9) can be expanded to be[31)]

$$P_r(F_1 \cup F_2 \cup \cdots \cup F_n) = P_r(F_1 \cup \cdots \cup F_{n-1}) + P_r(F_n) - P_r((F_1 \cup \cdots \cup F_{n-1}) \cap F_n) \qquad (4.17)$$

where the symbol " $\cap$ " signifies the intersection of the events.
The last term on the right side in Eq.(4.17) is lowly limited by the probability of the occurrence of two events.

$$P_r((F_1 \cup \cdots \cup F_{n-1}) \cap F_n) \geq P_r(F_k \cap F_n) \qquad (4.18)$$

where F_k is one of the events F_i (i=1, $\cdots$, n-1).
Thus, the upper bound of p_f can be reduced, that is,

$$p_f \leq P_r(F_1 \cup F_2 \cup \cdots \cup F_{n-1}) + P_r(F_n) - P_r(F_k \cap F_n) \qquad (4.19)$$

To obtain the closest upper bound, one should select the value which minimizes the last term of inequality (4.19). When the expansion is continued, a simple formula presenting an upper bound can be obtained.[32)]

$$p_f \simeq \sum_{i=1}^{n} P_r(F_i) - \sum_{i=1}^{n-1} \max_{j=1}^{i} (P_r(F_j \cap F_{i+1})) \qquad (4.20)$$

Here, assuming a statistically complete dependence between each mode, the failure probability becomes as follows :[33)]

$$P_f = P_r(F_{iw}) \tag{4.21}$$

where F_{iw} is the weakest mode.

On the other hand, assuming a probabilistic independence, it can be expressed as

$$p_f = \sum_{i=1}^{n} P_r(F_i) \tag{4.22}$$

It is apparent that Eq.(4.20) gives a better upper bound than Eq.(4.22), because the value calculated by Eq.(4.20) is less than that by Eq.(4.22) by the value of its second term.

When the failure modes do not have a strong dependence, Eq.(4.21) gives a value very far from the true solution. For such a case, the following equation may give a better result.

$$p_f \geq \sum_{i=1}^{n} P_r(F_i) - \sum_{0<i<j<n} P_r(F_i \cap F_j) \tag{4.23}$$

An Improvement on Evaluation of System Reliability

In the preceding section, a simple method is presented, which requires the probabilities that two events occur simultaneously. These probabilities can be obtained by introducing the inter-dependence between two modes through the coefficients of correlation. Using the approximate method developed by M. Tichy and M. Vorlicek[35], they can be calculated without integration.

When $P_r(F_i)$ is less than $P_r(F_j)$, the probability of the occurrence of two events, F_i and F_j, is expressed as

$$P_r(F_i \cap F_j) = P_r(F_j) \left\{P_r(F_i) + \gamma_{F_iF_j}^{\phi_j+2} (1-P_r(F_i))\right\} \tag{4.24}$$

where $\gamma_{F_iF_j}$: the coefficient of correlation between F_i and F_j

$$\phi_j = -\log_{10} P_r(F_j) \tag{4.25}$$

While the implementation of Eq.(4.20) needs only the failure probability of each mode and the coefficient of correlation, it may give a too conservative value for a case where the failure modes are considerably dependent. To examine the accuracy of this method, an

improvement on the lower bound is considered herein.

Eq.(4.9) can be rewritten in the terms of the intersections of the events as follows :

$$P_r(F_1 \cup \cdots \cup F_n) = \sum_{i=1}^{n} P_r(F_i) - \sum_{0<i<j<n} P_r(F_i \cap F_j) + \sum_{0<i<j<k<n} P_r(F_i \cap F_j \cap F_k) - \cdots\cdots + P_r(F_1 \cap F_2 \cap \cdots \cap F_n) \qquad (4.26)$$

It is evident that in Eq.(4.26) any term has a greater value than those of the successive terms. Also, the former is influential on the latter. Generally, higher terms are truncated in the calculation, assuming that those have small values. However, this assumption is not true for some cases, and the case treated here may be one of the exceptions. Therefore, we attempt to take additionally the third term of Eq.(4.26) into account, in order to improve the approximation. In order to obtain this probability analytically, a simple mathematical model is proposed.

In general, the failure probability of the i-th mode is calculated as the negative region shown in Fig. 4.2. Then, the circle with the same area as this region is transferred to express the failure event F_i and a similar treatment is used for the remainders, F_j and F_k. The probability of the occurrence of two events is given as the intersected region of two circles, as shown in Fig. 4.3. Also, the event that three modes occur at the same time can be specified as the shading part of Fig. 4.4. This procedure is summarized as follows :

Step 1 Specify the three circles, where their radii are determined by corresponding their areas to their failure probabilities.

Step 2 The distance between each two circles can be obtained by making the overlapped section areas equivalent to those of the two-events-occurrence probabilities.

Step 3 The three-events-occurrence probability can be calculated as the area of the induced curve-linear triangle.

It should be noted that the actual failure can never be exactly expressed by that simple figure, which may have a complicated boundary. The two-dimensional model employed here may be insufficient to express some special cases. Nevertheless, it can be considered to give the inter-dependence between three modes on the average, though it may include little physical meaning.

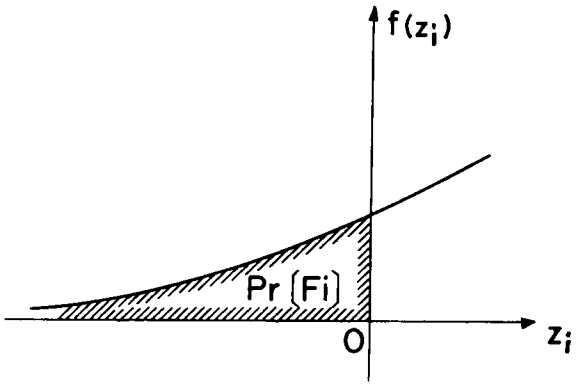

Fig. 4.2 Failure Probability of the i-th Mode

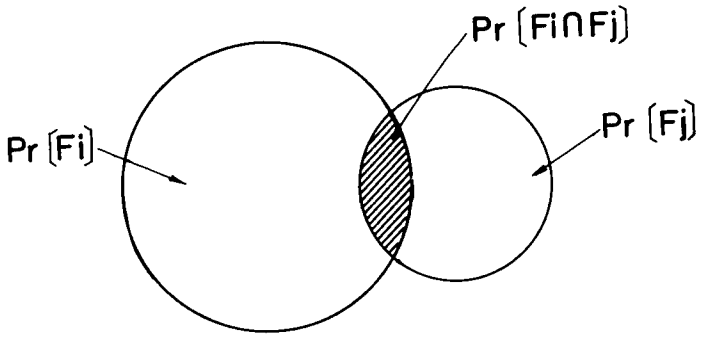

Fig. 4.3 Probability of Two-Events-Occurrence

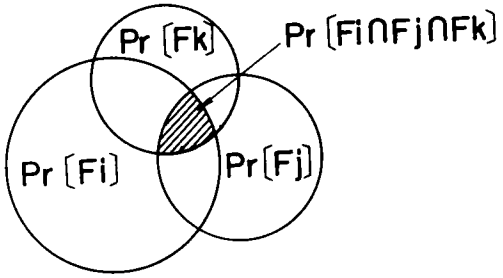

Fig. 4.4 Expression of $P_r(F_i \cap F_j \cap F_k)$

The system failure probability is calculated by using the first to the third terms of Eq.(4.26).

$$p_f \leq \sum_{i=1}^{n} P_r(F_i) - \sum_{0<i<j<n} P_r(F_i \cap F_j) + \sum_{0<i<j<k<n} P_r(F_i \cap F_j \cap F_k) \tag{4.27}$$

While this model is developed to improve the lower bound, the used equation will give an upper bound. It is natural that this approximation presents a conservative value when the model corresponds well to the actual event and the calculation is performed with a good accuracy. The obtained value will approach the true solution more closely, whether it is conservative or not.

The Relation between Proposed Method and Ordering Method

F. Moses and D. Kinser[36)37)] proposed the analysis method called the ordering method for estimating the overall failure probability. By using the relationship of mutually exclusive events, p_f can be written as

$$p_f = P_r(F_i) + P_r(F_2 \cap \overline{F}_1) + P_r(F_3 \cap \overline{F}_1 \cap \overline{F}_2) + \cdots\cdots$$

$$\cdots\cdots + P_r(F_n \cap \overline{F}_1 \cap \overline{F}_2 \cap \cdots \cap \overline{F}_{n-1}) \tag{4.28}$$

While this equation covers all possible failure events of the entire system, it requires enormous computations. Its implementation can be carried out solely when the correlations among all modes are found. It is apparent that the following relation exsists.

$$P_r(F_n \cap \overline{F}_1 \cap \cdots \cap \overline{F}_{n-1}) \leq P_r(F_n \cap \overline{F}_k) \tag{4.29}$$

where k is one of number 1 through $n-1$.
If k is selected as having the minimum value of $P_r(\overline{F}_i \cap F_n)$ ($i=1,\cdots\cdots, n-1$), that is,

$$P_r(\overline{F}_k \cap F_n) = \min_{i=1}^{n-1} P_r(\overline{F}_i \cap F_n) \tag{4.30}$$

the difference between the left and the right hands of inequality (4.29) will be the smallest. Now, the probability, $\min P_r(\overline{F}_i \cap F_n)$ can be rewritten by use of the failure event F_i as follows :

$$\min_{i=1}^{n-1} P_r(\bar{F}_i \cap F_n) = \min_{i=1}^{n-1} \{P_r(F_n) - P_r(F_i \cap F_n)\} \qquad (4.31)$$

Since $P_r(F_n)$ is constant, the minimum value is obtained when $P_r(F_i \cap F_n)$ indicates the maximum value.

$$\min_{i=1}^{n-1} P_r(\bar{F}_i \cap F_n) = P_r(F_n) - \max_{i=1}^{n-1} P_r(F_i \cap F_n) \qquad (4.32)$$

Using Eq.(4.32), Eq.(4.28) can be approximately expressed as follows :

$$P_f \simeq P_r(F_1) + (P_r(F_2) - P_r(F_2 \cap F_1)) + \{P_r(F_3) - \max_{i=1}^{2} P_r(F_i \cap F_2)\}$$

$$+\cdots + \{P_r(F_n) - \max_{i=1}^{n-1} P_r(F_i \cap F_n)\}$$

$$= \sum_{i=1}^{n} P_r(F_i) - \sum_{i=1}^{n-1} \max \{P_r(F_1 \cap F_{i+1}), \cdots, P_r(F_i \cap F_{i+1})\} \qquad (4.33)$$

Thus, the relationship between the proposed method and the ordering method is clarified. Namely, they are equivalent, if the ordering method accepts the approximation as shown in Eq.(4.29).

Design Examples

To illustrate the validity and the accuracy of the proposed method, some test examples are presented. In all examples, the loads and resistances are assumed to be normally distributed, because of the easiness of the treatment and the security of the central limit theorem. At first, the approximate method proposed by M. Tichy and M. Vorlicek is examined for some cases in which the ratio of $P_r(F_i)$ and $P_r(F_j)$ varies. The results are shown in Fig. 4.5(a) - (d), in which the abscissa is the coefficient of correlation. From these figures, this method seems to overestimate the joint probability density function when the probabilities of the i-th and j-th failure events have the same orders, or their coefficient of correlation is greater than 0.8. For other cases, this method presents unconservative values which are fairly close to the true solutions.

" Example 1 : Reliability Analysis of Portal Frame "

This simple model is used to explain the proposed method in detail.

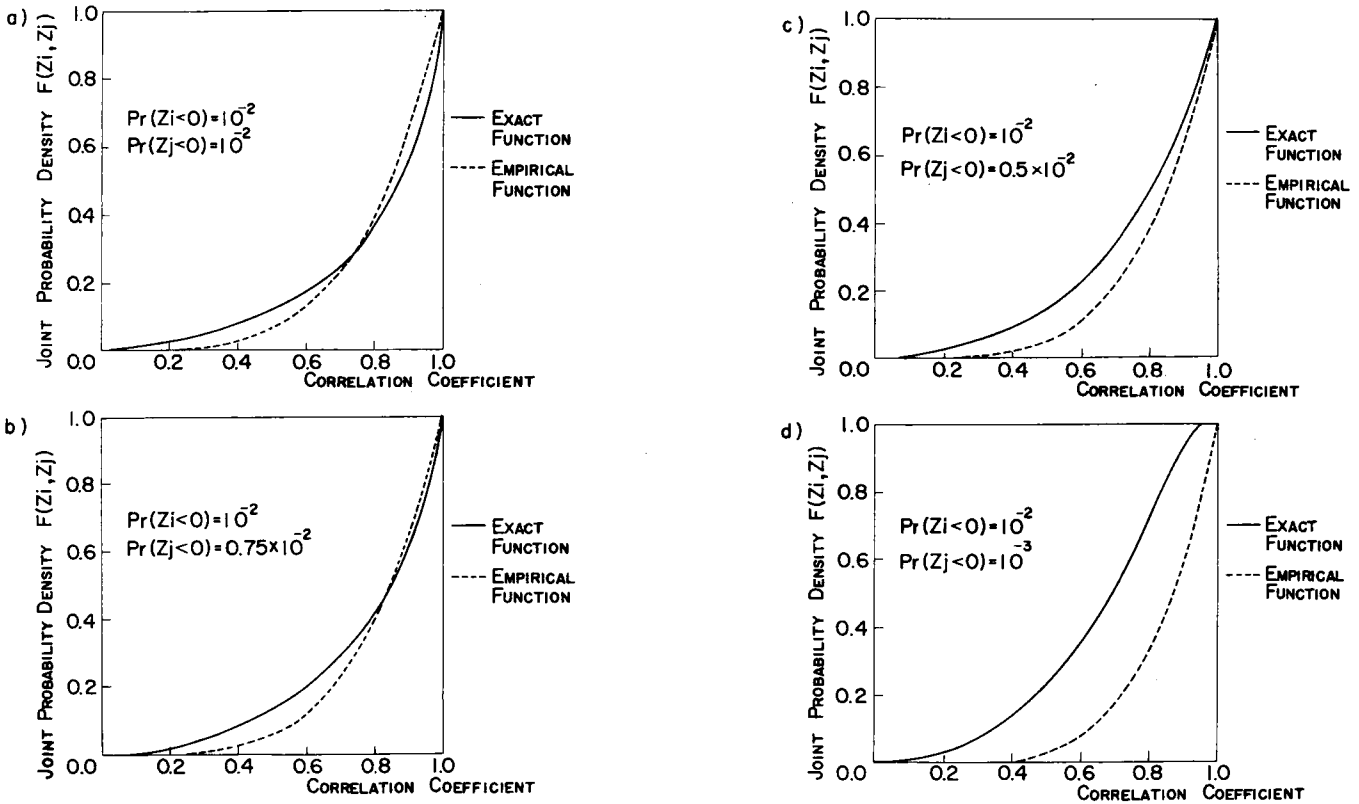

Fig. 4.5 Comparison of Empirical and Exact Functions
(Tichy's Method and Exact Solution)

Table 4.1 Reliability Analysis of Single Bent Frame

a) Condition of Input Data

Mean Value of Moment Resist. (K-FT)	Mean Value of Load		Coefficient of Variation	
	P_1 (K)	P_2 (K)	Resist.	Load
40	0.5	1.0	0.2	0.2

b) Calculated Probabilities of Failure

1	2	3	4	5	6
0.808×10^{-2}	0.920×10^{-2}	0.958×10^{-2}	0.886×10^{-2}	0.100×10^{-1}	0.150×10^{-1}
	0.8 sec.	5×10^4 trials	1.9 sec.	0.8 sec.	

1 : Dependent 2 : Lower Bound [Eq.(4.26)]

3 : Monte Carlo Simulation 4 : Stevenson's Method

5 : Upper Bound [Eq.(4.20)] 6 : Independent

The load condition and failure modes are illustrated in Fig. 4.1. The applied loads P_1 and P_2 are considered to be dependent and to have the mean values and the coefficient of variation presented in Table 4.1. Assuming the statistical independence and the complete dependence, the resulting band is considerably wide, and the proposed method gives an upper bound which is closer to the true solution than Eq.(4.22). By using a circle model, Eq.(4.27) presents a good lower bound. While the method by J. Stevenson shows a good agreement, it may lead to unconservative solutions, and also it requires twice the execution time of Eq.(4.20) in computing. (see Table 4.1)

" Example 2 : Reliability Analysis of One-Bay Two-Story Frame "

This model, whose geometry and applied load are shown in Fig. 4.6, is considered to have many dominant failure modes which are considerably inter-dependent on each other. Then, the assumption of statistical independence will give a too conservative value. By taking the correlation of two failure events into account, the proposed method improves the upper bound effectively. (see Table 4.2 and Table 4.3)

The failure probability decreases and approaches the result obtained by assuming the statistical independence, as the mean value of the load decreases. This phenomena can be explained by the fact that the coefficient of correlation between each mode becomes smaller according to the decrease of the load. However, this tendency accompanied with the decrease of failure probability is not observed when the coefficients of variation of the load and resistance decrease. The approximate solution by the method of M. Tichy and M. Vorlicek is compared with the exact solution for this model to show that this method always presents conservative values. Its application can be considered useful for ordinal structures, because it can reduce the execution time by the elimination of numerical integration.

Next, the failure probabilities are calculated for those cases in which the moment resistances have 60 and 70 (K-FT) as mean values. Then, the numerical results are summarized in Table 4.4, including the results of the improving method proposed here.

This method is considered to improve the lower bound. In the calculation processes, the curve-linear triangles, which correspond

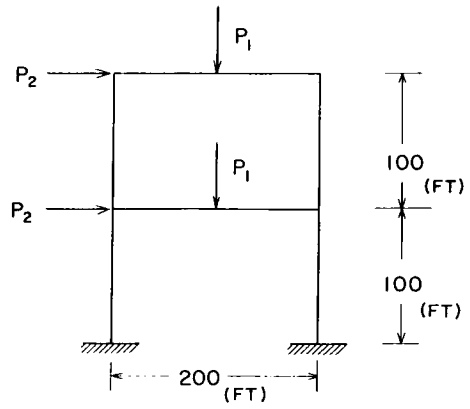

Fig. 4.6 Two-Story Single-Bay Rigid Frame

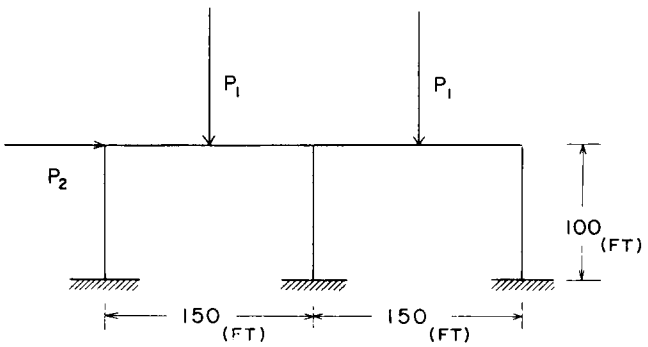

Fig. 4.7 One-Story Two-Bay Rigid Frame

Table 4.2 Reliability Analysis of Two-Story Single-Bay Frame (I)

a) Condition of Input Data

Case No.	Mean Value of Moment Resistance	Mean Value of Load		Coefficient of Variation		P_1 , P_2
		P_1	P_2	Moment Resistance	Load	
1	40	1.0	0.5	0.2	0.2	Dependent
2	40	0.8	0.4	0.2	0.2	Dependent
3	40	0.6	0.3	0.2	0.2	Dependent

b) Calculated Probabilities of Failure

Case No.	Dependent	Independent	Simulation		Stevenson's Method	Proposed Method
			Limit Analysis	Elastic Analysis		
1	0.941×10^{-1}	0.462	0.118	0.722	0.113	0.157 * 0.132
			10^4 trials	10^4 trials	7.8 sec.	2.5 sec.
2	0.841×10^{-2}	0.369×10^{-1}	0.131×10^{-1}	0.414	0.112×10^{-1}	0.160×10^{-1} 0.147×10^{-1}
			10^4 trials	10^4 trials	7.2 sec.	2.5 sec.
3	0.271×10^{-3}	0.831×10^{-3}	0.640×10^{-3}	0.109	0.587×10^{-3}	0.710×10^{-3}
			5×10^5 trials	10^4 trials	5.7 sec.	2.5 sec.

Proposed Method
* Upper Value by M. Tichy's Method
Lower Value by Numerical Integration

Table 4.3 Reliability Analysis of Two-Story Single-Bay Frame (II)

a) Condition of Input Data

Case No.	Mean Value of Moment Resistance	Mean Value of Load		Coefficient of Variation		P_1 , P_2
		P_1 (K)	P_2 (K)	Moment Resistance	Load	
1	40 (K-FT)	1.0	0.5	0.1	0.1	Dependent
2	40	0.8	0.4	0.1	0.1	Dependent

b) Calculated Probabilities of Failure

Case No.	Dependent	Independent	Simulation		Stevenson's Method	Proposed Method
			Limit Analysis	Elastic Analysis		
1	0.425×10^{-2}	0.969×10^{-2}	0.504×10^{-2}	0.776	0.480×10^{-2}	0.515×10^{-2}
			5×10^4 trials	10^4 trials	4.8 sec.	2.5 sec.
2	0.864×10^{-6}	0.113×10^{-5}		0.199	0.938×10^{-6}	0.961×10^{-6}
				10^4 trials	3.2 sec.	2.5 sec.

Table 4.4 Reliability Analysis of Two-Story Single-Bay Frame (III)

Mean Value of Moment Resistance	Dependent	Lower Bound by Eq.(4.27)	Proposed Method (Lower Bound)	Monte Carlo Simulation	Proposed Method (Upper Bound)	Independent
60	0.355×10^{-2}	0.947×10^{-2}	0.112×10^{-1}	0.121×10^{-1} (4.6×10^4 trials)	0.138×10^{-1}	0.170×10^{-1}
70	0.123×10^{-2}	0.375×10^{-2}	0.375×10^{-2}	0.380×10^{-2} (4.6×10^4 trials)	0.400×10^{-2}	0.407×10^{-2}

Mean Value of Load : $P_1 = 1.0$ (K) , $P_2 = 0.5$ (K)

Table 4.5 Reliability Analysis of One-Story Two-Bay Frame

a) Condition of Input Data

Case No.	Mean Value of Moment Resistance	Mean Value of Load		Coefficient of Variation		P_1 , P_2
		P_1 (K)	P_2 (K)	Moment Resistance	Load	
1	40 (K-FT)	1.0	0.5	0.2	0.2	Dependent
2	40	1.0	0.5	0.2	0.2	Independent

b) Calculated Probabilities of Failure

Case No.	Dependent	Independent	Simulation		Stevenson's Method	Proposed Method
			Limit Analysis	Elastic Analysis		
1	0.808×10^{-1}	0.200×10^{-1}	0.158×10^{-1}	0.736×10^{-1}	0.162×10^{-1}	0.169×10^{-1}
			5×10^4 trials	5×10^4 trials	4.2 sec.	1.8 sec.
2	0.808×10^{-2}	0.199×10^{-1}	0.158×10^{-1}	0.610×10^{-1}	0.163×10^{-1}	0.169×10^{-1}
			5×10^4 trials	5×10^4 trials	3.6 sec.	1.8 sec.

to the three-events-occurrence probabilities, are approximated by the linear triangles, in order to save the execution time and make the programming simple. In spite of this approximation, this method gives lower bounds very close to the solution obtained by Monte Carlo simulation. However, this method seems to have the possibility of presenting greater values for cases where the difference between the curve-linear triangles and the linear triangles is small, or the estimating method for the two-events-occurrence probability presents values that are too conservative. Nevertheless, these results show good agreement with the true solutions.

" Example 3 : Reliability Analysis of One-Story Two-Bay Frame "

In this model, the beam mechanism can be considered to be the most dominant mode, and to have less correlation among the modes. (see Fig. 4.7) Table 4.5 shows that all solutions are almost equal, excepting those obtained by assuming complete dependence or independence. Considering the matter of less calculation time, the proposed method is also useful for this case, though Stevenson's method presents the closest value to the true solution.

4.4 Reliability Analysis Including Statistical Uncertainty

In the foregoing section, the failure probability is calculated on the assumption that each uncertain quantity is normally distributed. As mentioned before, it is quite difficult to select an appropriate distribution for a random variable. It is said that the failure probability is sensitive and unstable, depending on the selected distribution function.[9)38)] Furthermore, even if a good estimation of distribution function can be done, it is impossible to obtain the mean value and variance of the population. In practice, the characteristics such as mean and variance are estimated from observations and experimental results. Then, the sample mean and variance obtained from the measured data with a small size are seldom consistent with the population mean and variance. Also, the difference between the sample and population characteristics may give a considerably large

influence on the calculation of failure probability.[39]

In this section, the effect of statistical uncertainty related to measured data on the reliability analysis is studied on the basis of the fiducial statistics and Bayesian concept. Furthermore, the optimum sampling number is discussed by use of the risk analysis.

Reliability Analysis Using the Fiducial Statistics

The fiducial statistics deals with the population mean and variance as random variables, whereas usual classical statistics treat the sample mean and variance as variables. By use of the peculiar property of the fiducial statistics, the statistical uncertainty can be evaluated in the calculation of failure probability.[40]

Sample mean $\bar{X}$ and variance S_X^2 with n independent samples, $X_1 - X_n$, are calculated as

$$\bar{X} = \frac{1}{n} \sum_{i=1}^{n} X_i^2 \tag{4.34}$$

$$S_X^2 = \frac{1}{n} \sum_{i=1}^{n} (X_i - \bar{X})^2 \tag{4.35}$$

Postulated that a variable X is normally distributed, those probability density functions are

$$f_{\bar{X}}(\bar{X}) = \frac{\sqrt{n}}{\sqrt{2\pi}\,\sigma_X} \exp\left(- n(\bar{X} - \mu_X)/2\sigma_X^2 \right) \tag{4.36}$$

$$f_{S_X}(S_X) = \frac{\sqrt{n}^{\,n-1}}{\sqrt{2}^{\,n-3}\,\Gamma((n-1)/2)} \frac{1}{\sigma_X} \left(\frac{S_X}{\sigma_X} \right)^{n-2} \exp(-nS_X^2/2\sigma_X^2) \tag{4.37}$$

where

$$f(X) = \frac{1}{\sqrt{2\pi}\,\sigma_X} \exp\left(-(X-\mu_X)^2/2\sigma_X^2 \right) \tag{4.38}$$

in which μ_X and σ_X^2 are the population mean and variance, respectively. Then, the joint probability density function of $\bar{X}$ and S_X can be obtained by assuming a statistical independence between them.

$$f_{\bar{X},S_X}(\bar{X},S_X) = C \frac{1}{\sigma_X^2}\left[\frac{S_X}{\sigma_X}\right]^{n-2} exp(-n(\bar{X}-\mu_X)^2/2\sigma_X^2)\ exp(-nS_X^2/2\sigma_X^2) \quad (4.39)$$

Here, the joint density function of μ_X and σ_X can be calculated by converting $d\bar{X}\cdot dS_X/S_X$ and $d\mu_X\cdot d\sigma_X/\sigma_X$ in Eq.(4.39).

$$f_{\mu_X,\sigma_X}(\mu_X,\sigma_X) = C \frac{1}{\sigma_X^2}\left[\frac{S_X}{\sigma_X}\right]^{n-1} exp(-n(\bar{X}-\mu_X)^2/2\sigma_X^2)\ exp(-nS_X^2/2\sigma_X^2) \quad (4.40)$$

where
$$C = n^{n/2} / (2^{n/2-1}\sqrt{\pi}\,\Gamma((n-1)/2) \quad (4.41)$$

$\Gamma(\cdot)$: gamma function

The conditional density function, $f(X|\bar{X},S_X)$, can be obtained by multiplying Eq.(4.38) with Eq.(4.40).

$$f(X|\bar{X},S_X) = \frac{\Gamma(n/2)}{\Gamma((n-1)/2)\sqrt{\pi(n+1)}}\left\{1+\frac{(X-\bar{X})^2}{S_X^2(n+1)}\right\}^{-n/2} \quad (4.42)$$

Using Eq.(4.42) for the load S and the resistance R which are independent, the failure probability including the statistical uncertainty can be formulated as

$$p_f = \iint_{R<S} f(R|\bar{R},S_R)\ f(S|\bar{S},S_S)\ dRdS \quad (4.43)$$

Reliability Analysis Based on Bayes Theorem[41)-43)]

Here, statistical uncertainty is introduced into the calculation of failure probability by using Bayesian statistical decision theory. A major contribution of this theory is the procedure for coupling the professional information and the information contained in the measured data. The coupling procedure is performed with the aid of Bayes theorem that the posterior probability, $P_r(H_i|A)$, of hypothesis, i, given observations A, is proportional to the prior probability, $P_r(H_i)$, times the likelihood of A, given H_i, $P_r(A|H_i)$:[44)]

$$P_r(H_i|A) \propto P_r(A|H_i)\ P_r(H_i) \quad (4.44)$$

In the continuous form, the above relation can be written as

$$f''(\theta) = \frac{g(\varepsilon|\theta)\ f'(\theta)}{\int_{-\infty}^{\infty} g(\varepsilon|\theta)\ f'(\theta)\ d\theta} \tag{4.45}$$

in which $f'(\theta)$: prior distribution function

$f''(\theta)$: posterior distribution function

θ : parameter

ε : measured data

$g(\varepsilon|\theta)$: likelihood function ($= L(\theta)$)

Using Eq.(4.45), Bayesian distribution of a variable can be deduced.

$$f_X''(X|\theta) = \int_{-\infty}^{\infty} f_X'(X|\theta)\ L(\theta)\ d\theta \tag{4.46}$$

Applying Eq.(4.46) for the load S and the resistance R, the failure probability can be formulated as

$$p_f = \iint_{R<S} f_R''(R|\theta)\ f_S''(S|\theta)\ dRdS \tag{4.47}$$

Application of Bayes Theorem to Proof-Load Test[45)46)]

Proof-load test is often performed for aerospace structures to improve the reliability and the statistical confidence. By eliminating the members with less strength than the proof load, more reliable structures can be obtained. Although usual proof-load tests can not be carried out for civil engineering structures with large members, these structures undergo tacit processes of proof-load test during the construction.[47)48)]

Let S_p be the stress induced by a proof-load test. Then, the members which pass the proof-load test have the following probability density function.

$$f_R(X)dX = P_r(X<R<X+dX \mid R>S_p)$$

$$= \frac{P_r((X<R<X+dX) \cap (R>S_p))}{P_r(R>S_p)}$$

$$= \frac{H(X-S_p)\ f_R(X)dX}{1-F_R(S_p)} \tag{4.48}$$

where $H(X)$ is Heaviside's unit step function and $F_R(X)$ is the probability

distribution function for the yield point before the test. Therefore, the probability function for the yield point after the test, $F_{\underline{R}}(X)$, becomes

$$F_{\underline{R}}(X) = \frac{H(X-S_p)\ \{F_R(X) - F_R(S_p)\}}{1 - F_R(S_p)} \tag{4.49}$$

Let the probability density function for the stress induced by the applied load be $f_S(X)$. Then, the failure probability is obtained as follows, if the load is statistically independent of the resistance.[49]

$$p_f = \int_0^\infty F_{\underline{R}}(X)\ f_S(X)\ dX \tag{4.50}$$

The distributional sensitivity of member is considerably improved by introducing the proof-load test which truncates the tail of distribution function of resistance. However, there still remain a problem with respect to the statistical uncertainty involved in the proof-load test. Here, the statistical uncertainty is treated on the basis of Bayesian decision theory.

Consider three experimental methods in which the informations obtained from the proof-load test (undestructive test) are reflected in the evaluation of failure probability in different manners.

Method 1 The data obtained from the yielding test are used as the samples, by which the likelihood function is calculated, whereas the proof load S_p is used merely to modify the distribution of resistance. Bayesian distribution of resistance R is expressed as

$$f''_R(R|\theta) = \int_{-\infty}^{\infty} f'_R(R|\theta)\ L(\theta)\ d\theta \tag{4.51}$$

in which

$$L(\theta) = \prod_{i=1}^{n} f(X_i|\theta) \tag{4.52}$$

$X_1 - X_n$: the data obtained from the yielding test

Method 2 The proof-load test is considered to be a kind of yielding tests, and hence the data obtained from the proof-load test are used for estimating the parameter θ. The likelihood function is calculated by using the strength S_p and the

yielding strength for the undestructive and destructive members under the proof-load test, respectively.

$$L(\theta) = \sum_{i=1}^{n} f(X_i|\theta) \sum_{i=n_1+1}^{n} f(S_p|\theta) \qquad (4.53)$$

where $X_i \leq S_p$ $\quad i \leq n_1$

$X_i > S_p$ $\quad n_1 < i \leq n$

Method 3 The yielding test is further carried out for the members which pass the proof-load test. Then, the proof load S_p is used for the modifications of the distribution and the likelihood functions.

$$L(\theta) = \prod_{i=1}^{n} \frac{H(X-S_p)\, f(X_i|\theta)}{1 - F(S_p|\theta)} \qquad (4.54)$$

In Method 1, the statistical uncertainty due to the lack of data is compensated by performing the yielding test with respect to structural members which are practically utilized. Method 2 gives an upper bound of the failure probability by treating the strength larger than S_p as the proof load. Comparing with these two methods, Method 3 is considered to provide the most accurate value for the failure probability.

Optimum Sampling Method Based on Risk Analysis

Risk analysis is an evaluation method of structural safety which has developed mainly in the field of nuclear engineering.[51] Structures, which indicate a great social loss in their destruction, should be designed based on the expected loss instead of the expected benefit. In risk analysis, structural safety is evaluated by defining the term " risk " as the multiplication of failure cost and failure probability.

Let E_j be the various events which cause the failure in structures and $p_{f,j}$ be the failure probability relating to the event E_j. If E_j are independent of each other, the total failure probability, p_f, is expressed as

$$p_f = P_r(E_1 \cup E_2 \cup \cdots\cdots \cup E_j) = \sum_j p_{f,j} \qquad (4.55)$$

Then, risk is defined as

$$Risk = C_m \, p_f = \sum_j C_{m,j} \, p_{f,j} \tag{4.56}$$

where C_m : total expected cost of failure

$C_{m,j}$: expected cost of the failure caused by E_j

It can be considered that the failure probability of a structure decreases by the protection action against for failure such as inspection. Then, the decreasing probability p'_f is expressed by using the prior probability p_f and the effectiveness of the added protection r.[52]

$$p'_f = p_f \, (1-r) \tag{4.57}$$

The value $r = 0$ indicates an ineffective measure, and also $r = 1$ indicates full (or 100 %) effectiveness implying $p'_f = 0$. By using Eqs (4.55) and (4.57), the effectiveness r is expressed as

$$p'_f = \sum_j p_{f,j} \, (1-r_j) \tag{4.58}$$

Combining Eqs (4.58) and (4.57), the effectiveness r is rewritten as

$$r = \frac{p_f - p'_f}{p_f} = \frac{p_f - \sum_j p_{f,j} \, (1-r_j)}{p_f}$$

$$= \sum_j \left(\frac{p_{f,j}}{p_f} \right) r_j \tag{4.59}$$

Then, the expected benefit b_m obtained by a protection is

$$b_m = C_m \, p_f - C_m \, p'_f = C_m \, p_f \, r \tag{4.60}$$

By use of the abovementioned formulation, the optimum sampling is studied, where the effectiveness is considered to be provided by the increase of sampling number instead of protection actions. The expected benefit b_m can be rewritten as

$$b_m = C_m \, p_f - (\, C_m \, p'_f(n) + C_t \, n \,) \tag{4.61}$$

in which C_t : expected cost for a sampling

n : sampling number

Numerical Examples

" Example of Bayesian Renewal Process "

The change of failure probability is calculated for the case where the data of resistance are newly obtained from the additive yielding tests. Then, it is assumed that the load is sufficiently specified. Numerical results are shown in Table 4.6, in which five sampling cases are considered. In each case, the failure probability considerably changes when the mean value is treated as the unkown parameter, whereas it hardly changes when the variance is the unknown parameter. This implies that the effect of new data can be reflected well in the evaluation of failure probability, by employing only mean values as the unknown parameter in Bayesian decision process.

" Influence of Sampling Number on Failure Probability "

Using the fiducial statistics, the relations between the mean value or variance and the sampling number are obtained, as shown in Fig. 4.8 and Fig. 4.9. These figures indicate that the statistical uncertainty becomes considerably small when the sampling number exceeds 50 or 60. Fig. 4.10 shows the change of failure probability according to the increase of sampling number. It is seen that p_f shows no difference in both the case with $n = 50$ and the case with $n = 100$, when the coefficient of variation of the load is large. This fact leads to the conclusion that it is impossible to remove the statistical uncertainty for the case with large δ_R, unless a great number of samples is obtained.

" Example of Proof-Load Test "

Three experiment methods described before are examined by using a numerical example. The numerical results are given in Fig. 4.11 to Fig. 4.13. Table 4.7 indicates the input data used for these calculations. In all cases, the calculted failure probabilities are large in the order of Method 2, Method 1 and Method 3. Considering that how the obtained data are used in these methods, it is obvious that Method 2 presents the most conservative value, and that Method 3 presents the most reliable value. However, the differences between the three methods tend to vanish when the parameter U, which is defined as $U = (\mu_R - S_p) / \sigma_R$, exceeds one. The reason is that in the case with small S_p,

Table 4.6 Bayesian Renewal Process (prior $p_f = 0.1107 \times 10^{-1}$)

μ : Variable ($\times 10^{-3}$)

Step	1	2	3	4	5	6	7	8	9	10
Case 1	1.6201	0.6840	0.6026	0.6226	0.4481	2.2414	0.3111	0.3766	0.3602	0.3704
Case 2	0.9330	0.4098	0.3830	0.3673	0.4997	0.7295	0.5082	0.5604	0.5232	0.7183
Case 3	2.0473	0.9290	1.1393	0.7689	0.7596	0.6715	1.0387	0.4366	0.4285	0.4394
Case 4	0.7262	0.3416	0.4086	0.3610	0.2640	0.2857	0.5992	0.2550	0.8415	0.3266
Case 5	1.3449	0.5466	1.0206	1.0582	1.7042	0.8323	0.8138	0.6806	0.6637	0.6625

σ : Variable ($\times 10^{-2}$)

Step	1	2	3	4	5	6	7	8	9	10
Case 1	1.0044	0.9953	0.9726	0.9433	0.9134	0.8759	0.8548	0.8355	0.8135	0.7931
Case 2	1.0050	0.9893	0.9637	0.9371	0.9175	0.8999	0.8746	0.8540	0.8308	0.8046
Case 3	1.0021	0.9936	0.9767	0.9477	0.9727	0.8997	0.8679	0.8448	0.8227	0.8026
Case 4	1.0039	0.9848	0.9558	0.9241	0.9000	0.8739	0.8436	0.8201	0.8060	0.7855
Case 5	1.0049	0.9885	0.9720	0.9635	0.9355	0.9107	0.8852	0.8594	0.8377	0.8143

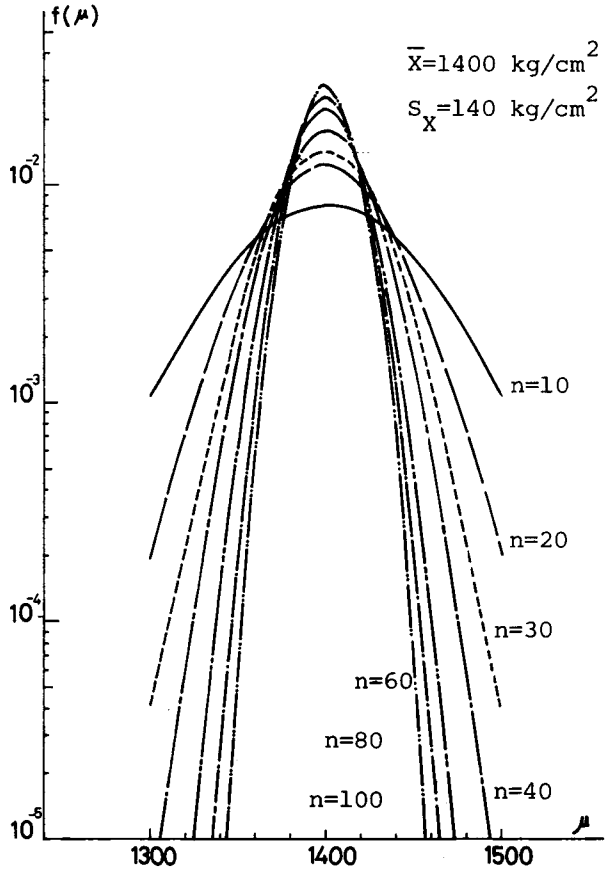

Fig. 4.8 P.D.F. of Mean Value

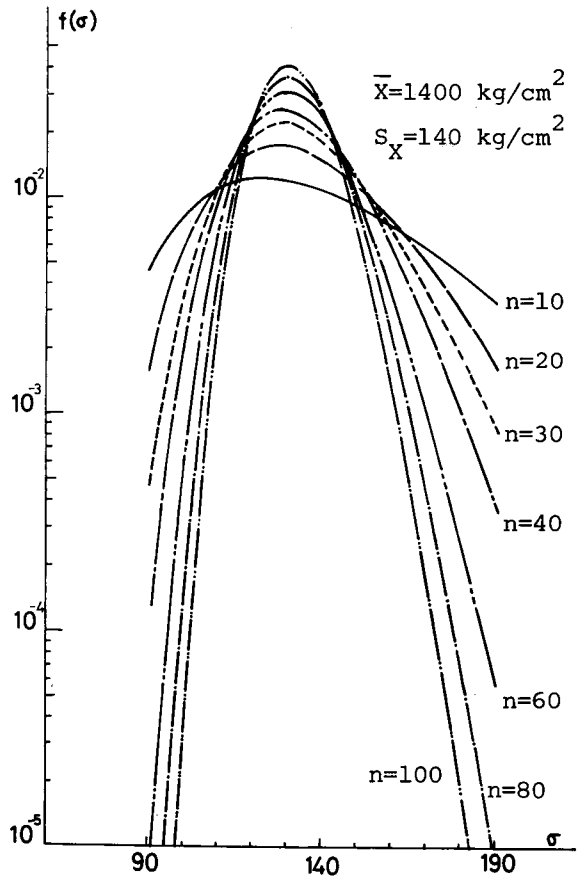

Fig. 4.9 P.D.F. of Standard Deviation

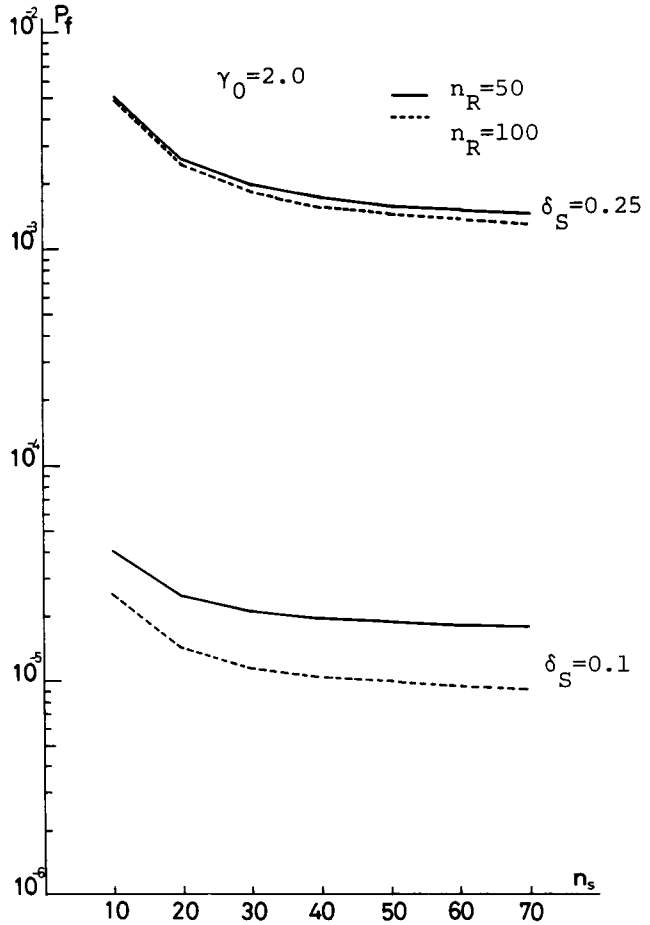

Fig. 4.10 Relation between p_f and n_s

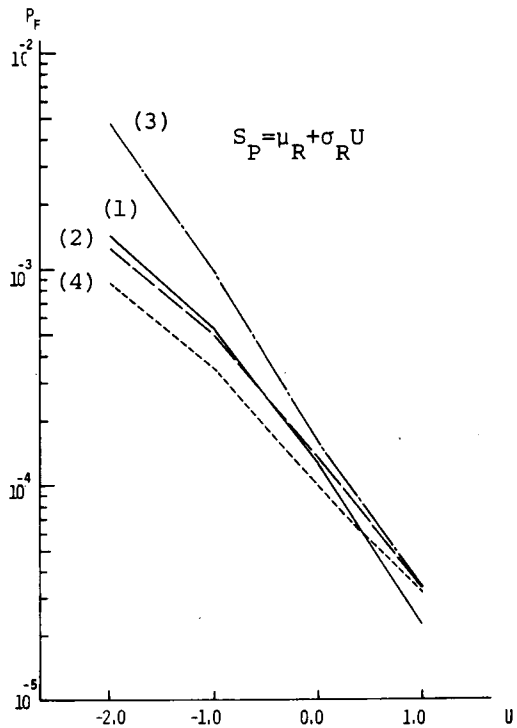

Fig. 4.11 Proof-Load Test (1)

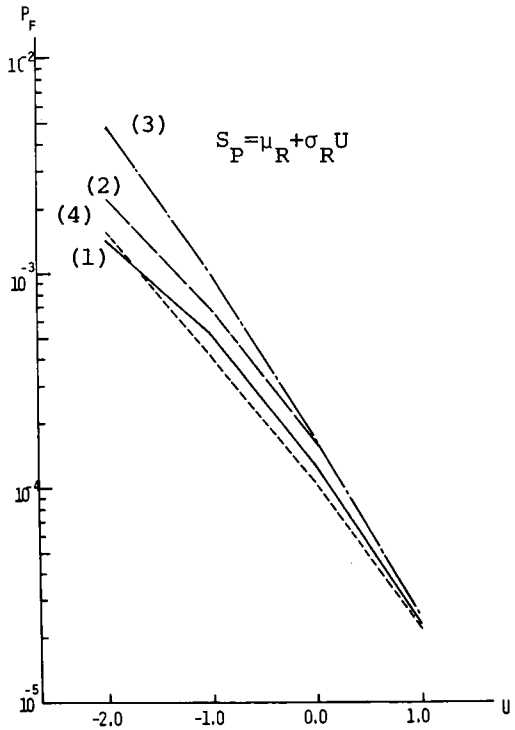

Fig. 4.12 Proof-Load Test (2)

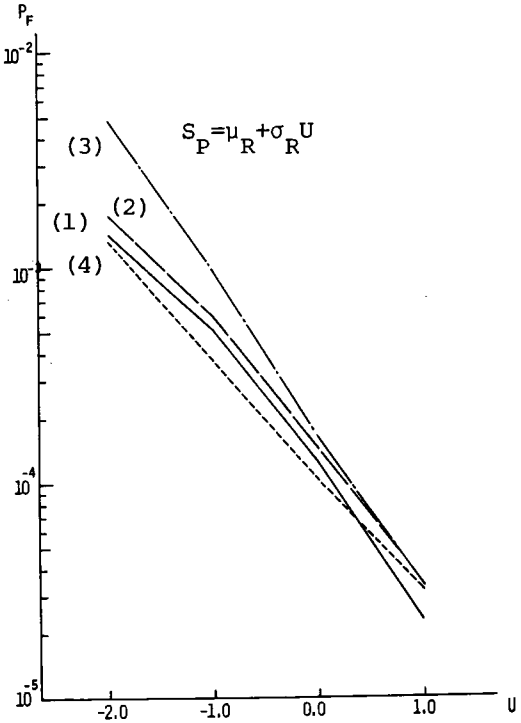

Fig. 4.13 Proof-Load Test (3)

Table 4.7 Input Data for Proof-Load Test

a) Data of Material Strength

Step	1	2	3	4	5	6	7	8	9	10
Case 1	2991.25	2095.39	2038.19	2637.04	2156.72	2010.36	2533.57	2459.23	2064.97	1729.95
	2438.67	2227.15	2029.25	2031.35	2355.01	2387.66	1624.72	2434.39	2182.58	2419.47
Case 2	1394.71	1959.25	2421.62	2030.88	2460.24	1780.85	1926.80	2420.33	2229.80	2228.54
	2268.73	2080.03	2486.01	2134.43	2445.24	2294.30	2555.56	2300.30	2137.09	2015.56
Case 3	1415.41	1986.13	2290.04	2242.10	2391.38	2475.53	2068.84	1819.74	2338.83	1978.98
	2119.30	1932.33	2286.54	2264.07	2338.64	2204.90	1719.93	2117.95	2320.45	2219.57

b) Sampling Number

U	-2.0	-1.0	0.0	1.0
Case 1	18	18	10	6
Case 2	19	16	11	6
Case 3	18	15	11	1

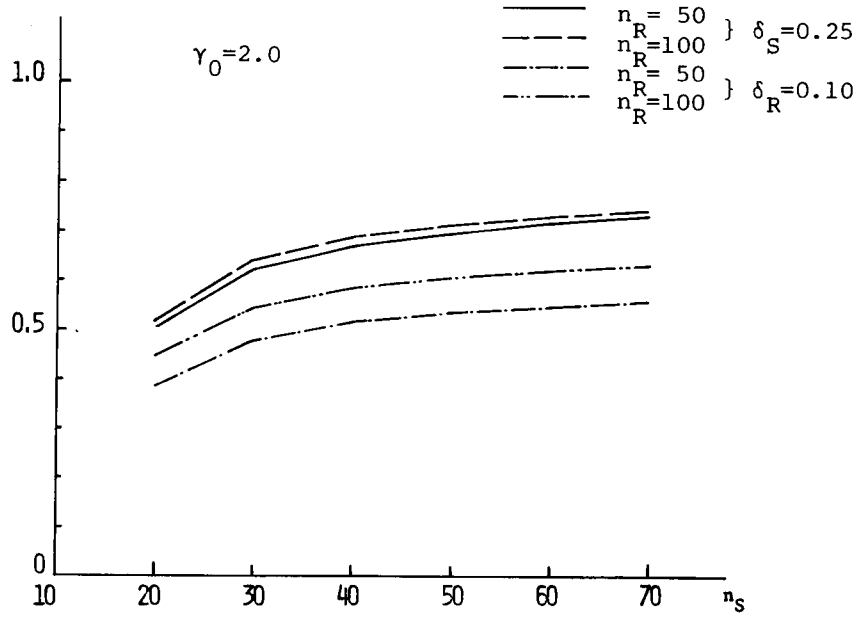

Fig. 4.14 Change of Effectiveness

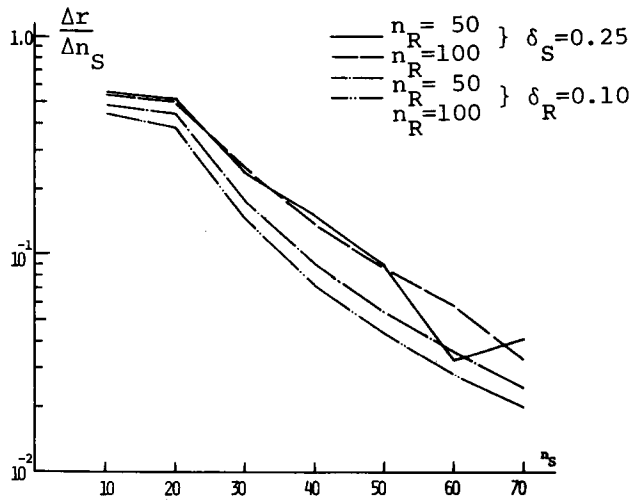

Fig. 4.15 Decreasing Ratio of Effectiveness

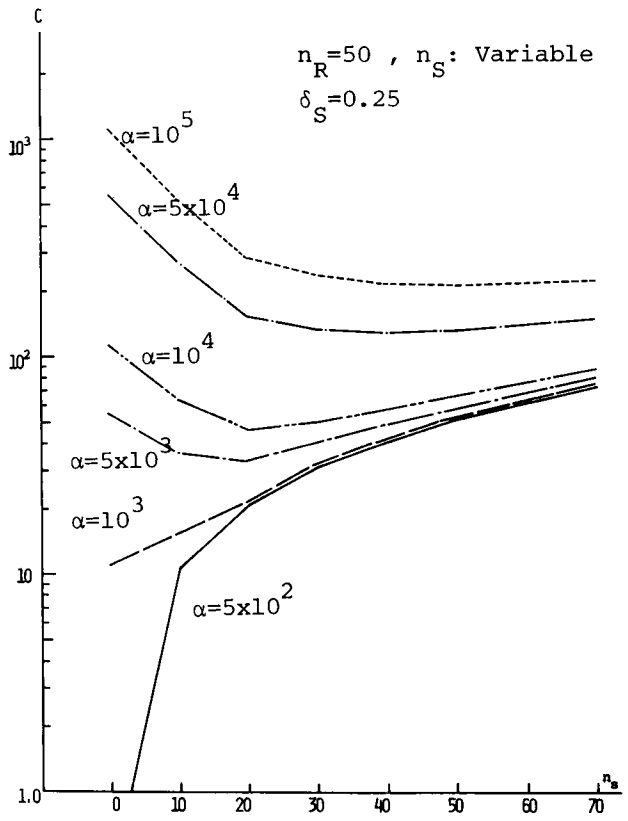

Fig. 4.16 Relation between Cost and Sampling Number

the likelihood function is quite sensitive to the obtained data, while in the case with large S_p it is insensitive to the data, because of the small number of obtained data.

" Optimum Sampling Number "

Based on the concept of the risk analysis, the optimum number of sampling is sought. Fig. 4.14 shows the change of effectiveness against the change of sampling number. As a matter of course, the effectiveness becomes larger as the sampling number increases. Comparing with the effectiveness obtained in the previous step, the sampling considered here is efficient to raise the effectiveness, within a range where the sampling number with respect to the load is less than 30. Fig. 4.16 gives the relation between cost C and sampling number n, where the parameter α denotes the ratio of failure cost C_f and sampling cost C_{yt}. It is seen in this figure that the optimum number of sampling, n_{opt}, becomes relatively large when α (e.g. C_f) is large. This implies that for the design of an important structure with a large failure cost, a large number of sampling is necessary to reduce the failure probability. Conversely, n_{opt} is very small or close to zero for small α. This tendency corresponds to the case where the sampling cost is often larger than the benefit obtained by the reduction of failure probability.

4.5 Minimum-Weight Design of Rigid Frames with Failure Probability Constraint

Design Formulation[53)]

In this section, the minimum-weight design of rigid frames is outlined based on the reliability concepts. As F. Moses[36)] and others mentioned, the minimization with a probability level moves the design away from having many active individual constraints. However, it is naturally anticipated that the safety analysis process will have more complicated and difficult features.

The minimum-weight design procedure is formulated as follows :

Find A_i $(i = 1, \cdots\cdots, m)$

such that

$$W = K \sum_{i=1}^{m} A_i L_i \rightarrow \text{Minimize} \qquad (4.62)$$

subject to

$$p_f \leq p_{fa} \qquad (4.63)$$

where A_i : the cross sectional area of the i-th member
L_i : the length of the i-th member
K : constant
m : number of members
W : total weight
p_{fa} : allowable failure probability

Then, according to Ridha's work[54], the cross sectional area can be expressed by the full plastic moment.

$$A_i = \frac{1}{3}\left(\frac{36}{S_{yi}}\right)^{2/3} M_i^{2/3} \qquad (4.64)$$

where S_{yi} : the yielding stress of the i-th member
M_i : the full plastic moment of the i-th member

Taking M_i as the design variable, this problem is reduced to a non-linear programming problem. The objective function is calculated from Eqs (4.62) and (4.64), and the overall failure probability p_f is obtained from Eq.(4.20).

There is, however, a point to be careful about in the use of Eq. (4.20) for the minimum-weight design. While the cross sectional areas of members are prescribed in the analysis, they are variables and are to be specified in the design procedure. Through the optimization, the dominant failure modes may move from one to others. Then, the ordering of possible modes is influential on the accuracy of Eq.(4.20). Its second terms (two-events-occurrence probabilities) are found to be the maximum value among those probabilities which are related to a failure mode. Here, the failure modes are successively ordered from

those with the largest failure probability. Since this process is employed in each design stage, it will require some time for computing the data.

Approximate Design Method Using Decomposition Technique[55)]

As mentioned above, the minimum-weight design of rigid frame is reduced to a mathematical programming problem. Then, using Eq.(4.20) for the safety analysis, it is easily performed with the aid of an appropriate mathematical programming technique. However, there still remain some problems in its direct application to large structural systems. As the number of the failure modes increases, the implementation of Eq.(4.20) will consume more time, especially in the calculation of the covariance matrices. This procedure, of course, does not require so many runnings different from the usual deterministic analysis. However, since this procedure appears many times in the design process, the total computation time will become enormous. In this study, an approximation based on the decomposition concepts is introduced to remove the problem concerned with computation. It is not likely that all collapse modes will be critical for the deterministic design. While the critical modes are active as constraints, the remainders are not and they don't contribute to the resulting solution. If the active modes whose numbers are the same as those of the design variables are taken as the constraints, the optimum set of values on weight and design variables can be obtained. This can be understood by corresponding the active modes to the " basis " of the coordinates of the design space.

Here, paying attention to this fact, the possible modes are divided into two groups : a basic group and non-basic group of modes, which correspond to the groups of active and non-active modes. It is, however, to be noted that this explicit classification of modes is hardly allowed in the probabilistic design. This is because all modes contribute to the evaluation of a system failure probability, even if some of them are very small. Furthermore, since the probabilistic design has only one constraint, a sufficient number of modes is not explicitly determined. Therefore, the basic and non-basic modes can

be expressed merely by the terms of " dominant " and " indominant ", respectively.

The basic modes are possibly selected in the following way. If the modes, which have the larger probability and are less correlated, are chosen to be part of the basic modes, the resulting solution may show a good agreement with the exact one. Then, the failure probability of the entire system is calculated by neglecting the effects of the non-basic modes.

$$p_f \simeq P_r(F_b) \tag{4.65}$$

where F_b denotes the failure event induced by at least one of the basic modes.

It should be noted that some treatment is necessary to use Eq. (4.65) for the design process, because it underestimates the failure probability. Assuming that the non-basic modes are independent of each other and uncorrelated to the basic modes, p_f can be expressed as

$$p_f = P_r(F_b) + \sum_{i=q+1}^{n} P_r(F_i) \tag{4.66}$$

in which q and n denote the numbers of the basic modes and all modes, respectively. While the use of this equation removes the problem of underestimation, it still involves the problem of the execution time for the case of complex structures having a large number of non-basic modes. For such cases, it is a considerably prohibitive task to calculate the failure probabilities of all the non-basic modes. Then, it is to be desired that safety is guaranteed without using the non-basic modes in the design process.

E. Vanmarcke[56] proposed an iterative design scheme for the design of large systems. At first, the design is performed by solving a relatively simple auxiliary problem in which only a set of basic modes are considered in computing system failure probabilities. Next, by changing the set of basic modes, new designs are successively generated. At every step, the upper bounds on the objective function are followed by solving the formulation :

Find A_i

such that the objective function

$$W = K \sum_i A_i L_i \rightarrow \textit{Minimize} \qquad (4.67)$$

subject to

$$p_f \leq p_{fa} - p'_f \qquad (4.68)$$

where p'_f can be found by subtracting $P_r(F_b)$ from the system failure probability which was obtained by using the design variables of the earlier stage. This method is very useful, because it not only saves the core size and the execution time but also easily gives good solutions which satisfy the design requirement. However, it seems to have problems in convergency and applicability such as how many modes are appropriate for the basic modes, and when or by what the iteration should be terminated. If the structural system to be designed has more dominant modes than the employed basic modes, the resulting upper and lower bounds will not converge, and the modified allowable failure level may become negative for some special cases.

An iterative design method is proposed herein, based on Vanmarcke's method. An improvement of convergency is attempted. The number of basic modes is not fixed and new dominant modes are successively added as the design stage proceeds. The procedure is summarized as follows : (see Fig. 4.17)

1) Construct the possible failure mechanisms. Specify the number of basic modes as that of the independent design variables. Give the allowable failure probability level. Assume the initial values for the design variables.
2) Perform the failure probability analysis for the current set of design variables. Obtain the system failure probability and find the basic modes.
3) Solve the problem :

$$\textit{Minimize} \qquad W \text{ (scaled weight)} = \sum_{i=1}^{m} M_i L_i \qquad (4.69)$$

$$\textit{subject to} \qquad P_r(F_b^{(I)}) \leq p_{fa}^{(I)} \qquad (4.70)$$

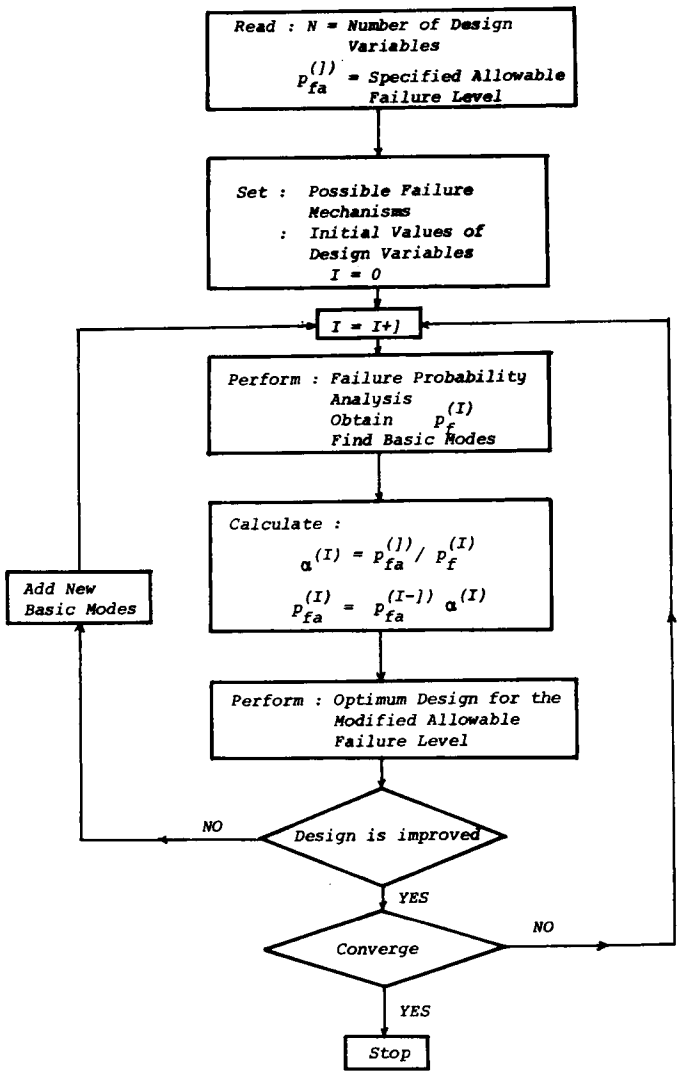

Fig. 4.17 Macro Flow Chart of Approximate Design Method Using Decomposition Technique

where $p_{fa}^{(I)}$ is the modified allowable failure level. This value is obtained by using the modification factor $\alpha^{(I)}$.

$$p_{fa}^{(I)} = p_{fa}^{(1)} \alpha^{(1)} \alpha^{(2)} \cdots\cdots\cdots \alpha^{(I-1)} \tag{4.71}$$

where

$$\alpha^{(I)} = p_{fa}^{(1)} / P_r(F_b^{(I)}) \tag{4.72}$$

Introducing the modification factor $\alpha^{(I)}$, the allowable failure level is forced to converge to an appropriate value.

4) If the improved design is not generated after two cycles, new basic modes are added for the next cycle. That number is found in the subsequent analysis by comparing the basic modes with those of the previous stage. If the design is improved, the basic modes are exchanged, but the number is unchanged.

5) Upon proceeding to the iterative process, the final design is achieved when the basic modes are not changed, or the difference between the predetermined failure level and the calculated failure probability is sufficiently small.

Design Examples

" Minimum-Weight Design of Portal Frame "

By using Eq.(4.20) for the safety analysis, a simple portal frame, shown in Fig. 4.1, is designed to minimize its total weight or its cost with some specified allowable probability levels. The obtained results are shown in Table 4.8 and Table 4.9, and compared with the results obtained by J. Stevenson[25] as well as the results based on the assumption of the independence of the failure modes. The probability of each failure mode is affected by its mean value and variance. For example, the failure modes, Z_1 and Z_2, have nearly equal central safety factors, but their failure probabilities have a relatively large difference. This is due to the difference of their variances. Then, one will reach the conclusion that the number of independent design variables, which are included in the failure modes, is very important in the probabilistic design. Therefore, the failure modes which are considered to be dominant in the deterministic design do not always become dominant from the probabilistic point of view.

Table 4.8 Input Data for Optimum Design of Single Bent Frame

L = 10 FT

Case No.	Initial Values (K-FT) M_C	M_B	Load (K) P_1	P_2	Coefficient of Variation M_C	M_B	P_1	P_2	Prob. of Failire to be allowed
1	220	260	20	30	0.10	0.10	0.10	0.10	0.08
2	320	360	20	30	0.10	0.10	0.10	0.10	0.008
3	320	360	20	30	0.10	0.10	0.10	0.10	0.0008
4	380	420	20	30	0.10	0.10	0.10	0.10	0.00008
5	320	360	20	30	0.10	0.10	0.05	0.05	0.0008
6	320	360	20	30	0.10	0.10	0.15	0.15	0.0008
7	320	360	20	30	0.10	0.10	0.20	0.20	0.0008

Table 4.9 Numerical Results of Single Bent Frame Example

a) Optimum Solutions

Case No.	Final (K-FT) M_C	M_B	Object Function	Prob. of Failure	Prob. of Failure (Independent)
1	171.12	188.01	197.41	0.888×10^{-1}	0.163
2	278.95	219.14	213.61	0.800×10^{-2}	0.160×10^{-1}
3	195.06	241.68	227.66	0.798×10^{-3}	0.149×10^{-2}
4	190.51	247.72	240.07	0.798×10^{-4}	0.124×10^{-3}
5	168.98	229.61	215.99	0.800×10^{-3}	0.142×10^{-2}
6	208.63	266.66	241.36	0.800×10^{-3}	0.151×10^{-2}
7	238.48	285.19	256.05	0.798×10^{-3}	0.157×10^{-2}

b) Failure Probabilities of Individual Modes

Case No.	z_1	z_2	z_3	z_4	z_5	z_6	z_7	z_8
1	0.573×10^{-2}	0.572×10^{-1}	0.543×10^{-1}	0.0	0.0	0.0	0.218×10^{-2}	0.183×10^{-2}
2	0.463×10^{-2}	0.653×10^{-2}	0.472×10^{-2}	0.0	0.0	0.0	0.115×10^{-3}	0.479×10^{-4}
3	0.635×10^{-3}	0.416×10^{-3}	0.434×10^{-3}	0.0	0.0	0.0	0.207×10^{-5}	0.137×10^{-5}
4	0.339×10^{-4}	0.577×10^{-4}	0.319×10^{-4}	0.0	0.0	0.0	0.358×10^{-6}	0.745×10^{-7}
5	0.499×10^{-3}	0.497×10^{-3}	0.413×10^{-3}	0.0	0.0	0.0	0.720×10^{-5}	0.256×10^{-5}
6	0.413×10^{-3}	0.669×10^{-3}	0.425×10^{-3}	0.0	0.0	0.0	0.459×10^{-5}	0.145×10^{-5}
7	0.547×10^{-3}	0.551×10^{-3}	0.469×10^{-3}	0.0	0.0	0.0	0.225×10^{-5}	0.121×10^{-5}

c) Safety Factors for Mean Load and Moment Resistance

Case No.	z_1	z_2	z_3	z_4	z_5	z_6	z_7	z_8
1	1.25	1.20	1.22	3.42	3.59	3.51	1.33	1.37
2	1.46	1.32	1.39	3.57	3.97	3.77	1.44	1.54
3	1.61	1.46	1.53	3.90	4.37	4.13	1.58	1.70
4	1.83	1.55	1.69	3.81	4.65	4.23	1.64	1.85
5	1.53	1.33	1.43	3.38	3.98	3.68	1.42	1.57
6	1.78	1.58	1.68	4.15	4.74	4.45	1.70	1.85
7	1.90	1.75	1.82	4.77	5.24	5.00	1.91	2.02

Table 4.10 Comparison of Proposed Method and Stevenson's Method

case No.	Final (K-FT)		Obj. Func.	Prob. of Failure	
	M_C	M_B		Stevenson's	Proposed M.
2	196.38	196.89	207.68	0.765×10^{-2}	0.325×10^{-1}
3	215.45	213.07	219.57	0.762×10^{-3}	0.831×10^{-2}

Table 4.10 indicates the failure probabilities calculated by the proposed method and Stevenson's method. The proposed method gives a greater value than Stevenson's method. The reasons are that Stevenson's method does not have the security of safety, and the assumption adopted in his work is not adequate, except for the case where the effect of variance is sufficiently small compared with the difference of the mean values.

" Minimum-Weight Design of Two-Story Single-Bay Frame "

A two-story single-bay model is employed to demonstrate the approximate design method based on the decomposition concept. The optimization is performed by the SUMT incorporating Powell's direct search technique, which does not require the derivatives of the functions. The possible modes are divided into basic and non-basic modes. This model has more than fifty collapse mechanisms. It is difficult to specify the appropriate basic modes at the start of the design process, because the dominant modes may change at any stage of the optimization. Here, their selection is automatically carried out at each design stage.

At first, the example frame model is designed by using Eq.(4.66) in computing the system failure probability. Then, sixteen modes are used for the basic modes. While this method needs less calculation time than the entire mode design, it gives a heavier design. (see Table 4.11)

Next, according to Vanmarcke's method, some designs are generated, where 8 and 16 are employed as the number of basic modes so as to investigate its influence. As shown in Table 4.11 and Fig. 4.18, infeasible designs are generated at the first design cycle. These are induced by the lack of effects of the non-basic failure modes. Next, upper and lower bounds on weight are produced in turn, and they are conservative and unconservative, respectively. In both cases, safety is examined by calculating the system failure probability with an analysis of all the modes.

For the case of 16 modes, the following items are observed from Table 4.11. The approximate method requires only 20 seconds of computation for one iteration, while the complete mode design requires

Table 4.11 Numerical Results of Two-Story Single-Bay Frame Design

a) Decomposition Design with 8 Basic Modes (Vanmarcke's M.)

Iteration Number	X_1	X_2	X_3	X_4	Scaled Weight	Prob. of Failure
1	69.83	39.12	62.73	62.53	46,842	0.0159
2	75.95	43.26	71.00	71.78	52,398	0.0051
3	69.54	41.14	65.23	61.28	47,438	0.0137
4	74.12	41.34	67.55	67.64	50,132	0.0078
5	69.54	41.14	65.23	61.28	47,438	0.0137
6	74.12	41.34	67.55	67.65	50,132	0.0078

$X_1 \sim X_4$: Design Variables (Moment Resistances [K-FT])

b) Decomposition Method with 16 Basic Modes (Vanmarcke's M.)

Iter. Number	X_1	X_2	X_3	X_4	Scaled Weight	Prob. of Failure
1	73.26	41.63	65.57	63.48	48,788	0.01025
2	72.07	40.42	66.91	65.49	48,978	0.00991
3	74.72	40.61	64.60	64.41	48,868	0.01021
4	73.89	38.96	68.08	64.69	49,002	0.009925
5	74.71	40.70	64.61	64.41	48,886	0.010167
6	75.31	40.58	66.21	62.14	49.020	0.009934

Calculation Time 20 sec./ Iteration

c) Entire Mode Design

Entire Design	71.69	40.79	67.25	64.93	48,932	0.009993

Calculation Time 150 sec.

d) Approximate Design (Using Eq.(4.66))

Approx. Design	79.52	38.98	66.30	65.53	49,066	0.009956

Calculation Time 120 sec.

e) Proposed Iterative Design Method

Iter. Number	X_1	X_2	X_3	X_4	P_{fa}	P_f	Scaled Weight	No. of Basic Modes
1	63.02	33.54	61.38	62.20	0.01000	0.03716	44,628	4
2	55.63	67.75	58.40	49.97	0.02691	0.03887	46,350	4
3	91.11	0.	91.03	91.91	0.00059	0.28290	54,808	4
4	69.83	39.12	62.73	62.53	0.01000	0.01592	46,842	8
5	71.28	42.85	68.30	67.72	0.00628	0.00791	50,030	8
6	74.39	39.21	65.73	65.41	0.00799	0.01015	48,948	8
7	72.09	39.36	68.08	65.31	0.00783	0.01019	48,968	8
8	71.17	42.56	64.80	66.39	0.00783	0.00971	48,984	8
9	70.32	42.82	64.31	62.35	0.01000	0.01211	47,960	12
10	77.52	40.22	65.60	65.51	0.00825	0.00866	49,770	12
11	71.08	41.81	66.43	63.07	0.00954	0.01007	48,878	12
12	73.57	40.90	64.24	65.89	0.00946	0.01001	48.920	12
13	73.57	40.89	64.33	65.93	0.00947	0.00995	48,944	12

X_i : Mean Plastic Moment of Member (K-FT)

i = 1, 3 : Beams of Upper and Lower Stories

i = 2, 4 : Columns of Upper and Lower Stories

Calculation Time 118 sec.

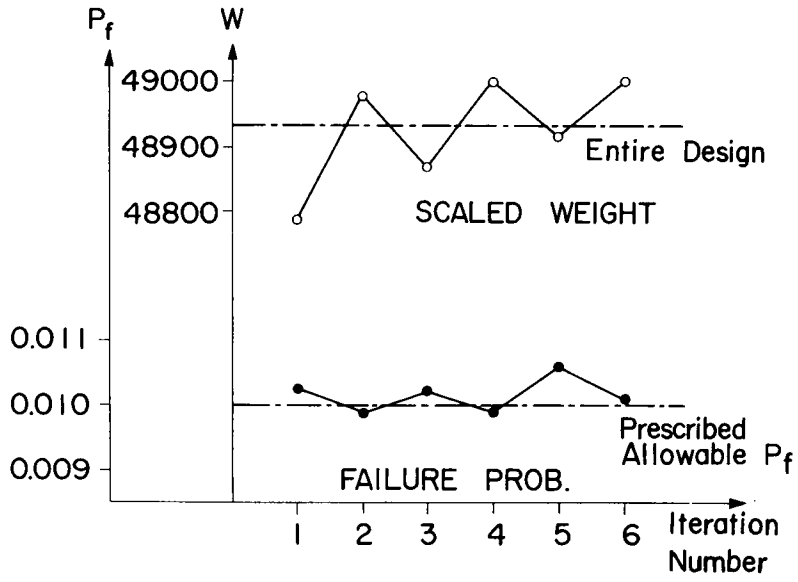

Fig. 4.18 Convergency of Decomposition Method

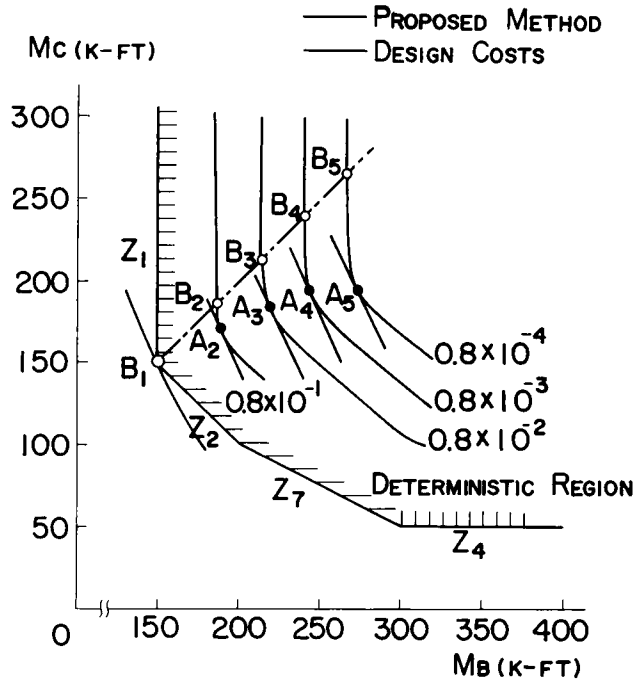

Fig. 4.19 Design Space of Single Bent Frame

150 seconds. Also, the results show acceptable values on weight, though the obtained values are slightly different in design variables from the exact values. Among the feasible designs, the second design shows the least weight, which is only 0.1 per cent heavier than the entire mode design. Other designs have larger failure probabilities than this design in spite of heavier weights. This fact may imply that the optimization for this problem is very sensitive to the change of the allowable failure level. It may also imply that the induced constraint surface does not have the distinct vertices which are observed in linear programming problems. The design space obtained for a two-variable problem indicates this tendency. (see Fig. 4.19)

Taking 8 as the numer of basic modes, this method does not give good solutions, for which the iterative procedure is terminated after four cycles, because the solutions hitherto bigin to diverge as shown in Table 4.11. Then, there are considerably large gaps on the weights of the upper and lower bounds. The accuracy of the decomposition method is explicitly dependent on how to select the basic modes. Table 4.11(e) presents the results obtained by the proposed iterative method. The design starts with the same number of basic modes as that of the independent variables. (i.e. 4) After three iterations, four modes are newly added to the basic modes. After five more cycles, the number is changed to 12, and an acceptable design is generated at the 13th cycle. This method requires 118 seconds in computation, but the calculation time can be reduced by starting from more basic modes. The first three steps contribute nothing to the final solution, and they should be eliminated. Also, this method gives a good design with only 8 basic modes. The obtained design is only 0.03 per cent heavier than the entire mode design. The convergency may be improved by introducing the modification factor.

4.6 Minimiu-Weight Design of Trussed Systems with Failure Probability Constraint[57)-59)]

The approximate design method proposed in the previous section is

applicable for the design of trussed systems. For indeterminate trusses, the failure modes can be formulated in the same fashion as that of rigid frames. In this section, the truss design including a variation of geometry is investigated on the basis of the reliability concept.

Optimality Condition

Based on the reliability concept, the minimum-weight design of trussed systems is formulated as

Find A_i , X_j

such that

$$Z = \rho \sum_{i=1}^{m} A_i(X_j)\ L_i(X_j) \rightarrow \textit{Minimize} \tag{4.73}$$

subject to

$$p_f(A_i, X_j) \leq p_{fa} \tag{4.74}$$

in which p_f is affected by the values of cross sectional areas and nodal coordinates.

Since the above design problem has a single constraint with respect to the system failure probability, it is useful to employ Lagrange's multiplier method as the optimization scheme. Then, the problem can be rewritten as

$$\left.\begin{aligned} \Phi &= Z(A,X) + \lambda(p_f(A,X) - p_{fa}) \\ \frac{\partial \Phi}{\partial X} &= \frac{\partial Z}{\partial X} + \lambda \frac{\partial p_f}{\partial X} = 0 \\ \frac{\partial \Phi}{\partial A} &= \frac{\partial Z}{\partial A} + \lambda \frac{\partial p_f}{\partial A} = 0 \\ \frac{\partial \Phi}{\partial \lambda} &= p_f - p_{fa} = 0 \end{aligned}\right\} \tag{4.75}$$

where Φ and λ are Lagrangean and Lagrange's multiplier, respectively.

For statically determinate truss problems, H. Switzky[60] presented an optimality condition which contributes to the minimum-weight design. The failure probability of statically determinate trusses can be

approximated for the case where the failure probability of each member, p_{fi}, is quite small.

$$p_f = \sum_{i=1}^{m} p_{fi} \tag{4.76}$$

By using Eqs (4.75) and (4.76), the partial derivative of the weight with respect to the weight of the i-th member is set equal to zero. This results in

$$\frac{\partial}{\partial z_i}\{ z + \lambda(p_{fa} - \sum_{i=1}^{m} p_{fi})\} = 1 - \lambda \frac{\partial p_{fi}}{\partial z_i} = 0 \tag{4.77}$$

$$\therefore \quad \frac{1}{\lambda} = \frac{\partial p_{fi}}{\partial z_i} \tag{4.78}$$

Eq.(4.78) implies that at an overall minimum weight, changes in the failure probability of each member are proportional to its change in weight, and that this ratio is independent of the respective members. Furthermore, if it is assumed that the ratio of the weight of a member to the overall weight is relatively insensitive to the overall failure probability, the following relation can be available for reducing a valuable optimality condition.

$$\left(\frac{z_i}{\Sigma z_i} \right)_{p_{f1}} = \left(\frac{z_i}{\Sigma z_i} \right)_{p_{f2}} \tag{4.79}$$

Eqs (4.77) and (4.79) are satisfied if

$$\frac{p_{fi}}{p_{fa}} = \frac{z_i}{z} \tag{4.80}$$

Eq.(4.80) indicates that a minimum-weight design will result when the failure probability of each component is proportional to its weight.

Approximate Design Method

By using the optimality condition (i.e. Eq.(4.80)) at each design step, the optimal geometry of the truss can be approximately sought as follows :

Step 1 Assume the initial geometry (i.e. nodal coordinates $X^{(0)}$)

Step 2 Perform the structural analysis of the truss with the geometry determined in the previous step.

Step 3 Obtain the optimum set of cross sectional areas by using the calculated values of member forces and member lengths.

Step 4 Search for the most effective direction in the design space which consists of nodal coordinates, and calculate the distance α with the aid of a one-dimensional optimization scheme.

Step 5 Then, the improved geometry can be defined as

$$X^{(I)} = X^{(I-1)} - \alpha S \tag{4.81}$$

Step 6 If the values of $X^{(I)}$ converge, the procedure is terminated. Otherwise, return to Step 2 and repeat Steps 3 - 5.

The direction S can be easily calculated for the case in which the member resistances and member forces have normal distributions. Differentiating the weight,

$$\frac{\partial Z}{\partial X_j} = \rho \left\{ \sum_{i=1}^{m} \left(\frac{\partial A_i(X)}{\partial X_j} L_i(X) + A_i(X) \frac{\partial L_i(X)}{\partial X_j} \right) \right\} \tag{4.82}$$

Then, the cross sectional areas $A_i(X)$ can be expressed by the member force $F_i(X)$ induced by the unit load, based on Switzky's optimality condition.

$$A_i(X) = \frac{\mu_S \mu_{R_i} + \beta_i \sqrt{(\sigma_{R_i}^2 \mu_S^2 + \mu_{R_i}^2 \sigma_S^2) - \beta_i^2 \sigma_{R_i}^2 \sigma_S^2}}{(\mu_{R_i}^2 - \beta_i^2 \sigma_{R_i}^2)} F_i(X)$$

$$= D_i F_i(X) \tag{4.83}$$

where μ_S , μ_{R_i} : the mean values of the applied force and member resistance of the i-th member

σ_S^2 , $\sigma_{R_i}^2$: the variances of the applied force and member resistance of the i-th member

$$\beta_i = -\Phi^{-1}(p_{fai})$$

p_{fai} and $\Phi(\cdot)$ denote the allowable level assigned to the i-th member and the standard normal distribution function, respectively.
Using Eq.(4.83), the weight and its derivatives can be found to be

$$Z = \rho \sum_{i=1}^{m} D_i F_i(X) L_i(X) \tag{4.84}$$

$$\frac{\partial Z}{\partial X_j} = \rho \{ \sum_{i=1}^{m} (D_i \frac{\partial F_i(X)}{\partial X_j} L_i(X) + D_i F_i(X) \frac{\partial L_i(X)}{\partial X_j})\} \tag{4.85}$$

Numerical Examples

Consider a 4-panel model, where the member resistances and applied load are random. Assume now that both of them have independent nomal distributions. The numerical results are given in Table 4.12 and Fig. 4.20, where the used mean values and standard deviations are μ_R = *2040 kg/cm*^{2}, μ_S = *20000 kg*, σ_R = *204 kg/cm*^{2} and σ_S = *4000 kg*, respectively. Also, the employed allowable level of failure probability is *0.04*. It can be found from Fig. 4.20 that the geometry obtained by the probabilistic method is not so different from that obtained by the deterministic method. That is, for statically determinate systems, both methods give an identical optimal geometry, though the values of the cross sectional areas differ somewhat from each other. It should be noted that it is impossible to compare both methods in volume because the employed value of the allowable level, 0.04, does not correspond to the safety factor of the deterministic approach.

From Table 4.12, it is obtained that the introduction of geoemtrical variations presents an economic design, whose volume is 34.5 per cent less than the Pratt truss with a fixed geometry. The convergency is shown in Fig. 4.21. This shows the efficiency of the proposed method. This method requires only 7 seconds to reach the optimum point. Though the convergency depends on the initial values, the search procedure was terminated at the 5th step. The results for some design cases are given in Table 4.13. The truss becomes heavier as the value of the allowable level becomes smaller. However, all geometries obtained for these conditions show no distinct difference. Next, the buckling effect is taken into account. The resulting geometry is shown in Fig. 4.22.

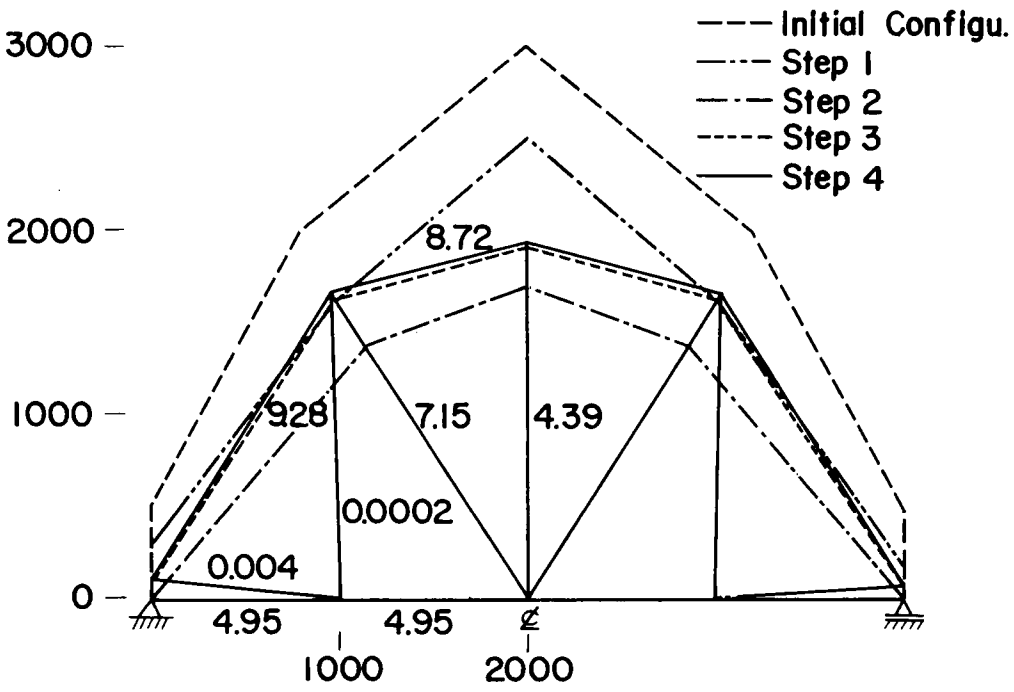

Fig. 4.20 Change of Geometry at Each Design Step

Table 4.12 Numerical Results of 4-Panel Model

	Pratt Truss	Variable Geometry
A_1 (cm^2)	8.66	9.61
A_2	8.66	8.98
A_3	11.76	4.99
A_4	0.0002	0.0002
A_5	8.66	0.49
A_6	16.64	8.93
A_7	11.76	7.15
A_8	8.66	4.96
A_9	0.0002	4.41
P_f	0.04	0.04
Volume (cm^3)	169101	112581

Table 4.13 Numerical Results under Some Design Conditions

	Case 1	Case 2	Case 3	Case 4	Case 5	Case 6	Case 7	Case 8	Case 9	Case 10	Case 11	Case 12	
A_1	11.71	17.29	15.02	10.75	10.26	19.38	15.45	12.12	12.48	12.94	13.82	15.15	(cm^2)
A_2	9.28	11.16	10.47	8.86	8.65	12.40	11.23	9.71	10.12	10.54	11.47	12.70	
A_3	0.00	0.06	0.04	0.07	0.04	0.04	0.04	0.04	0.06	0.01	0.04	0.04	
A_4	4.95	6.25	5.85	4.74	4.53	7.01	6.19	5.16	5.32	5.67	5.98	6.64	
A_5	0.00	0.04	0.04	0.04	0.04	0.04	0.04	0.04	0.04	0.04	0.04	0.04	
A_6	8.92	11.00	10.23	8.46	8.25	12.25	10.93	9.30	9.68	10.04	10.88	12.07	
A_7	7.15	8.68	8.13	6.81	6.66	9.68	8.69	3.51	7.78	8.09	8.78	9.36	
A_8	4.95	6.30	5.79	4.67	4.54	7.01	6.14	5.16	5.36	5.56	5.99	6.64	
A_9	4.39	5.44	5.06	4.19	4.05	6.06	5.41	4.61	4.76	4.98	5.34	5.93	
X_2	10.9	10.3	10.4	11.2	11.3	10.1	10.6	10.9	11.0	11.2	11.1	11.2	(m)
Y_2	19.3	18.3	18.3	19.5	19.9	17.8	18.0	19.2	19.5	19.5	19.6	19.7	
X_3	950.2	950.2	950.2	950.2	950.2	950.3	950.2	950.2	950.2	950.2	950.2	950.2	
Y_3	1675.4	1675.4	1675.4	1675.5	1675.5	1675.3	1675.4	1675.4	1675.4	1675.5	1675.4	1675.5	
Y_5	1939.8	1939.7	1939.7	1939.8	1939.8	1939.7	1939.8	1939.8	1939.8	1939.8	1939.8	1393.8	
P_{fa}	0.004	0.004	0.04	0.04	0.04	0.04	0.04	0.02	0.01	0.005	0.001	0.0001	
δ_p	0.2	0.2	0.2	0.2	0.2	0.3	0.3	0.2	0.2	0.2	0.2	0.2	
δ_R	0.1	0.17	0.15	0.07	0.05	0.17	0.13	0.1	0.1	0.1	0.1	0.1	
V	111768	137290	128118	106662	103823	152836	136829	117162	121658	126898	137105	152047	(cm^3)

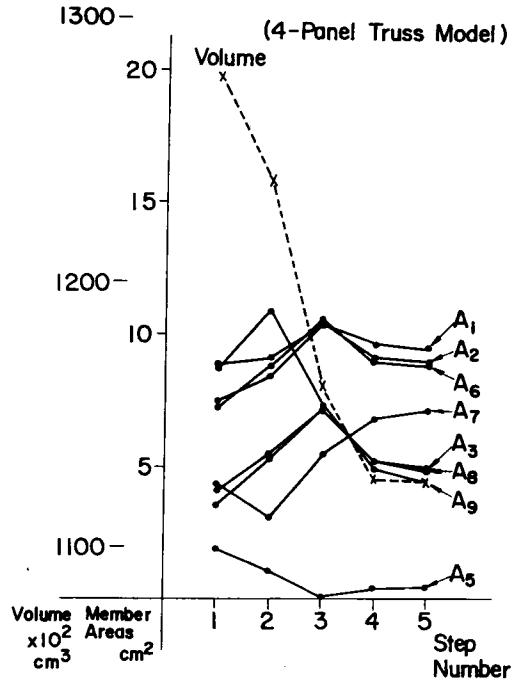

Fig. 4.21 Convergence of Objectives

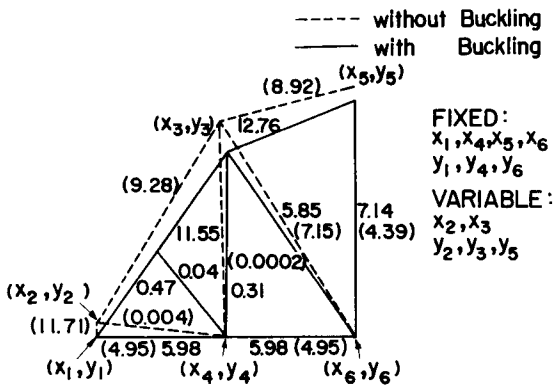

Fig. 4.22 Optimal Configuration of 4-Panel Model with Buckling Constraint

This shows a tendency similar to that of the deterministic method.

4.7 Conclusions

The safety analysis and minimum-weight design of framed structures are studied by using the failure probability as a measure of safety. The improvements on the upper and lower bounds of a system failure probability are attempted by considering the correlations between two or three failure events. With the aid of the fiducial statistics or Bayesian decision theory, the effect of statistical uncertainty with respect to the sampling on the estimation of failure probability is investigated. Based on the decomposition technique, an approximate design method is proposed to reduce the computational load. Also, a variation of geometry is treated in the design of truss, in which both the member strength and the applied load are considered to be random. Main results derived from the study in this chapter are as follows :

1) A considerably exact estimation of failure probability can be made for indeterminate structural systems, using the proposed method which takes the correlation between every two modes into account. This method is considered useful for practical computations, on account of less calculation load and the security of conservative evaluation of failure probability.
2) A simple mathematical model proposed herein proves to be acceptable for the rigid framed structures. A very close failure probability can be obtained by considering the effect of three-events-occurrence on the average. However, this model seems to be more suitable for examining the availability of the proposed method presenting an upper bound, because it consists of relatively complex procedures.
3) It is confirmed that statistical uncertainty can not be ignored in the evaluation of failure probability. Bayesian decision theory enables to combine the information obtained from sampling or experiments with the engineering judgements. However, it is difficult to apply Bayesian decision theory for all design cases, though it is of practical use to apply for the case where little information

is available.

4) Considering the effect of sampling number on the accuracy of the analysis of failure probability, the significance of information can be quantitatively recognized. By introducing the concept of risk analysis, the optimum number of sampling or experiment can be examined.

5) By taking the failure probability as the measure of safety, the minimum-weight design can be reduced to a mathematical programming problem with a single constraint, or to an unconstrained optimization problem. Many designs, whose weights are very close to the optimum one, are obtained through the optimization. This can be seen in the deterministic bridge design with the deflection constraint. If these designs are accepted as approximate solutions, the minimum-weight design will become simple and practical by utilizing the advantage that many various constraints can be reduced to one constraint.

6) The use of the decomposition technique makes the proposed analysis method effective in the redesign procedure. The classification of failure modes can clarify their contributions to the system failure. Conservative approximate designs can be obtained by using parts of possible modes. If a sufficient number of modes is taken as basic modes, the iterative scheme proposed by E. Vanmarcke is considered to be suitable. It can save the core size and make the calculation inexpensive. The iterative method proposed herein has similar merits. This method is superior to Vanmarcke's method with regard to convergency and applicability. There, the modified allowable failure level is forced to converge and the appropriate number of basic modes is sought for in the program.

7) By use of the optimality condition presented by H. Switzky, the optimal geometry can be easily obtained for statically determinate trusses in which the member strength and the applied load are random. Then, the obtained geometry is almost same as that of the deterministic design.

References for Chapter 4

1) The Task Committee on Structural Safety of the Administrative Committee on Analysis and Design of the Structural Division, " Structural Safety - A Literature Review ", Proc. ASCE, ST4, Apr., 1972, pp845-884
2) Ang, A. H-S. and Ellingwood, B. R., " Critical Analysis of Reliability Principles relative to Design ", Proceedings of the First International Conference on Applications of Statistics and Probability to Soil and Structural Engineering, Hong Kong, Sept., 1971, pp1-15
3) Freudenthal, A. M., " Safety of Structures ", Trans. ASCE, Vol.112, 1947, pp125-180
4) Freudenthal, A. M., " Safety and the Probability of Structural Failure ", Trans. ASCE, Vol.121, 1956, pp1337-1375
5) Freudenthal, A. M., " Safety, Reliability and Structural Design ", Proc. ASCE, ST3, March, 1961, pp1-16
6) Julian, O. G., " Synopsis of First Progress Report of Committee on Factors of Safety ", Proc. ASCE, ST4, July, 1957, pp1316(1)-1316(22)
7) Leve, H. L., " Reliability Framework for Structural Design ", Proc. ASCE, ST4, Aug., 1963, pp315-332
8) Broading, W. C., Diederich, F. W. and Parker, D. S., " Structural Optimization and Design Based on a Reliability Design Criterion ", J. of Spacecraft, Vol.1, No.1, Jan., 1964, pp56-61
9) Ang, A. H-S. and Amin, M., " Safety Factors and Probability in Structural Design ", Proc. ASCE, ST7, July, 1969, pp1389-1405
10) Brown, C. B., " Concepts of Structural Safety ", Proc. ASCE, ST12, Dec., 1960, pp39-59
11) Benjamin, J. R., " Probabilistic Structural Analysis and Design ", Proc. ASCE, ST7, July, 1968, pp1665-1679
12) Ang, A. H-S. and Amin, M., " Reliability of Structures and Structural Systems ", Proc. ASCE, EM2, Apr., 1968, pp671-691
13) Ang, A. H-S., " Extended Reliability Basis of Structural Design under Uncertainties ", Paper for Presentation at the SAE/AIAA/ ASME, 9th Reliability and Maintenability Conference, Detroit,

Michigan, July, 1970

14) Ellingwood, B. R. and Ang, A. H-S., " A Probabilistic Study of Safety Criteria for Design ", Tech. Rep. Univ. of Illinois, June, 1972

15) Ang, A. H-S., " Structural Risk Analysis and Reliability Based Design ", Proc. ASCE, ST9, Sept., 1973, pp1891-1909

16) Ellingwood, B. R. and Ang, A. H-S., " Risk-Based Evaluation of Design Criteria ", Proc. ASCE, ST9, 1974, pp1771-1787

17) Freudenthal, A. M., Garrelts, J. M. and Shinozuka, M., " The Analysis of Structural Safety ", Proc. ASCE, ST1, Feb., 1966, pp267-325

18) Veneziano, D., " A Theory of Reliability which Includes Statistical Uncertainty ", Proceedings of the 2nd International Conference on Applications of Statistics and Probability in Soil and Structural Engineering, Aachen, F.R.Germany, Sept., 1975, pp231-249

19) Yao, J. and Yeh, H., " Formulation of Structural Reliability ", Proc. ASCE, ST12, Dec., 1969, pp2611-2619

20) Shinozuka, M., Yao, J. and Nishimura, A., " On the Reliability of Redundant Structures ", Proceedings of the 6th International Symposium on Space Technology and Science, Tokyo, Dec., 1965

21) Hoshiya, M., " Reliability of Redundant Cable System ", Proc. ASCE, ST11, Nov., 1971, pp2773-2776

22) Hoshiya, M., " Monte Carlo Evaluation of Safety of Indeterminate Structure ", Proc. JSCE, No.205, Sept., 1972, pp147-154

23) Konishi, I., Shiraishi, N., Taniguchi, T. and Furuta, H., " Structural Analysis and Design of Rigid Frames Based on Plastic Theorem ", The Memoirs of the Faculty of Engineering, Kyoto Univ., Vol.37, Part 4, Oct., 1975, pp219-236

24) Ishikawa, N., " Iterative Optimal Plastic Design of Steel Frames ", Proc. JSCE, No.237, May, 1975, pp109-119

25) Stevenson, J., " Reliability Analysis and Optimum Design of Redundant Structural Systems with Application to Rigid Frames ", A Thesis submitted to Case Institute of Technology, 1968

26) Cohn, M. (Editor), " An Introduction to Structural Optimization Study No.1 ", Solid Mechanics Division, Univ. of Waterloo, 1969

27) Jorgenson, J. L. and Goldberg, J. E., " Probability of Plastic Collapse Failure ", Proc. ASCE, ST8, Aug., 1969, pp1743-1761

28) Castiati, E. and Sacci, G., " On the Reliability Theory of the Structures ", Meccanica, Dec., 1974, pp291-298

29) Moses, F., " Reliability of Structural Systems ", Proc. ASCE, ST9, Sept., 1974, pp1813-1819

30) Augusti, G. and Baratta, A., " Limit Analysis of Structures with Stochastic Strength Variations ", J. of Structural Mechanics, Vol.1, (1), 1972, pp43-62

31) Kawata, Y. et al, " Exercises of Mathematical Statistics (Suri Tokei Enshu) ", Shokabo Publishing, 1962 (in Japanese)

32) Shiraishi, N. and Furuta, H., " Safety Analysis and Minimum-Weight Design of Rigid Frames Based on Reliability Concept ", The Memoirs of the Faculty of Engineering, Kyoto Univ., Vol. XLI, Part 4, Oct., 1979, pp474-497

33) Cornell, C. A., " Bounds on the Reliability of Structural Systems ", Proc. ASCE, ST1, Feb., 1967, pp171-200

34) Tichy, M. and Vorlicek, M., " Safety of Reinforced Concrete Framed Structures ", International Symposium on the Flexural Mechanics of Reinforced Concretes, Miami, Fla., Nov., 1964, pp53-84

35) Tichy, M. and Vorlicek, M., " Statistical Theory of Concrete Structures ", Irish University Press, Shannon, 1972

36) Moses, F. and Kinser, D., " Optimum Structural Design with Failure Probability Constraints ", AIAA Journal, Vol.15, No.6, June, 1967, pp1152-1158

37) Moses, F. and Kinser, D., " Analysis of Structural Reliability ", Proc. ASCE, ST5, Oct., 1967, pp147-164

38) Moses, F., " Sensitivity Studies in Structural Reliability ", Chapter 1 of Structural Reliability and Codified Design (Editor N.C.Lind), Solid Mechanics Division No.3, Univ. of Waterloo, 1970, pp1-17

39) Baba, S., Nakagawa, N. and Naruoka, M., " Reliability Analysis with Uncertainties of the Measured Values ", Proc. JSCE, No.254, 1976, pp1-11 (in Japanese)

40) Fujino, Y., " Discussion to Reliability Analysis with Uncertainties of the Measured Values ", Proc. JSCE, No.268, 1977, pp193-133

(in Japanese)

41) Ang, A. H-S. and Tang, W. H., " Probability Concepts in Engineering Planning and Design, Volume I : Basic Principles ", John Wiley and Sons, Inc., 1975

42) Benjamin, J., " Probabilistic Models for Seismic Force Design ", Proc. ASCE, ST5, May, 1968, pp1175-1195

43) Turkstra, C. J., " Applications of Bayesian Decision Theory ", Structural Reliability and Codified Design (Editor : N.C.Lind), Study No.3, Univ. of Waterloo, 1970, pp49-71

44) Cornell, C. A., " Bayesian Statistical Decision Theory and Reliability-Based Design ", (Editor : A.M.Freudenthal), Pergamon Press, 1969, pp47-68

45) Fujino, Y. and Lind, N. C., " Proof-Load Factors and Reliability ", Proc. ASCE, ST4, Apr., 1977, pp853-870

46) Veneziano, D., Meli, R. and Rodriguez, M., " Proof Loading for Target Reliability ", Proc. ASCE, ST1, Jan., 1978, pp79-93

47) Shinozuka, M., " Method of Safety and Reliability Analysis ", (Editor : A.M.Freudenthal) Int. Conf. of Structural Safety and Reliability, Pergamon Press, 1969, pp11-45

48) Shinozuka, M., " Structural Safety and Optimum Proof Load ", Symposium on Concepts of Structural Safety and Methods of Design, IABSE, London, Sept., 1969, pp47-57

49) Konishi, I., Kitagawa, T. and Katsuragi, M., " Structural Reliability Analysis Considering Strength Assurance Level ", (Editor : A.M.Freudenthal et al), Reliability Approach in Structural Engineering, Maruzen, 1975, pp91-104

50) Shiraishi, N., Furuta, H., Nakano, M. and Goto, K., " A Consideration on Structural Reliability Analysis Based on Bayes Theorm ", Annual Meeting of JSCE, Kansai Branch, I-54, 1978 (in Japanese)

51) Konishi, I. and others, " Reliability and Safety of Steel Structures ", JSSC, Vol.13, No.144, 1977, pp1-40 (in Japanese)

52) Vanmarcke, E. H., " Risk and Decision in Engineering for Natural Hazards Protection ", Joint U.S.-S.E. Asia Symposium on Engineering for Natural Hazards Protection, Manila, Phillipine, Sept., 1977

53) Hilton, H. and Feigen, M., " Minimum Weight Analysis Based on

Structural Reliability ", J. of Aerospace Science, Vol.27, No.9, Sept., 1960, pp641-652

54) Ridha, R. and Wright, R., " Minimum Cost Design of Frames ", Proc. ASCE, ST4, Aug., 1967, pp165-183

55) Shiraishi, N., Taniguchi, T. and Furuta, H., " A Consideration on Optimum Design of Rigid Frames Based on Reliability Theory ", Annual Meeting of JSCE, Kansai Branch, I-23, 1976 (in Japanese)

56) Vanmarcke, E. H., " Matrix Formulation of Reliability Analysis and Reliability-Based Design ", Int. J. of Computers and Structures, Vol.3, 1971, pp757-770

57) Kalaba, R., " Design of Minimum-Weight Structures for Given Reliability and Cost ", J. of Aerospace Sciences, Vol.29, Sept., 1962, pp355-356

58) Switzky, H., " Minimum Weight Design with Structural Reliability ", AIAA 5th Annual Structures and Materials Conference, 1964, pp316-322

59) Ghista, D., " Structural Optimization with Probability of Failure Constraint " NASA TN-3777, 1966, pp1-15

60) Switzky, H., " Minimum Weight Design with Reliability ", J. of Aircraft, Vol.2, May-June, 1965, pp228-232

Chapter 5 Safety Index and Its Application to Reliability Analysis

5.1 Reliability Analysis Based on Second-Moment First-Order Approximation

It has been widely recognized that probability theory provides a more accurate engineering representation of reality. Namely, uncertainties in structural performance, which are due to the uncertainties involved in applied forces and in structural resistances, can be analyzed rationally only with probability. The classical reliability theory in which the failure probability is used as the measure of safety had been developed on the basis of pure probability theory, and its theoretical framework was already established in 1960's.

Despite of the various advantages in the safety analysis and design, this approach has not been explicitly adopted as a basis for the standard structural practice in civil engineering. As C. A. Cornell pointed out[1], there are several problems which obstruct the development of probability-based design in civil engineering. Those obstacles are related with the characteristic properties of civil engineering design :

1. The uncertain factors include those about which there is imcomplete knowledge and those for which the engineering analysis is possible but not economically justified.
2. Much of uncertainty, which is of a fundamentally nonstatistical nature, takes a quite important role in the performance predictions of civil engineering structures.
3. The new design code will presumably afford some minor increase in complexity over present codes.

In order to remove the above problems, C. A. Cornell[2)3)] proposed a new reliability approach called the second-moment first-order approach. In this approach, all uncertainties are treated in a uniform manner, namely the simplest and most familiar measures of dispersion : standard deviations or coefficients of variation. As the measure of

safety, he used the safety index which is determined solely from the means and the standard deviations or coefficients of variation. Because of the simplicity, flexibility and easiness of treatment, this approach has been proven greatly adaptable to application in practical structural design codes and are being implemented in several independent code systems in North America and Europe.[4)-6)]

However, the code formats using the safety index suffered to a greater or smaller degree from arbitrariness, lack of invariance under a change of formulation of the failure criteria consistent with the laws of algebra and mechanics. A. M. Hasofer and N. C. Lind[7)8)] presented a new definition of safety index, by which the " invariance " problem is almost overcome. By use of their definition of safety index, fundamental characteristics of safety index is studied here, placing attention on the following subjects : the physical and probabilistic significance of safety index, the effect of statistical uncertainty on the safety index, the calculation of safety index for the case with many possible failure modes.

5.2 The Influence of Statistical Uncertainty on Safety Index

In general, structural safety is examined in the following, by using structural resistance R and load effect S.

$$Z = R - S \tag{5.1}$$

where $Z \geq 0$: safe condition

$Z < 0$: failure condition

C. A. Cornell called Eq.(5.1) " safety margin " and also defined the safety index β by means of the mean value μ_Z and the standard deviation σ_Z of safety margin Z.

$$\beta = \mu_Z / \sigma_Z \tag{5.2}$$

Supposing that R and S are statistically independent of each other, β can be calculated as

$$\beta = (\mu_R - \mu_S) / \sqrt{\sigma_R^2 + \sigma_S^2} \tag{5.3}$$

μ and σ^2 in Eqs (5.2) and (5.3) represent the population mean and population variance, which should be probabilistically estimated from a lot of samples or data. It is, however, impossible to collect a sufficient number of available data for estimating the characteristics of the structural resistances and the applied forces in the field of civil engineering. Then, the population means and variances ought to be estimated by use of the means and variances of the measured data. If the number of available data is quite small, the value of safety index calculated by Eq.(5.3) becomes unreliable on account of the errors involved in the estimation of the characteristics. The concept of the fiducial statistics[9)10)] can be considered useful to deal with such statistical uncertainties in the calculation of safety index.

The probability density functions of the population mean and variance including the effect of statistical uncertainty can be obtained by using the fiducial statistics, because it treats the characteristics of population as variables different from usual classical statistics. Supposing that a random variable X is normally ditributed, the probability density function of X is

$$f_X(X) = \frac{1}{\sqrt{2\pi}\,\sigma_X} \exp\left(1 - \frac{(X - \mu_X)^2}{2\sigma_X^2} \right) \qquad (5.4)$$

in which μ_X and σ_X^2 are considered to be unknown.
If n independent samples are obtained from a population of X, the sample mean $\bar{X}$ and sample variance S_X^2 are independent of each other, and also $\bar{X}$ and nS_X^2/σ_X^2 follow to the normal distribution $N(\mu_X, \sigma_X^2/n)$ and χ^2- distribution $\chi^2(n-1)$, respectively. Then, the joint probability density function of $\bar{X}$ and S_X can be expressed as

$$f_{\bar{X},S_X}(\bar{X},S_X) = C \frac{1}{\sigma_X^2} \left(\frac{S_X}{\sigma_X} \right)^{n-2} \exp\left(- \frac{n}{2\sigma_X^2} \{ (\bar{X}-\mu_X)^2 + S_X^2 \} \right) \qquad (5.5)$$

where

$$C = \frac{2^{n/2}}{2^{n/2-1}\sqrt{\pi}\,\Gamma((n-1)/2)} \qquad (5.6)$$

$\Gamma(\cdot)$: gamma function

By use of the fiducial statistics, Eq.(5.5) can be transformed to the joint density function of μ_X and σ_X with the exchange of $d\bar{X} \cdot dS_X / S_X$ and $d\mu_X \cdot d\sigma_X / \sigma_X$.

$$f_{\mu_X,\sigma_X}(\mu_X,\sigma_X) = C \frac{1}{\sigma_X^2} \left(\frac{S_X}{\sigma_X} \right)^{n-1} exp\left(- \frac{n}{2\sigma_X^2} \{ (\bar{X}-\mu_X)^2 + S_X^2 \} \right) \quad (5.7)$$

When the structural resistance R and load effect S are independent and normally distributed, the safety margin Z (Eq.(5.1)) is also normally distributed. Then, the joint probability density function of μ_Z and σ_Z, $f_{\mu Z,\sigma Z}(\mu_Z,\sigma_Z)$, can be obtained in the same form as Eq.(5.7), by replacing X with Z. Furthermore, performing the transformation of (μ_Z, σ_Z) to (β,σ_Z), the joint probability density function of β and σ_Z can be obtained as follows :

$$f_{\beta,\sigma_Z}(\beta,\sigma_Z) = f_{\mu_Z,\sigma_Z}(\mu_Z,\sigma_Z) \left| \frac{\partial(\mu_Z,\sigma_Z)}{\partial(\beta,\sigma_Z)} \right|$$

$$= 2C \frac{1}{\sigma_Z} \left(\frac{S_Z}{\sigma_Z} \right)^{n-1} exp\left(- \frac{n}{2\sigma_Z^2} \{ (\bar{Z}-\beta\sigma_Z)^2 + S_Z^2 \} \right) \quad (5.8)$$

The probability density function of β, $f_\beta(\beta)$, can be calculated by integrating Eq.(5.8) with respect to σ_Z.

$$f_\beta(\beta) = 2C \int_0^\infty \frac{1}{\sigma_Z} \left(\frac{S_Z}{\sigma_Z} \right)^{n-1} exp\left(- \frac{n}{2\sigma_Z^2} \{ (\bar{Z}-\beta\sigma_Z)^2 + S_Z^2 \} \right) d\sigma_Z \quad (5.9)$$

Using Eq.(5.9), the mean and variance of safety index, μ_β and σ_β^2, can be obtained. However, the integration of Eq.(5.9) can not be performed in closed form, so the actual calculation must depend on a numerical integration which is often prohibitive and time-consuming.
For the reason, it is convenient to investigate the effect of statistical uncertainty on safety index with the aid of the first order approximation. Using the first order approximation, the expected value and variance of β can be expressed as

$$E[\beta] = E[\mu_Z] \; / \; E[\sigma_Z] \quad (5.10)$$

$$Var[\beta] = \frac{1}{E[\sigma_Z]^2} Var[\mu_Z] + \frac{E[\mu_Z]^2}{E[\sigma_Z]^4} Var[\sigma_Z] \qquad (5.11)$$

in which the expected values and variances of μ_Z and σ_Z are obtained by use of the probability density functions of μ_Z and σ_Z.

$$f_{\mu_Z}(\mu_Z) = C_\mu \frac{1}{S_Z} \left\{1 + \frac{(\bar{z}-\mu_Z)^2}{S_Z^2}\right\}^{-n/2} \qquad (5.12)$$

$$f_{\sigma_Z}(\sigma_Z) = C_\sigma \frac{1}{S_Z} \left(\frac{S_Z}{\sigma_Z}\right)^n exp\left(-\frac{nS_Z^2}{2\sigma_Z^2}\right) \qquad (5.13)$$

where

$$C_\mu = \frac{\Gamma(n/2)}{\sqrt{\pi}\,\Gamma((n-1)/2)} \quad , \quad C_\sigma = \frac{\sqrt{n}^{\,n-1}}{\sqrt{2}^{\,n-3}\,\Gamma((n-1)/2)} \qquad (5.14)$$

$$E[\mu_Z] = \bar{z} \qquad (5.15)$$

$$E[\sigma_Z] = S_Z\sqrt{\frac{n}{2}}\,\frac{\Gamma(n/2-1)}{\Gamma((n-1)/2)} \qquad (5.16)$$

$$Var[\mu_Z] = S_Z^2 / (n-3) \qquad (5.17)$$

$$Var[\sigma_Z] = S_Z^2\left[\frac{n}{n-3} - \frac{n}{2}\left\{\frac{\Gamma(n/2-1)}{\Gamma((n-1)/2)}\right\}^2\right] \qquad (5.18)$$

Substituting Eqs (5.15) - (5.18) to Eqs (5.10) and (5.11), the expected value and variance of β can be calculated.

Numerical Example

Let's consider that $\bar{z} = 800\ kg/cm^2$ and $S_Z = 210\ kg/cm^2$ are obtained as the sample mean and standard deviation, respectively. Then, using Eq.(5.9), the probability density function of β is obtained as shown in Fig. 5.1. Table 5.1 presents the means and standard deviations of β calculated by using the obtained probability density function and the first order approximation. These results indicate that the effect of statistical uncertainty is large when the number of measured data is

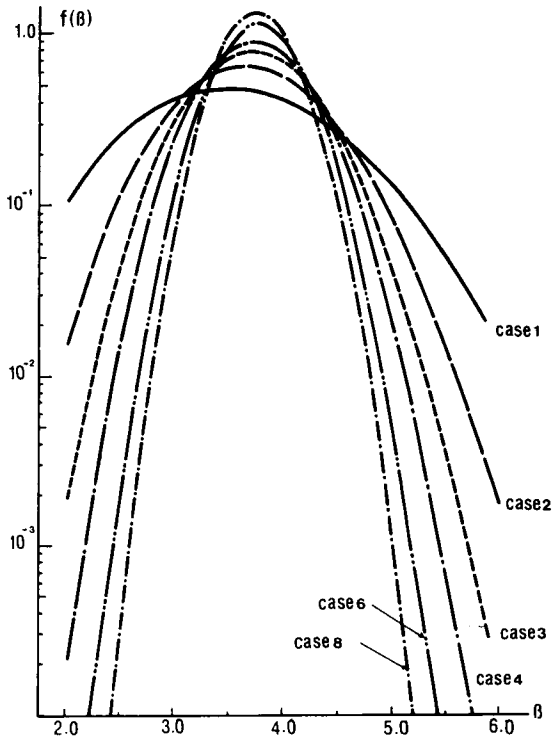

Fig. 5.1 Probability Density Function of Safet Index

Table 5.1 Mean Value and Standard Deviation of Safety Index

case	n	μ_β	σ_β	E[β]	$\sqrt{Var[\beta]}$
1	10	3.58703	1.02111	3.303	0.955
2	20	3.66991	0.78944	3.564	0.656
3	30	3.71389	0.65242	3.648	0.532
4	40	3.73767	0.56621	3.689	0.459
5	50	3.75208	0.50678	3.713	0.410
6	60	3.76170	0.46281	3.729	0.373
7	70	3.76853	0.42860	3.741	0.345
8	80	3.77367	0.40101	3.750	0.323

small. This implies that the safety index should be underestimated for the case where a large number of data is not available. According to the increase of the number of data, σ_β becomes smaller. This means that the safety index calculated by Eq.(5.2) becomes more reliable as the number of data increases. In this case, the dispersion of β tends to converge when n exceeds 70. The first order approximation gives a considerably good estimation for the mean value, whereas it gives a somewhat small value for the variance. It can be considered that the first order approximation is useful for examining the effect of statistical uncertainty, because it requires less calculation.

As described before, the fiducial statistics is useful for the estimation of safety index for a case in which statistical uncertainty is unavoidable. However, it is sometimes difficult even to obtain rough estimates of parameters, when the number of available data is quite small. In this case, the safety index should be estimated to some extent by means of engineering judgements, which are based on the inspirations and experiences of engineers. Then, such engineering judgements should be combined with the obtained statistical data. To do this, convenient is Bayesian decision theory in which engineering judgements are reflected in the determination of the prior distribution and the likelihood function.[11)-13)]

When a random variable Z is normally distributed, Bayesian decision theory presents the similar equations to Eqs (5.15) - (5.18) for estimating the characteristics of Z. However, simplification can possibly be achieved only when appropriate distributions of the characteristics are chosen by corresponding to the underlying random variable. Namely, if a " conjugate " of the distribution of the underlying random variable is chosen, a posterior distribution can be obtained. Otherwise, mathematical complications are unavoidable. For this reason, a more simplified manner is necessary to introduce both statistical uncertainty and engineering judgements into the safety analysis.

A. H-S Ang[14)] attempted to treat those effects by introducing a correction factor, such that

$$X = N_X \hat{X} \tag{5.19}$$

where X : random variable

$\hat{X}$: prediction model of X

N_X : correction factor

As he mentioned, his formulation is implicitly based on the philosophy of Bayesian probability. Fig. 5.2 shows the relationships between Ang's method and Bayesian treatment. It is seen that statistical uncertainty can be included in the correction factor and that the effects of other engineering uncertainties on safety index can be grasped.

The above comparison implies that it is convenient to take the statistical uncertainty into account by using the correction factor, ans also to perform the safety analysis by using the performance function including the correction factor. However, it should be noted that more sufficient examinations are necessary for the use of the simplified method proposed by A. Ang, because simplifications generally involve some large assumptions. Then, the strict treatment described before takes an important role in checking the availability of Ang's method.

5.3 Safety Index and Correction Factor

Before O. Ditlevesen[15], N. Lind[4] and others pointed out, it was widely believed that all second-moment formats were mutually consistent in the simple sense that the same safety margin could be prescribed. However, Cornell's format used in the previous section was found to prescribe relatively large safety margins if the resistance is highly dispersed, and as an alternative, Rosenblueth and Esteva's format[16] gave appreciably smaller values. A. M. Hasofer and N. C. Lind[7] presented a new definition of safety index to remove the inconsistency due to the lack of invariance under a change of formulation of the failure criteria.

Hasofer and Lind's Definition of Safety Index[7]

A. M. Hasofer and N. C. Lind defined the safety index as " the minimum value of distances from the origin to the failure region in the normalized space ".

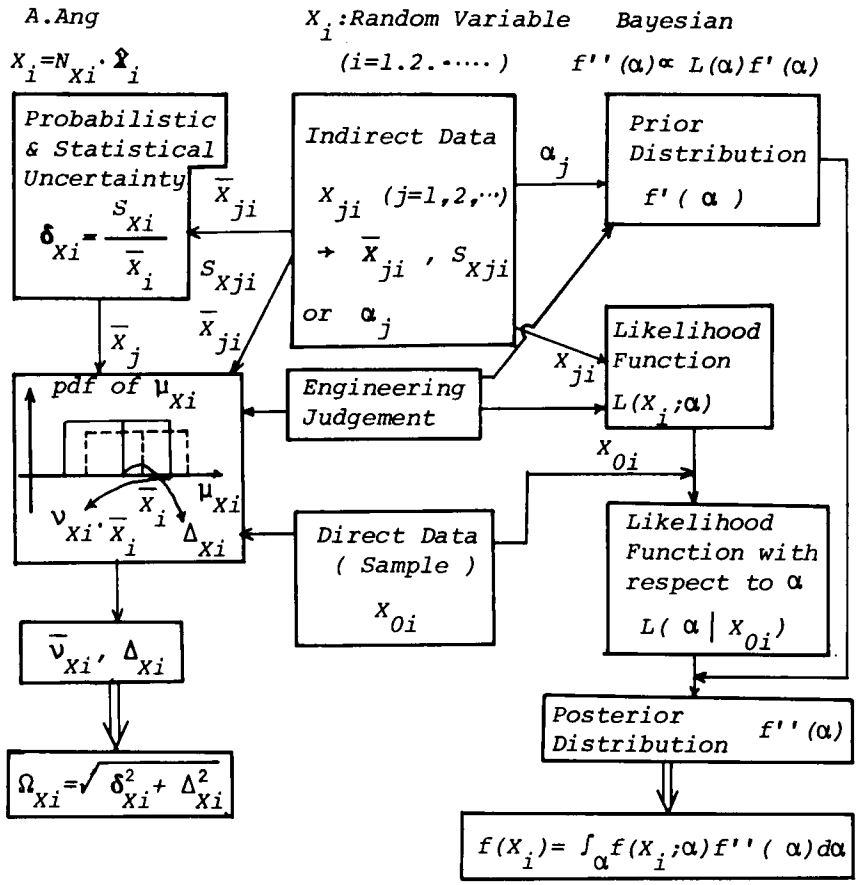

Fig. 5.2 Relation between Ang's Method and Bayesian Decision Theory

Let X be an independent random variable and x be a basic variable which is reduced by the following normalizing transformation.

$$x = \frac{X - \mu_X}{\sigma_X} \tag{5.20}$$

At any point of the normalized space, safety can be evaluated in a uniform manner, because the basic variable x is distributed without warping.

Consider R and S as random variables. By performing the normalizing transformation, the performance function $Z = F(R,S) = 0$, shown in Fig. 5.3(a), is reduced to $z = F(r,s) = 0$, as shown in Fig. 5.3(b). On this figure, the safety index β can be expressed as $\overline{OA}$ which indicates the shortest distance between the origin O and the boundary of the failure region ($F(r,s)<0$) and the safe region ($F(r,s)>0$). Here, the point A is called as " failure point ", which generally corresponds to the condition that the failure is most likely to occur. Since the safety index presented by Hasofer and Lind is defined only by using the failure point, not by using the other points in this space, it can be considered to be a quasi-probabilistic measure of safety.

The Relatioships between Safety Index and Correction Factor

In the previous section, the relationships between the correction factor and Bayesian decision theory is clarified. Here, the relationships between the correction factor and the safety index are discussed by use of the normalized space proposed by Hasofer and Lind.

Introducing the correction factor N with respect to the load effect S, the performance function becomes

$$Z = R - N S \tag{5.21}$$

If N is considered as a random variable, the reduced performance function is calculated as

$$z = F(r,s,n) = (\mu_R + r\sigma_R) - (\mu_n + n\sigma_n)(\mu_S + s\sigma_S) \tag{5.22}$$

in which μ_n and σ_n denote the mean and standard deviation of N, respectively. Since Eq.(5.22) is a nonlinear equation, the calculation of safety index needs a linearlizing technique and an iterative procedure.[7)]

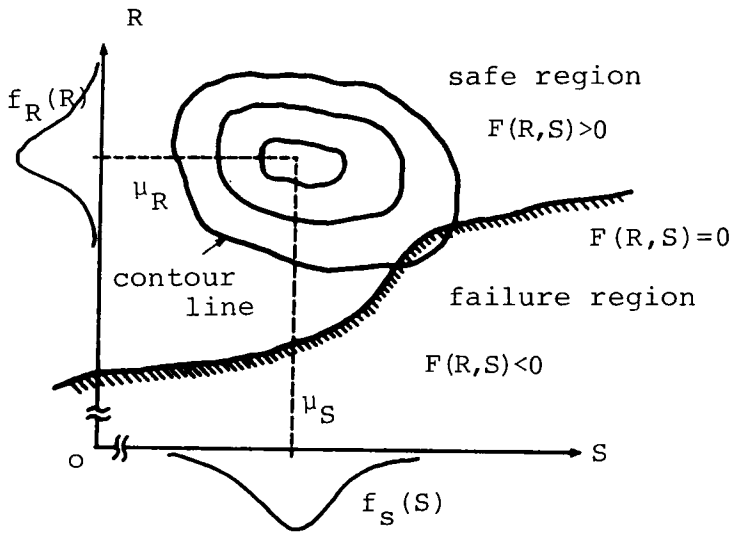

a) R - S Plane

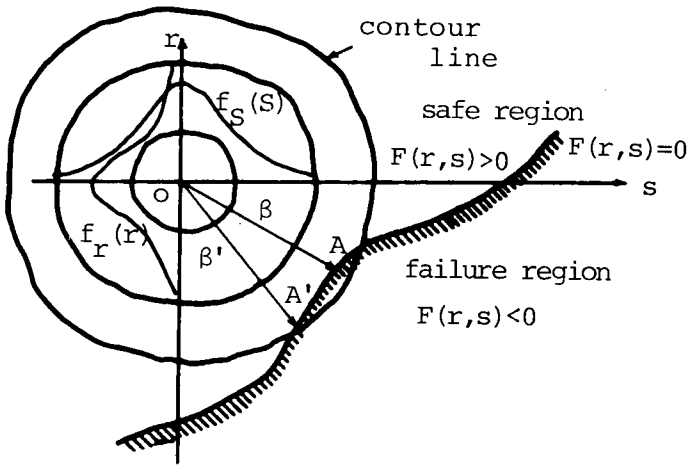

b) r - s Plane

Fig. 5.3 Definition of Failure Point

Here, a way different from Hasofer and Lind's treatment is employed to evaluate the effect of the correction factor. Namely, a three dimensional space is not taken as the normalized space, though the correction factor is considered to be a random variable. The effect of the correction factor is taken into account by the variation with respect to the angle of performance function. (see Fig. 5.4(a)) Then, the angle θ is related to N as follows :

$$\theta = \tan^{-1} N \tag{5.23}$$

$$d\theta = \frac{|dN|}{1 + N^2} \tag{5.24}$$

The increment of N yields the increments of R and S. The induced increments Δr and Δs can be obtained in the normalized space, as shown in Fig. 5.4(b).

$$\Delta r = \frac{\mu_S \, d\theta}{\sigma_R \cos^2\theta} = \frac{\mu_S}{\sigma_R} dN \tag{5.25}$$

$$\Delta s = \frac{\mu_R \, d\theta}{\sigma_S \cos^2\theta} = \frac{\mu_R}{\sigma_S} dN \tag{5.26}$$

Although Δr and Δs are induced by the change of N, it is possible to relate them with $d\sigma_R$ and $d\sigma_S$. When N has a small variation, Eqs (5.25) and (5.26) give the following relations.

$$\left.\begin{aligned} \frac{d\sigma_R}{\sigma_{R_0}} &= \frac{\Delta r}{\frac{\mu_R - \mu_n \mu_S}{\sigma_R}} = \frac{\mu_S}{\mu_R - \mu_n \mu_S} dN = \frac{1}{\theta_0 - N} dN \\ \frac{d\sigma_S}{\sigma_{S_0}} &= \frac{\theta_0}{\theta_0 - N} dN \end{aligned}\right\} \tag{5.27}$$

where θ_0 ($= \mu_R/\mu_S$) indicates the central safety factor.
Solving Eq.(5.27),

$$\sigma_R = \sigma_{R_0} \left(1 + \ln \frac{\theta_0 - 1}{\theta_0 - N} \right) = \sigma_{R_0} (1 + \lambda_R) \tag{}$$

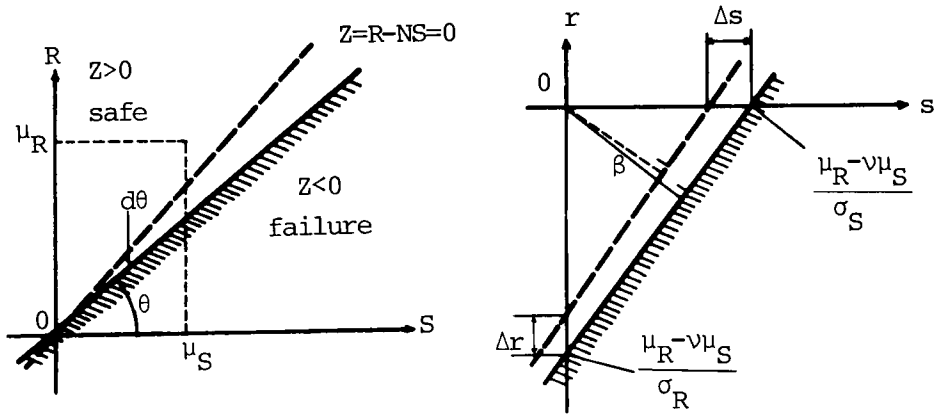

a) R - S Plane

b) r - s Plane

Fig. 5.4 Failure Line and Correction Factor

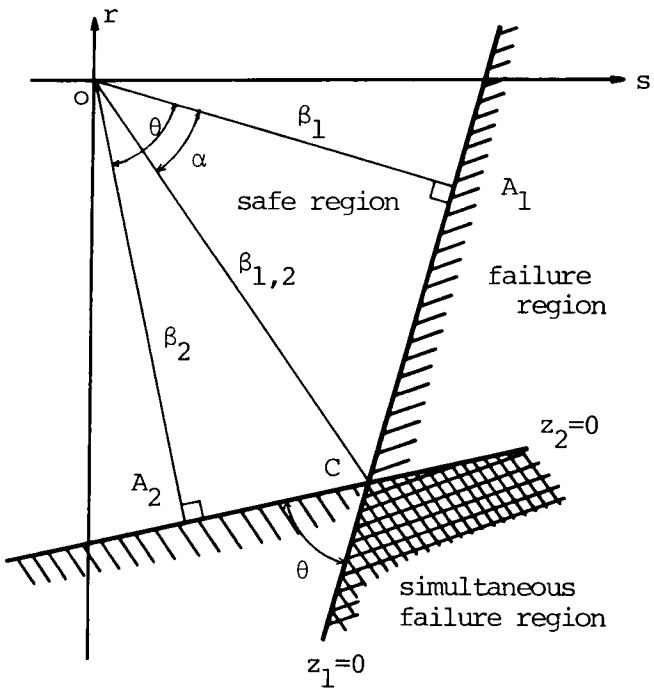

Fig. 5.5 Normalized Space with Two Failure Modes

$$\left.\begin{aligned} \sigma_S &= \sigma_{S_0}\left(1 + \theta_0 \ln \frac{\theta_0 - 1}{\theta_0 - N}\right) = \sigma_{S_0}\left(1 + \lambda_S\right) \end{aligned}\right\} \qquad (5.28)$$

where σ_{R0} and σ_{S0} are the values of σ_R and σ_S for $N = 1$. Similarly, σ_R and σ_S can be calculated as follows for the case where N has a large variation.

$$\left.\begin{aligned} \sigma_R &= \sigma_{R_0} \frac{\theta_0 - 1}{\theta_0 - N} \\ \sigma_S &= \sigma_{S_0} \left(\frac{\theta_0 - 1}{\theta_0 - N}\right)^{\theta_0} \end{aligned}\right\} \qquad (5.29)$$

Replacing σ_R and σ_S in Eqs (5.28) and (5.29) with σ'_R and σ'_S, the safety index is expressed in the following, for the case where the performance function includes the correction factor.

$$\beta = \frac{\mu_R - \mu_n \mu_S}{\sqrt{\sigma'^2_R + \sigma'^2_S}} \qquad (5.30)$$

When N follows to a certain kind of distribution, the expected value of β in Eq.(5.30) can be obtained by using the first order approximation.

$$E[\beta] = \frac{\mu_R - \mu_n \mu_S}{\sqrt{E[\sigma'_R]^2 + E[\sigma'_S]^2}} \qquad (5.31)$$

For N with small variation,

$$E[\beta] = \frac{\mu_R - \mu_n \mu_S}{\sqrt{\sigma^2_{R_0}(1+E[\lambda_R])^2 + \sigma^2_{S_0}(1+E[\lambda_S])^2}} \qquad (5.32)$$

Using Eqs (5.28) - (5.32), it is possible to discuss the effect of the correction factor on the failure region, the relation between the safety factor and the applied load (or structural resistance). The detail is presented in reference 17 with some numerical examples.

5.4 Reliability Analysis of Structural Systems with Multiple Failure Modes

Many investigations have been made for the reliability analysis of structures with many possible failure modes.[18] However, most of them use the failure probability as the measure of safety, and only few can be enumerated as the studies which are based on the second-moment theory : the one in which the safety index for the failure of the overall system is specified as the minimum value of the safety indices calculated for individual failure modes[7], or the one in which the overall safety index is calculated by weighting each failure mode.[8] This problem has such a property that even if the basic variables like structural resistances and load effects are statistically independent, each failure mode, which consists of those variables, is generally correlated with each other.

Here, an analysis method is proposed for structural systems with many possible failure modes, calling attention to the characteristic properties of the normalized space.

For simplicity, let's consider a simple case where only two modes, Z_1 and Z_2, exsist. In this case, the normalized space is expressed as Fig. 5.5. Comparing with the case with a single failure mode, the following informations can be newly obtained :

(1) Intersecting angle θ of Z_1 and Z_2

As shown in Appendix, the cosine of θ corresponds to the correlation coefficient ρ between Z_1 and Z_2. Also, this angle θ is equal to the intersecting angle of $\vec{\beta}_1$ and $\vec{\beta}_2$ which are the position vectors relating the safety indices for Z_1 and Z_2, respectively. (see Fig. 5.5)

(2) Simultaneous-failure region

It is probabilistically possible that two failure events with regard to Z_1 and Z_2 occur simultaneously in the shading region of Fig. 5.5. The probability of the simultaneous failure is written as

$$P_{f1,2} = P_r(Z_1<0 \cap Z_2<0) \tag{5.33}$$

(3) Intersecting point C

When the intersecting point C is the nearest to the origin O in the simultaneous region, this point will become important to evaluate the safety for the simultaneous failure.

In this study, the point which gives the minimum distance from the origin within the simultaneous-failure region is defined as " failure point ". The distance between the failure point and the origin seems to have a relationship with $p_{f1,2}$. Generally, the overall probability p_{f12} can be calculated as

$$p_{f12} = P_r(Z_1<0 \cup Z_2<0)$$

$$= p_{f1} + p_{f2} - p_{f1,2} \qquad (5.34)$$

Supposing that R and S are normally distributed, the following relation exsists between the safety index and the failure probability.[19]

$$1 - p_f = \Phi(\beta) \qquad (5.35)$$

where $\Phi(\cdot)$ signifies the standard normal distribution function. Substituting Eq.(5.35) into Eq.(5.34), the overall safety index is derived as

$$\beta_{12} = \Phi^{-1} \{\Phi(\beta_1) + \Phi(\beta_2) - \Phi(\beta_{1,2})\} \qquad (5.36)$$

in which β_1 and β_2 are the safety indices obtained for Z_1 and Z_2, respectively, and also $\beta_{1,2}$ is the safety index which corresponds to $p_{f1,2}$.

Here, we attempt to express $\beta_{1,2}$ by using β_1, β_2 and ρ (= $cos\theta$). As seen in Fig. 5.5, the intersecting point C is the nearest to the origin in the simultaneous-failure region, when $\theta - \alpha \geq 0$. That is, C is the failure point if the following condition is satisfied. This condition is derived from the condition $sin(\theta-\alpha)\geq 0$.

$$\bar{\beta}_{1,2} \leq \beta_1 / \rho \qquad (5.37)$$

where $\bar{\beta}_{1,2}$ denotes the distance between O and C, and β_1 is assumed to be less than β_2.

Then, $\bar{\beta}_{1,2}$ can be calculated as follows. From Fig. 5.5, the following relations can be obtained.

$$\bar{\beta}_{1,2} \cos\alpha = \beta_1 \tag{5.38}$$

$$\bar{\beta}_{1,2} \cos(\theta-\alpha) = \beta_2 \tag{5.39}$$

Eliminating α from the above two equations, $\bar{\beta}_{1,2}$ is found to be

$$\bar{\beta}_{1,2} = \sqrt{\frac{\beta_1^2 + \beta_2^2 - 2\rho\beta_1\beta_2}{1-\rho^2}} \tag{5.40}$$

On the other hand, the nearest point to the origin is A_2 within a range $\theta-\alpha < 0$. Then, $\beta_{1,2}$ is equivalent to β_2 :

$$\beta_{1,2} = \beta_2 \qquad (\text{for } \bar{\beta}_{1,2} > \beta_1 / \rho) \tag{5.41}$$

From Eqs (5.40) and (5.41), the safety index for the simultaneous failure can be expressed in the terms of β_1, β_2 and ρ.

$$\beta_{1,2} = \begin{cases} \bar{\beta}_{1,2} = \sqrt{\dfrac{\beta_1^2 + \beta_2^2 - 2\rho\beta_1\beta_2}{1-\rho^2}} & (\bar{\beta}_{1,2} \leq \beta_1/\rho) \\ \beta_2 & (\bar{\beta}_{1,2} > \beta_1/\rho) \end{cases} \tag{5.42}$$

The overall safety index can be calculated by using Eqs (5.42) and (5.36).

E. H. Vanmarcke[20] proposed the following equation for estimating the overall failure probability.

$$p_f = p_{f1} + a_{21}\, p_{f2} \tag{5.43}$$

where

$$a_{21} \simeq 1 - \frac{g(\max\{\beta_1/\rho, \beta_2\})}{g(\beta_2)} \tag{5.44}$$

$g(\cdot)$: the function which relates the safety index to the failure probability

When the underlying variables are normally distributed, the overall safety index can be obtained as

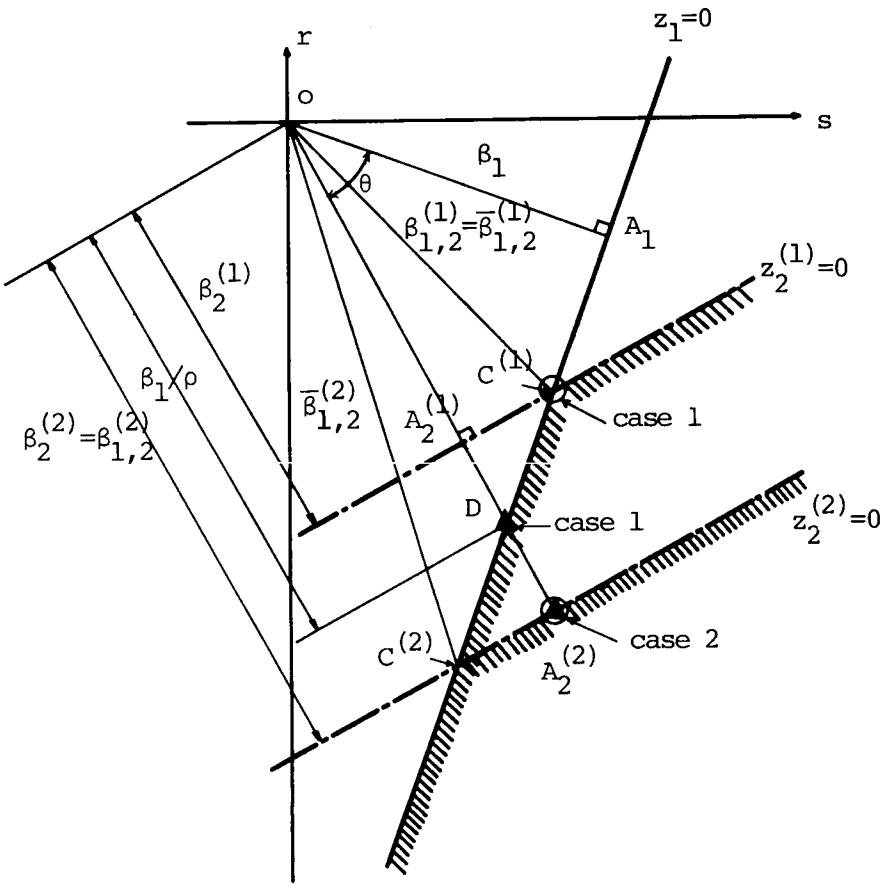

Fig. 5.6 Comparison of Proposed Method and Vanmarcke's Method

$$\beta_{12} = \Phi^{-1}(\Phi(\beta_1) + \Phi(\beta_2) - \Phi(max\{\beta_1/\rho, \beta_2\}) \qquad (5.45)$$

Although Eqs (5.36) and (5.45) are quite similar, they differ in the process of calculating the safety index for the simultaneous failure. Namely, max { β_1/ρ , β_2 } is used in Vanmarcke's method, whereas $\beta_{1,2}$ (Eq.(5.42)) is used in the proposed method. Fig. 5.6 shows the difference between both methods, where z_1 is fixed and two performance functions $z_2^{(1)}$ and $z_2^{(2)}$ are considered for z_2. In both cases, it is postulated that $\theta = cos^{-1}\rho$ is equal and also that the condition, $\beta_2^{(1)} < \beta_1/\rho < \beta_2^{(2)}$, is satisfied. In this example, A_1, $A_2^{(1)}$ and $A_2^{(2)}$ are the failure points of z_1, $z_2^{(1)}$ and $z_2^{(2)}$, respectively. And β_1, $\beta_2^{(1)}$ and $\beta_2^{(2)}$ denote the safety indices for z_1, $z_2^{(1)}$ and $z_2^{(2)}$, respectively. It is first seen in this figure that β_1/ρ is equal to the distance from O to D, where D is the intersecting point of z_1 and the line perpendicular to $z_2^{(1)}$ ($z_2^{(2)}$) starting from the origin.

According to Eqs (5.36) and (5.45), the significant points for estimating the safety for the simultaneous failure are obtained as the points expressed by the signatures, O (the proposed method) and ▲ (Vanmarcke's method). When $z_2^{(2)}$ is employed, both methods provide the same safety index, namely $\beta_{1,2}^{(2)} = \beta_2^{(2)}$. However, when $z_2^{(1)}$ is used, the proposed method and Vanmarcke's method give $\bar{\beta}_{1,2}^{(1)}$ and β_1/ρ for $\beta_{1,2}^{(1)}$, which correspond to the points $C^{(1)}$ and D, respectively. From this example, it is concluded that when the difference between β_1 and β_2 is not large, the proposed method gives a smaller value for β_{12} than Vanmarcke's method, and they provide the same value when the difference is large. Despite of the difference in calculating $\beta_{1,2}$, these methods are based on the same concept that the simultaneous failure can be approximately evaluated by use of a representative point in the normalized space.

5.5 Evaluation of the Effects of Each Failure Mode on System Reliability

How each failure mode affects the evaluation of the overall safety

index is discussed in the normalized space. To do so, it is inevitable to pay attention to the components of the vector $\vec{\beta}$ as well as the absolute value of $\vec{\beta}$, and to disclose the influence of the combination of the failure modes on the evaluation of the overall safety index. As the components of $\vec{\beta}$ can be expressed by the coordinates of the failure point, we can solve the problem what failure mode should be thought of, or what order the failure mode should be combined, by investigating how the combination of failure modes will change the coordinates of the failure point.

Consider a case with two failure modes, as shown in Fig. 5.7(a), where the performance functions are assumed to be linear so as to make the discussion simple. As described previously, the intersecting angle of the vectors, $\vec{\beta}_1$ and $\vec{\beta}_2$, which correspond to the safety indices for the underlying modes, is related to the correlation coefficient between these failure modes. Then, the direction of the vector $\vec{\beta}_{12}$, cooresponding to the overall safety index β_{12}, is likely to lie whithin an angle which consists of $\vec{\beta}_1$ and $\vec{\beta}_2$, because the points, A_1 and A_2, which are the ends of $\vec{\beta}_1$ and $\vec{\beta}_2$, become the failure points for individual modes. Furthermore, since β_{12} $(=|\vec{\beta}_{12}|)$ is less than β_1 and β_2, the end of $\vec{\beta}_{12}$, which corresponds to the failure point of the system failure, will locate within a region surrounded by OA_1CA_2O. Based on the above assumptions, the overall performance function, which is composed of Z_1 and Z_2, is modeled as that the performance function with small safety index, Z_1, changes and results in the overall performance function Z_{12} on account of the effect of another failure mode Z_2.

If all the performance functions are considered to be linear, Z_{12} is derived through translation, rotation and both. Here, only the rotation is employed to change Z_1, because the gradient of performance function has a close relation to the dispersions of random variables. Z_{12} is obtained by rotating Z_1 around the point A_1 which is the failure point of Z_1. This process is illustrated in Fig. 5.7(b), where α is the rotating angle. In this figure, the overall safety index can be obtained as the minimum distance from the origin to the resulting performance function. Then, $\vec{\beta}_{12}$ rotates by α from $\vec{\beta}_1$ to $\vec{\beta}_2$, and the end of $\vec{\beta}_{12}$ represented by A_{12} becomes the failure point of Z_{12}.

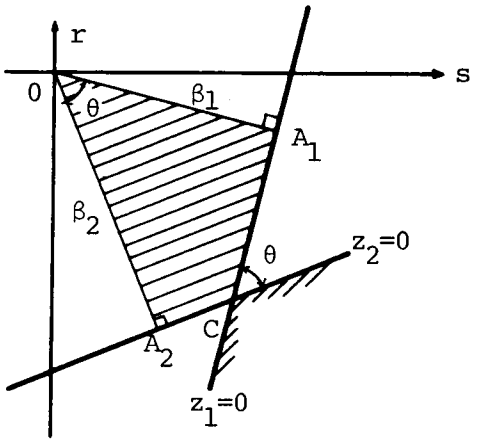

a) Normalized Space with Two Performance Functions

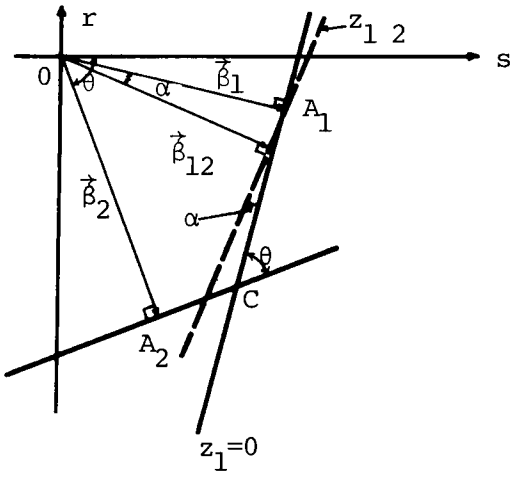

b) Expression of Overall Performance Function

Fig. 5.7 Change of Failure Point

Observing Fig. 5.7(b), $\vec{\beta}_{12}$ is calculated as

$$\vec{\beta}_{12} = \frac{\cos\alpha\{\ \beta_2 \sin(\theta-\alpha)\vec{\beta}_1 + \beta_1 \sin\alpha \vec{\beta}_2\ \}}{\beta_{12}\sqrt{\sin^2(\theta-\alpha)+\sin^2\alpha+2\sin\alpha\sin(\theta-\alpha)\cos\theta}} \qquad (5.46)$$

In calculating Eq.(5.46), we face the problem how to determine α. Here, we attempt to express α in the terms of β_1, β_2 and ρ, by using Eq.(5.35) which relates p_f to β. In general, α is written as

$$\alpha = func.(\ \beta_1, \beta_2, \rho\ ) \qquad (5.47)$$

Moreover, Eq.(5.47) is approximately written as a multiplication form.

$$\alpha = f_1(\rho)\ f_2(\beta_1, \beta_2) \qquad (5.48)$$

For instance, the following equation can be obtained through some numerical calculations :

$$\alpha = \alpha_0\{\ 1 - exp[-a(1-\rho)]\}exp[-\{b(\beta_1-2)+(c\beta_1+d)(\beta_2-\beta_1)\}] \qquad (5.49)$$

where α is expressed by degree,

$$\alpha_0 = 30\ ,\ a = 15\ ,\ b = 0.265\ ,\ c = 0.325\ ,\ d = 0.5$$

Substituting Eq.(5.49) to Eq.(5.46), $\vec{\beta}_{12}$ can be computed. Its components give the coordinates of the failure point. It is also possible to calculate $\vec{\beta}_{12}$ by using Eq.(5.46) and the relation that $\alpha = \cos^{-1}(\beta_{12}/\beta_1)$. In the case with more than three failure modes, the process of changing the failure point can be examined by a successive use of the above procedure.

5.6 Numerical Examples[21] (Documentation)

Example of Rigid Frame[22]

To demonstrate the applicability of the method proposed in this chapter, a simple portal frame model is employed. The representative failure modes and the applied loads, vertical load P and horizontal load H, are shown in Fig. 5.8. In this example, it is assumed that the

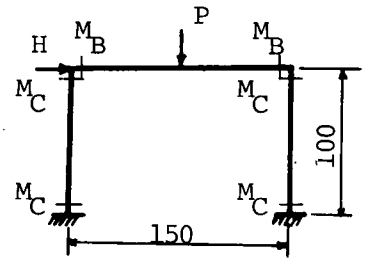

Mode 1

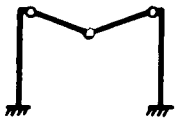

Mode 2

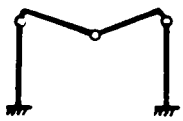

Mode 3

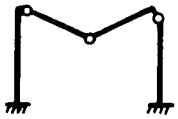

Mode 4

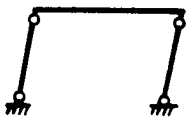

Mode 5

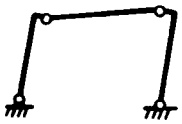

Mode 6

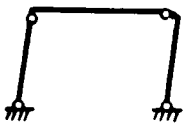

Mode 7

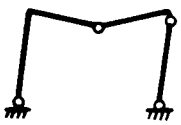

Mode 8

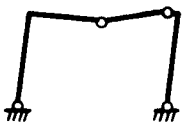

R ; $\mu_{M_B} = \mu_{M_C} = 40$

$\sigma_{M_B} = \sigma_{M_C} = 4$

S ; $\mu_P = 1$, $\mu_H = 0.5$

$\sigma_P = 0.2$, $\sigma_H = 0.1$

Performance function

$Z_1 = 4M_B - 75P$

$Z_2 = 2M_B + 2M_C - 75P$

$Z_3 = 3M_B + M_C - 75P$

$Z_4 = 4M_C - 100H$

$Z_5 = 2M_B + 2M_C - 100H$

$Z_6 = M_B + 3M_C - 100H$

$Z_7 = 2M_B + 4M_C - 75P - 100H$

$Z_8 = 4M_B + 2M_C - 75P - 100H$

Fig. 5.8 Failure Modes of Portal Frame

Table 5.2 Example of Portal Frame

a) Performance Functions ($Z_1 - Z_8$)

$$Z_1 = 4\,M_B - 75\,P \qquad Z_5 = 2\,M_B + 2\,M_C - 50\,P$$

$$Z_2 = 2\,M_B + 2\,M_C - 75\,P \qquad Z_6 = M_B + 3\,M_C - 50\,P$$

$$Z_3 = 3\,M_B + M_C - 75\,P \qquad Z_7 = 2\,M_B + 4\,M_C - 125\,P$$

$$Z_4 = 4\,M_C - 50\,P \qquad Z_8 = 4\,M_B + 2\,M_C - 125\,P$$

b) Covariance Matrix

	Z_1	Z_2	Z_3	Z_4	Z_5	Z_6	Z_7	Z_8
Z_1	1.	0.957	0.969	0.362	0.840	0.605	0.746	0.936
Z_2		1.	0.958	0.784	0.980	0.918	0.982	0.982
Z_3			1.	0.578	0.938	0.778	0.887	0.993
Z_4				1.	0.800	0.960	0.872	0.652
Z_5		S.Y.M.			1.	0.937	0.952	0.952
Z_6						1.	0.957	0.827
Z_7							1.	0.932
Z_8								1.

c) Safety Indices for Individual Failure Modes

Mode i	$\vec{\beta}_i$ m_B	m_C	p	β_i
1	-2.827	0	2.651	3.876
2	-1.926	-1.926	3.612	4.524
3	-2.649	-0.883	3.312	4.331
4	0	-4.944	3.090	5.830
5	-3.860	-3.860	4.825	7.286
6	-1.692	-5.077	4.231	6.822
7	-0.974	-1.947	3.042	3.741
8	-1.947	-0.974	3.042	3.741

Table 5.3 Changes of Failure Point and Safety Index
(by Eq.(5.49))

case	step / item	1	2	3	4
1	modes	7,8	78,1	781,3	7813,2
	β_j	3.741	3.876	4.332	4.524
	$\rho_{i,j}$	0.932	0.869	0.997	0.973
	$\alpha_{i,j}$	12.1°	11.5°	0.25°	1.38°
	β_{ij}	3.660	3.528	3.587	3.587
2	modes	7,1	71,8	718,3	7813,2
	β_j	3.876	3.741	4.332	4.524
	$\rho_{i,j}$	0.746	0.993	0.980	0.992
	$\alpha_{i,j}$	14.7°	1.52°	1.53°	0.48°
	β_{ij}	3.617	3.615	3.615	3.615
3	modes	7,1	71,3	713,2	7132,8
	β_j	3.876	4.332	4.524	3.741
	$\rho_{i,j}$	0.746	0.971	0.994	0.996
	$\alpha_{i,j}$	14.7°	2.08°	0.37°	0.92°
	β_{ij}	3.617	3.616	3.616	3.615

Table 5.4 Changes of Failure Point and Safety Index
(by the Method Using the Simultaneous Region)

case	step / item	1	2	3	4
1	modes	7,8	78,1	781,3	7813,2
	β_j	3.741	3.876	4.332	4.524
	$\rho_{i,j}$	0.932	0.847	0.983	0.993
	$\alpha_{i,j}$	9.61°	7.31°	0°	0°
	β_{ij}	3.688	3.658	3.658	3.658
2	modes	7,1	71,8	718,3	7183,2
	β_j	3.876	3.741	4.332	4.524
	$\rho_{i,j}$	0.746	0.985	0.960	0.999
	$\alpha_{i,j}$	11.3°	0°	0°	0°
	β_{ij}	3.668	3.668	3.668	3.668
3	modes	7,1	71,3	713.2	7132,8
	β_j	3.876	4.332	4.524	3.741
	$\rho_{i,j}$	0.746	0.960	0.999	0.985
	$\alpha_{i,j}$	11.3°	0°	0°	0°
	β_{ij}	3.668	3.668	3.668	3.668

a) Failure Point

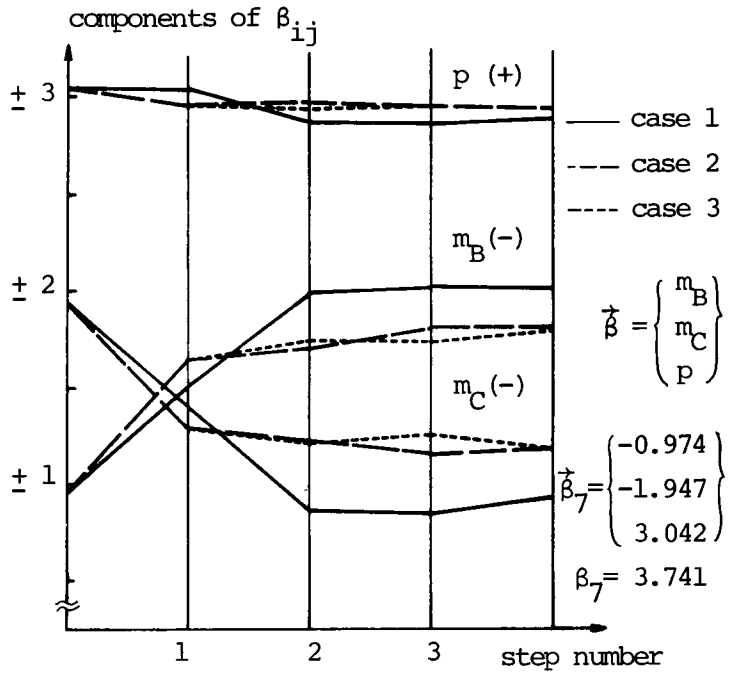

b) Safety Index

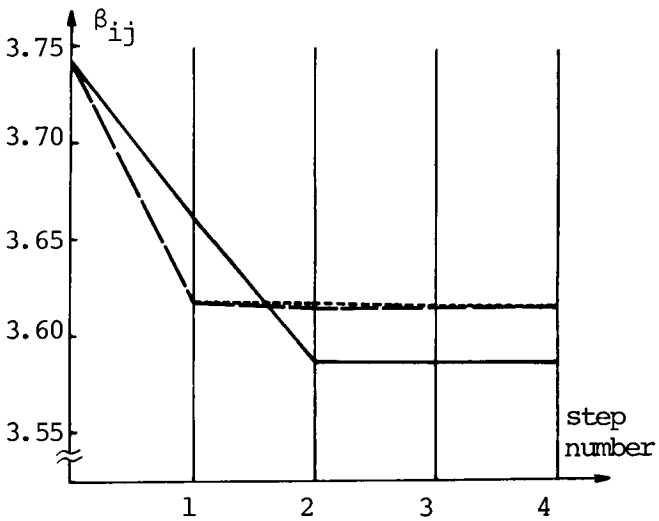

Fig. 5.9 Changes of Failure Point and Safety Index
(by Eq.(5.49))

a) Failure Point

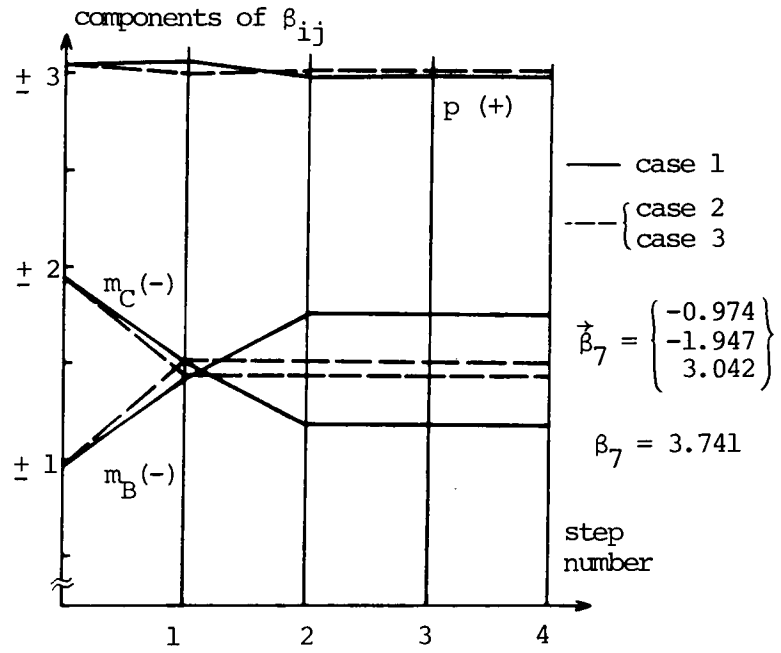

b) Safety Index

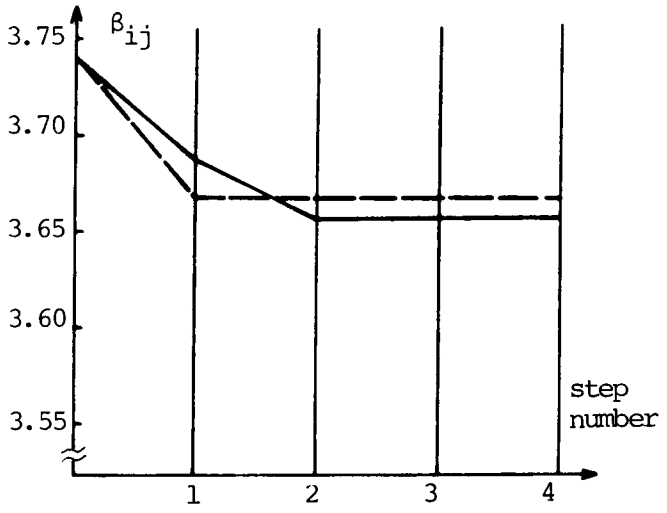

Fig. 5.10 Changes of Failure Point and Safety Index
(by the Method Using the Simultaneous Region)

full plastic moments of beam and column, M_B and M_C, are independent, and that P and H are completely dependent. The performance functions for individual modes and the coefficients of correlation between them are presented in Table 5.2(a) and (b). Table 5.2(c) shows the calculated values of β_i and the components of $\vec{\beta}_i$ ($i=1,\cdots,8$). The changes of safety index and failure points due to the combination of the failure modes are shown in Table 5.3, Table 5.4, Fig. 5.9 and Fig. 5.10. Table 5.3 and Fig. 5.9 are obtained by using Eq.(5.49). In this case, attention is placed on the 7th mode with the smallest value of safety index. In case 1, the failure modes are combined with the 7th mode in the order of those with smallest safety index. In case 2, the 7th mode is combined with the first mode which has the least correlation among the modes with relatively small safety indices, and next mode 8 is combined. In case 3, the mode with the least correlation coefficient is combined at each step. Observing the results obtained at the 4th step, case 1 provides the most conservative value of safety index. While case 1 and case 2 show the convergence at the 4th step, case 3 does not. Although the obtained results somewhat differ in those three cases, the value of safety index decreases by 3 or 4 per cent from that of the weakest failure mode.

Table 5.4 and Fig. 5.10 present the numerical results obtained by the method proposed in section 5.4. Comparing with the results shown in Table 5.3 and Fig. 5.9, the overall safety index is overestimated for each case. This is why this method is derived by extending the definition of safety index proposed by Hasofer and Lind. They define the safety index by only the minimum distance, and do not use the information with respect to the form of performance function. Namely, the performance function is always treated in the normalized space as a line perpendicular to the vector $\vec{\beta}$. Then, the simultaneous failure region is estimated larger than the real region. Since this approximation leads to the overestimation of safety index for the simultaneous failure, the proposed method provides small values for the overall safety index.

Example of Beam Buckling[23)]

In the previous example, the failure mechanisms due to the formation of plastic hinges are employed as failure modes. In this example, differ-

ent types of failure are considered. Let's consider the buckling phenomena of beam. Here, Euler buckling and lateral buckling are taken as representative ones. The former occurs by the effect of compressive load, and the latter occurs through the loss of stability for the lateral direction due to the bending moment around the principal axis.

If a safety is checked in the term of stress for both the structural resistance and the load effect, the performance function is expressed as

$$Z = f_R - f_S \tag{5.50}$$

in which f_R and f_S represent the allowable stress and the stress induced by the applied load, respectively.

For Euler buckling, f_R is written as

$$f_R = f_{R1} = \frac{\pi^2 E}{\lambda^2} \tag{5.51}$$

in which E and λ denote Young's modulus and the slenderness ratio, respectively.

For a lateral buckling with respect to slender beams with symmetrical cross section, f_R is given as

$$f_R = f_{R2} = \frac{\pi^2}{2\ell^2} \frac{I_y E}{A_f + A_w/6} \tag{5.52}$$

where ℓ : beam length

I_y : moment inertia with respect to the y-axis

A_f : cross sectional area of the flange

A_w : cross sectional area of the web

The I-beam shown in Fig. 5.11 is analyzed, where the span length is *20 m*. For simplicity, only Young's modulus E is treated as a random variable and other quantities are considered deterministic. Assume that the mean and coefficient of variation of E are 2.1×10^6 *kg/cm*^{2} and *0.1*, respectively. Then, the standard deviation of E is 2.1×10^5 *kg/cm*^{2}, and also f_{R1} and f_{R2} become completely dependent. The loading condition is shown in Fig. 5.11(b) in which the axial force P with the eccentricity e and the bending moment M, which are independent of each other, are taken into consideration.

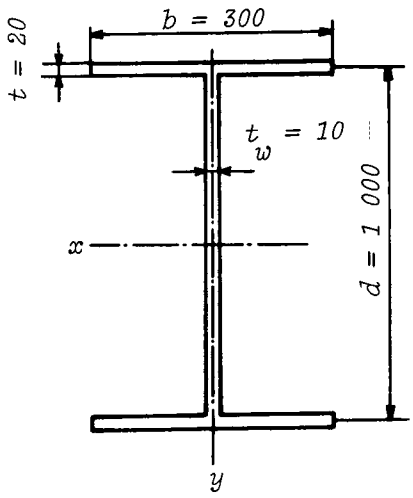

a) Cross Section

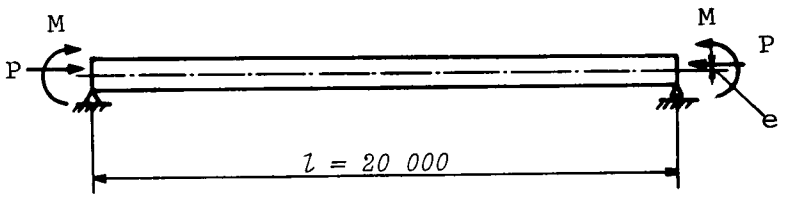

b) Applied Load

Fig. 5.11 I-Shaped Beam

Since the compressive load P and the resulting bending moment $M + P \cdot e$ give rise to Euler buckling and lateral buckling, respectively, the stress induced by those loads are expressed as

$$f_{S1} = P / A \tag{5.53}$$

$$f_{S2} = \frac{M + Pe}{I_X} \frac{d}{2} \tag{5.54}$$

in which A : total cross sectional area

I_x : moment inertia with respect to the x-axis

d : height of cross section

Supposing that the means of P and M are $\mu_P = 200\ t$ and $\mu_M = 100\ tm$, and that the coefficient of variation is 0.2 for both loads, the standard deviations are calculated as $\sigma_P = 60\ t$ and $\sigma_M = 20\ tm$. It is also assumed that $\mu_e = 5\ cm$ and $\sigma_e = 2\ cm$.

By performing the normalizing transformation, the performance functions are obtained as follows :

Euler buckling : $$Z_1 = 212.0 \cdot r - 272.8 \cdot p + 756 \tag{5.55}$$

Lateral buckling : $$Z_2 = 304.1 \cdot r - \frac{100}{6.2} \{20 \cdot m + (3+0.6 \cdot p) \times (5+2 \cdot \tilde{e})\} + 1428 \tag{5.56}$$

where r, p, m and $\tilde{e}$ are the reduced variables for E, P, M and e, respectively.

Then, the safety indices β_i ($i=1,2$) and vectors $\vec{\beta}_i = (r , p , m , \tilde{e})$ ($i=1.2$) are calculated as

$$\vec{\beta}_1 = (-1.343, 1.728, 0, 0)^t , \quad \beta_1 = 2.188$$

$$\vec{\beta}_2 = (-1.717, 0.337, 1.821, 0.583)^t , \quad \beta_2 = 2.592$$

$$\rho_{12} = 0.509$$

Using the above quantities, the overall safety index and the coordinates of the failure point are calculated by means of the two methods

used in the previous example and Vanmarcke's method.

1) Using $\alpha = 17.49°$ which is calculated by Eq.(5.49), the overall safety index is obtained through Eq.(5.46) as follows :

$$\vec{\beta}_{12} = 0.740\ \vec{\beta}_1 + 0.281\ \vec{\beta}_2 = (-1.476, 1.373, 0.512, 0.164)^t$$

2) Using Eq.(5.42), $\beta_{1,2}$ is obtained as

$$\beta_{1,2} = 2.782 \quad (< \beta_1/\rho = 4.299)$$

Then,

$$\beta_{12} = \Phi^{-1}(0.9836) = 2.135$$

$$\alpha = 12.64°$$

$$\vec{\beta}_{12} = 0.826\ \vec{\beta}_1 + 0.209\ \vec{\beta}_2 = (-1.468, 1.498, 0.381, 0.122)^t$$

3) By use of Vanmarcke's method, β_{12} and $\vec{\beta}_{12}$ are calculated as

$$\beta_{12} = \Phi^{-1}(0.9809) = 2.073 , \quad \alpha = 18.66°$$

$$\vec{\beta}_{12} = 0.718\ \vec{\beta}_1 + 0.297\ \vec{\beta}_2 = (-1.474, 1.741, 0.541, 0.173)^t$$

Comparing the results of case 1) - case 3), the value of β_{12} is the largest in case 2) and the smallest in case 3).

5.7 Conclusions

In this chapter, the probabilistic meaning of safety index is analytically studied on the basis of the fiducial statistics. Also, the statistical or physical significance of safety index is discussed through a graphical interpretation. The examination of the normalized space presented by Hasofer and Lind offers new informations to calculate the safety index for the structural systems with many possible failure modes. The main results obtained in this chapter are as follows :

1) Although the safety index is essetially a deterministic quantity, it is possible to treat it as a random variable with the aid of the

fiducial statistics or Bayesian decision theory, and further possible to disclose the effect of statistical uncertainty on the evaluation of safety index.

2) However, for a practical use, it is convenient to deal with the statistical uncertainty by means of the correction factor proposed by Ang. It is possible to evaluate the effects of various engineering uncertainties in the form of the increase of the standard deviation of each random variable, using the relations between the correction factor and the safety index which are derived here.

3) A new approach based on the second-moment theory is proposed to evaluate the safety of structures with multiple failure modes, by extending the definition of safety index proposed by Hasofer and Lind. The concept of the failure point used here is applicable to the case where the performance function is nonlinear, and also to the case where more than three failure modes exist.

4) By paying attention to the failure point, the problem how the failure modes are combined to make the calculation accurate can be discussed. Numerical results imply that the value of safety index for each mode and the correlation between the modes are important factors for estimating the overall safety. The order of combining the failure modes affects the accuracy of the resulting solutions. A relatively conservative estimation is achieved without difficulty, by successively combining the modes in the order of those with the smallest safety index.

5) The coordinates of the failure point in the normalized space express the ratio of the underlying variables at the most weakest failure condition. This means that the failure point will take an important role in the reliability-based design.

References for Chapter 5

1) Cornell, C. A., " A Probability-Based Structural Code ", ACI Jour. Dec., 1969, pp974-985
2) Cornell, C. A., " Structural Safety Specifications Based on Second-Moment Reliability Analysis ", IABSE Symposium on Concepts of Safety of Structures and Methods of Design, Final Report, London, 1969, pp235-245
3) Cornell, C. A., " A First-Order Reliability Theory for Structural Design ", Chapter 6 of Structural Reliability and Codified Design (Editor : N.C.Lind), Study No.3, Solid Mechanics Division, Univ. of Waterloo, 1970, pp87-111
4) Lind, N. C., " An Invariant Second-Moment Reliability Format ", Paper No.113, Solid Mechanics Division, Univ. of Waterloo, 1972
5) Ellingwood, B. R., " Reliability of Current Reinforced Concrete Designs ", Proc. ASCE, ST4, Apr., 1979, pp699-712
6) Ellingwood, B. R., " Reliability Based Criteria for Reinforced Concrete Design ", Proc. ASCE, ST4, Apr., 1979, pp713-727
7) Hasofer, A. M. and Lind, N. C., " An Exact and Invariant Second-Moment Code Format ", Proc. ASCE, EM1, Feb., 1974, pp111-124
8) Lind, N. C., " Formulation of Probabilistic Design ", Proc. ASCE, EM2, Apr., 1977, pp273-284
9) Fujimoto, H., " Tokei-Suri no Kiso to Ohyo ", Nikkan-Kogyo Shinbunsha, 1968, pp171-174 (in Japanese)
10) Fujino, Y., " Discussions to Reliability Analysis with Uncertainties of the Measured Values (by S.Baba et al) ", Proc. JSCE, No.268, 1977, pp129-132 (in Japanese)
11) Antchison, J. and Sculthorpe, D., " Some Problems of Statistical Prediction ", Biometrika, 52, 3 and 4, 1965, pp469-483
12) Bartholomew, D. J., " A Comparison of Some Bayesian and Frequentist Inferences ", Biometrika, 52, 1 and 2, 1965, pp19-35
13) Ang, A. H-S. and Tang, W., " Probability Concepts in Engineering Planning and Design, Volume I : Basic Principles ", John Wiley and Sons, Inc., 1975
14) Ang, A. H-S., " Series of Lectures on Structural Reliability and

Probability-Based Design ", Lecture Note, Apr., 1976

15) Ditlevesen, O., " Structural Reliability Analaysis and the Invariant Problem ", Tech. Rep. No.22, Solid Mechanics Division, Univ. of Waterloo, 1973

16) Rosenblueth, E. and Esteva, L., " Use of Reliability Theory in Building Codes ", Proceedings of the 1st International Conference on Applications of Statistics and Probability to Soil and Structural Engineering, Hong Kong, Sept., 1971, pp17-34

17) Shiraishi, N., Furuta, H. and Nakano, M., " Fundamental Consideration on Reliability Analysis Based on Second-Moment Theory ", The 33rd Annual Meeting of JSCE, I-149, 1978, pp284-285 (in Japanese)

18) for example, Moses, F. and Kinser, D., " Analysis of Structural Reliability ", Proc. ASCE, ST5, Oct., 1967, pp147-164

19) Ang, A. H-S. and Cornell, C. A., " Reliability Bases of Structural Safety and Design ", Proc. ASCE, ST9, Sept., 1974, pp1755-1769

20) Vanmarcke, E. H., " Matrix Formulation of Reliability Analysis and Reliability-Based Design ", Int. J. of Computers and Structures, Vol.3, 1971, pp757-770

21) Shiraishi, N., Furuta, H. and Nakano, M., " Some Considerations on Application of Safety Index to Reliability Analysis ", to appear in Proc. JSCE, No.301, Sept., 1980 (in Japanese)

22) Shiraishi, N., Furuta, H. and Tarumi, K., " Fundamental Study on Estimation of Reliability of Redundant Structures ", Annual Meeting of JSCE, Kansai Branch, I-71, 1976 (in Japanese)

23) Konishi, I. and others, " Kokyo : Kiso-hen ", Maruzen, 1977, pp437, (in Japanese)

Appendix Reduction of the Relation : $\cos\theta = \rho$

Consider first the safety index and the corresponding vector in a case with a single failure mode. When the boundary of failure region forms the hyperplane in a multi-dimensional space, the performance function Z is expressed by the linear combination of the resistances R_i ($i=1,\cdots\cdots,m$) and the load effects S_j ($j=1,\cdots\cdots,n$).

$$Z = \sum_{i=1}^{m} a_i R_i - \sum_{j=1}^{n} b_j S_j \qquad \text{(A1)}$$

where a_i and b_j are constants.
Performing the normalizing transformation,

$$Z = \sum_{i=1}^{m} a_i \sigma_{R_i} r_i - \sum_{j=1}^{n} b_j \sigma_{S_j} s_j + \left(\sum_{i=1}^{m} a_i \mu_{R_i} - \sum_{j=1}^{n} b_j \mu_{S_j} \right) \qquad \text{(A2)}$$

In this $(m+n)$-dimensional space, β can be expressed by the minimum distance from the origin to the hyperplane $Z = 0$, and also the components of $\vec{\beta}$ can be given by the coordinates of the point which gives the minimum distance.

$$\beta = \frac{\left| \sum_{i=1}^{m} a_i \mu_{R_i} - \sum_{j=1}^{n} b_j \mu_{S_j} \right|}{\sqrt{\sum_{i=1}^{m} a_i^2 \sigma_{R_i}^2 + \sum_{j=1}^{n} b_j^2 \sigma_{S_j}^2}} = \frac{\mu_Z}{\sigma_Z} \qquad \text{(A3)}$$

$$\vec{\beta} = \frac{-\left| \sum_{i=1}^{m} a_i \mu_{R_i} - \sum_{j=1}^{n} b_j \mu_{S_j} \right|}{\sum_{i=1}^{m} a_i^2 \sigma_{R_i}^2 + \sum_{j=1}^{n} b_j^2 \sigma_{S_j}^2} \begin{pmatrix} a_1\sigma_{R_1} \\ \vdots \\ a_m\sigma_{R_m} \\ b_1\sigma_{S_1} \\ \vdots \\ b_n\sigma_{S_n} \end{pmatrix} = -\frac{\mu_Z}{\sigma_Z^2} \begin{pmatrix} a_1\sigma_{R_1} \\ \vdots \\ a_m\sigma_{R_m} \\ b_1\sigma_{S_1} \\ \vdots \\ b_n\sigma_{S_n} \end{pmatrix} \qquad \text{(A4)}$$

From Eq.(A2), it is obtained that the gradient of the hyperplane $Z = 0$ is closely related to the standard deviation of each variable.

Next, consider a case where many possible failure modes exsist. Using Eqs (A3) and (A4) for the modes Z_p and Z_q,

$$\vec{\beta}_p = -\frac{\mu_{Z_p}}{\sigma_{Z_p}} \begin{Bmatrix} a_{1p}\sigma_{R_1} \\ \vdots \\ a_{mp}\sigma_{R_m} \\ -b_{1p}\sigma_{S_1} \\ \vdots \\ -b_{np}\sigma_{S_n} \end{Bmatrix} \qquad \vec{\beta}_q = -\frac{\mu_{Z_q}}{\sigma_{Z_q}} \begin{Bmatrix} a_{1q}\sigma_{R_1} \\ \vdots \\ a_{mq}\sigma_{R_m} \\ -b_{1q}\sigma_{S_1} \\ \vdots \\ -b_{nq}\sigma_{S_n} \end{Bmatrix} \tag{A5}$$

$$\beta_p = \mu_{Z_p} / \sigma_{Z_p} \qquad \beta_q = \mu_{Z_q} / \sigma_{Z_q} \tag{A6}$$

Then, the intersecting angle of the vectors, $\vec{\beta}_p$ and $\vec{\beta}_q$, can be calculated as

$$\cos\theta = \frac{(\vec{\beta}_p, \vec{\beta}_q)}{|\vec{\beta}_p| \cdot |\vec{\beta}_q|} = \frac{\mu_{Z_p}/\sigma_{Z_p} \cdot \mu_{Z_q}/\sigma_{Z_q}}{\beta_p \cdot \beta_q} \left(\sum_{i=1}^{m} a_{ip}a_{iq}\sigma^2_{R_i} + \sum_{j=1}^{n} b_{jp}b_{jq}\sigma^2_{S_j} \right)$$

$$= \frac{\sigma_{Z_pZ_q}}{\sigma_{Z_p} \cdot \sigma_{Z_q}} = \rho_{pq} \tag{A7}$$

where $\sigma_{Z_pZ_q}$ $\left(= \sum a_{ip}a_{iq}\sigma^2_{R_i} + \sum b_{jp}b_{jq}\sigma^2_{S_j} \right)$ represents the covariance. Eq.(A7) proves that the cosine of the intersecting angle is equal to the coefficient of correlation between the underlying failure modes.

Chapter 6 Structural Design Based on Second-Moment Theory

6.1 Second-Moment Design Format

In the design format based on the allowable stress criterion, various uncertainties involved in the design process are taken into account by means of " safety factor ". The value of safety factor is determined from measurements or experiments through the statistical and probabilistic operations. However, the determination of safety factor may not be performed in a unified manner, because this approach is essentially based on the deterministic design philosophy. On account of the complexity of design process and the variety of uncertainties, it is desirable to establish a design method in which statistical data and engineering judgements can be reasonably combined without computational difficulty.

From the above standpoint of views, the second-moment theory, which uses the safety index as the measure of safety, is considered as one of excellent design approaches. At present, the efficiency and simplicity of the second-moment format are widely recognized, and also its application to actual design codes is attempted with the aid of " code calibration ". However, usual design formulations[1)-7)] frequently involve some mathematical approximations in the reduction of basic equations. Those approximations may deprive the underlying quatities of physical meaning and also may induce the unreasonability that the obtained design is too conservative or unconservative.

In this chapter, the reliability-based design format is discussed with emphasis on the reduction of basic formula. By use of the coordinates of the failure point in the normalized space, a geometrical interpretation is provided for the split coefficients which are used to relate the second-moment format to the load factor design. Using some design examples, the resistance and load factors derived here are examined in comparison with the triangular approximation method[1)], Ang's method[2)] and Shah's method.[9)]

6.2 Usual Reliability-Based Design Methods

Generally, the factors such as economy, safety, convenience and aesthetics should be taken into account in the structural design. Safety must be the most important among those factors for civil engineering design, considering the public utility and the enormous loss in failure. Here, a design formulation is simplified by paying attention to the safety of structure.

Let's consider a simple design case with two variables, R and S, where the safety is guaranteed when

$$Z = R - S \geq 0 \tag{6.1}$$

If R and S are statistically independent, the safety index is expressed in the following, as described before.

$$\beta = \frac{\mu_R - \mu_S}{\sqrt{\sigma_R^2 + \sigma_S^2}} \tag{6.2}$$

It is assumed that the most economic design is obtained when the prescribed allowable safety level is exactly achieved, that is, $P_r(R \geq S) = 1 - p_{fa}$. This assumption is valid for a simple case considered herein, but is not always valid for a case with a nonlinear performance function or with many design variables. Using the above simplification, the problem treated here can be specified " to determine the mean of structural resistance (μ_R) which satisfies the condition $P_r(R \geq S) = 1 - p_{fa}$, when the coefficients of variation of load and resistance (δ_S and δ_R) and the mean of load (μ_S) are given ".

If the allowable safety level is prescribed as β_d in the term of the safety index, μ_R can be derived from Eq.(6.2).

$$\mu_R = \frac{1 + \beta_d \sqrt{\delta_R^2 + \delta_S^2 - \beta_d^2 \delta_R^2 \delta_S^2}}{1 - \beta_d^2 \delta_R^2} \mu_S \tag{6.3}$$

where the coefficient of μ_S corresponds to the central safety factor θ_0 ($= \mu_R / \mu_S$).

Eq.(6.3) is one of the design formats which are immediately applicable. However, this equation is inconvenient to a practical use, because it includes the quantities with respect to R and S in a combined form. In practice, the statistical data are independently accumulated and analyzed, so it is desirable to treat R and S separately. For that reason, the design problem is formulated as a form based upon the load factor design[10)-14)] in which R and S are treated separately.

Introducing the characteristic values, the design condition, Eq. (6.1), can be written as

$$\phi R^{*} \geq \gamma S^{*} \tag{6.4}$$

in which R^{*} and S^{*} are the characteristic values of R and S, respectively, and also ϕ and γ denote the resistance factor and the load factor, respectively.

R^{*} and S^{*} are expressed as

$$R^{*} = \mu_R - k_p \sigma_R \tag{6.5}$$

$$S^{*} = \mu_S + k_q \sigma_S \tag{6.6}$$

Then, the mean value of resistance is written as

$$\mu_R = \mu_S + k_q \sigma_S + k_p \sigma_R \tag{6.7}$$

where k_p and k_q are the fractiles of individual distributions which correspond to the prescribed small probabilities p and q such that

$$p = P_r(R < R^{*}) \tag{6.8}$$

$$q = P_r(S > S^{*}) \tag{6.9}$$

Thus, the design problem is reduced to a problem how to determine the values of k_p and k_q to satisfy the prescribed safety level. By replacing β with β_d, Eq.(6.2) can be rewritten as follows :

$$\mu_R = \mu_S + \beta_d \sqrt{\sigma_R^2 + \sigma_S^2} \tag{6.10}$$

In order to correspond to Eq.(6.7), the square root term in Eq.(6.10)

must be linearized. Denoting the split (linearizing) coefficient by α_{RS},

$$\mu_R = \mu_S + \beta_d \alpha_{RS} (\sigma_R + \sigma_S) \tag{6.11}$$

From Eq.(6.11), k_p and k_q are obtained as

$$k_p = k_q = \beta_d \alpha_{RS} \tag{6.12}$$

The above linearization needs a mathematical approximation. For instance, N. Lind[1] employed the following approximation called " triangular approximation ".

$$\sqrt{X_1^2 + X_2^2} \simeq 0.75X_1 + 0.75X_2 \tag{6.13}$$

Although this approximation shows a good accuracy within $1/3 < X_1/X_2 < 3$, it is impossible to absolutely make Eq.(6.7) and Eq.(6.10) equivalent.

The error due to this approximation is illustrated by use of a simple design example. If $\delta_R = 0.10$, $\delta_S = 0.20$, $\mu_S = 1400\ kg/cm^2$ and $\beta_d = 3.090$ are given as a design condition, μ_R is calculated as $2667\ kg/cm^2$, by using Eqs (6.11) and (6.13). ($\beta_d = 3.090$ corresponds to $p_f = 10^{-3} = 1 - \Phi(\beta_d)$) On the other hand, Eq.(6.3) presents $\mu_R = 2575.5\ kg/cm^2$ for the same condition. Then, using Eq.(6.2), the safety indices are obtained as 3.281 and 3.090 for $\mu_R = 2667\ kg/cm^2$ and $\mu_R = 2575.5\ kg/cm^2$, respectively. This implies that the triangular approximation provides a somewhat large value for μ_R. Next, consider that δ_R changes to 0.05. In this case, the triangular approximation provides $2318\ kg/cm^2$ for μ_R, whereas μ_R is calculated as $2397\ kg/cm^2$ by Eq.(6.3). As observed from this example, the triangular approximation method presents conservative or unconservative designs, depending on the design condition. This inconsistency is due to the error involved in the linearization, which is caused by the approximations that the coefficients of σ_R and σ_S are considered equivalent, and that its value is specified as 0.75. While the latter assumption is mathematically supported to some extent, the former assumption is not well-grounded.

6.3 Failure Point

The " failure point " is defined in the previous chapter as " the point which lies at the boundary of failure region ($Z = 0$) and whose distance from the origin is the shortest ". Although this point is generally called as " design point " from the standpoint of designing,[14] the term " failure point " is used in this study to correspond to the definition in the previous chapter. Here, the physical meaning of the failure point is discussed with the aid of the relation between the safety index and the failure probability.

Probabilistically, it is true that a failure occurs at the points other than A (failure point) in the normalized space. Namely, it can be merely said that the failure point has larger possibility of failure. According to Veneziano's work[15)16)], safety index can be defined in a different way from that of Hasofer and Lind.[17)] A safety can be also measured by the expected value of the distances between the origin and the boundary of failure region. The comparison of Hasofer and Lind's and Veneziano's definitions of safety index is illustrated in Fig. 6.1. In the former, p_f and β are related along the line $\overline{OA}$. On the contrary, in the latter, all the points on the boundary are taken into account, and also the area of the safe region is related to the volume of the joint density function $f_{rs}(r,s)$ on the failure region.

If the distance between the origin and the boundary, β', is expressed as a function of the reduced angle $\underline{\alpha}^-$, the failure probability p_f is given as

$$1 - p_f = \int_{\substack{0 \le \alpha_i \le 2\pi \\ \cos\underline{\alpha}^{-t} \cos\underline{\alpha}^- \le 1}} d\underline{\alpha}^- \int_0^{\beta'(\underline{\alpha}^-)} f_{\underline{\alpha}^-,\beta}(\underline{\alpha}^-,\beta)\, d\beta \qquad (6.14)$$

in which $f_{\underline{\alpha}^-,\beta}(\underline{\alpha}^-,\beta)$ is the joint probability density function which is derived from $f_{r,s}(r,s)$ through the polar transformation, and α_i is the angle between the generic oriented direction and the i-th coordinate axis. The reduced vector $\underline{\alpha}^-$ is obtained from $\underline{\alpha} = [\alpha_1, \alpha_2, \cdots, \alpha_k]^t$ by deleting the last term.

To illustrate the difference between both definitions, a simple

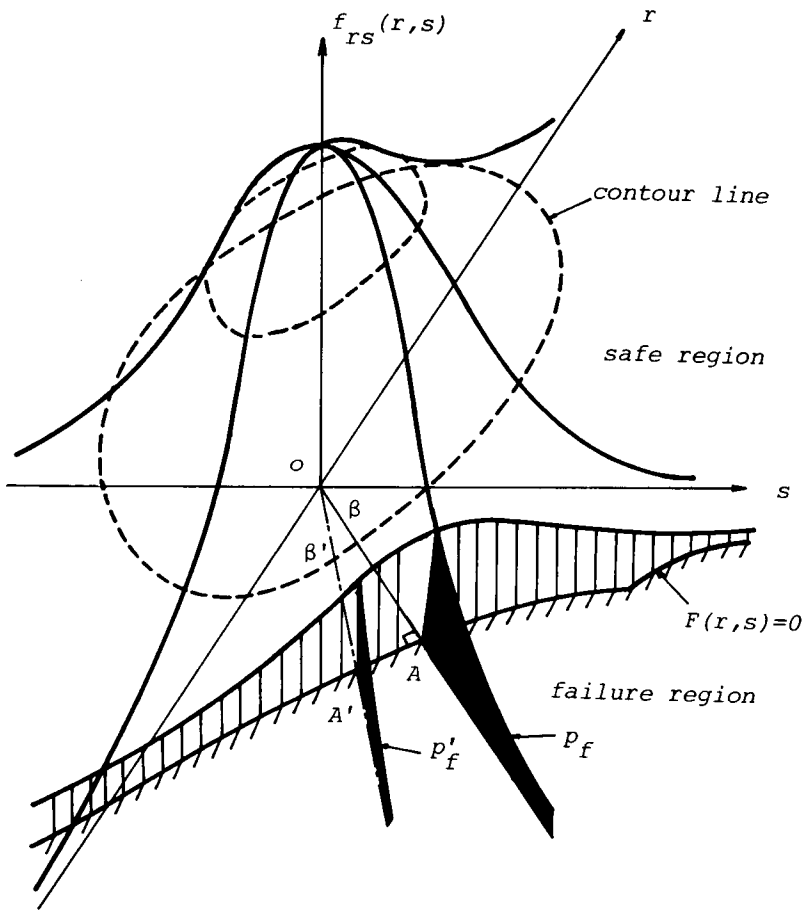

Fig. 6.1 Comparison of Hasofer & Lind's Method and Veneziano's Method

example is employed. Assume that the random variables R and S are normally distributed and their statistical properties are

$$\mu_R = 2100\ kg/cm^2\ ,\ \delta_R = 0.1 \quad \therefore\ \sigma_R = 210\ kg/cm^2$$
$$\mu_S = 1400\ kg/cm^2\ ,\ \delta_S = 0.2 \quad \therefore\ \sigma_S = 280\ kg/cm^2$$

Using the performance function that $Z = R - S$, the boundary of failure region is expressed as follows in the terms of the basic variables r and s.

$$r = \frac{4}{3} s - \frac{10}{3} \tag{6.15}$$

According to the definition proposed by Hasofer and Lind, the coordinates of the failure point and the safety index are found as

$$\vec{\beta} = -\frac{\mu_Z}{\sigma_Z} \begin{pmatrix} \sigma_R \\ -\sigma_S \end{pmatrix} = -\frac{2100 - 1400}{210^2 + 280^2} \begin{pmatrix} 210 \\ -280 \end{pmatrix} = \begin{pmatrix} -1.2 \\ 1.6 \end{pmatrix} \tag{6.16}$$

$$\beta = \mu_Z / \sigma_Z = 2. \tag{6.17}$$

When the random variables are normally distributed, $f_{\underline{\alpha}^-,\beta}(\underline{\alpha}^-,\beta)$ in Eq. (6.14) is reduced to a function expressed solely by β.

$$f_{\underline{\alpha}^-,\beta}(\underline{\alpha}^-,\beta) = \beta\, e^{-\beta^2/2} / 2\pi \tag{6.18}$$

Then, Eq.(6.14) is expressed in a form of summation.[18]

$$1 - p_f = \frac{1}{m} \sum_{i=1}^{m} \int_0^{\beta_i'^2/2} e^{-t}\, dt$$

$$= \frac{1}{m} \sum_{i=1}^{m} \left(1 - e^{-\beta_i'^2/2} \right)$$

$$= \frac{1}{m} \sum_{i=1}^{m} F_{\beta_i'}(\beta_i') \tag{6.19}$$

where m is the dividing number.

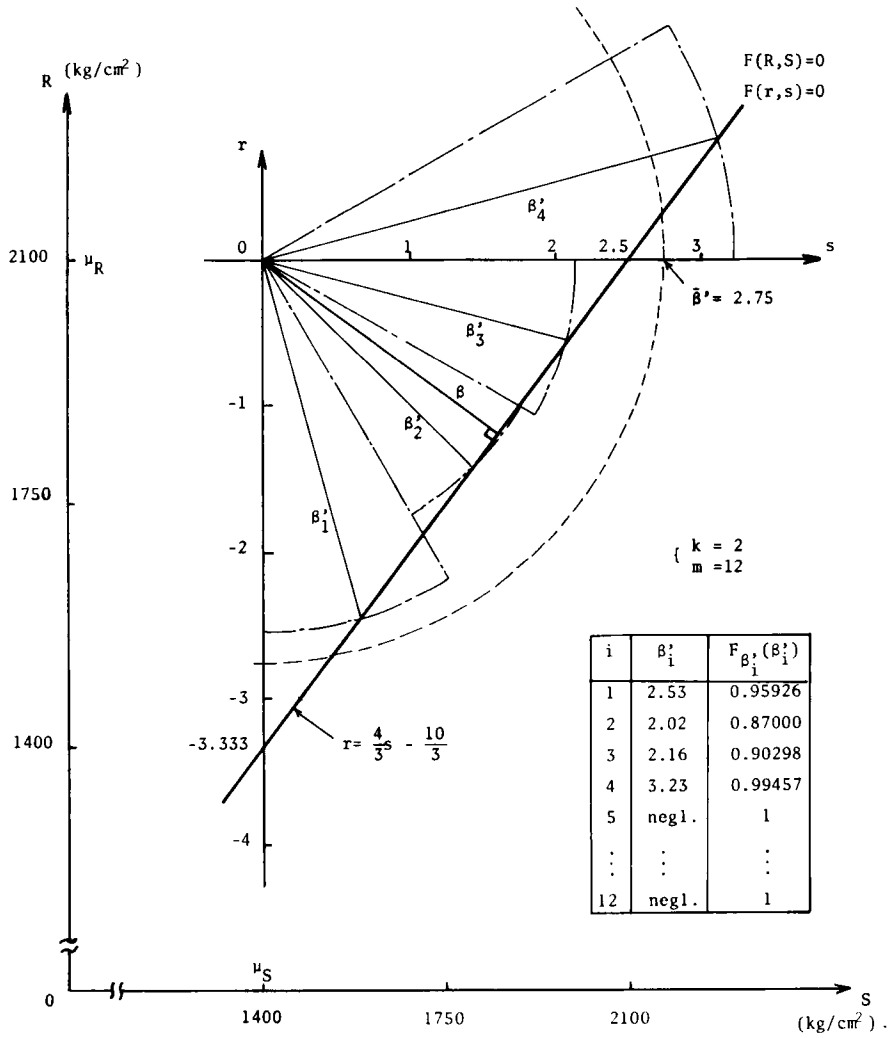

i	β_i'	$F_{\beta_i'}(\beta_i')$
1	2.53	0.95926
2	2.02	0.87000
3	2.16	0.90298
4	3.23	0.99457
5	negl.	1
⋮	⋮	⋮
12	negl.	1

Fig. 6.2 Example for Veneziano's Method

For $m = 12$, the values of β'_i and $F_{\beta'}(\beta')$ are calculated in Fig. 6.2. Finally, $1 - p_f$ is obtained as

$$1 - p_f = 0.977234 \tag{6.20}$$

By use of the inverse transformation with respect to $(1 - p_f)$, the expected value of β' is obtained as

$$\bar{\beta}' = F^{-1}_{\beta'} (1 - p_f) = \sqrt{-2 \ln p_f} = 2.75 \tag{6.21}$$

As seen in this example, the expected value is larger than the safety index calculated by Hasofer and Lind's definition. Although Veneziano's definition can precisely take the information with respect to the failure region into account, the calculation becomes more complicated. It can be considered that Hasofer and Lind's definition is superior in the computation and is sufficient for a practical use, because of the simple formulation and the underestimation of the safety index.

6.4 Iterative Design Method Using Failure Point

As stated previously, the triangular approximation method has a problem which is due to a mathematical approximation used in the determination of the split coefficients, k_p and k_q. In this section, the determination of those coefficients are carried out by use of the coordinates of failure point.

Since the coordinates of the normalized space are measured by the standard deviations of the respective random variables, the coordinates of each point, (r_i , s_i), represent the various combinations of k_p and k_q. From Eq.(5.20), the ordinal variables, R and S, are expressed in the terms of the basic variables, r and s.

$$R = \mu_R + \sigma_R r_i \tag{6.22}$$

$$S = \mu_S + \sigma_S s_i \tag{6.23}$$

The above equations mean that the set of the characteristic values with respect to R and S can be specified by the coordinates, (r_i , s_i).

Here, we attempt to find a rational combination of k_p and k_q, by paying attention to the failure point which specifies the safety index and provides the largest probability of failure. (strictly speaking, for the bell-shaped distribution like the normal distribution) The coordinates of the failure point, (r_0 , s_0), are calculated for an allowable safety level β_d as follows :

The performance function Z $(= R - S = 0)$ can be expressed in the terms of the basic variables through the normalizing operation.

$$Z = (\mu_R + \sigma_R r) - (\mu_S + \sigma_S s) = 0 \tag{6.24}$$

Eq.(6.24) is rewritten as

$$r = \frac{\sigma_S}{\sigma_R} s - \frac{\mu_R - \mu_S}{\sigma_R} \tag{6.25}$$

Then, the failure point must satisfy the relation such as

$$\frac{s_0}{r_0} = - \frac{\sigma_S}{\sigma_R} \tag{6.26}$$

for $r_0 < 0$ and $s_0 > 0$.
Also, r_0 and s_0 are related to the prescribed allowable level β_d as follows :

$$r_0^2 + s_0^2 = \beta_d^2 \tag{6.27}$$

Solving Eqs (6.26) and (6.27), the coordinates of the failure point can be obtained as

$$\left.\begin{aligned} r_0 &= \frac{-\beta_d \sigma_R}{\sqrt{\sigma_R^2 + \sigma_S^2}} \quad (< 0) \\ s_0 &= \frac{\beta_d \sigma_S}{\sqrt{\sigma_R^2 + \sigma_S^2}} \quad (> 0) \end{aligned}\right\} \tag{6.28}$$

Expressing (r_0 , s_0) in the (R , S) - coordinates and substituting them to Eq.(6.24), the following relation is given.

$$\mu_R (1 + r_0 \delta_R) = \mu_S (1 + s_0 \delta_S) \qquad (6.29)$$

Then, the resistance factor ϕ and load factor γ can be obtained by corresponding Eq.(6.29) to the load factor formula Eq.(6.4). Considering the mean values as the characteristic values, ϕ and γ become

$$\left.\begin{aligned} \phi &= 1 - \frac{\beta_d \sigma_R}{\sqrt{\sigma_R^2 + \sigma_S^2}} \delta_R \\ \gamma &= 1 + \frac{\beta_d \sigma_S}{\sqrt{\sigma_R^2 + \sigma_S^2}} \delta_S \end{aligned}\right\} \qquad (6.30)$$

By use of the above equations, it is possible to calculate the necessary mean value of the resistance without approximation. However, the calculation needs an iterative procedure for a case where the dispersion of the resistance is given by its coefficient of variation, because Eqs (6.28) and (6.30) involve the standard deviation of the resistance. The iterative procedure consists of the following steps :

Step 1 Assume the initial value of μ_R.

Step 2 Calculate the values of (r_0 , s_0) by use of σ_R which is obtained by the assumed μ_R and the given δ_R.

Step 3 Calculate the new value of μ_R, using the values of (r_0 , s_0) obtained in the previous step.

Step 4 Repeat the above steps until μ_R converges.

Consider the same example as that used in the previous section, in order to examine the accuracy of the iterative method proposed here. The numerical results are shown in Table 6.1. Starting from the initial value that $\mu_R = 2000\ kg/cm^2$, the final solutions can be obtained after three iterations.

$$\mu_R = 2575.5\ kg/cm^2 \ , \ \phi = 0.791 \ , \ \gamma = 1.455$$

The results imply that the proposed method provides a reasonable solution which is equivalent to the solution obtained by Eq.(6.3), and also

Table 6.1 Numerical Results Obtained by the Proposed Iterative Method

Repetition Number	μ_R	r_0	s_0
1	2000	-1.796	2.514
2	2564.5	-2.087	2.279
3	2575.7	-2.092	2.274
4	2575.5	-2.092	2.274

Table 6.2 Numerical Results for a Case with Nonlinear Performance Function

	r	s
Initial Value	-1.	2.924
Step 1	-1.287	2.809
Step 2	-1.259	2.822
Step 3	-1.263	2.820
Step 4	-1.262	2.821
Step 5	-1.262	2.821
Final Solution	-1.262	2.821

imply that it enables to determine the resistance and load factors without difficulty.

Furthermore, the proposed method is applied for a case in which the performance function is nonlinear. As well as a linear case, the following performance function is considered.

$$Z = F\ (\ R\ ,\ S\ ) = F\ (\ r\ ,\ s\ ;\ \mu_R\ ) = 0 \qquad (6.31)$$

In this case, the failure point is defined as the point which minimizes the mean value of the structural resistance and which satisfies the condition that the distance from the origin is equal to the prescribed safety level β_d. Then, the problem reduces to a nonlinear optimization problem.

Find r *and* s

such that the objective function

$$P = \mu_R(\ r,s\ ) \quad \rightarrow \quad \textit{Minimize} \qquad (6.32)$$

subject to

$$\sqrt{r^2 + s^2} = \beta_d \qquad (6.33)$$

$$F\ (\ r\ ,\ s\ ;\ \mu_R\ ) = 0 \qquad (6.34)$$

Using Lagrange's multiplier method, the above optimization problem can be expressed as

Find r *and* s

such that

$$\Phi\ (\ r\ ,\ s\ ,\ \lambda\ ) = \mu_R(\ r\ ,\ s\ ) - \lambda\ (\sqrt{r^2 + s^2} - \beta_d\ )$$

$$\rightarrow \quad \textit{Minimize} \qquad (6.35)$$

in which Φ and λ denote Lagrangean and Lagrange's multiplier, respectively. From the stationary condition, the following relations are derived.

$$\left.\begin{array}{l} \dfrac{\partial \Phi}{\partial r} = 0 \ ; \quad \dfrac{\partial \mu_R(r,s)}{\partial r} - \dfrac{\lambda\, r}{\sqrt{r^2+s^2}} = 0 \\ \end{array}\right\}$$

$$\left.\begin{aligned} \frac{\partial \Phi}{\partial s} &= 0 \;;\quad \frac{\partial \mu_R(r,s)}{\partial s} - \frac{\lambda\, s}{\sqrt{r^2+s^2}} = 0 \\ \frac{\partial \Phi}{\partial \lambda} &= 0 \;;\quad \sqrt{r^2+s^2} - \beta_d = 0 \end{aligned}\right\} \qquad (6.36)$$

Eq.(6.36) results in

$$\frac{r}{s} = \frac{\partial \mu_R / \partial r}{\partial \mu_R / \partial s}$$

$$\therefore \quad r = \frac{\partial \mu_R / \partial r}{\partial \mu_R / \partial s} \cdot s \qquad (6.37)$$

and

$$s = \sqrt{\beta_d^2 - r^2} \qquad (6.38)$$

It is convenient to use a one-by-one approximation method for the actual computation. The outline of this method is as follows :

Step 1 Find the function $\mu_R(r,s)$ from the performance function $F(r,s;\mu_R) = 0$.

Step 2 Derive the relation expressed by Eq.(6.37).

Step 3 Calculate the value of s through Eq.(6.38), by using the prescribed β_d and the assumed r.

Step 4 Calculate a new value of r by substituting the values of r and s obtained in the previous steps to Eq.(6.37).

Step 5 Repeat Step 3 and Step 4 until the convergence is achieved.

Step 6 The design value of μ_R is obtained from the function $\mu_R(r,s)$, by using the final solutions of r and s.

This procedure is illustrated by use of a simple design example. Let's consider the following performance function.

$$Z = F(R, S) = R - \frac{S^2}{20000} \qquad (6.39)$$

Introducing the basic variables r and s, the mean value of the resistance is obtained as

$$\mu_R(r, s) = \frac{(1+\delta_S^2 \cdot s)^2 \mu_S^2}{20000(1+\delta_R \cdot r)} \qquad (6.40)$$

Then, Eq.(6.37) gives the following relation :

$$r = -\frac{\delta_R}{2\delta_S} \frac{1+\delta_S s}{1+\delta_R r} s \qquad (6.41)$$

Assuming that $\beta_d = 3.090$, $\delta_R = 0.1$, $\sigma_S = 280\ kg/cm^2$ and $\mu_S = 1400\ kg/cm^2$, Eqs (6.38) and (6.41) are calculated as

$$s = \sqrt{3.090^2 - r^2} \qquad (6.42)$$

$$r = -\frac{1+0.2s}{4(1+0.1r)} s \qquad (6.43)$$

These simultaneous equations can be solved by the iterative procedure, as shown in Table 6.2. Then, the final solutions are

$$\mu_R = 2744\ kg/cm^2$$

$$(r_0, s_0) = (-1.262, 2.821)$$

6.5 Determination of Partial Load Factors

In the foregoing section, all load effects are treated as involved in a random variable S. However, actual structures are generally subjected to several different kinds of loads at the same time, and various combinations of those loads can be considered. In order to introduce rationally the characteristics of each load (i.e. intensity, frequency of occurrence, etc.) into the design process, the load factor design seems to be more convenient than the allowable stress criterion method in which the combination of loads is taken into consideration by increasing the allowable stress limit.

Here, the iterative design method is extended and used to determine the partial load factors. Consider that only dead load D and live load

L are independently applied to a structure. Then, the total load S is given as

$$S = D + L \tag{6.44}$$

where its mean μ_S and variance σ_S^2 are

$$\mu_S = \mu_D + \mu_L \tag{6.45}$$

$$\sigma_S^2 = \sigma_D^2 + \sigma_L^2 \tag{6.46}$$

where μ_D , μ_L : mean values of D and L
σ_D^2 , σ_L^2 : variances of D and L

Using $Z = R - (D + L)$ for the performance function, the safety index is calculated as

$$\beta = \frac{\mu_R - (\mu_D + \mu_L)}{\sqrt{\sigma_R^2 + (\sigma_D^2 + \sigma_L^2)}} \tag{6.47}$$

Eq.(6.47) can be rewritten in the following :

$$\mu_R = (\mu_D + \mu_L) + \beta\sqrt{\sigma_R^2 + (\sigma_D^2 + \sigma_L^2)} \tag{6.48}$$

In usual, the partial load factors γ_D and γ_L are determined by corresponding Eq.(6.48) to the formula of the load factor design shown below.

$$\phi \mu_R \geq \gamma_D \mu_L + \gamma_L \mu_L \tag{6.49}$$

The equalization between Eqs (6.48) and (6.49) has been carried out by introducing the linearizing coefficients. The split coefficient α_{RS} is firstly employed for the linearization with respect to R and S.

$$\mu_R = (\mu_D + \mu_L) + \beta \alpha_{RS} (\sigma_R + \sqrt{\sigma_D^2 + \sigma_L^2}) \tag{6.50}$$

Next, introducing α_{DL} into the linearization with respect to D and L,

$$\mu_R = (\mu_D + \mu_L) + \beta \alpha_{RS} \{\sigma_R + \alpha_{DL} (\sigma_D + \sigma_L)\} \tag{6.51}$$

From Eqs (6.49) and (6.51), the resistance factor ϕ and partial load factors γ_D and γ_L can be obtained.

$$\left.\begin{aligned} \phi &= 1 - \alpha_{RS}\,\beta\,\delta_R \\ \gamma_D &= 1 + \alpha_{RS}\,\alpha_{DL}\beta\,\delta_D \\ \gamma_L &= 1 + \alpha_{RS}\,\alpha_{DL}\beta\,\delta_L \end{aligned}\right\} \qquad (6.52)$$

As representative methods for determining α_{RS} and α_{DL}, the following methods can be enumerated :

(1) Triangular Approximation Method[1)]

As stated before, both of α_{RS} and α_{DL} are approximately specified as *0.75*. (It is also possible to use the values other than *0.75* for α_{RS} or α_{DL}[2)]) Although this method includes errors in the determination of the design resistance, it requires the least computation load.

(2) Shah's Method[9)]

In this method, α_{RS} and α_{DL} are related to σ_R, σ_D and σ_L as follows :

$$\alpha_{RS} = \frac{\sqrt{\sigma_R^2 + \sigma_S^2}}{\sigma_R + \sigma_S} \qquad (6.53)$$

$$\alpha_{DL} = \frac{\sqrt{\sigma_D^2 + \sigma_L^2}}{\sigma_D + \sigma_L} \qquad (6.54)$$

(3) Ang's Method[8)]

A. Ang proposed a method in which α_{RS} is treated as *0.75* to exclude the complicated computations, while α_{DL} is determined based on Shah's method.

In the above three methods, the same coefficient α_{RS} (α_{DL}) is used for *R* (*D*) and *S* (*L*). While this treatment enables to make the calculation easier, it induces some gaps between the calculated safety index and the prescribed safety level as clarified in section 6.3.

Here, we attempt to determine the partial load factors by extending

the design method based on the failure point. In this case, the vector $\vec{\beta}_0$, which gives the coordinates of the failure point, can be expressed as

$$\vec{\beta}_0 = \begin{pmatrix} r_0 \\ d_0 \\ \ell_0 \end{pmatrix} = \frac{\beta_d}{\sqrt{\sigma_R^2 + \sigma_D^2 + \sigma_L^2}} \begin{pmatrix} -\sigma_R \\ \sigma_D \\ \sigma_L \end{pmatrix} \tag{6.55}$$

in which r, d and ℓ are the basic variables of R, D and L, respectively. Transforming the coordinates (r_0 , d_0 , ℓ_0) to the (R , D , L) - coordinates and substituting them to the performance function, the following design formula is obtained.

$$(1 + r_0\delta_R) \mu_R = (1 + d_0\delta_D) \mu_D + (1 + \ell_0\delta_L) \mu_L \tag{6.56}$$

From this formula, ϕ, γ_D and γ_L can be calculated as

$$\left.\begin{aligned} \phi &= 1 + r_0\delta_R = 1 - \frac{\beta_d\sigma_R}{\sqrt{\sigma_R^2 + \sigma_D^2 + \sigma_L^2}} \delta_R \\ \gamma_D &= 1 + d_0\delta_D = 1 + \frac{\beta_d\sigma_D}{\sqrt{\sigma_R^2 + \sigma_D^2 + \sigma_L^2}} \delta_D \\ \gamma_L &= 1 + \ell_0\delta_L = 1 + \frac{\beta_d\sigma_L}{\sqrt{\sigma_R^2 + \sigma_D^2 + \sigma_L^2}} \delta_L \end{aligned}\right\} \tag{6.57}$$

It is possible to deal with a case with more than three loads in the same fashion. It is to be noted that Eq.(6.57) presents the values equivalent to the resistance and load factors which are obtained by using the Taylor expansion of performance function with respect to random variables.[19)]

By comparing with the afore-mentioned three methods, the validity and applicability of the proposed method are discussed hereafter.

Observing Eqs (6.52) and (6.57), it is obtained that both equations include the coefficients of variation of the variables, R, D and L, which are used to extend or shrink the axes of coordinates in the normalizing transformation. The normalizing transformation gives the property of isotropy for the resulting space. Then, a design is specified in this space by the condition that $Z = R - (D + L)$. The difference between the proposed method and the three methods depends on how to use the informations obtained from the design condition. For example, the triangular approximation method utilizes only the value of safety index, and always treats the ratio of the resistance factor and the load factor, which corresponds to a direction generated from the origin, as a constant. On the other hand, the proposed method utilizes the direction perpendicular to the boundary of failure region, by means of the coordinates of the failure point. Namely, the following relations are used instead of the split coefficients α_{RS} and α_{DL}.

$$\left.\begin{aligned} &\alpha_{RS} \sim -\sigma_R / \sqrt{\sigma_R^2 + \sigma_D^2 + \sigma_L^2} \\ &\alpha_{RS}\,\alpha_{DL} \sim \sigma_D / \sqrt{\sigma_R^2 + \sigma_D^2 + \sigma_L^2} \quad or \quad \sigma_L / \sqrt{\sigma_R^2 + \sigma_D^2 + \sigma_L^2} \end{aligned}\right\} \qquad (6.58)$$

Eq.(6.58) means that in the proposed method, the resistance and load factors are obtained by alloting the allowable level β_d to R, D and L, according to the ratio of the standard deviations. Then, the denominator in Eq.(6.58) is interpreted as the normalizing coefficient. Shah's method and Ang's method have the similar form to that of the proposed method, but they don't utilize the direction perpendicular to the line specified by the performance function.

Next, we consider a case where the performance function is given in a logarithmic form. In this case, Z and β are expressed as

$$Z = ln\ R - ln\ S = ln\ (R/S) \qquad (6.59)$$

$$\beta = (\mu_{ln\ R} - \mu_{ln\ S}) / \sqrt{\sigma_{ln\ R}^2 + \sigma_{ln\ S}^2} \qquad (6.60)$$

When δ_R and δ_S are smaller than 0.3, β can be approximately written as

$$\beta = ln\ (\mu_R / \mu_S) / \sqrt{\delta_R^2 + \delta_S^2} \qquad (6.61)$$

Table 6.3 Comparison of Some Load Factor Design Methods

(Z = ln (R / S))

	Triangular Approx.	A. Ang's Method	Proposed Method
Design Format	$\exp(-0.75\beta_d\delta_R)\cdot\mu_R$ $= \exp(0.75^2\beta_d\delta_D)\cdot\mu_D$ $+ \exp(0.75^2\beta_d\delta_L)\cdot\mu_L$	$\exp(-0.75\beta_d\delta_R)\cdot\mu_R$ $= \exp(0.75\beta_d\delta_S)\cdot\mu_S$ $= \exp(0.75\alpha\beta_d\delta_D)\mu_D$ $+ \exp(0.75\alpha\beta_d\delta_L)\mu_L$	$\exp\left(-\frac{\beta_d\delta_R^2}{\sqrt{\delta_R^2+\delta_S^2}}\right)\mu_R$ $= \exp\left(\frac{\beta_d\delta_S^2}{\sqrt{\delta_R^2+\delta_S^2}}\right)\mu_S$ $= \exp\left[\frac{\beta_d(\delta_D^2+\rho^2\delta_L^2)}{(1+\rho)^2 V}\right](\mu_D+\mu_L)$ $= \alpha'\left(\exp\left[\frac{\beta_d\delta_D^2}{(1+\rho)^2V}\right]\mu_D + \exp\left[\frac{\beta_d\rho^2\delta_L^2}{(1+\rho)^2V}\right]\mu_L\right)$ where $V=\sqrt{\delta_R^2+\frac{\delta_D^2+\rho^2\delta_L^2}{(1+\rho)^2}}$
Determination of α and α'		$(1+\rho)\exp\left[\frac{0.75\beta_d}{1+\rho}\times\sqrt{\delta_D^2+\rho^2\delta_L^2}\right]$ $=\exp(0.75\alpha\beta_d\delta_D)$ $+\rho\exp(0.75\alpha\beta_d\delta_L)$	$\alpha' = \frac{(1+\rho)\exp\left[\frac{\beta d(\delta_D^2+\rho^2\delta_L^2)}{(1+\rho)^2V}\right]}{\exp\left[\frac{\beta_d\delta_D^2}{(1+\rho)^2V}\right]+\rho\exp\left[\frac{\beta_d\rho^2\delta_L}{(1+\rho)^2V}\right]}$
Load Factors	$\phi = \exp(-0.75\beta_d\delta_R)$ $\gamma_D = \exp(0.75^2\beta_d\delta_D)$ $\gamma_L = \exp(0.75^2\beta_d\delta_L)$	$\phi = \exp(-0.75\beta_d\delta_R)$ $\gamma_D = \exp(0.75\alpha\beta_d\delta_D)$ $\gamma_L = \exp(0.75\alpha\beta_d\delta_L)$	$\phi = \exp[-\beta_d\delta_R^2/V]$ $\gamma_D = \alpha'\exp[\beta_d\delta_D^2/(1+\rho)^2V]$ $\gamma_L = \alpha'\exp(\beta_d\rho^2\delta_L/(1+\rho)^2V]$

By rewriting Eq.(6.61) in the exponential form and introducing the linearizing coefficient, the following formula can be obtained.

$$exp(-\alpha_{RS}\ \beta\delta_R\ )\ \mu_R = exp(\ \alpha_{RS}\ \beta\ \delta_S\ )\ \mu_S \qquad (6.62)$$

Since the total load S is the summation of D and L, δ_S is calculated as

$$\delta_S = \frac{\sqrt{\delta_D^2 + \rho^2\ \delta_L^2}}{1 + \rho} \qquad (6.63)$$

in which ρ is μ_L/μ_D.

Then, the partial load factors can be obtained by use of the triangular approximation method or Ang's method. In Table 6.3, the proposed method is shown together with the above two methods. In Ang's method, the coefficient α is introduced to linearize the right hand term of Eq.(6.62). While Ang's method equally allots the allowable safety level β_d to D and L by means of α, the proposed method decomposes the effect of the total load by use of the coordinates of the failure point. However, as well as Ang's method, the coefficient α', which equates the magnitudes of total load and summation of partial loads, should be approximately determined by the iterative procedure, because it is impossible to reduce the partial load factors directly from the coordinates of the failure point.

6.6 Numerical Examples[20)]

Example 1

To compare the proposed method with the usual methods, the combination of dead load D and live load L is considered. As a safety level, five cases with p_s ($= 1 - p_f$) $= 0.9,\ 0.99,\ 0.999,\ 0.9999,\ 0.99999$ are employed. Corresponding to these values, the allowable safety indices are obtained as $\beta_d = 1.282,\ 2.326,\ 3.090,\ 3.720,\ 4.266$, respectively, through the inverse transformation such as $\beta = \Phi^{-1}(p_s)$. Then, the statistical data are given as[9)]

$$\mu_D = 60\ lb/ft^2\ ,\ \sigma_D = 5\ lb/ft^2$$

$$\mu_L = 80\ lb/ft^2\ ,\ \sigma_L = 20\ lb/ft^2$$

The mean value of the resistance μ_R and the reduced partial load factors γ_1' ($= \gamma_1/\phi$) and γ_2' ($= \gamma_2/\phi$) are calculated for some cases with different coefficients of variation of the resistance. (subscript *1* and *2* correspond to dead load and live load, respectively) In Fig. 6.3 - Fig. 6.5, the results are illustrated for the case with the performance function that $Z = R - S$. Fig. 6.6 - Fig. 6.8 show the results obtained for $Z = ln\ (R/S)$. From these figures, the following conclusions are obtained :

- Although there is little difference between the triangular approximation method and Ang's method, Ang's method presents somewhat large values for μ_R, γ_1' and γ_2'.
- In Shah's method, the values of μ_R, γ_1' and γ_2' are quite sensitive to the change of δ_R. The proposed method is less sensitive than Shah's method, but more sensitive than the triangular approximation and Ang's method. (see Fig. 6.3)
- The proposed method provides larger values for γ_2' when δ_R is small. This is why the proposed method tends to give a large load factor for a load whose standard deviation is large.
- While in the proposed method, the increasing rates of μ_R, γ_1' and γ_2' become larger as the increase of δ_R, those in the triangular approximation or Ang's method are almost constant.
- In spite of the choice of performance function, the probability of reliability or the safety index is not so varied for the changes of γ_1' and γ_2'. Especially, this tendency is remarkable for small δ_R. This is due to the fact that in the proposed method the error involved in the determination of γ_1' and γ_2' is hardly influential on the value of β in the design process.
- For a case with $Z = ln\ (R/S)$, the values of μ_R, γ_1' and γ_2' change proportional to the change of p_s or β_d. This tendency means that the performance function with a logarithmic form is more convenient to estimate the changes of μ_R, γ_1' and γ_2' according to the change of the design condition.

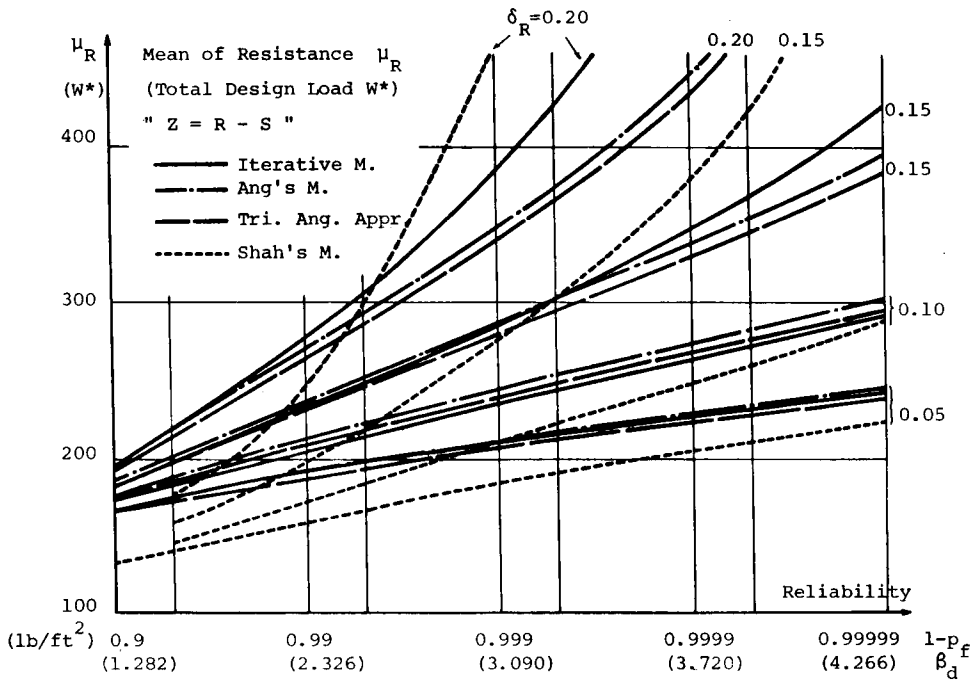

Fig. 6.3 Mean Value of Resistance (Z = R - S)

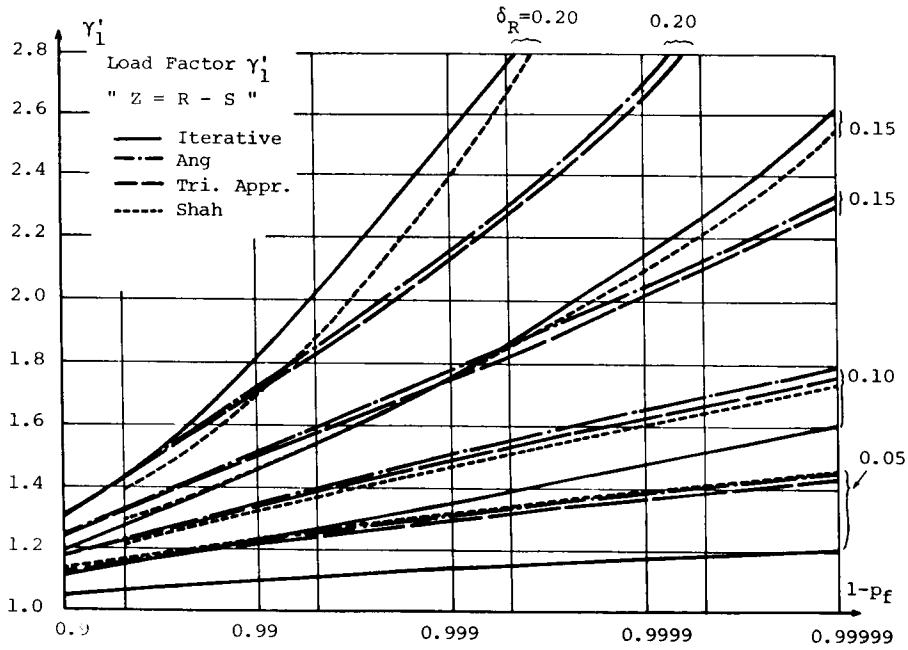

Fig. 6.4 Load Factor γ_1' (Z = R - S)

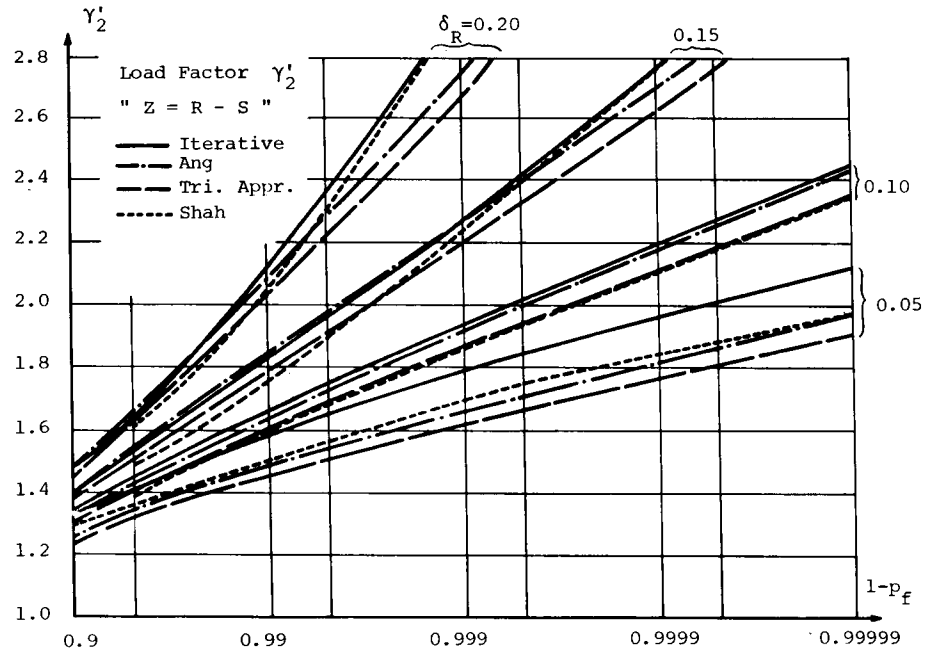

Fig. 6.5 Load Factor γ_2' (Z = R - S)

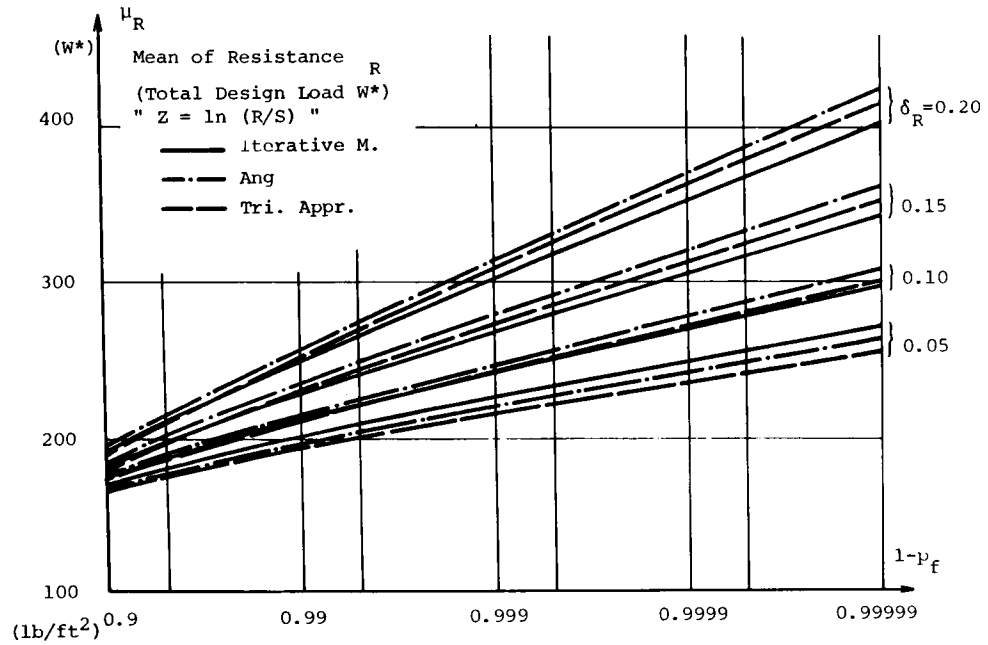

Fig. 6.6 Mean Value of Resistance (Z = ln (R/S))

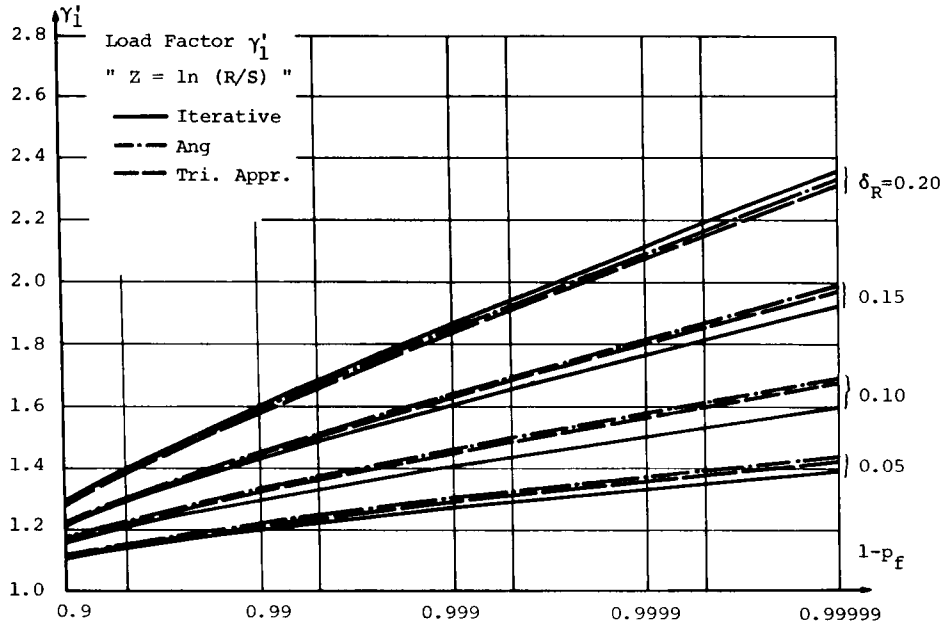

Fig. 6.7 Load Factor γ_1' (Z = ln (R/S))

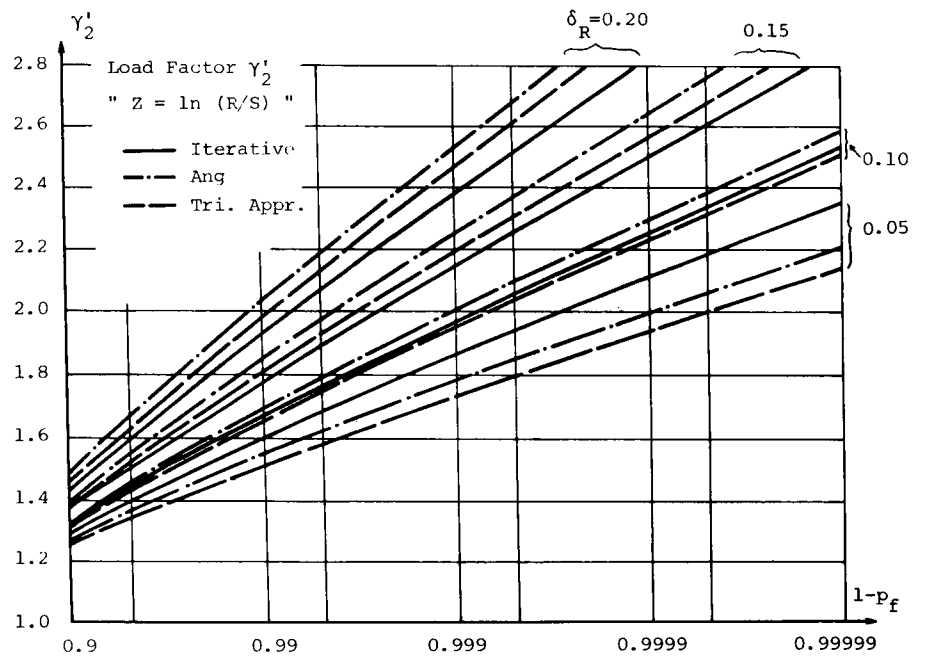

Fig. 6.8 Load Factor γ_2' (Z = ln (R/S))

Example 2

As a more practical case, let's consider the design of a rigid frame which is subjected to dead load D, live load L, wind load W and earthquake load E.[21] Its dimension and rigidity are presented in Fig. 6.9(a), and the applied loading condition is shown in Fig. 6.9(b), where $\mu_D = 60\ lb/ft^2$, $\mu_L = 80\ lb/ft^2$, w_1 (uniform load due to D) = $1.2\ klb/ft$, w_2 (uniform load due to L) = $1.6\ klb/ft$, Q_1 (wind load) = $3.3\ klb$ and Q_2 (earthquake load) = $2.4\ klb$.

If a failure occurs at the beam or column by the induced bending moment, the points A - E have a large probability of failure. The bending moments induced at those points are calculated and listed in Table 6.4(a). Five load combinations are considered here and presented in the same table. Since the point B has the largest bending moment, the design is performed by paying attention to this point. Table 6.4 (b) shows the mean values, standard deviations and coefficients of variation of the bending moments induced by the individual loads. Subscript 1, 2, 3 and 4 correspond to D, L, W and E, respectively. The correlation coefficient between the loads is 0.5 for D and E, and zero for other sets of loads. Also, the coefficient of variation of the resistance is 0.10 and the allowable safety level is specified as 3.720, which corresponds to $p_s = 0.9999$.

Under the above design conditions, the mean value of the resistance μ_R and the laod factors γ'_{ij} (i and j mean the combination of loads and the individual load, respectively.) are determined. The obtained numerical results are shown in Table 6.5(a) in comparison with those obtained by Shah's method.[21] (see Table 6.5(b)) The comparison of Table 6.5(a) and Table 6.5(b) leads to the following conclusions :

- Observing the results obtained for case 4, it is said that in the proposed method, the coefficient of variation is more influential on the determination of load factors, compared with Shah's method. That is, the proposed method provides large factors for the load with high dispersion.
- Despite of the difference between individual load factors, both methods present almost same design loads for each load combination.

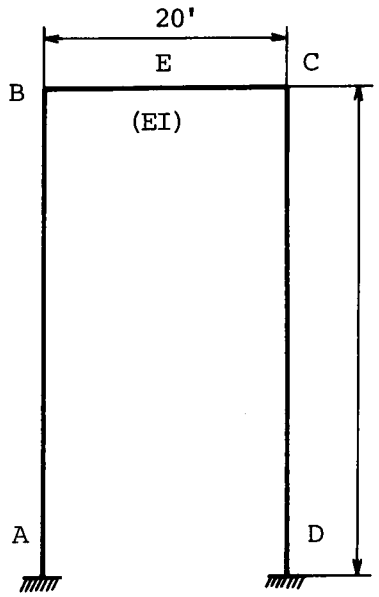

a) Configuration and Rigidity

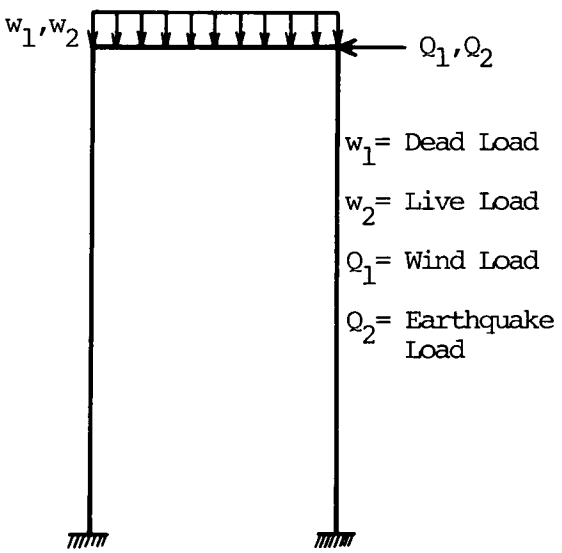

b) Applied Loads

Fig. 6.9 Portal Frame Example

Table 6.4 Bending Moments

a) Bending Moments at Points A - E

Load / Point	D	L	W	E	D + L	D + W	D + E	D+L+W	D+L+E
A	13.4	18.0	47.1	34.3	31.4	60.5	47.7	78.5	65.7
B	-26.7	-35.7	-35.4	-25.7	-62.4	-62.1	-52.4	-97.8	-88.1
C	-26.7	-35.7	35.4	27.7	-62.4	8.7	-1.0	-27.0	-36.7
D	13.4	18.0	-47.1	-34.3	31.2	-33.7	-17.9	-15.9	-3.1
E	33.3	44.5	0.	0.	77.8	33.3	33.3	77.8	77.8

(kip-ft)

b) Bending Moments at Point B for Individual Loads

Load (i)	μ_i (kip-ft)	δ_i	σ_i (kip-ft)
1	26.7	0.083	2.22
2	35.7	0.25	8.93
3	35.4	0.20	7.08
4	25.7	0.25	6.43

Table 6.5 Comparison of Proposed Method and Shah's Method

a) Numerical Results by the Proposed Method

Case	Loading Condition	ϕ_i	γ_{i1} γ'_{i1}	γ_{i2} γ'_{i2}	γ_{i3} γ'_{i3}	γ_{i4} γ'_{i4}	Design Load μ_i
1	D + L	0.707	1.046 1.480	1.555 2.201	0. 0.	0. 0.	118.1
2	D + W	0.690	1.051 1.523	0. 0.	1.392 2.017	0. 0.	112.1
3	D + E	0.707	1.136 1.607	0. 0.	0. 0.	1.552 2.195	99.3
4	D+L+W	0.687	1.032 1.502	1.388 2.020	1.246 1.814	0. 0.	176.3
5	D+L+E	0.699	1.085 1.552	1.412 2.020	0. 0.	1.345 1.924	163.0

(kip-ft)

b) Numerical Results by Shah's Method

Case	Loading Condition	γ'_{i1}	γ'_{i2}	γ'_{i3}	γ'_{i4}	Design Load μ_i
1	D + L	1.61	2.13	0.	0.	119
2	D + W	1.61	0.	1.96	0.	113
3	D + E	1.61	0.	0.	2.08	96.8
4	D+L+W	1.57	1.97	1.85	0.	177
5	D+L+E	1.58	1.97	0.	1.97	163

(kip-ft)

Example 3

Let's determine the cross sectional areas of the lower chord T of a trussed bridge which is shown in Fig. 6.10(a).[22] Since the bridge is considered to belong to the first-class bridges, *TL-20* load is employed as an applied load.

At first, the cross sectional area is calculated by use of the allowable stress design format. Using the nominal safety factor θ^* and the nominal load ratio ρ^* which corresponds to the calculated cross sectional area, an equivalent safety index is obtained. Next, the truss is redesigned to satisfy the obtained safety level, by using the proposed reliability-based design method, and the obtained results are compared with those obtained by the allowable stress design.

It is postulated that the dead load including the weights of the pavements, deck plate, lateral members, etc. is *3.75 t/m*, and that the line load, the uniform load, the impact load, etc. are taken as the live load. Then, the member force, T_0, which is induced by the dead and live loads are obtained as

$$\textit{Member force due to the dead load} : T_D = 360.1 \text{ t}$$

$$\textit{Member force due to the live load} : T_L = 182.9 \text{ t}$$

$$T_0 = T_D + T_L = 543.0 \text{ t}$$

The total member force is obtained by adding T'_D, which is the force due to the self-weights of the main truss members, to T_0. In this case, T'_D is calculated as $0.3215A$ (t) when the density of steel is *7.85*. Then, the cross sectional area of the member T is determined as $A = 344 \text{ cm}^2$, if *SM50* steel is employed. Since the allowable stress limit and the nominal yield stress of *SM50* steel are 1900 kg/cm^2 and 3200 kg/cm^2, the nominal safety factor becomes *1.684*.

Next, the load factor design format is applied for determining the necessary cross sectional area. Taking $Z = R - S$ as the performance function, the safety index is expressed in the term of safety factor.

$$\beta = \frac{\theta - 1}{\sqrt{\theta^2 \delta_R^2 + \delta_S^2}} \tag{6.64}$$

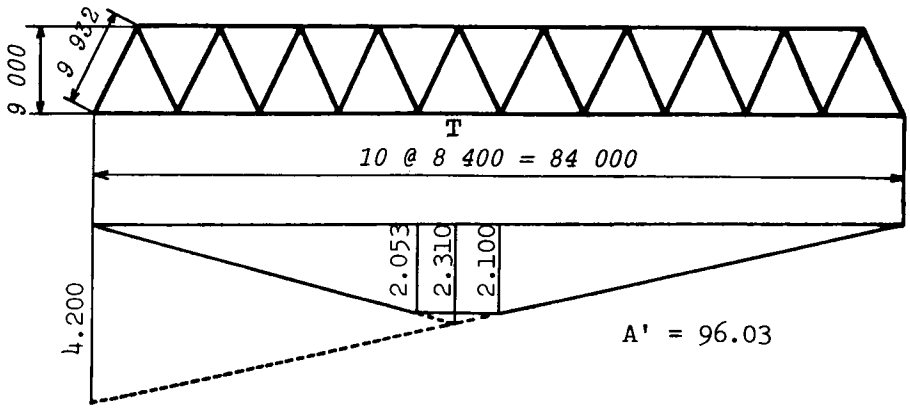

a) Influence Line of Member T

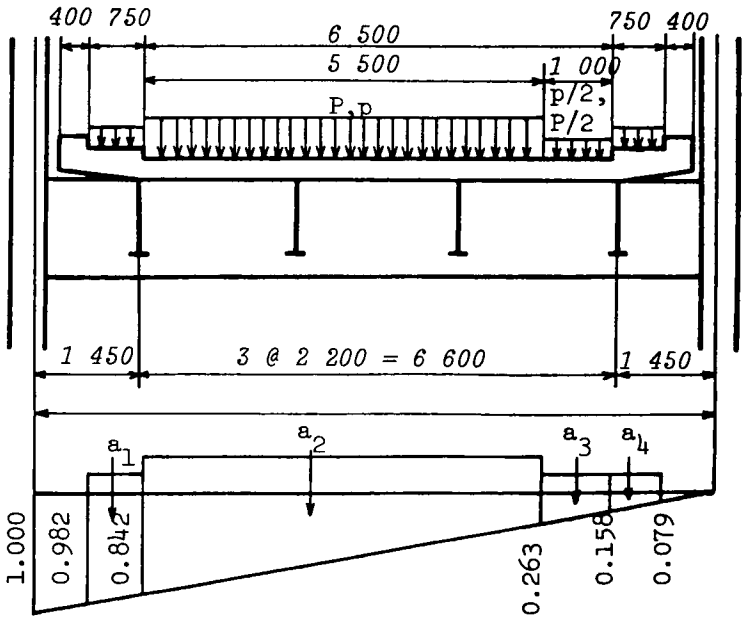

a_1=0.661, a_2=3.039, a_3=0.211, a_4=0.089

b) Design Load

Fig. 6.10 Warren Truss with Parallel Chords

Table 6.6 Numerical Results by the Proposed Method

δ_R	δ_D	δ_L	β	ϕ	γ_D	γ_L	γ_D'	γ_L'	R* (t)	A (cm^2)
0.05	0.05	0.15	8.864	0.734	1.138	1.485	1.550	2.023	1099.6	343.6
		0.20	8.436	0.777	1.125	1.781	1.448	2.292	1100.8	344.0
		0.25	7.972	0.823	1.112	2.088	1.351	2.537	1099.8	343.7
	0.10	0.15	7.793	0.839	1.428	1.375	1.702	1.617	1100.9	344.0
		0.20	7.501	0.866	1.397	1.617	1.613	1.867	1100.8	344.0
		0.25	7.168	0.895	1.362	1.889	1.522	2.101	1100.5	343.9
0.10	0.05	0.15	4.873	0.636	1.402	1.147	1.638	1.803	1101.0	344.1
		0.20	4.798	0.653	1.041	1.252	1.594	1.917	1101.1	344.1
		0.25	4.708	0.673	1.039	1.380	1.544	2.051	1101.9	344.3
	0.10	0.15	4.670	0.682	1.154	1.135	1.692	1.664	1100.8	344.0
		0.20	4.605	0.696	1.149	1.233	1.651	1.772	1101.1	344.1
		0.25	4.524	0.714	1.144	1.351	1.602	1.892	1100.1	343.8
0.15	0.05	0.15	3.313	0.613	1.019	1.068	1.662	1.742	1101.1	344.1
		0.20	3.290	0.622	1.019	1.119	1.638	1.799	1100.0	343.8
		0.25	3.260	0.632	1.019	1.182	1.612	1.870	1101.0	344.1
	0.10	0.15	3.247	0.636	1.074	1.065	1.689	1.675	1101.1	344.1
		0.20	3.225	0.644	1.073	1.114	1.666	1.730	1100.6	343.9
		0.25	3.197	0.654	1.072	1.175	1.639	1.797	1100.1	343.8

Table 6.7 Numerical Results of the Triangular Approximation Method

δ_R	δ_D	δ_L	β	ϕ	γ_D	γ_L	γ_D'	γ_L'	R (t)	A (cm^2)
0.10	0.05	0.15	4.872	0.762	1.137	1.411	1.492	1.852	1030.6	322.1
		0.20	4.792	0.768	1.135	1.540	1.478	2.005	1055.7	329.9
		0.25	4.706	0.776	1.132	1.662	1.459	2.142	1074.6	335.6
	0.10	0.15	4.671	0.780	1.263	1.394	1.619	1.787	1086.8	339.6
		0.20	4.605	0.786	1.259	1.518	1.602	1.931	1108.3	346.3
		0.25	4.524	0.793	1.255	1.636	1.583	2.063	1126.2	351.9

where δ_S^2 can be calculated from Eq.(6.63) and also ρ and θ can be obtained from ρ^* and θ^*. Then, ρ^* is computed as

$$\rho^* = \frac{T_L}{T_D + T'_D} = \frac{182.9}{360.1 + 0.3215\ A} \qquad (6.65)$$

Using the safety index calculated by Eq.(6.64), the cross sectional area and the load factors are determined by both the proposed method and the triangular approximation method. Table 6.6 presents the results of the proposed method. It is seen that the proposed method provides the cross sectional area which is almost equal to that obtained by the allowable stress design. This result can be easily anticipated, considering a good accuracy of the proposed method, as shown in section 6.4. On the other hand, the triangular approximation method gives different cross sectional areas, which are conservative or unconservative, according to the values of the coefficient of variation. This inconsistency is due to the approximation involved in the linearizing process.

Consequently, it can be said that the proposed method gives a good correspondence between the allowable stress design and the load factor design. This means that the proposed method enables to make a rational calibration between the safety factor and the load factors, which is inevitable to establish a design code based upon the reliability-based philosophy.[23)]

Example 4

The safety of present road bridges is examined by use of the statistical data obtained by the observation and simulation.[24)] Special attention is placed on the relation between span length and safety.

According to Ref. 24, the safety level of current road bridges, whose span lengths are longer than *20 m*, can be evaluated as follows : The central safety factor θ is

$$\theta = \frac{\mu_R}{\mu_S} = \frac{\nu_R \cdot p\ \{1 + 1/\rho^* + 20/(50+\ell)\}}{\mu_E(\ \nu_D/\rho^* + \nu_L\ )} \qquad (6.66)$$

Then, the nominal safety factor θ^* becomes

$$\theta^* = \frac{R^*}{S^*} = \frac{\mu_R / \nu_R}{\mu_S / \nu_S} = \frac{\nu_S}{\nu_R}\,\theta \qquad (6.67)$$

in which ν denotes the ratio of the mean value and the nominal value, and also p represents the safety factor used in the current design code. The safety index is expressed as follows :

for $Z = R - S$

$$\beta = \frac{\theta - 1}{\sqrt{\theta^2\delta_R^2 + \delta_E^2 + (\delta_D^2 + \rho^2\delta_L^2) / (1+\rho)^2}} \qquad (6.68)$$

for $Z = \ln (R/S)$

$$\beta = \frac{\ln \theta}{\sqrt{\delta_R^2 + \delta_E^2 + (\delta_D^2 + \rho^2\delta_L^2) / (1+\rho)^2}} \qquad (6.69)$$

The calculation is implemented by using the following data :[24)]

Resistance R ; $\nu_R = 1.2$, $\delta_R = 0.15$, *Error* E ; $\nu_E = 1.0$, $\delta_E = 0.05$

Load S ; $\nu_D = 1.0$, $\delta_D = 0.05$ *Safety Factor* p ; $p = 1.7$

Other Data ; given in the left columns of Table 6.8

The nominal safety factor calculated from the above data is illustrated in Fig. 6.11. The nominal safety factor has somewhat larger values than *1.7* which is given in the current design specifications. Fig. 6.12 shows the relation between span length and safety index. The right columns of Table 6.8 present the numerical results of safety index and load factors. It is obtained from Fig. 6.12 that the values of safety index differ by about one, depending on the choice of the performance function. Also, it is seen that the safety index changes unevenly within $\ell = 20 - 100$ *m*. This uneven change is probably due to the use of actually measured data. Roughly speaking, the safety index changes against span length with a similar tendency, despite of the performance function.

In Fig. 6.13, the load factors are obtained for both the performance functions, $Z = R - S$ and $Z = \ln (R/S)$, corresponding to $\phi = 0.90$ and the values of β shown in Fig. 6.12. The proposed method does not give

Table 6.8 Statistical Data of Live Load and Calculated Results

Span Length (m)	Statistical Data of Live Load				Calculated Values *		
						Load Factors (ϕ=0.9)	
	ν_L	δ_L	$\rho^* = \frac{L^*}{D^*}$	Freq. of Live Load	β	γ_D	γ_L
20	0.93	0.20	1.26	0.249	3.76	1.65	1.85
					4.67	1.57	1.92
40	1.01	0.16	0.80	0.415	3.55	1.57	1.75
					4.57	1.57	1.79
60	0.99	0.14	0.63	0.18	3.52	1.55	1.66
					4.62	1.61	1.69
80	0.96	0.15	0.53	0.073	3.51	1.58	1.61
					4.61	1.62	1.61
100	0.98	0.14	0.45	0.034	3.46	1.56	1.59
					4.55	1.61	1.61
150	0.94	0.13	0.34	0.025	3.44	1.56	1.54
					4.54	1.59	1.47
200	0.87	0.14	0.29	0.013	3.47	1.56	1.38
					4.61	1.62	1.38
250	0.84	0.14	0.27	0.005	3.47	1.56	1.33
					4.62	1.62	1.32
300	0.73	0.13	0.25	0.003	3.53	1.58	1.16
					4.73	1.67	1.18

*

Upper Row $Z = R - S$
Lower Row $Z = \ln(R/S)$

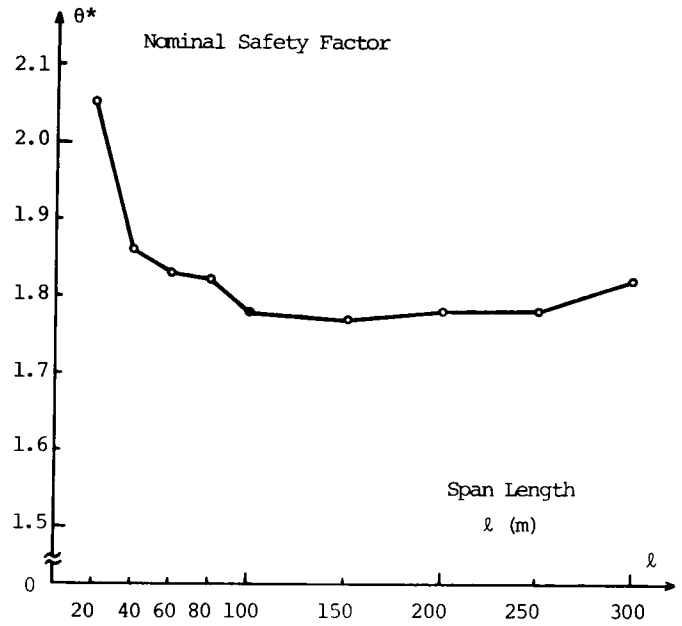

Fig. 6.11 Relation between Nominal Safety Factor and Span Length

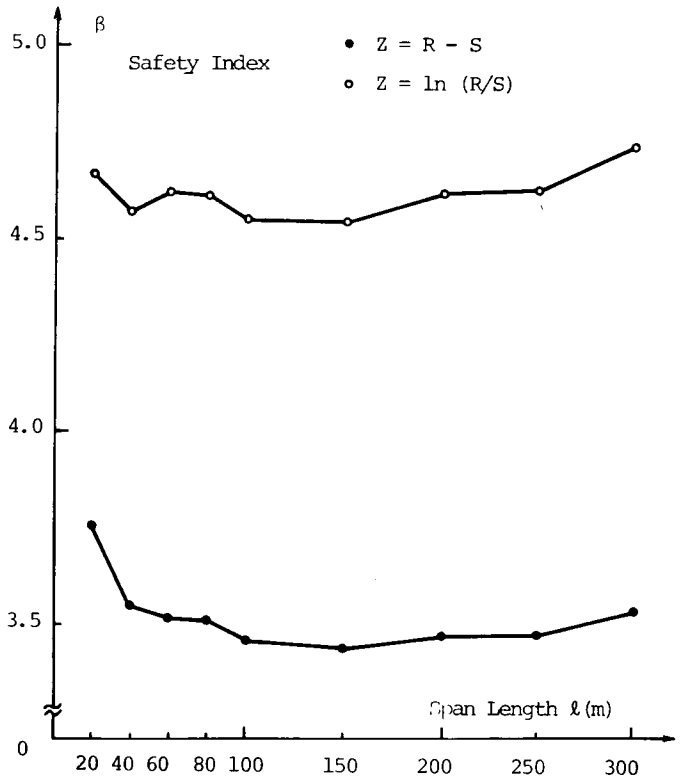

Fig. 6.12 Relation between Safety Index and Span Length

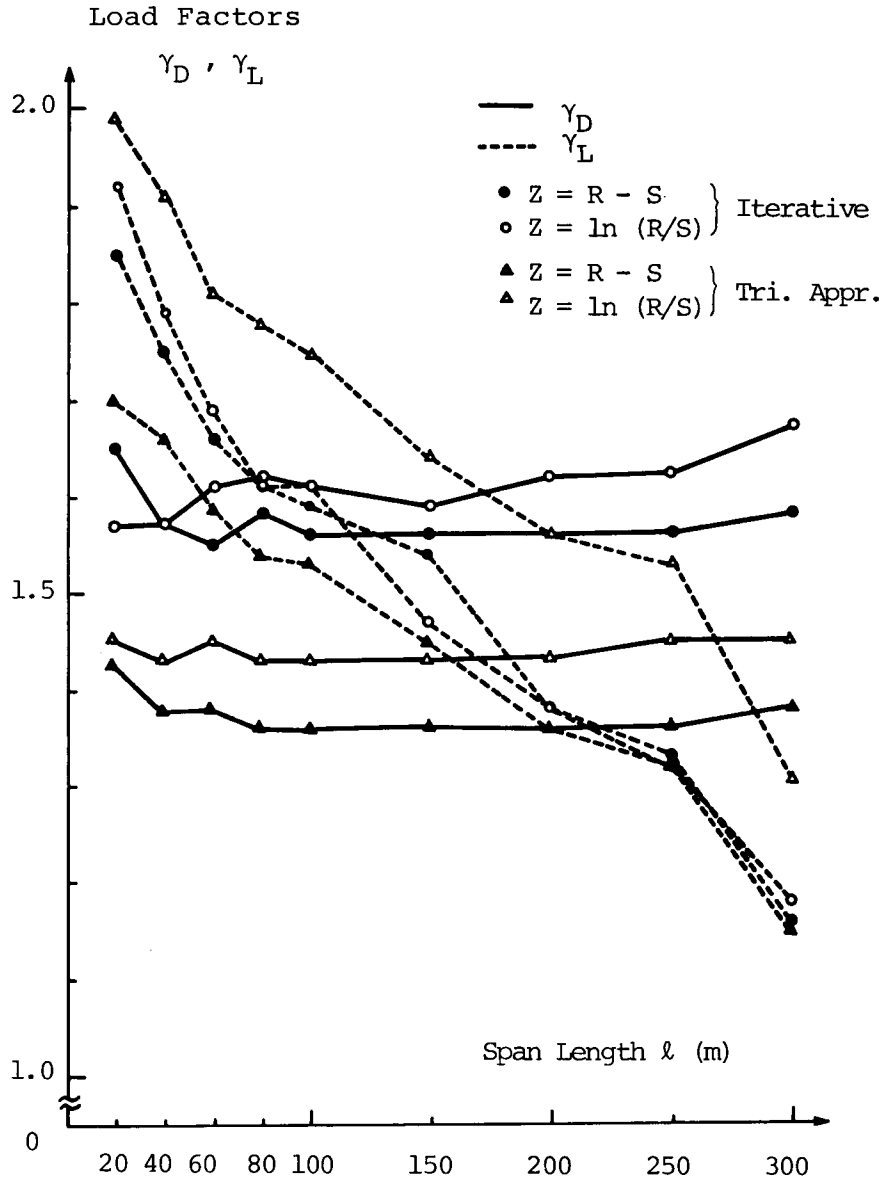

Fig. 6.13 Relation between Load Factors and Span Length

so different values of γ_D and γ_L for both the performance functions, and also gives larger value for γ_D than the triangular approximation method does. This reason is that in the proposed method, the load factors are determined by corresponding to the magnitude of its standard deviation. On the other hand, in the triangular approximation method, the values of the load factors are considerably affected by the selection of performance function, and especially the difference is remarkable for γ_L. Despite of the difference of the values, the relations between the load factors and span length have the similar tendency for both the performance functions.

Next, the sensitivity of the load factors to the safety index is examined. The mean and minimum values of the safety indices calculated for several span lengths are employed as representative ones. Fig. 6.14 presents the results of γ_D and γ_L, which are obtained for $Z = R - S$ by using $\beta = 3.59$ (mean) and $\beta = 3.44$ (minimum) for the entire range of span length. Fig. 6.15 shows the results obtained for $Z = ln\ (\ R/S\ )$, in which $\beta = 4.61$ (mean) and $\beta = 4.54$ (minimum) are employed. It is seen that the proposed method is more sensitive to the change of the safety index in the determination of the load factors. Although excessive sensitivity is not desirable in the actual design, the sensitivity appeared in this case is considered reasonable, because it is natural that the values of the load factors change as the change of the safety index.

It can be also considered that the values of θ^* and γ are obtained through the calibration which uses an appropriate value of β. Comparing the results of θ^*, γ_D and γ_L, θ^* and γ_D tend to change similarly against span length. Then, the proposed method enables to perform a rational calibration in spite of the choice of performance function, because the difference of the load factors due to the selection of Z is not so large in the proposed method.

Through the above numerical results, the following conclusions are obtained :

- The nominal safety factor θ^* lies within a range from 1.8 to 1.9, and the load factor with respect to the dead load is about 1.6.
- However, the load factor with respect to the live load varies

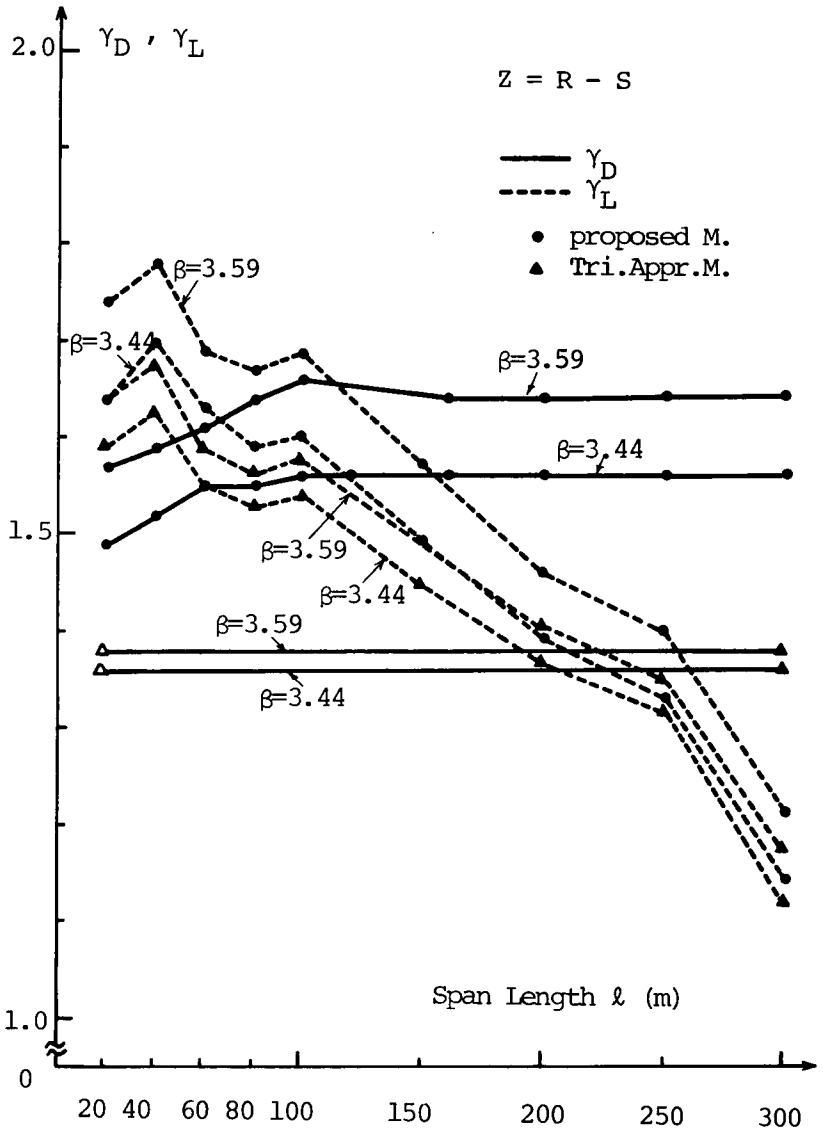

Fig. 6.14 Comparison of the Proposed Method and the Triangular Approximation Method (Z = R - S)

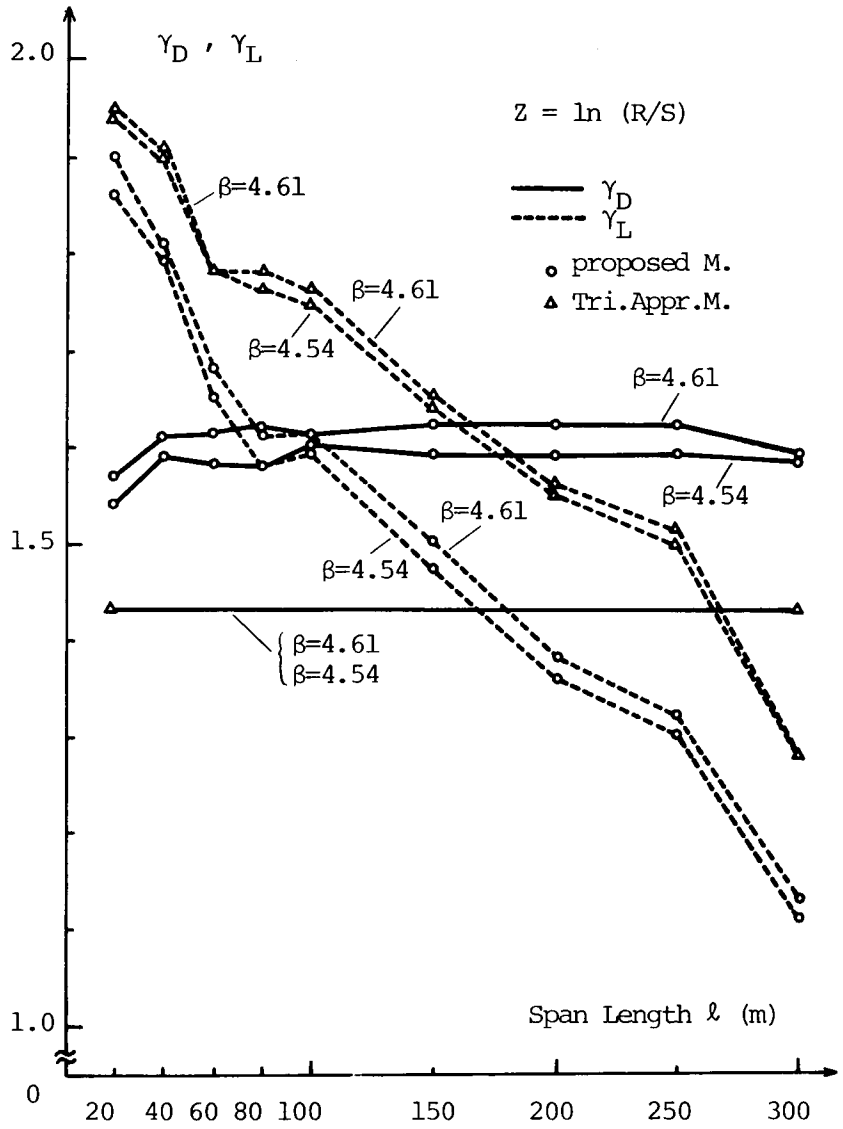

Fig. 6.15 Comparison of the Proposed Method and the Triangular Approximation Method (Z = ln (R/S))

according to the span length, namely

$$\gamma_L = 1.9 \qquad \text{for } \ell = 20\ m$$

$$\gamma_L = 1.6 \qquad \text{for } \ell = 100\ m$$

$$\gamma_L = \text{more than } \gamma_D \qquad \text{for } \ell > 100\ m$$

6.7 Conclusions

In this chapter, an iterative design method is derived on the basis of the second-moment theory. The design load, resistance factor and load factors can be calculated without mathematical approximations, by using the coordinates of the failure point in the normalized space. The proposed method and usual methods are compared and examined through some design examples. The main results derived here are as follows :

1) Usual methods often provide unreasonable designs because of the mathematical approximation involved in the reduction of the basic formula. On the contrary, the proposed method makes it possible to obtain an accurate design with relatively less computation load.
2) By using the concept of the failure point defined in the normalized space, the physical meaning of the split coefficients can be graphically interpreted. The basic design formula derived herein provides the assurance of well correspondence between the first-order second-moment design format and the load factor design format.
3) It is possible to easily perform a rational calibration between the safety factor and the load factors, by using the safety index as the measure of safety.
4) Comparing with the triangular approximation method, the proposed method is liable to undergo an influence of the change of the safety index in the determination of the load factors, while less influence of the choice of performance function.
5) As well known, current road bridges tend to become more reliable when the span length is more than *100 m*, but the increasing rate is not so large as expected.

References for Chapter 6

1) Lind, N. C., " Consistent Partial Safety Factors ", Proc. ASCE, ST6, June, 1971, pp1651-1669

2) Ravindra, M. K., Lind, N. C. and Siu, W., " Illustrations of Reliability-Based Design ", Proc. ASCE, ST9, Sept., 1974, pp1789-1811

3) Ang, A. H-S. and Cornell, C. A., " Reliability Bases of Structural Safety and Design ", Proc. ASCE, ST9, Sept., 1974, pp1755-1769

4) Strating, J., " Loading Function ", Planning and Design of Tall Buildings, Structural Design of Tall Steel Buildings, Volume II, ASCE/IABSE, State of Art Report No.3, 1972, pp849-859

5) Galambos, T. V., " Response Function ", Planning and Design of Tall Buildings, Structural Design of Tall Steel Buildings, Volume II, ASCE/IABSE, State of Art Report No.4, 1972, pp861-867

6) Mrazik, A., " Limit State of Steel Structures According to Czechoslovak Standard ", Proceedings of the 2nd International Conference of Application of Statistics and Probability in Soil and Structural Engineering, W.Germany, Sept., 1975, pp305-317

7) Cho, T. and Koyama, K., " Code Calibration for Reinforced Concrete Design ", Proc. JSCE, No.287, July, 1979, pp115-125 (in Japanese)

8) Ang, A. H-S., " Series of Lectures on Structural Reliability and Probability-Based Design ", Lecture Note, Apr., 1976

9) Shah, H. C., " Statistical Evaluation of Load Factors in Structural Design ", Structural Reliability and Codified Design (Editor : N.C. Lind), Study No.3, Solid Mechanics Division, Univ. of Waterloo, 1970, pp129-153

10) Committee of JSCE, " Concepts of Design for Steel Bridges ", JSSC, Vol.9, No.86, 1973, pp5-54 (in Japanese)

11) Heins, C. P. and Kurzweil, A. D., " Load Factor Design of Continuous-Span Bridges ", Proc. ASCE, ST6, June, 1976, pp1213-1228

12) Porter, J. C., " Load Factor Analysis for Design of Bridges ", Proc. ASCE, ST5, May, 1976, pp891-897

13) Lingu, D. and Ghiocel, D., " Towards a Reliability-Based Concrete Structural Code ", Proceedings of the 2nd International Conference

of Applications of Statistics and Probability in Soil and Structural Engineering, W.Germany, 1975, pp190-199

14) Lind, N. C., " Formulation of Probabilistic Design ", Proc. ASCE, EM2, Apr., 1977, pp273-284

15) Veneziano, D., " A Theory of Reliability which Includes Statistical Uncertainty ", Proceedings of the 2nd International Conference of Applications of Statistics and Probability in Soil and Structural Engineering, W.Germany, 1975, pp231-249

16) Veneziano, D., " New Index of Reliability ", Proc. ASCE, EM2, Apr., 1979, pp277-295

17) Hasofer, A. M. and Lind, N. C., " Exact and Invariant Second-Moment Code Format ", Proc. ASCE, EM1, Feb., 1974, pp111-121

18) Nakano. M., " Fundamental Study on Reliability Analysis and Design Using Safety Index ", Master of Engineering Thesis, Kyoto Univ., 1979 (in Jpanese)

19) Paloheimo, E. and Hannus, M., " Structural Design Based on Weighted Fractiles ", Proc. ASCE, ST7, July, 1974, pp1367-1378

20) Shiraishi, N., Furuta, H. and Nakano, M., " Fundamental Study on Structural Design Based on Second-Moment Theory ", (contributing to Proc. JSCE) (in Japanese)

21) Tang, W., Shah, H. and Benjamin, J., " Statistical Evaluation of Load Factors in Structural Design ", IABSE Symposium on Concepts of Safety of Structures and Methods of Design, Final Report, London, England, 1969, pp99-107

22) Kikuchi, Y. and Sasado, M., " Design Examples of Bridges ", Ohmu-sha Publishing, June, 1975 (in Japanese)

23) Cho, T., Koyama, K. and Imao, Y., " Code Calibration for Ultimate Strength Design of RC Beam ", The 32nd Annual Meeting of JSCE, V-163, Oct., 1977, pp311-312 (in Japanese)

24) Kinoshita, S., Ito, M. and Fujino, Y., " Evaluation of Load Factors for Steel Road Bridges Based on Reliability Approach ", The 33rd Annual Meeting of JSCE, I-150, Oct., 1978, pp286-287 (in Japanese)

Chapter 7 Concluding Remarks

In this dissertation, two main subjects, geometrical configuration and reliability of structural systems, have been investigated and discussed with emphasis on how they should be introduced or related to the design process. Although these two subjects can be contained in a category of structural design, it would be better to consider them independent at the present time, because their basic philosophies and their objectives are different. The characteristics of geometrical configurations have been argued on the basis of the current design format, i.e., the allowable stress criterion format, while the reliability-based design treated in the latter part aims to disclose the intrinsic inconsistency involved in the current codes, and further to quantitatively introduce various uncertainties, which are unavoidable to small or great extent, into the design process.

If the ultimate goal of structural engineers is to obtain a rational design, or to establish a rational design method in a wider sense, the two subjects considered here should be treated and discussed in a unified manner. It is, however, quite difficult to establish a well-grounded method which satisfies the above requirement, because of the existence of many unresolved problems related to the essense or philosophy of design.

In this conclusive chapter, the objectives of this study and the main results derived from the foregoing chapters will be reviewed comprehensively to discuss commonly the conclusions related to proposals for structural design and also in relation to the prospect for future studies to be continued.

In chapter 2, the geometrical configurations of framed structures were recognized by means of a graphical representation. In order to determine the effective configuration, the topological and geometrical systems can be considered useful for the design of trussed bridges. By corresponding those systems to a hierarchy of structural design, an effective design procedure can be found out through some numerical experiments :

1) Determine the supporting condition.

2) Assume the number of nodes and the topology of members.

3) Perform the optimization by taking the nodal coordinates and the cross sectional areas of members as design variables.

Using the abovementioned procedure, a practical design method including a geometrical variation was proposed in chapter 3 on the basis of a two-level treatment. This method showed a considerable efficiency or applicability by a design example of large continuous truss bridge, though some problems in conjunction with computations remain. It is also to be noted that there are some design requirements to be accounted for in the application of the proposed method to the actual bridge design. Nevertheless, the results obtained in this study confirmed that the quantitative introduction of geometrical variations has a large possibility of presenting a more rational structure even in the present designs.

While the topology of members was not significant for the weight-minimization of trussed bridges, it has become significant for the design of arched bridges. This may imply that a variation of topology will take an important role in the selection of the type of bridges. To this problem, further investigations should be made, broadening our views to the cable-stayed bridge or other typed bridges.

Chapter 4 has been devoted to developments of the classical reliability theory. Although many researchers have pointed out some problems involved in the classical theory, nobody can deny the firm and sophisticated base in its theoretical framework. On account of the easiness of treatment and the explicitness of physical meaning, the failure probability will remain as one of the excellent measure of safety. By use of the fiducial statistics or the statistical decision theory, the effect of statistical uncertainty or the optimum sampling method can be evaluated or achieved. However, it may be said that the reliability approach using the failure probability is not suitable for an actual complicate design, but for a conceptual basic design.

From a practical point of views, the reliability theory based on the second-moment theory has been investigated in chapter 5 and chapter 6. Among the reliability-based designs presented up to date, the second-moment design format can be considered the most convenient and flexible

to account for the various uncertainties, some of which are not tractable in a mathematical form. In chapter 5, major concerns are the physical meaning of safety index and the treatment of combinatorial problems based on the second-moment expression. By paying attention to the normalized space presented by Hasofer and Lind, it is possible to evaluate the safety of structural systems with many possible failure modes, as well as that of structural systems with a single failure mode. The coordinates of the failure point, which defines the safety index, express the ratio of the underlying variables at the most weakest failure condition.

Chapter 6 has dealt with the problem how the engineering uncertainties must be introduced into the design process. By giving special attention to the failure point, a basic formula can be reduced in the form of the load factor design format, without mathematical approximations. Since the proposed formula does not involve the errors due to the approximation, an accurate calibration, which is important to transfer the current design code to the load factor design or the limit-state design, can be achieved.

Throughout this study, special interest may be taken in the fundamental features of structural design, and also some assumptions have been employed to make the discussion simple. For these reasons, the results obtained in this study may not be immediately applicable or sufficient for the actual design works, they may serve to present some valuable suggestions for the advance of the design of bridge structures.